GEOLOGIJA

2017 | št.: **60/1**

Gostujoči uredniki / Guest Editors:
Mihael Brenčič, Barbara Čenčur Curk, Luka Gale & Timotej Verbovšek

GeoZS
Geološki zavod
Slovenije

ISSN
Tiskana izdaja / Print edition: 0016-7789
Spletna izdaja / Online edition: 1854-620X

GEOLOGIJA

60/1 – 2017

GeoZS
Geološki zavod Slovenije

GEOLOGIJA	2017	60/1	1-168	Ljubljana

GEOLOGIJA
ISSN 0016-7789

Izdajatelj: Geološki zavod Slovenije, zanj direktor Miloš Bavec
Publisher: Geological Survey of Slovenia, represented by Director Miloš Bavec
Financirata Javna agencija za raziskovalno dejavnost Republike Slovenije in Geološki zavod Slovenije
Financed by the Slovenian Research Agency and the Geological Survey of Slovenia

Vsebina številke 60/1 je bila sprejeta na seji Uredniškega odbora, dne 5. 6. 2017.
Manuscripts of the Volume 60/1 accepted by Editorial and Scientific Advisory Board on June 5, 2017.

Naslov uredništva / Editorial Office: GEOLOGIJA Geološki zavod Slovenije / Geological Survey of Slovenia
Dimičeva ulica 14, SI-1000 Ljubljana, Slovenija
Tel.: +386 (01) 2809-700, Fax: +386 (01) 2809-753, e-mail: urednik@geologija-revija.si
URL: http://www.geologija-revija.si/

GEOLOGIJA izhaja dvakrat letno. / GEOLOGIJA is published two times a year.
GEOLOGIJA je na voljo tudi preko medknjižnične izmenjave publikacij. /
GEOLOGIJA is available also on exchange basis.

Izjava o etičnosti
Izdajatelji revije Geologija se zavedamo dejstva, da so se z naglim naraščanjem števila objav v svetovni znanstveni literaturi razmahnili tudi poskusi plagiatorstva, zlorab in prevar. Menimo, da je naša naloga, da se po svojih močeh borimo proti tem pojavom, zato v celoti sledimo etičnim smernicam in standardom, ki jih je razvil odbor COPE (Committee for Publication Ethics).

Publication Ethics Statement
As the publisher of Geologija, we are aware of the fact that with growing number of published titles also the problem of plagiarism, fraud and misconduct is becoming more severe in scientific publishing. We have, therefore, committed to support ethical publication and have fully endorsed the guidelines and standards developed by COPE (Committee on Publication Ethics).

Baze, v katerih je Geologija indeksirana / Indexation bases of Geologija: Scopus, Directory of Open Access Journals, GeoRef, Zoological Record, Geoscience e- Journals, EBSCOhost

Cena / Price

Posamezni izvod / Single Issue	Letna naročnina / Annual Subscription
Posameznik / Individual: 15 €	Posameznik / Individual: 25 €
Institucija / Institutional: 25 €	Institucija / Institutional: 40 €

Tisk / Printed by: Birografika BORI d.o.o.

Slika na naslovni strani: Školjka iz karnijskih amfiklinskih plasti pri Crngrobu (foto: M. Križnar)

Cover page: Bivalve from Carnian Amphiclina beds near Crngrob (photo: M. Križnar)

VSEBINA – CONTENTS

GEOLOGIJA 60/1, 5-8, Ljubljana 2017
https://doi.org/10.5474/geologija.2017.000

Uvodnik

Oddelek za geologijo Univerze v Ljubljani se približuje svoji stoti obletnici. V celotnem obdobju svojega delovanja se je razvil in kadrovsko okrepil ter dosegel pomembne rezultate na pedagoškem, znanstvenem in strokovnem področju. Na Oddelku so različne stopnje akademske izobrazbe dosegli številni geologi, ki danes uspešno delujejo tako v Sloveniji, kot tudi v tujini. Vse to je zasluga današnje in mnogih predhodnih generacij, ki so v preteklosti delovale na Oddelku. Zato je prav, da se današnji člani Oddelka in vsi ostali slovenski geologi zavedamo svojih korenin in zaslug, ki jih imajo za naš razvoj profesorji, pri katerih smo začenjali svoje prve korake v svet geologije in se kasneje pri njih tudi izpopolnjevali. V tednu Univerze v Ljubljani decembra leta 2016 smo na Oddelku za geologijo počastili okrogle življenjske obletnice štirih naših učiteljev, ki so v preteklosti nesebično razdajali svoje znanje številnim generacijam študentov. Profesorji Jožef Pezdič, Mihael Ribičič, France Šušteršič in Miran Veselič, kakor tudi drugi profesorji, so s svojim pedagoškim, znanstvenim in strokovnim delom pomembno zaznamovali slovensko geologijo ter Oddelek za geologijo. Njihovemu delu so posvečeni članki v obeh številkah 60. letnika revije Geologija, ki so jih napisali njihovi učenci, predvsem diplomanti in doktorski študentje, zato je prav, da si v uvodniku prve številke na kratko ogledamo tudi življenje in delo slavljencev.

Redni prof. dr. Jožef Pezdič, univ. dipl. inž. geol., se je rodil 8. marca 1945 v Radovljici. Tam je obiskoval osnovno šolo in se nato vpisal v gimnazijo v Kranju, ki jo je zaključil leta 1964. Istega leta se je vpisal na Fakulteto za naravoslovje in tehnologijo v Ljubljani, smer geologija. Svojo raziskovalno smer je začrtal že v diplomi leta 1985 z naslovom »Izotopske značilnosti mineralne vode na področju Rogaške Slatine«, šest let kasneje pa je doktoriral s področja izotopov, z naslovom disertacije »Izotopi v termo-mineralnih vodnih sistemih«. Njegova prva zaposlitev leta 1965 je bila na inštitutu Jožef Stefan, kjer je ostal vse do leta 1996, ko se je istega leta kot visokošolski učitelj zaposlil na takratni Fakulteti za naravoslovje in tehnologijo v Ljubljani. Leta 1992 je bil izvoljen v naziv docenta, 1998 v izrednega profesorja in 2004 v naziv rednega profesorja.

Ukvarjal se je z različnimi geološkimi in kemičnimi tematikami, največji pečat pa je pustilo njegovo delo na področju izotopske geokemije in laboratorijskih tehnik, s katerim se je ukvarjal celotno svojo kariero. Poleg tematike izotopov se je ukvarjal tudi s termomineralnimi vodami (predvsem v Prekmurju), geokemičnim modeliranjem, raziskovanjem fluidov (plinov in vode), s posebnim poudarkom na CO_2 ciklusu in s sorpcijo plinov v Velenjskem premogovniku. Rezultati njegovega raziskovalnega dela so vidni v številnih objavah in publikacijah. Tako je bil prvi avtor ali soavtor 88 izvirnih znanstvenih člankov, že zelo zgodaj pa je izkazoval veliko citiranost v mednarodnih revijah (do sedaj skupaj 416 citatov sistemu v Web of Science od tega 319 čistih citatov). Bil je tudi soavtor poglavij v treh tujih znanstvenih monografijah. Njegov pomemben pedagoški in znanstveni dosežek je visokošolski učbenik z naslovom »Izotopi in geokemijski procesi«, s katerim je povzel znanje in številne primere uporabe stabilnih in radioaktivnih izotopov v geologiji. Njegova strokovna dejavnost obsega 48 strokovnih poročil in elaboratov s tematike geokemije, izotopov, termalnih vod in rudišč ter 75 ekspertiz s področja ocene različnih posegov v okolje. V sistemu COBISS je v njegovi bibliografiji skupaj zabeleženih 326 del. Že od leta 1970 dalje je bil vključen v številne raziskovalne projekte. Sodeloval je pri sedmih ARRS projektih, od tega je bil pri dveh (Mehanizmi nastajanja, prenosa in kopičenja plinov v premogovnih slojih in Geokemija supergene cone v Sloveniji) tudi vodja. Vodil je IAEA mednarodni projekt in bil nosilec bilateralnih in mednarodnih projektov (InterReg in IGCP). Profesor Pezdič je bil mednarodno dejaven tudi z gostovanjem in pedagoškim delom v tujini (Nemčija, Češka), izvajal je vabljena predavanja v več državah Evrope in v Kanadi, pedagoško je cel semester deloval na Masarykovi univerzi v Brnu ter opravil polletno raziskovalno specialistično delovanje na UFZ Leipzig (Nemčija). Bil je tudi organizator nekaterih mednarodnih kongresov, med drugim 4th Isotope Workshop v Portorožu. Vrsto let je bil glavni in odgovorni urednik revije RMZ-Materials and Geoenvironment ter član uredniškega odbora biltena Mineralne surovine.

Njegovo pedagoško delo je bilo zelo pestro. V času svojega delovanja na fakulteti je imel predavanja iz predmetov Geokemija in okolje, Ekonomska geologija, Organske surovine, Tehnična geologija 1 in Sklepne terenske vaje. Poleg tega je bil tudi nosilec predmetov na podiplomskem študiju geologije in varstva okolja. V času svojega pedagoškega delovanja je bil mentor 28 diplomantom (ter dvakrat somentor), trem magistrantom (Andreji Ramšak, Roku Pencu, Tjaši Kanduč ter dvema somentor - Mateju Karahodžiču in Nataši Kukar). Pod njegovim mentorstvom je doktoriralo osem doktorjev znanosti: Jože Uhan, Tamara Teršič, Miloš Markič, Timotej Verbovšek, Tjaša Kanduč, Simon Zavšek, Branka Trček, Sonja Lojen, bil pa je tudi somentor pri doktorski disertaciji Mateja Dolenca. Po upokojitvi je ustanovil lastno podjetje GEORIS - raziskovanje, izobraževanje in svetovanje, Jožef Pezdič s.p., preko katerega aktivno sodeluje s Premogovnikom Velenje in številnimi drugimi organizacijami v javnem in zasebnem sektorju.

Izredni prof. dr. France Šušteršič, univ. dipl. inž. geol., se je rodil 8.6.1945 v Ljubljani, kjer je obiskoval II. gimnazijo. Po končani maturi se je leta 1966 vpisal na Oddelek za geologijo in študij dokončal leta 1976 z diplomsko nalogo z naslovom »Kvartarni sedimenti v zasutih breznih notranjskega krasa«. Leta 1985 je doktoriral s tezo »Uporabnost Fourierjeve analize v fizikalni speleologiji«. Kariero profesorja Šušteršiča so v celoti zaznamovali kras, jamarstvo in speleologija. Že v srednješolskih letih je postal aktiven jamar in član Društva za raziskovanje jam Ljubljana. To svojo strast je zadržal vse do danes, prenesel jo je v svoje znanstveno raziskovalno delo ter tudi na svoje učence. Že pred diplomo se je leta 1974 zaposlil na Inštitutu za raziskovanje krasa v Postojni, kjer je ostal vse do leta 1988, ko se je zaposlil na Oddelku za geologijo Fakultete za naravoslovje in tehnologijo, na katerem je deloval vse do svoje upokojitve leta 2008. V naziv docenta je bil izvoljen leta 1988 in v naziv izrednega profesorja leta 1994. Na Oddelku je v letih 1998 do 2000 opravljal tudi funkcijo predstojnika.

Znanstveno delovanje profesor Šušteršiča sega na številna področja krasoslovja, pri tem je dosegel pomembne uspehe in tudi širši odmev v mednarodnem merilu. Temeljito se je posvečal teoriji razvoja krasa, v okviru katere je postavil »Model čistega krasa«, prav tako temeljen je njegov premislek na področju speleogeneze, ki sega od splošnih principov, pa vse do speleogeneze posameznih jam različnih velikosti. Zelo veliko pozornosti je posvečal nastanku in razvoju vrtač in udornic ter tudi geomorfologiji kraških polj. Pri svojem znanstvenem delu je vpeljeval številne matematične modele in metode. Do sedaj je sam ali v soavtorstvu objavil 34 izvirnih znanstvenih člankov, 8 preglednih znanstvenih člankov, 30 strokovnih člankov, 25 poljudnih člankov, 2 poglavji v znanstvenih monografijah in 3 poglavja v strokovnih monografijah. V okviru naštevanja njegovih zaslug, je potrebno omeniti tudi njegov jamarski prispevek, ki je tesno povezan z njegovim znanstvenim delom. Skupaj s prijateljem Matjažem Pucem sta že v študentskih letih na noge postavila kataster jam, ki predstavlja temelje sodobnega katalogiziranja jam in je vzor številnim jamarskim katastrom po svetu. Seveda je v ta kataster kot prvopristopnik prispeval številne zapisnike. Med njegove najpomembnejše jamarske dosežke sodijo raziskave Najdene jame pri Lazah na Planinskem polju, kjer si je tudi ustvaril svoj dom. Je dolgoletni član uredništva revije Naše jame in nekaj časa tudi njihov urednik.

Na Oddelku za geologijo je poučeval številne predmete. Na dodiplomskem študiju so bili to Geologija krasa, Statistika v geologiji, Fizikalna geologija z geomorfologijo in Opisna geometrija. Bil je tudi nosilec predmetov na podiplomskem študiju. Svoje bogato krasoslovno znanje je na študente prenašal tudi v Speleološkem krožku. O krasu je predaval na univerzah Aix-en-Provance, Clausthal, Padova in Brno. Bil je mentor petim diplomantom in somentor šestim diplomantom. Mileni Zlokulica je bil mentor pri magisteriju ter mentor pri doktoratih Martinu Knezu, Tereziji Lenarčič, Nadji Zupan Hajna in Marku Vrabcu. Profesor Šušteršič ostaja strokovno in znanstveno aktiven tudi po svoji upokojitvi. Tako nemalokrat vodi ekskurzije študentov geologije in tudi druge skupine, ki se zanimajo za kras. Še vedno je aktiven jamar, publicist ter pisec zlasti polemičnih jamarskih zapisov.

Izredni prof. dr. Mihael Ribičič, univ. dipl. inž. geol., se je rodil 20. 5. 1946 v Ljubljani, kjer je tudi obiskoval osnovno šolo in gimnazijo. Leta 1964 se je vpisal na študij geologije na takratni Fakulteti za naravoslovje in tehnologijo Univerze v Ljubljani. Študij geologije – praktična smer – je leta 1973 zaključil z diplomskim delom "Geološke razmere med Podutikom in Jamo" in se zaposlil na Geološkem zavodu Ljubljana, kjer je deloval na področju inženirske geologije.

Svoje znanje je stalno nadgrajeval, s svojimi idejami pa je zagotovo pustil velik pečat v razvoju inženirske geologije pri odkopavanju premoga v rudniku lignita Velenje, saj je s sodelavci razvil odkopne metode na območju lignita, kjer preti nevarnost vdorov vode, blata, peska in plina v jamske prostore Premogovnika Velenje. Razvijal je tudi metode za in-situ preiskave - meritve napetosti z različnimi hidravličnimi celicami in hidravlično frakturizacijo so bile v premogovniku uporabljene celo prvič na svetu. Bil je tudi pionir pri uvajanju geotomografske seizmične metode za proučevanje rušnih procesov pri širokočelnem odkopavanju premoga z vertikalnim pridobivanjem. V tem obdobju je leta 1986 zagovarjal magistrsko nalogo "Matematično modeliranje zarušnih procesov pri odkopavanju premoga v Rudniku lignita Velenje z metodo končnih elementov", leta 1988 pa doktorsko nalogo "In-situ meritve za določitev pogojev odkopavanja v debelih premoških slojih, kjer preti nevarnost vdorov vode in tekočih mas". Leta 1988 je opravil tudi projektantski izpit in postal samostojni projektant v rudarstvu.

V drugi polovici kariere se je ukvarjal predvsem z naravnimi nesrečami, predvsem s plazovi in potresi. Preučeval je posledice potresov v naravi in kako na tej osnovi ocenimo jakost potresa ter napovemo potencialno ogroženost glede na intenziteto potresa. Na področju varstva pred plazovi je uvedel metodologijo popisa fosilnih plazov s pomočjo GIS-a in metodologijo določanja verjetnosti pojavljanja plazov, podorov, drobirskih tokov ter kart ogroženosti. Bil je tudi član Strokovnega odbora za plazove večjega obsega pri Ministrstvu za okolje in prostor. Stalna želja po znanju ga je vodila v uvajanje novih pristopov v geološko stroko: matematično modeliranje, GIS, daljinsko zaznavanje, umetna inteligenca, nevronske mreže in še bi lahko naštevali. Del njegovega znanstvenega dela je bil vezan tudi na gradnjo prometnic, kjer je proučeval merske in raziskovalne metode ter vpliv geološke zgradbe na pogoje odkopavanja in vpliv tehnologije odkopavanja na okolje. Strokovno delo je zahtevalo tudi projektiranje in nadzor, zato je leta 1997 opravil projektantski izpit in postal samostojni projektant v gradbeništvu. V bogati strokovni in znanstveni karieri je napisal 17 izvirnih znanstvenih člankov, 2 pregledna znanstvena članka in 25 strokovnih člankov. Izdal je nekaj znanstvenih monografij, med katerimi so tudi karte dovzetnosti pojavljanja plazov in drobirskih plazov.

Akademsko kariero je začel leta 1989, ko je bil prvič izvoljen v naziv docenta. Do leta 2004, ko se je redno zaposlil na Naravoslovnotehniški fakulteti, je poleg redne zaposlitve pogodbeno predaval Inženirsko geologijo I in II, Tehnično geologijo ter se udeleževal Sklepnih terenskih vaj, kjer je podajal inženirsko geološke tematike. Bil je tudi nosilec predmetov na podiplomskem študiju geologije in varstva okolja. Vsi ti predmeti so ozko usmerjeni, zato je zanje potrebno široko izkustveno znanje, ki ga je pridobil v svoji dolgoletni strokovni in znanstveni karieri. Ravno zaradi tega so bila njegova predavanja vedno zelo zanimiva. Že na začetku akademske kariere je napisal skripta, ki se uporabljajo še danes. Leta 2006 je bil izvoljen v izrednega profesorja. Vzgojil je mnoge mlade inženirske geologe, saj je bil mentor 67 diplomantom in somentor devetim diplomantom. Poleg tega je bil mentor osmim magistrandom (Tomaž Beguš, Anton Dular, Magda Čarman, Karmen Fifer Bizjak, Janez Hafner, Mitja Janža, Albin Križnič, Katarina Žnideršič) ter somentor pri treh magisterijih. Mentor je bil pri desetih doktoratih (Tomaž Beguš, Magda Čarman, Karmen Fifer Bizjak, Janez Hafner, Mitja Janža, Marko Komac, Drago Ocepek, Matevž Uroš Pavlič, Mojca Videnič, Renato Vidrih).

Izredni prof. dr. Miran Veselič se je rodil 6.11.1946 v Mariboru. V Ljubljani je obiskoval II. gimnazijo, na kateri je tudi maturiral. Po končanem srednješolskem izobraževanju se je vpisal na Oddelek za geologijo takratne Fakultete za naravoslovje in tehnologijo, ki ga je obiskoval v letih 1966 do 1972. Študij geologije je zaključil z diplomsko nalogo z naslovom »Hidrogeologija akumulacijskega bazena Završnica«. Po diplomi se je zaposlil na Geološkem zavodu Ljubljana na Oddelku za inženirsko geologijo in hidrogeologijo, ki je deloval v okviru organizacijske enote Geologija, geotehnika in geofizika. Na svojem prvem delovnem mestu je nadaljeval z delom na področju hidrogeologije, ki ga je pritegnila že kot študenta. To je v prihodnosti postalo tudi glavno torišče njegovega strokovnega in znanstveno raziskovalnega dela. Želja po znanju ga je vodila na Univerzo v Bordeauxu I v Franciji, kjer je leta 1975 najprej magistriral s tezo posvečeno vodni bilanci in izračunu evapotranspiracije, leta 1978 pa je na isti univerzi še doktoriral s tezo posvečeno problematiki črpanja podzemne vode iz polzaprtih vodonosnikov.

Profesor Veselič je že na začetku svoje kariere prevzel številne strokovne naloge, tako je v času svoje zaposlitve v letih od 1974 do 1993 na Geološkem zavodu Ljubljana vodil številne projekte, med katere so sodili tako projekti usmerjeni v posamezne hidrogeološke ekspertize, kot tudi projekte velikega obsega, ki so terjali vključitev širokega spektra geologov, kot tudi drugih strokovnjakov. Njegovo dejavnost zaznamujejo številni elaborati in ekspertize. Med najpomembnejše strokovne prispevke k razvoju hidrogeologije ter izkoriščanju mineralnih surovin nedvoumno sodi obsežno in dolgoletno delo v Premogovniku Velenje, kjer je hidrogeološka problematika zelo izpostavljena. Sam in v sodelovanju s sodelavci v svojem strokovnem timu je razvil številne strokovne, tehnološke in ekonomske rešitve, ki so omogočile učinkovito in varno izkoriščanje premoga ter imele svoj odmev tudi izven meja. Pomembno področje njegovega delovanja je bila tudi geotermija, kjer je raziskoval tako v Sloveniji, kot tudi v Bosni in Srbiji. Leta 1993 se je za kratek čas zaposlil na Fakulteti za naravoslovje in tehnologjo, nato pa je leta 1994 prevzel vodenje takratnega Rudarskega inštituta Ljubljana, ki se je pod njegovim vodstvom preimenoval v Inštitut za rudarstvo, geotehnologijo in okolje – IRGO ter razširil področje svojega delovanja. Inštitut je vodil do leta 2002, ko je prevzel mesto direktorja Agencije za radioaktivne odpadke, ki jo je vodil do leta 2008. V času njegovega vodenja so bili uspešno izpeljani postopki umeščanja odlagališča nizko in srednje radioaktivnih odpadkov v prostor.

Tako kot je bilo pestro njegovo strokovno delo, je tudi v znanosti posegal na številna področja hidrogeologije. Svoje strokovno delo na področju geotermije in rudniške hidrogelogije je nadgradil tudi z znanstvenimi objavami. Poleg že navedenih tematik se je znanstveno ukvarjal še s problematiko upravljanja in zaščite vodnih virov ter s hidrogeologijo krasa. Samostojno in v soavtorstvu je napisal 26 znanstvenih člankov, 2 pregledna znanstvena članka, 5 poglavij v znanstvenih monografijah, številne strokovne članke, pogosto pa je na različnih znanstvenih in strokovnih dogodkih sodeloval kot vabljeni predavatelj. Pri pregledu dosežkov profesorja Veseliča ne moremo mimo dejstva, da je sodeloval v številnih strokovnih združenjih in da je bil dolgo vrsto let prvi predsednik

Slovenskega komiteja mednarodnega združenja hidrogeologov, v tem združenju pa je opravljal tudi pomembno funkcijo na mednarodnem nivoju. Prav tako je pomembno tudi njegovo predsedovanje Mednarodnemu združenju za rudniške vode, kjer mu je bil za njegove zasluge podeljen tudi naziv častni predsednik.

Profesor Veselič je predaval tako na Oddelku za geologijo, kot tudi na Oddelku za rudarstvo. Predaval je predmeta Hidrogeologija in Hidrodinamika v kamninah. Bil pa je tudi nosilec predmetov Metode hidrogeoloških raziskav in Dinamika podzemne vode na podiplomskem študiju. Pogosto je bil član komisij za zagovor doktoratov, tako na Univerzi v Ljubljani, kot tudi na tujih univerzah. Organiziral pa je tudi šole s področja hidrogeologije. V času svojega pedagoškega delovanja je bil mentor 24 diplomantom, 8 magistrantom (Mihael Brenčič, Barbara Čenčur Curk, Nina Mali, Andrej Lapanje, Metka Petrič, Joerg Prestor, Goran Vižintin, Vesna Zupanc) in mentor pri 4 doktorskih disertacijah (Mihael Brenčič, Barbara Čenčur Curk, Metka Petrič, Branka Trček). Poleg tega je opravil še številna delovna mentorstva mladim raziskovalcem ter mentorstva na strokovnem usposabljanju.

Profesor Veselič ostaja strokovno in znanstveno aktiven tudi po svoji upokojitvi, saj pri številnih projektih, na podlagi svojih bogatih izkušenj, sodeluje kot konzultant in recenzent.

Jubileju naših učiteljev je v posameznih sklopih posvečeno skupaj 14 člankov. V prvi številki Geologije so profesorju Pezdiču posvečeni trije članki. Avtorji Tjaša Kanduč, David Kocman in Timotej Verbovšek so prispevali članek z naslovom »Biogeokemija izbranih slovenskih rek (Kamniška Bistrica, Idrijca in Sava v Sloveniji): vpogled v rečno vodno geokemijo, stabilne izotope ogljika in snovne tokove preperevanja«. Jože Uhan je prispeval članek »Ranljivost podzemne vode glede na nitratno onesnaženje v aluvialnih vodonosnikih Slovenije – primer Spodnje Savinjske doline«. Avtorja Branka Trček in Albrecht Leis sta prispevala članek »Pregled izotopskih raziskav podzemne vode v razpoklinskem vodonosnem sistemu na območju Rogaške Slatine«. V prvi številki revije so jubileju profesorja Ribičiča posvetili članek »Retencijske lastnosti trdnih meljev« avtorji Barbara Likar, Vikica Kuk, Karmen Fifer Bizjak.

V sklop člankov posvečenih pomembnim življenskim obletnicam naših učiteljev sodijo še naslednji članki: Luka Gale, Uroš Novak, Teja Kolar Jurkovšek, Matija Križnar in France Stare: »Značaj okremenjene fosilne združbe zgornjekarnijskih amfiklinskih plasti pri Crngrobu (osrednja Slovenija)«; Rok Gašparič, Matija Križnar: »Spodnjemiocenska rakovica *Retropluma slovenica* Gašparič & Hyžný, 2014 iz govških plasti Tunjiškega gričevja«; Matija Križnar, Davo Preisinger: »Novo najdišče pleistocenske sesalske favne v kamnolomu pri Črnem Kalu (Primorska, Slovenija) ter problematika zaščite in ohranjanja najdišč v kamnolomih«.

V drugi številki 60. letnika Geologije bodo izšli članki posvečeni vsem štirim slavljencem. Profesorju Veseliču bodo posvečeni članki: Mihael Brenčič, Teja Keršmanc: »Hidrogeološke razmere na poplavni ravnici – primer reke Mure pri Hrastju Mota (SE Slovenija)«; Metka Petrič: »Študij dinamike toka vode v kraškem vodonosniku z metodami sledenj z naravnimi in umetnimi sledili: primer kraških izvirov Malenščica in Unica«; in Branka Trček: »Uporaba naravnih sledil za študij drenažnega sistema nezasičene cone vodonosnika Ljubljanskega polja«. Profesorju Šušteršiču bosta posvečena članka Marko Vrabec, Galena Jordanova: »Analiza sistematične razpokanosti eocenskih flišnih kamnin Slovenske obale«; in Mihael Brenčič, Mateja Jelovčan, Teja Keršmanc: »Poplavljanje Planinskega polja – izboljšani katalog poplavnih dogodkov«. Profesorju Ribičiču bo posvečen članek Marko Komac, Matevž Pavlič: »Nadgradnja ploskovnega erozijskega modela z območji erozije v strugah – primer občine Bohinj«. Profesorju Pezdiču bo posvečen članek Miloš Markič: »Visoka vsebnost arzena (As) v premoški snovi iz neogenskih sedimentov Panonskega bazena na območju Slovenije«.

Avtorji prispevkov, gostujoči uredniki člankov posvečenih jubilantov, kakor tudi vsi ostali kolegi želimo slavljencem še naprej uspešno in ustvarjalno znanstveno, raziskovalno in strokovno delo. Pričujoči članki pa naj predstavljajo skromno zahvalo za ves trud vložen v izobraževanje na področju geologije, kakor tudi za prispevek k razvoju stroke v najširšem pomenu.

Mihael Brenčič, Barbara Čenčur Curk, Luka Gale, Timotej Verbovšek
(gostujoči uredniki)

GEOLOGIJA 60/1, 9-26, Ljubljana 2017

https://doi.org/10.5474/geologija.2017.001

Biogeochemistry of some selected Slovenian rivers (Kamniška Bistrica, Idrijca and Sava in Slovenia): insights into river water geochemistry, stable carbon isotopes and weathering material flows

Biogeokemija izbranih slovenskih rek (Kamniška Bistrica, Idrijca in Sava v Sloveniji): vpogled v rečno vodno geokemijo, stabilne izotope ogljika in snovne tokove preperevanja

Tjaša KANDUČ[1], David KOCMAN[1] & Timotej VERBOVŠEK[2]

[1]Jožef Stefan Institute, Department of Environmental Sciences, Jamova cesta 39, SI-1000 Ljubljana, Slovenia; e-mail: tjasa.kanduc@ijs.si
[2]Department of Geology, Faculty of Natural Sciences and Engineering, University of Ljubljana, Privoz 11, SI-1000 Ljubljana, Slovenia;

Prejeto / Received 19. 10. 2016; Sprejeto / Accepted 23. 5. 2017; Objavljeno na spletu / Published online 9.6.2017

Dedicated to Professor Jože Pezdič on the occasion of his 70th birthday

Key words: water geochemistry, biogeochemistry, carbon stable isotopes, weathering fluxes, rivers
Ključne besede: vodna geokemija, biogeokemija, stabilni izotopi ogljika, snovni tokovi, reke

Abstract

Review of biogeochemical processes studied in three Slovenian rivers (River Kamniška Bistrica, River Sava in Slovenia and River Idrijca), which represent an ideal natural laboratory for studying biogeochemical processes and anthropogenic impacts in catchments with high weathering capacity is presented. The River Kamniška Bistrica, the River Sava in Slovenia and the River Idrijca water chemistry is dominated by HCO_3^-, Ca^{2+} and Mg^{2+}, and Ca^{2+}/Mg^{2+} molar ratios indicate that calcite/dolomite weathering is the major source of ions to the river system. The Kamniška Bistrica River, the River Sava and River Idrijca and its tributaries are oversaturated with respect to calcite and dolomite. pCO_2 concentrations were on average up to 25 times over atmospheric values for River Kamniška Bistrica, 20 times for River Sava and 13 times over atmospheric values for River Idrijca. $\delta^{13}C_{DIC}$ values ranged from -12.7 to -2.7 ‰ in River Kamniška Bistrica, from -12.7 to -6.3 ‰ in River Sava in Slovenia, from -10.8 to -6.6 ‰ in River Idrijca, respectively. In all investigated rivers we found out that carbonate dissolution is the most important biogeochemical process affecting carbon isotopes in the upstream portions of the catchment, while carbonate dissolution and organic matter degradation control carbon isotope signatures downstream, except for River Idrijca where both processes contribute equally from source to outflow to River Soča.

Izvleček

Predstavljen je pregled biogeokemisjkih procesov, ki smo jih preučevali v treh slovenskih rekah (Kamniška Bistrica, Sava v Sloveniji in Idrijci) in predstavljajo idealen naravni laboratorij za študij biogeokemisjkih procesov in antropogenih vplivov v porečjih z visoko intenzivnostjo preperevanja. Vodna geokemija Kamniške Bistrice, Save v Sloveniji in Idrijce je dominirana s HCO_3^-, Ca^{2+} in Mg^{2+} ter Ca^{2+}/Mg^{2+} molarnim razmerjem in kaže da je kalcitno/dolomitno preperevanje glavni vir ionov v rečnem sistemu. Kamniška Bistrica, reka Sava v Sloveniji in Idrijca ter njeni pritoki so prenasičeni glede na kalcit in dolomit. Koncentracije pCO_2 so v povprečju 25 krat nad atmosferskimi vrednostmi v Kamniški Bistrici, 20 krat nad atmosferskim v reki Savi v Sloveniji ter 13 krat v reki Idrijci. $\delta^{13}C_{DIC}$ vrednosti se v Kamniški Bistrici spreminjajo od -12,7 do -2,7 ‰, od -12,7 do -6,3 ‰ v reki Savi v Sloveniji in od 10,8 do -6,6 ‰ v reki Idrijci. V vseh raziskanih rekah je raztapljanje karbonatov najpomembnejši biogeokemijski proces, ki vpliva na izotopsko sestavo ogljika v zgornjem delu porečja, medtem ko raztapljanje karbonatov in razgradnja organske snovi kontrolirata izotopsko sestavo ogljika v spodnjem delu porečja, razen v reki Idrijci, kjer oba procesa vplivata enako od izvira do izliva v reko Sočo.

Introduction

Systematic studies of river water geochemistry provide important information on chemical weathering of bedrock/soil and natural and anthropogenic processes that may control the dissolved chemical loads (Schulte et al., 2011; Gibbs, 1972; Reeder et al., 1972; Huh et al., 1998; Négrel & Lachassagne, 2000). Since carbonate weathering largely dominates the water chemistry of river waters, characterization of rivers draining carbonate-dominated terrain is crucial to precisely identify the various contributions of the different sources of water solutes, and to estimate the weathering fluxes of the continental crust and associated CO_2 consumption (Liu & Zhao, 2000).

Freshwaters cover small fraction of the Earth's surface area, inland freshwater ecosystems (particularly lakes, rivers and reservoirs) have rarely been considered as potentially important quantitative components of the carbon cycle at either global or regional scales (Cole et al., 2007). Rivers are the major pathways for the transport of carbon (C) from the continents top the oceans. Global river carbon fluxes are estimated to be 0.4 Pg C/year of organic C (evenly divided between particulate and dissolved phases) and 0.4 Pg C/year for dissolved inorganic carbon (DIC). Bulk fluxes are small components of the global C cycle but are significant compared to net oceanic uptake of anthropogenic CO_2 (Sarmiento & Sundquist, 1992).

Concentrations of DIC and its isotopic composition of dissolved inorganic carbon ($\delta^{13}C_{DIC}$) are governed by processes occurring in the river system and vary seasonally. Changes of DIC concentrations result from carbon addition or removal from the DIC pool, while changes of its isotopic composition result from the fractionation accompanying transformation of carbon or mixing of carbon from different sources (Atekwana & Krishnamurthy, 1998). The major sources of carbon to riverine DIC loads are dissolution of carbonate minerals, soil CO_2 derived from root respiration and from microbial decomposition of organic matter and exchange with atmospheric CO_2. The major processes removing riverine DIC are carbonate mineral precipitation, CO_2 degassing, and aquatic photosynthesis (Atekwana & Krishnamurthy, 1998). Rivers in Slovenia represents an "ideal natural laboratory" for studying biogeochemical processes and tracing the riverine carbon cycle as a result of its geologically heterogeneous composition, relatively high specific discharge, and limited aquatic photosynthesis (Germ et al., 1999).

The relative contributions of C3 and C4 vegetation to an ecosystem can be reconstructed using the isotopic composition of particulate organic carbon (POC, e.g. $\delta^{13}C_{POC}$), because of their different isotopic composition, which ranges from -32.0 to -20.0 ‰ for C3 plants and from -15.0 to -9.0 ‰ for C4 plants (Deines, 1980). Vegetation of the River Sava watershed in Slovenia is described in detail in Kanduč et al. (2007) and references therein. Detail evaluation of some selected sites of River Sava watershed was described with aquatic moss *Fontinalis antipyretica* (Mechora & Kanduč, 2016). Hydrogeochemical and isotopic characterization of River Pesnica, Slovenia was described in detail in Kanduč et al. (2016).

Application of stable isotopes and biogeochemical processes in environmental studies is presented in Pezdič (1999). In this study we represent summary (review) of biogeochemical research with application of stable isotope analysis of river systems; three rivers were subject of investigation during years 2004–2011 in different time related to national research projects and program founding P1-0143 in Slovenia: River Kamniška Bistrica (Kanduč et al., 2013), River Sava in Slovenia (Kanduč et al., 2007) and River Idrijca (Kanduč et al., 2008) presented in the Figures 1 and 2.

Study area

Catchment and hydrological characteristics of gravel bed rivers

River Kamniška Bistrica is the left tributary of the River Sava, which is the largest river in Slovenia (Figs. 1 and 2). Kamniška Bistrica emerges at the southern foothills of Kamnik-Savinja Alps at 630 m a.s.l. elevation. The river is 32.8 km long and drains an area of 380 km^2, with an average discharge of 15.4 m^3/s at its confluence with River Sava. The average discharge at the mouth of the River Kamniška Bistrica measured during this study was 0.7-12.1 m^3/s. According to discharge regimes of all rivers and streams in Slovenia, River Kamniška Bistrica has an alpine high mountain snow-rain regime (Hrvatin, 1998). The maximum discharge occurs in autumn (November) and spring (May) and minimum occurs in summer (August) and winter (February). Major

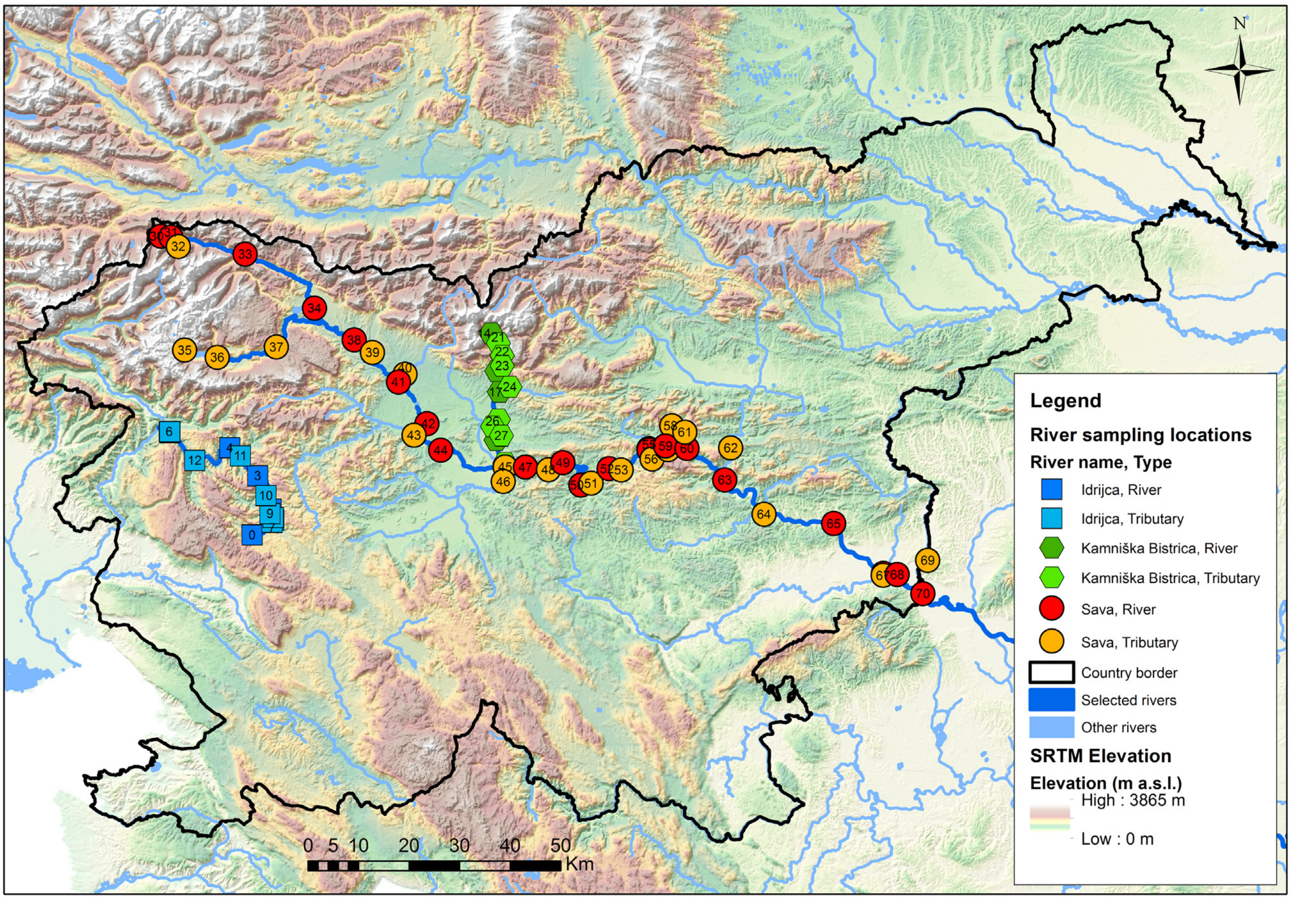

Fig. 1. General topographic map of the major river network in Slovenia, with a detailed location map of the numbered sampling sites for the rivers Kamniška Bistrica, Sava (Slovenian part) and Idrijca. Digital elevation model (DEM) was obtained from the Shuttle Radar Topography Mission (SRTM) dataset (Internet 1). Numbers correspond to the sampling points IDs (see Tables 1 and 2).

tributaries of the River Kamniška Bistrica are the Črna and Nevljica rivers on the left and River Pšata on the right. In the upper reaches, from the headwater spring to Stahovica (at the confluence with River Črna), River Kamniška Bistrica changes over a short distance (6.8 km downstream) from a clean alpine river to industrially and agriculturally affected river at the confluence with the tributary River Črna, which carries sediments and waste waters from the abandoned Črna kaolin mine (Radinja et al., 1987).

Discharge regimes of the River Sava are controlled by precipitation and the configuration of the landscape. In the upper part of the River Sava a snow-rain regime prevails and in the central and lower part a rain-snow regime (Hrvatin, 1998). Annual discharge maxima are characteristic in spring and late summer, while discharge minima occur in the summer and winter months. The mean annual long term discharge (from the years 1960–1991) for the gauging stations increases from 17 m^3/s of the upper section of the River Sava at Radovljica (location 35, Table 1, Fig. 1) to 182 m^3/s of the central section at Hrastnik (location 60, Table 1, Fig. 1) and to 290 m^3/s in the lower section of the river at Čatež (location 68, Table 1, Fig. 1) (Internet 2). Discharges are also controlled by hydropower outflows along the Sava River. The discharge conditions for the River Sava and its tributaries during the study ranged from 2 to 344 m^3/s during spring 2004, from 1 to 144 m^3/s during late summer 2004, and from 0.3 to 128 m^3/s during winter, respectively. The River Idrijca joins the River Soča in the middle stretch at the village of Most na Soči. Both rivers have torrential characteristics. Detail description of the Idrijca catchment is described in Kanduč et al. (2008). High peaks and steep mountain slopes prevent air circulation in the valley and induce severe erosion. Characteristic long-term discharge data (from the years 1949 to 2015) according to the Slovenian Environment Agency for the gauging station on the Idrijca at Hotešk, which is located above the confluence with the River Soča, are as follows: low long-term discharge varies from 3.4 to 8.5 m^3/s, mean long-term discharge varies from 14.3 to 39 m^3/s, and high long-term discharge varies from 113 to 644 m^3/s (Internet 2).

General geological setting of selected river watersheds

This chapter summarizes the general geological setting of the river watershed areas, as the geological composition of each river basin is very complex (Fig. 1). Therefore, the prevailing geological units are described below. Detailed general description of geological setting of investigated Slovenian rivers is described in detail in Kanduč et al. (2007, 2008 and 2013).

River Kamniška Bistrica. The upper part of the River Kamniška Bistrica is underlain by massive and stratified limestone and dolomite of middle and upper Triassic age (Fig. 2), and carbonates generally prevail in the watershed. The middle part of the river is underlain by marlstone and limestone of Miocene age (Buser, 1987). The lower reaches of the River Kamniška Bistrica, along the right bank and before the confluence with the River Sava, is underlain by Pleistocene and Holocene age gravels, while the left bank is underlain by Permo-Carboniferous shales with a cover of Quaternary gravel. The River Kamniška Bistrica is also one of the Slovenian watersheds identified as having a high weathering capacity, due to the predominance of carbonate bedrock and high relief and precipitation (Kanduč et al., 2013).

River Sava in Slovenia. The valley of the Sava River extends in a NW-SE direction comprising almost half the surface area of Slovenia and has a very heterogeneous geological composition. Both branches of the Sava River (Sava Bohinjka and Sava Dolinka rivers) emerge in the Julian Alps, composed mostly of Triassic limestones and dolomites. Leaving the Alps approximately at the confluence of the Sava Bohinjka and Sava Dolinka rivers, river then flows on the Holocene and Pleistocene fluvioglacial sediments (terraces) (Žlebnik, 1971). Eastwards from the city of Ljubljana, the watershed in Sava folds is mainly composed of Permo-Carbonian clastic sediments, which alternate with some Triassic carbonates, with Miocene sandstones, clays and gravels in some of the valleys. Leaving the Sava folds, the watershed in the Krško-Brežice area mainly consists of terraced Holocene and Pleistocene sediments - sands and gravels. The catchments of the River Sava's tributaries are composed of Triassic and Jurassic carbonates, Permo-Carbonian sandstones and siltstones, Oligocene clay and volcanic rocks, Miocene clastic rocks and Pleistocene sediments (Buser, 1987).

River Idrijca. The beds in the upper part of the River Idrijca are composed of various sedimentary and volcanic rocks, predominantly massive and stratified Triassic limestones and dolomites. Along Idrijca, Middle Permian mica quartz sandstone and red sandstone with conglomerate are exposed as the oldest rocks. In the lower part of the flow, before the confluence with the River Soča, stratified and massive Upper Triassic dolomites and Cretaceous limestones with marls appear (Buser, 1987). In general, the Idrija region has a very complex tectonic structure (Mlakar & Čar 2009; Čar, 2010) with several major faults dissecting the area and tectonic nappes overlying several units.

Materials and methods

Sampling and used methods

Surface water sampling locations (Fig. 1, Tables 1 and 2) were selected based on their relationship to confluence of the major and minor streams, typically sampled before and after the confluence. Sampling of river water and tributaries was performed at different sampling seasons according to discharge regimes (Hrvatin, 1998; Fratar, 2005). Temperature, conductivity, dissolved oxygen (DO), and pH measurements were performed in the field. The precision of dissolved oxygen saturation and conductivity measurements was ±5 %. The field pH was determined on the NBS scale using two buffer calibrations with reproducibility of ±0.02 pH unit. Total alkalinity was measured within 24h of sample collection by Gran titration (Gieskes, 1974) with a precision of ±1%. Carbonate rocks from hinterland of river watershed were ground to powder in an agate mortar and then approximately 2 mg of sample was first flushed with He and then transformed to CO_2 by H_3PO_4 acid treatment. NBS 18 and NBS 19 were used as reference materials. The isotopic composition of carbonate ($\delta^{13}C_{CaCO3}$) was measured with a Europa Scientific 20-20 continuous flow IRMS ANCA-TG preparation module. All methods are described in detail in Kanduč et al. (2007, 2008 and 2013).

All stable isotope results for carbon are expressed in the conventional delta (δ) notation, defined as per mil (‰) deviation from the reference standards VPDB. Precision was ±0.2 ‰ for $\delta^{13}C_{DIC}$, $\delta^{13}C_{POC}$ and $\delta^{13}C_{CaCO3}$.

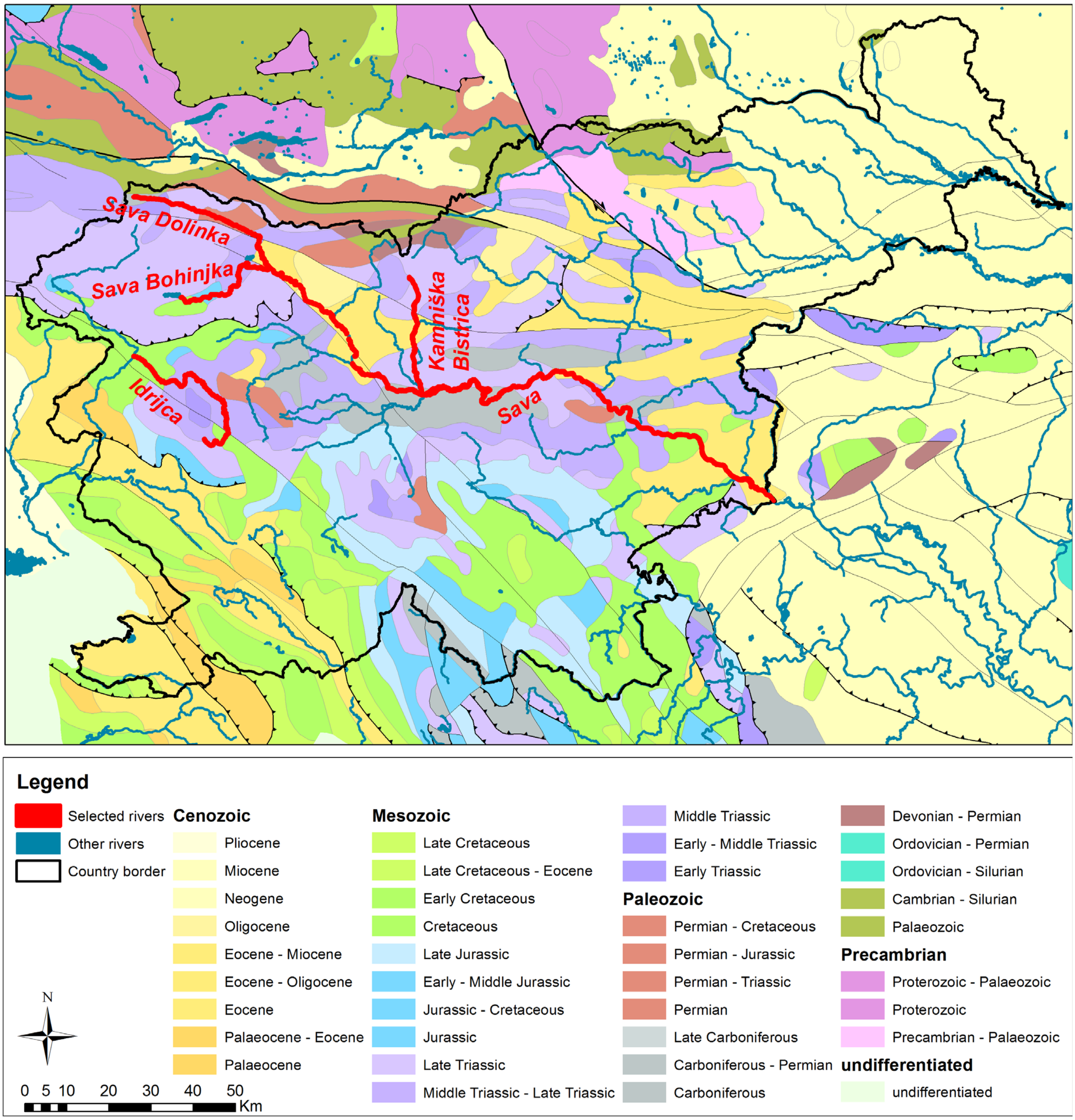

Fig. 2. General geological map of Slovenia with selected three rivers: Kamniška Bistrica, Sava in Slovenia and Idrijca. Geological data were obtained from the 1: 5 Million International Geological Map of Europe and Adjacent Areas (IGME 5000) dataset (Internet 3).

Major and minor cation chemistry was measured by inductively coupled plasma optical emission spectroscopy (ICP-OES) technique. The precision of the method was ±2% for major (Ca^{2+}, Mg^{2+}, Na^{+} and K^{+}) and ±5% for minor elements (Sr and Si). The stable isotope composition of dissolved inorganic carbon ($\delta^{13}C_{DIC}$) was determined with a Europa Scientific 20-20 continuous flow IRMS ANCA-TG preparation module. Phosphoric acid (H_3PO_4, 100 %) was added (100-200 µl) to a septum-sealed vial which was then purged with pure He. The water sample (6 mL) was injected into a septum tube and headspace CO_2 was measured (modified after Miyajima et al., 1995; Spötl, 2005). In order to determine the optimal extraction procedure for surface water samples, a standard solution of Na_2CO_3 (Carlo Erba) with a known $\delta^{13}C_{DIC}$ of -10.8 ‰ ± 0.2 ‰ was prepared with a concentration of either 4.8 mol/L (for samples with alkalinity above 2 mmol/L) or of 2.4 mmol/L (for samples with alkalinity below 2 mmol/L). The carbon stable isotope composition of particulate organic carbon ($\delta^{13}C_{POC}$) was determined with a

Table 1. Sampling locations and geochemical data for spring sampling season (sampling years: Idrijca: 2006-2007, Kamniška Bistrica: 2010-2011, Sava: 2004-2005). ID numbers correspond to the locations in Figure 1.

ID	Name	River	Type	LAT (°)	LON (°)	Z (m)	T (°C)	pH (-)	Alkal. mmol/L	EC (μS/cm)	Ca^{2+} mmol/L	Mg^{2+} mmol/L	Na^{+} mmol/L	K^{+} mmol/L	Si mmol/L	SO_4^{2-} mmol/L	Cl^{-} mmol/L	NO_3^{-} mmol/L	pCO_2 (bar)	$SI_{calcite}$ (-)	$SI_{dolomite}$ (-)	$\delta^{13}C_{DIC}$ (‰)
0	Idrijca	Confluence Idrijca/Belca	River	45.963396	13.981281	389	9.00	8.43	4.12	333.0	0.82	0.74	0.05	0.00	0.00	0.04	0.03	0.06	-3.14	0.66	1.17	-9.4
1	Idrijca	Podroteja	River	45.990652	14.035864	325	7.30	7.92	4.20	353.0	0.93	0.75	0.07	0.00	0.00	0.05	0.07	0.09	-2.62	0.20	0.16	-10.6
2	Idrijca	Kolektor	River	46.009519	14.028858	316	10.8	8.43	4.33	367.0	1.15	0.87	0.11	0.05	0.02	0.11	0.10	0.05	-3.12	0.84	1.48	-10.1
3	Idrijca	Travnik	River	46.068869	13.993716	267	11.4	8.44	4.43	485.0	1.00	1.22	0.10	0.02	0.02	0.72	0.10	0.05	-3.12	0.80	1.62	-9.2
4	Idrijca	Kozarska grapa	River	46.117877	13.921682	227	11.7	8.29	4.26	416.0	1.01	0.89	0.11	0.02	0.03	0.36	0.11	0.04	-2.97	0.66	1.21	-9.3
5	Idrijca	Before Bača	River	46.143312	13.767604	153	13.0	8.82	4.27	383.0	1.16	0.85	0.10	0.05	0.00	0.00	0.00	0.47	-3.53	1.22	2.27	-8.4
6	Idrijca	After Bača	River	46.144954	13.765608	152	12.7	8.77	4.20	356.0	1.15	0.84	0.11	0.05	0.02	0.00	0.00	0.05	-3.48	1.16	2.15	-8.3
7	Idrijca	Zala	Tributary	45.986561	14.031768	328	10.6	8.09	4.87	420.0	1.27	0.98	0.17	0.04	0.03	0.07	0.15	0.06	-2.72	0.60	1.00	-9.7
8	Idrijca	Ljubevšča	Tributary	45.995142	14.034411	325	10.2	8.54	5.04	444.0	1.32	1.05	0.30	0.05	0.07	0.10	0.29	0.05	-3.17	1.04	1.90	-9.6
9	Idrijca	Nikova	Tributary	46.00197	14.026078	325	10.1	8.67	4.81	418.0	1.31	0.91	0.20	0.06	0.04	0.10	0.13	0.04	-3.33	1.14	2.03	-9.4
10	Idrijca	Kanomljica	Tributary	46.033902	14.015139	302	10.8	8.29	4.33	368.0	1.23	0.87	0.08	0.05	0.04	0.15	0.00	0.04	-2.93	0.78	1.32	-9.4
11	Idrijca	Cerknica	Tributary	46.103916	13.948576	245	11.8	8.35	3.52	349.0	1.25	0.47	0.19	0.06	0.10	0.19	0.12	0.02	-3.12	0.75	1.00	-7.6
12	Idrijca	Trebuščica	Tributary	46.094549	13.832344	188	11.6	8.37	4.01	181.0	1.00	0.85	0.06	0.04	0.02	0.05	0.03	0.05	-3.08	0.71	1.29	-8.0
13	Idrijca	Bača	Tributary	46.144888	13.767263	154	12.2	8.37	3.15	282.0	1.18	0.32	0.08	0.05	0.07	0.08	0.00	0.05	-3.21	0.74	0.86	-6.9
14	Kamniška Bistrica	Spring	River	46.3257344	14.58846446	623	5.70	8.29	1.55	188.5	0.70	0.18	0.04	0.00	0.00	0.01	0.00	0.03	-3.42	0.04	-0.68	-2.7
15	Kamniška Bistrica	before Stahovica	River	46.28567753	14.61692482	530	7.10	8.40	2.33	194.0	0.80	0.24	0.03	0.00	0.01	0.02	0.01	0.04	-3.36	0.39	0.10	-5.0
16	Kamniška Bistrica	after Stahovica	River	46.25867675	14.60364769	450	7.70	8.63	2.38	198.6	0.90	0.27	0.05	0.00	0.01	0.03	0.03	0.04	-3.60	0.64	0.62	-5.6
17	Kamniška Bistrica	Kamnik	River	46.2215134	14.61034338	378	10.6	8.61	2.86	238.4	1.04	0.33	0.11	0.01	0.02	0.03	0.06	0.04	-3.54	0.80	0.97	-7.4
18	Kamniška Bistrica	Vir	River	46.14710269	14.60453603	310	14.6	8.73	2.82	239.3	1.04	0.32	0.09	0.01	0.02	0.01	0.03	0.02	-3.59	0.98	1.45	-6.9
19	Kamniška Bistrica	Domžale	River	46.13584974	14.60277837	300	9.50	8.54	3.35	282.7	1.20	0.42	0.21	0.02	0.03	0.06	0.16	0.04	-3.34	0.85	1.15	-7.3
20	Kamniška Bistrica	Videm	River	46.08835696	14.62594168	260	12.5	8.34	4.39	368.3	1.50	0.50	0.38	0.05	0.05	0.04	0.16	0.11	-3.01	0.91	1.36	-9.6
21	Kamniška Bistrica	Dolski Graben	Tributary	46.30851523	14.60699003	570	7.80	8.15	2.92	239.7	1.21	0.18	0.05	0.00	0.35	0.03	0.02	0.05	-3.00	0.41	-0.13	-9.8
22	Kamniška Bistrica	Bistričica	Tributary	46.28606501	14.61710383	470	9.90	8.49	3.79	317.1	1.17	0.66	0.13	0.02	0.06	0.08	0.06	0.05	-3.25	0.85	1.36	-8.7
23	Kamniška Bistrica	Črna	Tributary	46.26802869	14.61710383	470	8.70	8.47	2.72	291.0	1.12	0.50	0.24	0.02	0.06	0.08	0.22	0.05	-3.36	0.66	0.86	-8.7
24	Kamniška Bistrica	Nevljica	Tributary	46.23068024	14.63750483	460	10.4	8.42	4.53	358.4	1.72	0.43	0.18	0.02	0.07	0.11	0.11	0.05	-3.07	0.99	1.28	-11.0
25	Kamniška Bistrica	Radomeljska Mlinščica	Tributary	46.17251455	14.60803291	340	8.90	8.54	2.91	234.0	1.05	0.32	0.11	0.01	0.02	0.04	0.07	0.04	-3.40	0.74	0.85	-7.10
26	Kamniška Bistrica	Pšata	Tributary	46.16032599	14.59330627	338	16.1	8.34	4.25	409.4	1.20	0.35	0.24	0.04	0.04	0.09	0.23	0.22	-2.96	0.82	1.11	-10.5
27	Kamniška Bistrica	Rača	Tributary	46.14401047	14.61606564	310	13.5	8.38	4.33	390.3	0.60	0.38	0.21	0.02	0.03	0.09	0.41	0.05	-3.04	0.59	0.96	-10.7
28	Kamniška Bistrica	Homška Mlinščica	Tributary	46.09543708	14.62563539	290	10.5	8.61	3.09	243.9	1.05	0.33	0.19	0.01	0.02	0.05	0.17	0.05	-3.43	0.85	1.12	-6.9
29	Kamniška Bistrica	Pšata channel	Tributary	46.08835696	14.62594168	280	9.80	8.38	3.58	327.1	1.40	0.41	0.22	0.04	0.08	0.08	0.16	0.09	-3.15	0.80	0.96	-10.9
30	Sava	Sava Dolinka, spring	River	46.49238108	13.73738958	830	8.60	7.83	2.98	276.0	1.02	0.52	0.05	0.00	0.03	0.06	0.00	0.03	-2.67	0.04	-0.34	-10.7
31	Sava	Sava Dolinka, Podkoren	River	46.4910896	13.76249572	829	8.90	8.14	2.62	244.0	0.00	0.00				0.10	0.15	0.02	-3.80			-10.3
32	Sava	Pišnica at Kranjska gora	Tributary	46.47464479	13.78197234	819	7.60	8.36	2.37	216.0	0.82	0.44	0.07	0.00	0.01	0.07	0.00	0.04	-3.31	0.36	0.31	-7.9
33	Sava	Sava Dolinka, Dovje	River	46.46265059	13.95393196	704	9.70	8.28	2.81	251.0	1.00	0.53	0.07	0.00	0.03	0.13	0.00	0.03	-3.15	0.45	0.54	-8.6
34	Sava	Sava Dolinka, Šobec	River	46.36797849	14.13464505	459	9.70	8.48	3.19	283.0	1.12	0.43	0.09	0.00	0.02	0.15	0.00	0.04	-3.30	0.75	0.98	-9.6

ID	Name	River	Type	LAT (°)	LON (°)	Z (m)	T (°C)	pH (-)	Alkal. mmol/L	EC (µS/cm)	Ca^{2+} mmol/L	Mg^{2+} mmol/L	Na^{+} mmol/L	K^{+} mmol/L	Si mmol/L	SO_4^{2-} mmol/L	Cl^{-} mmol/L	NO_3^{-} mmol/L	pCO_2 (bar)	$SI_{calcite}$ (-)	$SI_{dolomite}$ (-)	$\delta^{13}C_{DIC}$ (‰)
35	Sava	River Savica	Tributary	46.29039117	13.80250167	700	6.20	8.32	2.00	172.3	0.76	0.18	0.01	0.00	0.01	0.03	0.00	0.04	-3.34	0.21	-0.37	-5.8
36	Sava	Lake Bohinj, outlet	Tributary	46.278398	13.8863417	557	12.3	8.26	2.35	201.0	0.90	0.20	0.05	0.00	0.01	0.04	0.00	0.04	-3.19	0.38	0.06	-8.3
37	Sava	Sava Bohinjka, Nomenj	Tributary	46.29801526	14.03757249	509	9.50	8.43	2.30	203.0	1.01	0.19	0.03	0.00	0.01	0.04	0.03	0.04	-3.39	0.54	0.26	-9.1
38	Sava	Sava Otočec	River	46.31216997	14.23744784	415	10.3	8.57	2.91	254.0	1.10	0.33	0.07	0.00	0.02	0.09	0.00	0.04	-3.43	0.80	0.99	-9.0
39	Sava	Tržiška Bistrica, Bistrica	Tributary	46.29011458	14.28442503	422	11.0	8.95	2.60	277.0	1.22	0.44	0.09	0.00	0.03	0.36	0.00	0.04	-3.89	1.12	1.73	-6.8
40	Sava	Kokra, Kranj	Tributary	46.25204699	14.36869104	407	12.1	8.10	2.64	264.0	1.08	0.43	0.07	0.00	0.02	0.19	0.00	0.04	-2.98	0.33	0.20	-7.0
41	Sava	Sava, Kranj	River	46.23782813	14.35202318	350	10.5	8.59	2.89	246.0	1.15	0.35	0.08	0.01	0.02	0.12	0.08	0.05	-3.45	0.83	1.07	-9.5
42	Sava	Sava, Smlednik	River	46.16419816	14.42555633	336	10.6	8.42	2.79	305.0	1.18	0.38	0.13	0.03	0.02	0.14	0.00	0.06	-3.29	0.67	0.76	-10.2
43	Sava	Sora, Ladja	Tributary	46.14358732	14.39285266	313	10.2	8.37	2.48	260.0	0.93	0.43	0.12	0.01	0.05	0.12	0.00	0.09	-3.29	0.48	0.52	-11.2
44	Sava	Sava, Tacen	River	46.11722401	14.46118304	280	10.4	8.43	3.16	302.0	1.15	0.39	0.10	0.00	0.03	0.14	0.00	0.07	-3.25	0.72	0.88	-10.7
45	Sava	Kamniška Bistrica, Beričevo	Tributary	46.08842291	14.62648002	260	11.2	8.17	3.90	381.0	1.42	0.46	0.35	0.03	0.04	0.17	0.00	0.21	-2.89	0.64	0.72	-12.4
46	Sava	Ljubljanica, Zalog	Tributary	46.06220617	14.62169268	267	10.9	8.10	4.01	391.0	1.47	0.50	0.17	0.00	0.03				-2.81	0.60	0.67	-13.5
47	Sava	Sava, Dolsko	River	46.08799496	14.67835027	265	10.9	8.23	3.27	338.0	1.36	0.45	0.17	0.00	0.03	0.15	0.00	0.10	-3.03	0.61	0.66	-12.7
48	Sava	Jevnica, Jevnica	Tributary	46.08360965	14.73719533	240	13.0	7.79	0.39	62.3	0.15	0.08	0.13	0.03	0.16	0.07	0.07	0.03	-3.47	-1.56	-3.46	-8.1
49	Sava	Sava, Kresnice	River	46.09632929	14.77395623	235	11.1	8.20	3.60	324.0	1.33	0.45	0.17	0.01	0.03	0.14	0.00	0.09	-2.56	0.61	0.68	-12.5
50	Sava	Sava, Litija	River	46.05646171	14.82051447	230	12.1	8.27	3.28	323.0	1.34	0.45	0.16	0.00	0.03	0.15	0.00	0.12	-3.06	0.66	0.79	-12.3
51	Sava	Reka pri Bregu, Litija	Tributary	46.05962086	14.84614684	245	13.4	8.18	2.59	272.0	0.80	0.62	0.17	0.03	0.11	0.14	0.00	0.08	-3.05	0.29	0.43	-13.2
52	Sava	Sava, Log	River	46.08563083	14.89206999	230	11.2	8.18	3.00	344.0	1.26	0.45	0.15	0.01	0.03	0.14	0.16	0.09	-3.01	0.50	0.98	-12.0
53	Sava	Polšnik, Sava	Tributary	46.08337901	14.92308091	260	8.40	8.17	1.87	208.0	0.57	0.45	0.15	0.03	0.14	0.15	0.09	0.03	-3.21	-0.06	-0.36	-11.6
54	Sava	Medija, Zagorje	Tributary	46.12125638	14.99434953	240	8.70	8.16	4.15	491.0	1.64	0.76	0.29	0.05	0.10	0.38	0.00	0.12	-2.87	0.66	0.87	-13.0
55	Sava	Sava, Zagorje	River	46.11889003	14.99455671	225	10.4	8.10	3.32	380.0	1.34	0.48	0.17	0.00	0.03	0.16	0.17	0.10	-2.89	0.48	0.41	-11.0
56	Sava	Šklendrovec, Zagorje	Tributary	46.10301833	15.00215046	350	8.70	8.34	4.26	424.0	1.48	0.91	0.15	0.01	0.05	0.25	0.16	0.05	-3.04	0.80	1.28	-12.4
57	Sava	Mitovšica, Trbovlje	Tributary	46.11971806	15.04299911	350	8.40	8.19	3.34	318.0	1.57	0.34	0.03	0.00	0.03	0.17	0.05	0.08	-2.99	0.60	0.41	-12.6
58	Sava	Trboveljščica, Trbovlje	Tributary	46.16192117	15.05268008	230	10.1	8.31	3.56	389.0	0.91	0.76	0.39	0.04	0.12	0.28	0.01	0.11	-3.08	0.53	0.89	-10.5
59	Sava	Sava, Trbovlje	River	46.12621671	15.03632723	220	10.7	8.08	3.57	395.0	1.37	0.49	0.20	0.01	0.03	0.21	0.18	0.10	-2.84	0.50	0.46	-11.5
60	Sava	Sava, Hrastnik	River	46.12155113	15.0916258	210	10.8	8.08	3.38	349.0	1.32	0.47	0.18	0.01	0.02	0.16	0.17	0.10	-2.86	0.46	0.39	-11.5
61	Sava	Boben, Hrastnik	Tributary	46.15057264	15.08592694	220	11.0	8.10	4.48	573.0						1.13	0.21	0.15	-2.74			-9.5
62	Sava	Savinja, Rimske Toplice	Tributary	46.12262895	15.20328147	200	14.4	8.98	3.04	375.0	1.30	0.43	0.32	0.03	0.03	0.30	0.00	0.12	-3.85	1.27	2.06	-8.5
63	Sava	Sava, Radeče	River	46.06552039	15.18817906	193	11.6	8.10	3.66	375.0	1.34	0.47	0.20	0.02	0.03	0.19	0.00	0.10	-2.84	0.53	0.54	-11.1
64	Sava	Mirna, Dol Bostanj	Tributary	46.0042524	15.28807396	191	12.9	8.48	4.57	443.0	1.66	0.82	0.11	0.00	0.07	0.19	0.00	0.05	-3.14	1.07	1.80	-11.5
65	Sava	Sava, Brestanica	River	45.98708882	15.46596947	150	13.4	8.42	3.17	383.0	1.38	0.48	0.19	0.01	0.03	0.18	0.16	0.10	-3.23	0.82	1.14	-10.0
66	Sava	Sava, Brežice	River	45.89794945	15.59147525	145	14.2	8.04	3.39	396.0	1.42	0.52	0.21	0.02	0.03	0.22	0.00	0.10	-2.53	0.50	0.54	-11.9
67	Sava	Krka, Čatež	Tributary	45.89436142	15.59106334	140	13.5	8.32	4.33	423.0	1.67	0.50	0.11	0.00	0.04	0.10	0.00	0.09	-2.99	0.92	1.30	-12.9
68	Sava	Sava, Mostec	River	45.89565401	15.62699197	140	13.4	8.28	3.52	412.0	1.52	0.50	0.16	0.00	0.03	0.16	0.16	0.10	-3.04	0.76	1.02	-11.1
69	Sava	Sotla, Rakovec	Tributary	45.92058244	15.70479521	140	14.0	8.15	5.22	570.0	2.33	0.68	0.37	0.05	0.09	0.41	0.29	0.11	-2.74	0.95	1.35	-11.8
70	Sava	Sava, Bregana	River	45.86110493	15.69178091	135	13.8	8.23	3.75	398.0	1.48	0.50	0.17	0.01	0.03	0.19	0.00	0.09	-2.96	0.74	0.98	-11.1

Table 2. Sampling locations and geochemical data for autumn sampling season (sampling years: Idrijca: 2006-2007, Kamniška Bistrica: 2010-2011, Sava: 2004-2005). ID numbers correspond to the locations in Figure 1.

GIS_ ID	Name	River	Type	LAT (°)	LON (°)	Z (m)	T (°C)	pH	Alkal. mmol/L	EC µS/cm	Ca^{2+} mmol/L	Mg^{2+} mmol/L	Na^{+} mmol/L	K^{+} mmol/L	Si mmol/L	SO_4^{2-} mmol/L	Cl^{-} mmol/L	NO_3^{-} mmol/L	pCO_2 bar	SI_{cal}	SI_{dol}	$\delta^{13}C_{DIC}$ (‰)
0	Idrijca	Confluence Idrijca/Belca	River	45.963396	13.981281	389	8.8	8.17	4.35	338.0	1.05	0.76	0.06	0.02	0.03	0.07	0.04		-2.77	0.61	0.96	-10.1
1	Idrijca	Podroteja	River	45.990652	14.035864	325	8.0	7.96	3.88	327.0	1.23	0.68	0.06	0.01	0.02	0.06	0.07		-2.61	0.42	0.44	-9.3
2	Idrijca	Kolektor	River	46.009519	14.028858	316	6.5	7.73	3.93	364.0	1.16	0.78	0.07	0.01	0.02	0.08	0.07		-2.38	0.14	-0.05	-10.8
3	Idrijca	Travnik	River	46.068869	13.993716	267	8.5	8.34	4.01	375.0	1.18	0.94	0.08	0.02	0.02	0.14	0.08		-2.98	0.78	1.33	-10.1
4	Idrijca	Kozarska grapa	River	46.117877	13.921682	227	9.0	8.06	3.99	409.0	1.26	0.97	0.12	0.06	0.02	0.35	0.11		-2.70	0.54	0.86	-9.4
5	Idrijca	Before Bača	River	46.143312	13.767604	153	9.5	8.82	4.21	410.0	1.26	1.03	0.09	0.01	0.02	0.37	0.08		-2.92	0.80	1.41	-9.2
6	Idrijca	After Bača	River	46.144954	13.765608	152	9.6	8.26	4.66	412.0	1.26	1.00	0.11	0.03	0.02	0.38	0.10		-2.83	0.80	1.40	-9.0
7	Idrijca	Zala	Tributary	45.986561	14.031768	328																
8	Idrijca	Ljubevšča	Tributary	45.995142	14.034411	325	8.3	8.29	5.10	465.0	1.37	1.09	0.33	0.04	0.05	0.17	0.31		-2.83	0.87	1.53	-10.4
9	Idrijca	Nikova	Tributary	46.00197	14.026078	325	8.4	8.23	4.70	434.0	1.38	0.89	0.23	0.04	0.04	0.14	0.19		-2.80	0.80	1.28	-9.9
10	Idrijca	Kanomljica	Tributary	46.033902	14.015139	302	8.2	8.34	4.08	378.0	1.26	0.90	0.07	0.02	0.03	0.21	0.06		-2.98	0.81	1.34	-8.7
11	Idrijca	Cerknica	Tributary	46.103916	13.948576	245	9.5	8.19	3.63	378.0	1.35	0.51	0.37	0.05	0.09	0.09	0.78		-2.86	0.65	0.80	-6.9
12	Idrijca	Trebuščica	Tributary	46.094549	13.832344	188	8.6	7.77	3.89	348.0	1.01	0.86	0.05	0.01	0.02	0.07	29.76		-2.41	0.16	0.12	-8.2
13	Idrijca	Bača	Tributary	46.144888	13.767263	154	9.2	8.27	3.09	282.0	1.17	0.34	0.08	0.02	0.06	0.10	0.04		-3.01	0.63	0.62	-6.6
14	Kamniška Bistrica	Spring	River	46.3257344	14.58846446	623	5.9	7.35	1.93	160.7	0.73	0.18	0.05	0.00	0.01	0.01	0.01	0.03	-2.37	-0.77	-2.34	-3.6
15	Kamniška Bistrica	before Stahovica	River	46.28567753	14.61692482	530	6.5	8.02	2.74	211.0	0.96	0.29	0.07	0.01	0.01	0.02	0.02	0.04	-2.89	0.15	-0.39	-6.7
16	Kamniška Bistrica	after Stahovica	River	46.25867675	14.60364769	450	6.8	8.10	3.00	225.5	1.00	0.32	0.07	0.01	0.03	0.03	0.03	0.04	-2.90	0.28	-2.95	-7.3
17	Kamniška Bistrica	Kamnik	River	46.2215134	14.61034338	378	7.7	8.15	3.48	269.3	1.21	0.35	0.11	0.02	0.05	0.06	0.06	0.06	-2.91	0.48	0.28	-9.2
18	Kamniška Bistrica	Vir	River	46.14710269	14.60453603	310	9.3	8.23	3.51	277.9	1.29	0.35	0.12	0.02	0.06	0.06	0.07	0.06	-2.98	0.61	0.54	-9.7
19	Kamnišk Bistrica	Domžale	River	46.13584974	14.60277837	300	9.1	8.18	3.72	259.7	1.30	0.39	0.17	0.02	0.07	0.07	0.12	0.07	-2.91	0.61	0.59	-10.1
20	Kamniška Bistrica	Videm	River	46.08835696	14.62594168	260	9.7	7.92	4.19	334.8	1.43	0.45	0.25	0.03	0.07	0.08	0.20	0.11	-2.59	0.42	0.24	-10.7
21	Kamniška Bistrica	Dolski Graben	Tributary	46.30851523	14.60699003	570	7.0	7.82	3.61	259.7	1.34	0.19	0.10	0.01	0.02	0.03	0.02	0.05	-2.57	0.20	-0.60	-10.8
22	Kamniška Bistrica	Bistričica	Tributary	46.28606501	14.61710383	470	7.3	8.12	4.31	267.0	1.27	0.66	0.11	0.02	0.07	0.07	0.04	0.06	-2.79	0.54	0.64	-10.0
23	Kamniška Bistrica	Črna	Tributary	46.26802869	14.61710383	470	6.8	8.26	3.25	272.6	1.07	0.41	0.17	0.02	0.07	0.07	0.12	0.09	-3.06	0.49	0.41	-9.9
24	Kamniška Bistrica	Nevljica	Tributary	46.23068024	14.63750483	460	8.3	8.04	4.58	355.6	1.93	0.22	0.12	0.01	0.06	0.09	0.06	0.10	-2.68	0.67	0.28	-12.6
25	Kamniška Bistrica	Radomeljska Mlinščica	Tributary	46.17251455	14.60803291	340	8.3	8.21	3.55	274.5	1.24	0.35	0.11	0.02	0.05	0.06	0.06	0.06	-2.96	0.56	0.45	-9.2
26	Kamniška Bistrica	Pšata	Tributary	46.16032599	14.59330627	338	8.4	8.07	3.90	309.1	1.46	0.33	0.16	0.03	0.10	0.08	0.11	0.10	-2.78	0.53	0.29	-12.1
27	Kamniška Bistrica	Rača	Tributary	46.14401047	14.61606564	310	9.0	8.03	3.92	329.1	1.29	0.52	0.30	0.04	0.09	0.10	0.25	0.09	-2.73	0.45	0.39	-12.7
28	Kamniška Bistrica	Homška Mlinščica	Tributary	46.09543708	14.62563539	290	8.8	8.25	3.45	276.4	1.21	0.35	0.15	0.02	0.00	0.07	0.09	0.07	-3.01	0.59	0.52	-8.8
29	Kamniška Bistrica	Pšata channel	Tributary	46.08835696	14.62594168	280	9.5	7.93	4.12	338.0	1.51	0.42	0.17	0.03	0.09	0.09	0.13	0.11	-2.61	0.44	0.23	-12.6
30	Sava	Sava Dolinka, spring	River	46.49238108	13.73738958	830	5.6	7.54	2.63	279.0	0.91	0.47	0.07	0.01	0.02	0.05	0.07	0.03	-2.44	-0.39	-1.25	-7.8
31	Sava	Sava Dolinka, Podkoren	River	46.4910896	13.76249572	829	7.1	7.56	2.67	380.0	0.93	0.47	0.13	0.00	0.05	0.10	0.30	0.03	-2.45	-0.34	-1.12	-8.6
32	Sava	Pišnica at Kranjska gora	Tributary	46.47464479	13.78197234	819	7.6	7.82	3.36	239.0	0.86	0.44	0.05	0.02	0.01	0.05	0.04	0.03	-2.61	-0.01	-0.44	-5.4
33	Sava	Sava Dolinka, Dovje	River	46.46265059	13.95393196	704	8.5	7.86	2.65	286.0	1.00	0.51	0.07	0.02	0.03	0.40	0.06	0.06	-2.76	-0.04	-0.50	-7.3
34	Sava	Sava Dolinka, Šobec	River	46.36797849	14.13464505	459	10.7	8.31	3.06	311.0	1.12	0.51	0.10	0.01	0.03	0.19	0.12	0.06	-3.14	-0.58	0.73	-7.3

GIS_ ID	Name	River	Type	LAT (°)	LON (°)	Z (m)	T (°C)	pH	Alkal. mmol/L	EC µS/cm	Ca^{2+} mmol/L	Mg^{2+} mmol/L	Na^{+} mmol/L	K^{+} mmol/L	Si mmol/L	SO_4^{2-} mmol/L	Cl^{-} mmol/L	NO_3^{-} mmol/L	pCO_2 bar	SI_{cal}	SI_{dol}	$\delta^{13}C_{DIC}$ (‰)
35	Sava	River Savica	Tributary	46.29039117	13.80250167	700	6.0	8.08	2.19	190.0	0.75	0.23	0.01	0.00	0.01	0.03	0.01	0.03	-3.06	0.01	-0.68	-3.3
36	Sava	Lake Bohinj, outlet	Tributary	46.278398	13.8863417	557	9.5	7.85	4.11	369.0	2.33	0.51	0.28	0.02	0.04	0.06	0.24	0.09	-2.56	0.52	0.28	-12.8
37	Sava	Sava Bohinjka, Nomenj	Tributary	46.29801526	14.03757249	509	12.0	8.11	2.69	247.0	1.08	0.24	0.04	0.01	0.02	0.08	0.08	0.05	-2.98	0.35	-0.01	-7.2
38	Sava	Sava Otočec	River	46.31216997	14.23744784	415	12.2	8.26	3.24	305.0	1.18	0.47	0.11	0.03	0.03	0.15	0.10	0.05	-3.06	0.60	0.74	-7.3
39	Sava	Tržiška Bistrica, Bistrica	Tributary	46.29011458	14.28442503	422	11.3	8.44	2.81	378.0	1.38	0.60	0.11	0.01	0.05	0.58	0.06	0.04	-3.31	0.73	1.04	-6.4
40	Sava	Kokra, Kranj	Tributary	46.25204699	14.36869104	407	10.7	8.20	3.22	333.0	1.23	0.54	0.09	0.01	0.05	0.21	0.06	0.05	-3.01	0.53	0.61	-7.5
41	Sava	Sava, Kranj	River	46.23782813	14.35202318	350	14.7	7.57	3.22	632.0	1.38	0.52	0.17	0.01	0.04	0.18	0.19	0.10	-2.35	0.02	-0.41	-8.8
42	Sava	Sava, Smlednik	River	46.16419816	14.42555633	336	12.8	8.17	4.76	307.0	1.22	0.42	0.11	0.02	0.03	0.13	0.10	0.06	-2.80	0.69	0.87	-8.1
43	Sava	Sora, Ladja	Tributary	46.14358732	14.39285266	313	12.5	7.48	4.51	379.0	1.38	0.63	0.19	0.05	0.07	0.15	0.19	0.15	-2.13	0.03	-0.33	-10.5
44	Sava	Sava, Tacen	River	46.11722401	14.46118304	280	13.2	7.32	2.99	379.0	0.00	0.00				0.13	0.11	0.07	-2.11			-8.6
45	Sava	Kamniška Bistrica, Beričevo	Tributary	46.08842291	14.62648002	260	13.8	7.74	4.60	554.0	1.72	0.58	0.74	0.17	0.07	0.18	0.51	0.69	-2.38	0.39	0.29	-9.3
46	Sava	Ljubljanica, Zalog	Tributary	46.06220617	14.62169268	267	15.7	7.93	4.79	500.0	1.72	0.74	0.52	0.06	0.04	0.14	0.46	0.10	-2.54	0.62	0.88	-11.8
47	Sava	Sava, Dolsko	River	46.08799496	14.67835027	265	14.0	8.08	3.44	366.0	1.34	0.50	0.23	0.04	0.04	0.15	0.19	0.12	-2.84	0.52	0.59	-9.9
48	Sava	Jevnica,Jevnica	Tributary	46.08360965	14.73719533	240	11.9	7.24	0.84	118.5	0.30	0.14	0.16	0.03	0.19	0.08	0.09	0.03	-2.60	-1.51	-3.42	-9.0
49	Sava	Sava, Kresnice	River	46.09632929	14.77395623	235	11.5	7.29	3.58	387.0	1.45	0.49	0.18	0.04	0.05	0.15	0.14	0.10	-2.04	-0.25	-1.03	-11.8
50	Sava	Sava, Litija	River	46.05646171	14.82051447	230	12.1	7.81	3.48	393.0	1.48	0.49	0.23	0.05	0.05	0.15	0.18	0.12	-2.57	0.27	0.01	-10.9
51	Sava	Reka pri Bregu, Litija	Tributary	46.05962086	14.84614684	245	13.6	7.89	3.93	416.0	0.00	0.00				0.15	0.30	0.11	-2.57			-11.6
52	Sava	Sava, Log	River	46.08563083	14.89206999	230	13.6	8.32	3.81	378.0	1.44	0.49	0.17	0.03	0.05	0.14	0.14	0.10	-3.05	0.81	1.13	-10.2
53	Sava	Polšnik, Sava	Tributary	46.08337901	14.92308091	260	12.7	8.34	2.59	316.0	0.00	0.00				0.18	0.09	0.03	-3.20		1.13	-10.4
54	Sava	Medija, Zagorje	Tributary	46.12125638	14.99434953	240	18.5	8.64	4.89	574.0	1.69	1.00	0.41	0.09	0.11	0.31	0.26	0.12	-3.27	1.31		-11.0
55	Sava	Sava, Zagorje	River	46.11889003	14.99455671	225	13.7	8.35	3.63	403.0	1.49	0.52	0.18	0.02	0.06	0.15	0.16	0.10	-3.01	0.92	2.44	-9.8
56	Sava	Šklendrovec, Zagorje	Tributary	46.10301833	15.00215046	350	14.7	8.74	5.15	487.0	1.52	0.00	0.12	0.00	0.06	0.24	0.11	0.05	-3.37	1.33	1.35	-10.1
57	Sava	Mitovšica, Trbovlje	Tributary	46.11971806	15.04299911	350	15.0	8.72	4.03	414.0	1.54	0.55	0.06	0.03	0.04	0.23	0.07	0.07	-3.44	1.24	2.53	-10.9
58	Sava	Trboveljščica, Trbovlje	Tributary	46.16192117	15.05268008	230	12.5	8.04	4.22	512.0	1.41	1.00	0.71	0.10	0.15	0.13	0.10	0.06	-2.72	0.55	2.04	-11.4
59	Sava	Sava, Trbovlje	River	46.12621671	15.03632723	220	17.2	8.48	3.54	403.0	1.48	0.52	0.22	0.04	0.05	0.18	0.16	0.11	-3.23	0.99	0.90	-10.9
60	Sava	Sava, Hrastnik	River	46.12155113	15.0916258	210	13.5	8.52	3.45	376.0	1.43	0.51	0.19	0.04	0.05	0.15	0.15	0.17	-3.30	0.96	1.56	-10.2
61	Sava	Boben, Hrastnik	Tributary	46.15057264	15.08592694	220	17.3	8.34	3.42	575.0	1.67	1.01	0.77	0.12	0.13	0.44	0.41	0.10	-3.11	0.87	1.44	-11.6
62	Sava	Savinja, Rimske Toplice	Tributary	46.12262895	15.20328147	200	14.3	8.82	3.42	473.0	1.62	0.56	0.68	0.08	0.10	0.51	0.34	0.12	-3.63	1.25		-10.2
63	Sava	Sava, Radeče	River	46.06552039	15.18817906	193	14.4	8.54	3.36	397.0	1.46	0.53	0.32	0.04	0.06	0.24	0.21	0.10	-3.33	0.98	1.55	-9.9
64	Sava	Mirna, Dol Bostanj	Tributary	46.0042524	15.28807396	191	14.4	8.99	5.49	511.0	1.73	1.15	0.23	0.09	0.09	0.18	0.14	0.05	-3.63	1.59	2.04	-11.2
65	Sava	Sava, Brestanica	River	45.98708882	15.46596947	150	14.6	8.63	3.60	453.0	0.00	0.00				0.25	0.23	0.12	-3.35		1.51	-10.4
66	Sava	Sava, Brežice	River	45.89794945	15.59147525	145	14.4	7.86	3.29	428.0	1.57	0.56	0.37	0.06	0.07	0.28	0.24	0.11	-2.64	0.35	3.01	-10.8
67	Sava	Krka, Čatež	Tributary	45.89436142	15.59106334	140	14.5	8.77	4.65	459.0	0.00	0.00				0.10	0.16	0.12	-3.09			-11.1
68	Sava	Sava, Mostec	River	45.89565401	15.62699197	140	14.7	8.20	3.74	412.0	1.49	0.54	0.34	0.05	0.06	0.27	0.23	0.10	-2.93	0.71	0.97	-11.5
69	Sava	Sotla, Rakovec	Tributary	45.92058244	15.70479521	140	12.4	8.61	6.02	630.0	2.38	0.84	0.67	0.17	0.16	0.39	0.39	0.13	-3.18	1.41	2.33	-12.2
70	Sava	Sava, Bregana	River	45.86110493	15.69178091	135	14.0	7.93	3.51	424.0	1.52	0.55	0.30	0.05	0.06	0.22	0.06	0.04	-2.68	0.42	0.37	-10.8

Europa-Scientific 20-20 continuous flow IRMS ANCA-SL preparation module. For POC 1 L of the water sample was filtered through a Whatman GF/F glass fiber filter (0.7 μm). Filters and soil were treated with 1 M HCl to remove carbonate.

Thermodynamic geochemical modeling was used to evaluate CO_2 partial pressures (pCO_2) and the saturation state of calcite and dolomite ($SI_{calcite}$ and $SI_{dolomite}$) using pH, alkalinity, and temperature as inputs to the PHREEQC speciation program (PARKHURST & APPELO, 1999).

Results and discussion

Aquatic geochemistry of selected gravel bed rivers in Slovenia

The temperature of surface water in River Kamniška Bistrica, pH and conductivity ranged from 1.7 to 26.6 °C, 7.1 to 8.8, and 160.7 to 497.4 μS/cm. DO saturation varied seasonally from 59.6 to 76.8 % in the winter and from 68 to 140 % (KANDUČ et al., 2013). In River Idrijca water temperature was 7.3 to 13.0 °C, conductivity ranged from 181 to 465 μS/cm, pH ranged from 7.77 to 8.82 (KANDUČ et al., 2008). Temperature in River Sava water ranged from 0.4 to 15.7 °C, conductivity ranged from 62.3 to 632 μS/cm and pH ranged from 7.24 to 8.99, respectively (KANDUČ, 2006; KANDUČ et al., 2007). All results are described in detail in KANDUČ et al. (2007, 2008 and 2013).

The major solute composition of selected gravel-bed rivers was dominated by HCO_3^-, Ca^{2+} and Mg^{2+}. Concentrations varied seasonally according to discharge, with higher concentrations observed in autumn at lower discharge and lower concentrations during the spring sampling season. Dissolved Ca^{2+} and Mg^{2+} are largely supplied by the weathering of carbonates (Fig. 3), which are the most dominant rocks in the watersheds, and prone to chemical dissolution, with smaller contributions from silicate weathering, as indicated by the relatively high HCO_3^- and low Si concentrations (KANDUČ, 2006; KANDUČ et al., 2007, 2008 and 2013).

Figure 3 presents $Ca^{2+} + Mg^{2+}$ versus alkalinity for all three selected gravel bed rivers in Slovenia. Most of the samples have a 2:1 mole ratio of HCO_3^- to $Ca^{2+} + Mg^{2+}$ following the reactions (GAILLARDET et al., 1999):

Calcite: $CaCO_3 + CO_2 + H_2O \Leftrightarrow Ca^{2+} + 2HCO_3^-$ (1)

Dolomite:

$Ca_{0.5}Mg_{0.5}(CO_3) + CO_2 + H_2O \Leftrightarrow Ca^{2+} + Mg^{2+} + 2HCO_3^-$ (2)

Some samples deviate from 2:1 line due to weathering of other minerals in river watershed, like albite and anorthite:

$$\underset{\text{Anorthite}}{CaAl_2Si_2O_8} + 3H_2O + 2CO_2 \rightarrow \underset{\text{Kaolinite}}{Al_2Si_2O_5(OH)_4} + Ca^{2+} + 2HCO_3^- \quad (3)$$

$$\underset{\text{Albite}}{NaAlSi_3O_8} + CO_2 + {}^{11}/_2\, H_2O \rightarrow Na^+ + ½\, \underset{\text{Kaolinite}}{Al_2Si_2O_5(OH)_4} + 2H_4SiO_4 + HCO_3^- \quad (4)$$

The pH, temperature and pCO_2 of a watershed determine the carbonate speciation, controlling the HCO_3^- carrying capacity. In Slovenian watersheds, total alkalinity comprises carbonate alkalinity (KANDUČ, 2006; KANDUČ et al., 2007), and therefore the total alkalinity is assumed as HCO_3^-, which is also the main DIC species at the pH of 7.0 to 9.0 measured in all investigated watersheds. Concentrations of HCO_3^- in main channel of River Kamniška Bistrica (Fig. 3A) vary seasonally from 1.93 to 4.19 mM in autumn 2010, from 1.88 to 4.99 mM in winter 2011, from 1.55 to 4.39 mM in spring 2011 and from 1.70 to 5.57 mM in summer 2011, respectively. Concentrations of HCO_3^- (alkalinity) in tributaries vary seasonally and range from 3.25 to 4.58 mM in autumn 2010 (Fig. 3A). The alkalinity concentrations in the main channel sampling sites varied seasonally in River Sava (Fig. 3B) in the main channel from 2.60 to 3.75 mM in spring, from 2.63 to 4.79 mM in late summer 2004, and from 2.67 to 4.17 mM during winter. The upper alpine headwater catchments of the River Sava have thin soils developed on carbonate bedrock. In the central and lower part of the River Sava watershed, tributary streams have more variable alkalinity concentrations, ranging from about 0.39 to 6.02 mM (KANDUČ et al., 2007). River Idrijca (Fig. 3C) had alkalinities in range from 3.88 to 4.66 mM in autumn 2006 and from 4.12 to 4.43 mM in spring 2007, while in tributaries alkalinities range from 3.09 to 5.10 mM in autumn 2006 and in spring 2007 from 3.15 to 5.04 mM (KANDUČ et al., 2008).

Differences in alkalinities in carbonate-bearing watersheds are related to the geological composition of the watershed (Fig. 2), the relief (Fig. 1), the mean annual temperature, the depth of the weathering zone, the soil thickness and the water residence time in the system. Weathering rates increase in thicker soils like shales due to the higher residence time of shallow groundwater in contact with minerals in comparison to watersheds composed of carbonate minerals.

Mg^{2+} versus Ca^{2+} relations indicate the relative contribution of calcite/dolomite to carbonate weathering intensity in gravel bed rivers (Fig. 4). Most of the samples indicate that weathering of calcite is dominant over the entire River Kamniška Bistrica, especially in the upper and central reaches (Fig. 4A). A Mg^{2+}/Ca^{2+} ratio around 0.33 is typical for weathering of calcite for the entire length of the River Kamniška Bistrica as well as for rivers comprising Danube watershed (Kanduč et al., 2013). In contrast, rivers comprising St. Lawrence watershed (North America) have ratios Mg^{2+}/Ca^{2+} greater than 0.33 (Szramek et al., 2007). Most of the samples in River Sava (Fig. 4B) fall below 0.22 line, indicating weathering of calcite, only some samples in River Sava tributaries fall above 0.5 Mg^{2+}/Ca^{2+} line indicating weathering of dolomite. From Figure 4C it can be observed that most of the samples indicate that weathering of dolomite is dominant over the entire River Idrijca,

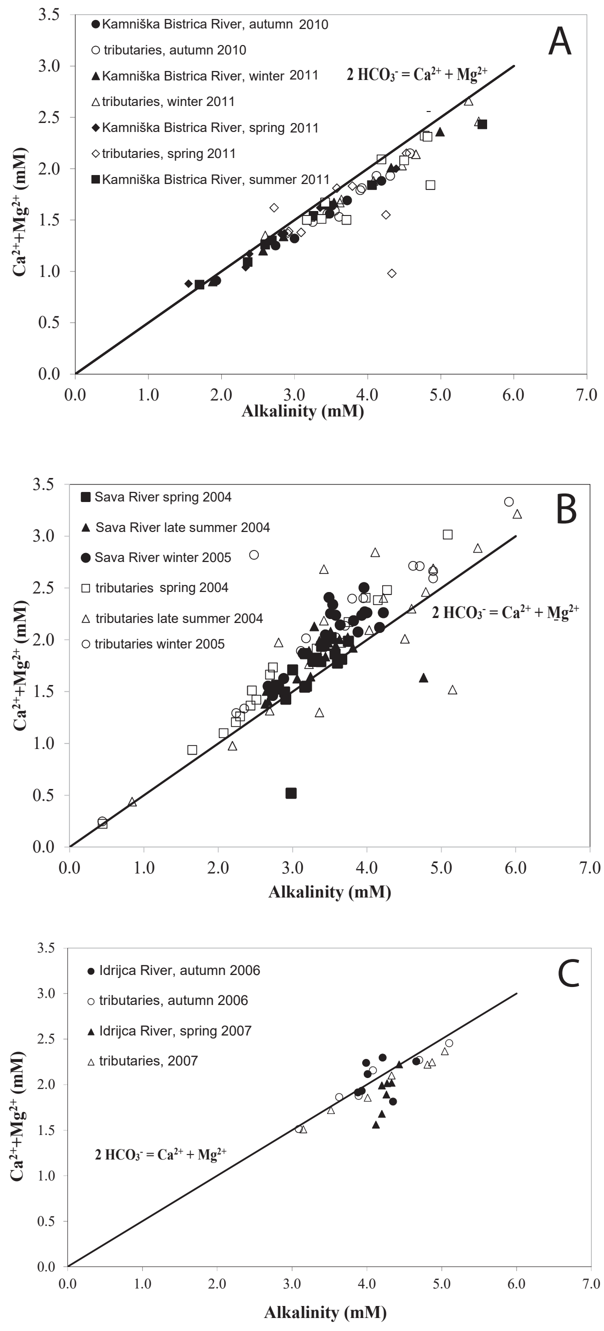

Fig. 3. $Ca^{2+}+Mg^{2+}$ ratio versus alkalinity with line 1: 2 indicating weathering of carbonates in the watershed (rivers: A: Kamniška Bistrica, B: Sava in Slovenia, C: Idrijca).

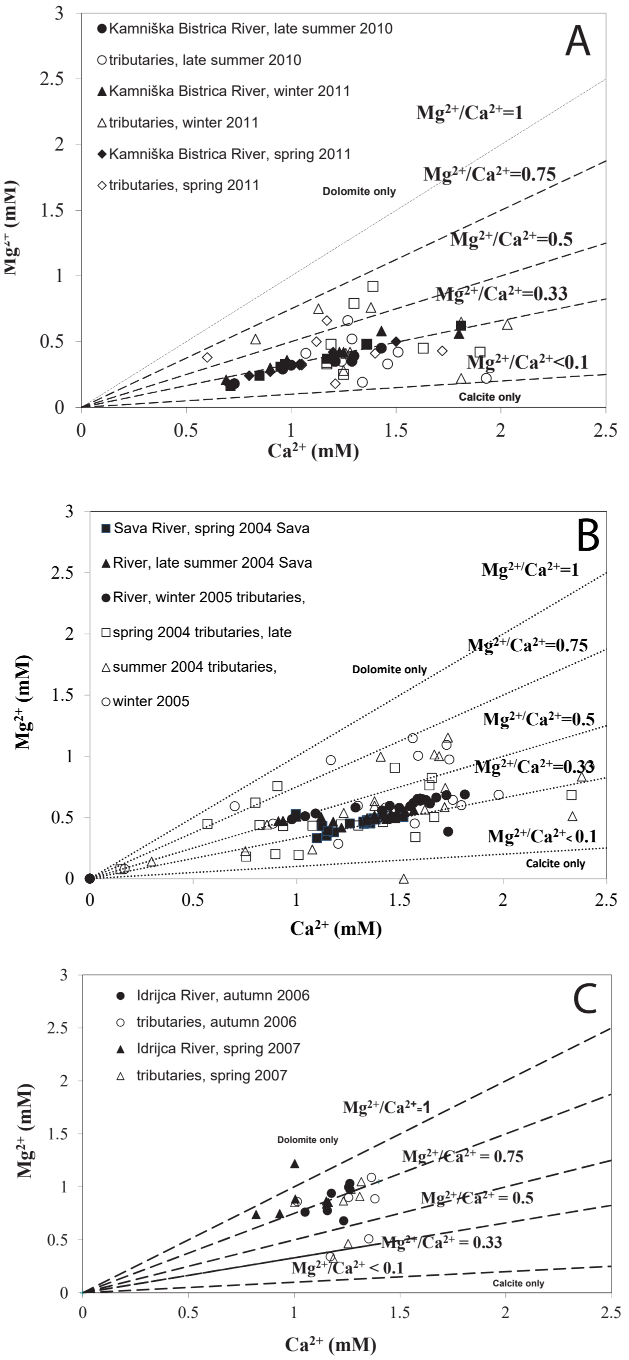

Fig. 4. Mg^{2+} versus Ca^{2+} indicating weathering of calcite and dolomite in watershed (rivers: A: Kamniška Bistrica, B: Sava in Slovenia, C: Idrijca).

especially in the upper and central flow of the river. A Mg^{2+}/Ca^{2+} ratio around 0.33 is characteristic only in the lowland tributaries of the River Idrijca composed mainly of limestone.

The major control on carbonate weathering intensity is runoff (Amiotte Suchet & Probst, 1993). Carbonate weathering intensity normalized to drainage area, quantifies HCO_3^- produced from mineral weathering. Figure 5 compares carbonate weathering intensities as a function of specific runoff for the River Idrijca watershed, combining new data from this study with published official data for the River Sava, River Kamniška Bistrica and data from Berner & Berner (1996) for world rivers and the River Danube. Global theoretical models of CO_2 consumption in carbonate watersheds show an alkalinity value around 3 mmol/L determined from a best-fit line (Amiotte Suchet & Probst, 1993). The climate and topographic relief in Slovenian watersheds importantly influence the carbonate weathering intensity and specific runoff. Roy et al. (1999) noted that linked factors such as lithology, residence time of water, mechanical erosion, etc., have more influence together than they do separately. The watershed of the River Idrijca is typically an environment where enhanced mechanical weathering increases chemical weathering (Fairchild et al., 1999; Anderson et al., 2000; Jacobson et al., 2000) and causes a high carbonate weathering intensity, since the river is a steep mountain river with torrential character, e.g. River Idrijca with 80 mmol/l·km²·s (Fig. 5) and Kamniška Bistrica with the highest weathering intensity of 150 mmol/l·km²·s (Fig. 5).

The world average value for carbonate weathering intensity is 7 mmol/l km² s (Berner & Berner, 1996). For the River Sava and its tributaries, the mean long term weathering intensity is from 37 to 140 mmol/l km² s.

Also carbonate weathering intensity (HCO_3^- in mmol/l km² s) of some other world rivers (Mississippi, World, Danube) is presented on Figure 5. From Figure 5 it can be observed that Slovenian gravel bed rivers have higher HCO_3^- weathering intensity in comparison to world rivers.

Thermodynamic modeling and isotope geochemistry with emphasize on carbon cycle

Thermodynamical modeling software PHREEQC for Windows was used to calculate pCO_2 and saturation indices for calcite and dolomite ($SI_{calcite}$ and $SI_{dolomite}$) along the main water channel and tributaries. In all investigated bed rivers a high value of pCO_2 was observed during all sampling seasons, meaning that rivers represent sources of CO_2 into air.

Calculated pCO_2 varied from 977 to 4,169 ppm in autumn and from 295 to 2,398 ppm in the spring sampling season. Normal atmospheric pressure is around 316 ppm according to Clark & Fritz (1997). Calculated pCO_2 varied from near atmospheric up to 25-fold supersaturated at River Kamniška Bistrica at Videm in summer season in year 2010 to 2011. Partial pressure in River Sava and its tributaries ranges from 128.8 to 2,951 ppm in April 2004, in September 2004

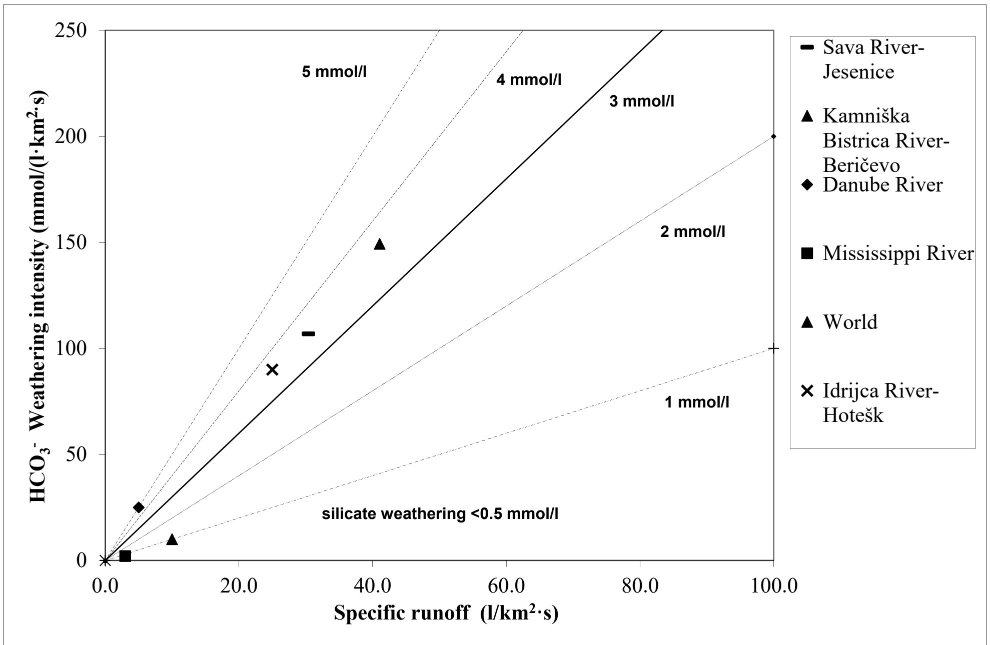

Fig. 5. Carbonate weathering intensity (HCO_3^- in mmol/l km² s) versus specific runoff (1/km²s) indicating high carbonate weathering intensity in selected rivers in Slovenia (River Kamniška Bistrica, River Sava in Slovenia, River Idrijca) and in the world. Data include mean long-term data of discharge and alkalinity from the Slovenian Environment Agency (2004-2011) for the Slovenian rivers, and Berner & Berner (1996) for world rivers, River Danube and Mississipi River.

from 234.4 to 9,120 ppm in April and from 223.9 to 4,074 ppm in January 2005 (Kanduč, 2006). In autumn all sampling locations on the River Idrijca watershed are above equilibrium with atmospheric CO_2. These higher partial pressures in autumn are probably due to higher degradation of organic matter in the river and due to lower discharge (Dever et al., 1983). Lower pCO_2 (below normal atmospheric pressure at locations 5 and 6, Table 1, Fig.1) in the spring are observed due to the higher pH of the water, which lowers the evasion of CO_2 from water.

The calcite saturation index ($SI_{calcite}$=log([-Ca^{2+}]*[CO_3^{2-}])/$K_{calcite}$; where $K_{calcite}$ is the solubility product of calcite and was generally well above equilibrium ($SI_{calcite}$=0)), indicates that calcite was supersaturated and precipitation was thermodynamically favoured along most of the course of all selected gravel bed rivers in Slovenia (Fig. 6). Calcite and dolomite were supersaturated and carbonate precipitation was thermodynamically favoured along most of the course of River Kamniška Bistrica (Fig. 6A). $SI_{calcite}$ and $SI_{dolomite}$ seasonally change in River Sava and their tributaries and reach oversaturation in central and lower flow of the river, while in upper part of the river rarely reach saturation (Fig. 6B). Low $SI_{calcite}$ and $SI_{dolomite}$ are observed at tributary location of River Sava (Fig. 6B). In most of the samples of River Idrijca and its tributaries calcite and dolomite are oversaturated, only one sample in River Idrijca is undersaturated with respect to dolomite (Fig. 6C).

Mass balance calculation with evaluation of biogeochemical processes in selected gravel bed rivers in Slovenia

Mass balance calculations were performed in previous studies (Kanduč et al., 2007, 2008 and 2013).

The $\delta^{13}C_{DIC}$ value can determine the contributions of organic matter decomposition, carbonate mineral dissolution, and exchange with atmospheric CO_2 to DIC in selected gravel bed rivers in Slovenia. The $\delta^{13}C_{DIC}$ values of the main channel of the river varied seasonally (year 2010–2011) from -10.9 ‰ (River Kamniška Bistrica, location 20, Table 1, Fig. 1) to -2.7 ‰ (River Kamniška Bistrica Spring, location 14, Table 1, Fig. 1) while $\delta^{13}C_{DIC}$ in tributaries ranged from -12.7 ‰ (Rača, location 27, Table 1, Fig.1) to -6.9 ‰ (Kamniška Bistrica Spring, location 14, Table 1, Fig.1) (Kanduč et al., 2013). The $\delta^{13}C_{DIC}$ in River Sava varied seasonally from -12.7 to -8.6 ‰ in spring 2004, from -11.8 to -7.3 ‰ in late summer 2004 and from -10.6 to -6.3 ‰ in winter 2005. The River Sava tributaries had $\delta^{13}C_{DIC}$ values that varied from -13.5 to -5.8 ‰ in spring 2004, from -12.8 to 3.3 ‰

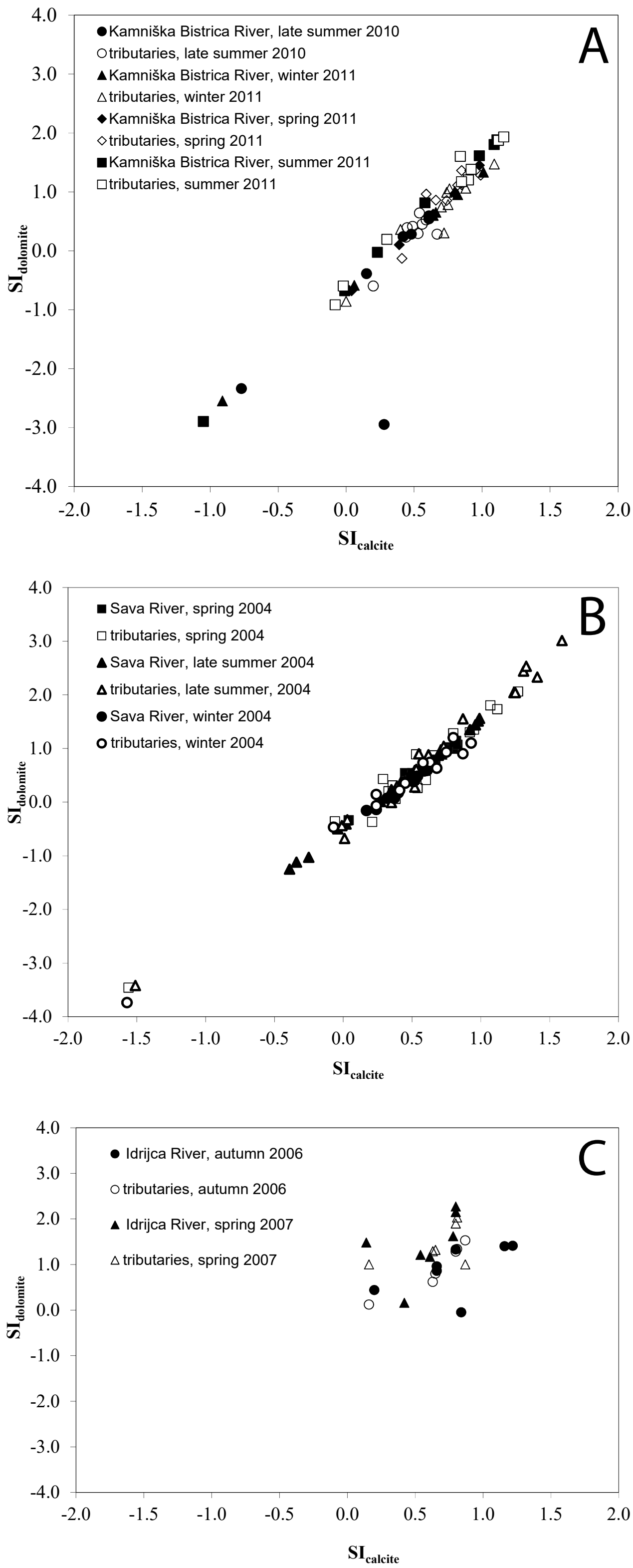

Fig. 6. $SI_{calcite}$ versus $SI_{dolomite}$ in different sampling seasons in different periods for the selected rivers (A: Kamniška Bistrica, B: Sava in Slovenia, C: Idrijca).

in late summer 2004, and from -11.9 to -4.2 ‰ in winter 2005 (Kanduč et al., 2007). $\delta^{13}C_{DIC}$ varied seasonally in River Idrijca watershed from -10.8 to -9.0 ‰ in autumn 2006 and from -10.6 to -8.3 ‰ in spring 2007. The $\delta^{13}C_{DIC}$ value of the river water is controlled by the geological composition of the watershed. Along the River Idrijca flow the dissolution of carbonates is the major contributor to $\delta^{13}C_{DIC}$ values, but some parts of the watershed also drain shales, mudstones, and sandstones (Kanduč et al., 2008). Thus, in those parts $\delta^{13}C_{DIC}$ is much lower (central part of the River Idrijca, lower reaches of River Kamniška Bistrica and central and lower flow of River Sava in Slovenia) since the thickness of soil is on this bedrock much higher and soil CO_2 contributes much more to DIC than on carbonate bedrocks. $\delta^{13}C_{DIC}$ was also generally lower during spring season at higher discharge (Fig. 7). The average $\delta^{13}C$ value of Mesozoic carbonate rocks ($\delta^{13}C_{CaCO3}$) in the hinterland of River Kamniška Bistrica is +2.4 ‰ (Kanduč et al., 2013). The $\delta^{13}C$ of Mesozoic carbonate rocks ($\delta^{13}C_{CaCO3}$) from the River Sava watershed ranged from -1.4 to +2.7 ‰, with an average of +1.4±1.3 ‰ (N=12) (Kanduč et al., 2007). The $\delta^{13}C$ value of Mesozoic carbonate rocks ($\delta^{13}C_{CaCO3}$), which forms the slopes in the watershed of the River Idrijca is on average +2.0±0.7 ‰ (N = 8) (Kanduč et al., 2008).

Figure 7 shows a plot of $\delta^{13}C_{DIC}$ versus alkalinity in different sampling seasons for selected gravel bed rivers in Slovenia. Changes over the course of the rivers indicate processes affecting $\delta^{13}C_{DIC}$, e. g. degradation of organic matter (line 3), carbonate mineral dissolution (line 2), and equilibration with atmospheric CO_2 (line 1) (Barth et al., 2003).

At River Kamniška Bistrica source carbonate dissolution prevails, while in central and lower part of the river degradation of organic matter and dissolution of carbonates prevails (Fig. 7A). The $\delta^{13}C_{DIC}$ values from the River Idrijca watershed (Fig. 7C) indicate that nonequilibrium carbonate dissolution predominates along the flow of river, since the watersheds are mainly composed of carbonate rocks with inclusions of clastic rocks, approaching a $\delta^{13}C_{DIC}$ value of -12.3 ‰. In tributaries of the River Idrijca watershed (Fig. 7C), River Kamniška Bistrica (Fig. 7A) and River Sava in Slovenia (Fig. 7B) dissolution of carbonate minerals prevails, which leads to higher $\delta^{13}C_{DIC}$ values. Mineralization of organic matter appears to be the dominant source of $\delta^{13}C_{DIC}$ along

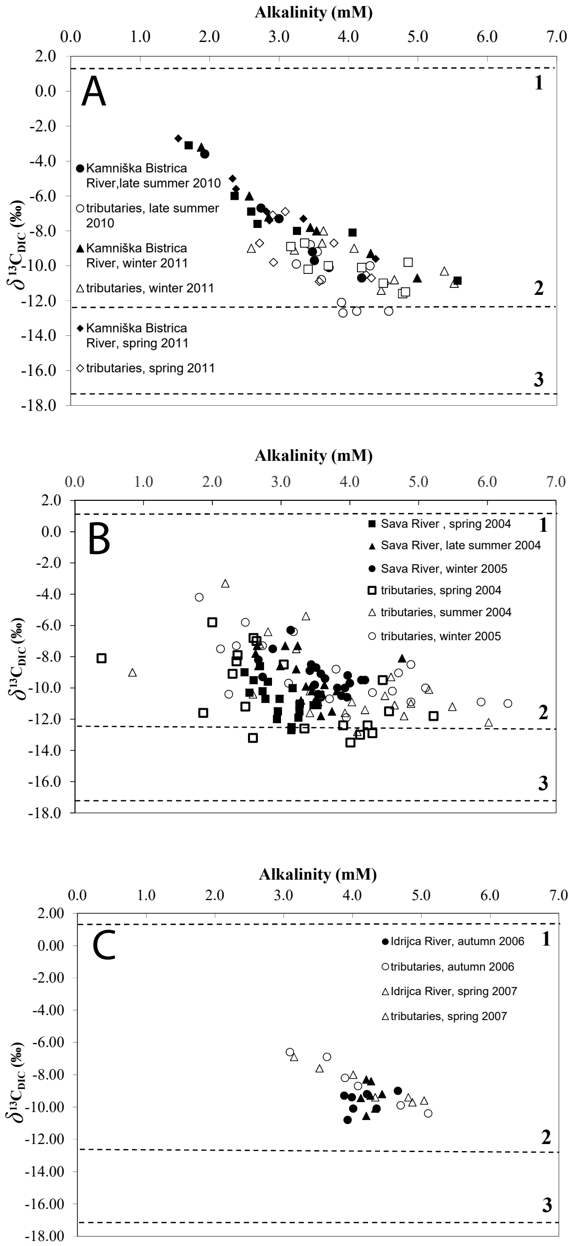

Fig. 7. $\delta^{13}C_{DIC}$ versus alkalinity of selected gravel bed rivers in Slovenia (rivers: A: Kamniška Bistrica, B: Sava in Slovenia, C: Idrijca).

the Idrijca flows (Fig. 7C), where the greater soil thickness enables accumulation of soil CO_2 due to the greater degree of silicate rock weathering, which leads to more a negative $\delta^{13}C_{DIC}$.

The evasion of CO_2 from the River Kamniška Bistrica, River Sava in Slovenia and River Idrijca can be calculated (equation 5) based on the thin-film diffusive gas exchange model (Broecker, 1974; Raymond et al., 2012):

$$[DIC]_{ex} = D/z * ([CO_2]_{eq} - [CO_2]) \quad (5)$$

where D is the CO_2 diffusion coefficient in water of 1.26 $*10^{-5}$ cm^2/s at a temperature of 10 °C and 1.67 $*10^{-5}$ cm^2/s at a temperature of 20 °C (Jähne et al., 1987), and z is the empirical thickness of the liquid layer [cm].

A simple isotopic mass balance calculation was performed in order to quantify different sources of DIC in all three selected gravel bed rivers: at River Kamniška Bistrica mouth (location 20, Table 1, Fig.1), at the River Idrijca mouth (location 6, Table 1, Fig. 1), at River Sava in Slovenia mouth (location 70, Table 1, Fig.1) considering the sum of tributary inputs and biogeochemical processes in the watershed. The major inputs to the DIC flux (DIC_{RI}) and $\delta^{13}C_{DIC}$ originate from tributaries (DIC_{tri}), degradation of organic matter (DIC_{org}), exchange with the atmosphere (DIC_{ex}), and dissolution of carbonates (DIC_{ca}) can be estimated by Eqs. (6 and 7):

$$DIC_{RI} = DIC_{tri} - DIC_{ex} + DIC_{org} + DIC_{ca} \quad (6)$$

$$DIC_{RI}*\delta^{13}C_{RI} = DIC_{tri}*\delta^{13}C_{tri} - DIC_{ex}*\delta^{13}C_{ex} + DIC_{org}*\delta^{13}C_{POC} + DIC_{ca}*\delta^{13}C_{CaCO3} \quad (7)$$

The contribution of rainwater to riverine DIC is considered to be minimal as it contains only a small amount of DIC (Yang et al., 1996).

DIC_{RI} and DIC_{tri} were calculated from the concentrations of alkalinity and water discharge, with the corresponding measured $\delta^{13}C$ values for $\delta^{13}C_{RI}$ and $\delta^{13}C_{tri.}$ The average diffusive flux of CO_2 from the river to the atmosphere, DIC_{ex}, estimated from Eq. (5), was taken into account. In Eqs. (5 and 6) the minus sign indicates outgassing of CO_2, which is observed in autumn, but not in the spring season. The $\delta^{13}C_{ex}$ value was calculated according to the equation for equilibrium isotope fractionation between atmospheric CO_2 and carbonic acid in water (Zhang et al., 1995), where a $\delta^{13}C$ value of -7.8 ‰ for atmospheric CO_2 was used (Levin et al., 1987). The isotopic composition of the contribution of equilibration between atmospheric CO_2 and DIC ($\delta^{13}C_{ex}$) would then be +1.4 ‰ in the autumn and +1.8 ‰ in the spring sampling season, considering atmospheric CO_2 as the ultimate source of CO_2 in the River Sava in Slovenia, River Idrijca and River Kamniška Bistrica drainage system. For $\delta^{13}C_{POC}$ and $\delta^{13}C_{CaCO3}$ average values of -26.6 ‰ and +2.0 ‰ were used in the mass balance equations.

Contributions of DIC from various biogeochemical processes were determined using steady state equations for different sampling seasons at the mouth of the River Kamniška Bistrica; results indicate that: (1) 1.9-2.2 % of DIC came from exchange with atmospheric CO_2, (2) 0-27.5 % of DIC came from degradation of organic matter, (3) 25.4–41.5 % of DIC came from dissolution of carbonates and (4) 33.0–85.0 % of DIC came from tributaries (Kanduč et al., 2013). In both sampling seasons the most important biogeochemical process is weathering of carbonates, while degradation of organic matter is more expressed in the spring sampling season. A less significant process in both sampling seasons is exchange with atmospheric CO_2 and is not marked in the spring sampling season due to the pCO_2 value (at location 28, Table 1, Fig.1), which is near equilibrium with atmospheric CO_2 pressure. In River Sava mouth among biogeochemical processes dissolution of carbonates contributes the highest proportion in both sampling seasons, which moves $\delta^{13}C_{DIC}$ to more positive values. Mass balances for riverine inorganic carbon suggest that carbonate dissolution contributes up to 26 %, degradation of organic matter ~17 % and exchange with atmospheric CO_2 up to 5 %. The concentration and stable isotope diffusion models indicated that atmospheric exchange of CO_2 predominates in streams draining impermeable shales and clays while in the carbonate-dominated watersheds dissolution of the Mesozoic carbonate predominates (Kanduč et al., 2007). The calculated contributions to the average DIC budget from DIC_{tri}:DIC_{ex}:DIC_{org}:DIC_{ca} at the River Idrijca mouth were 61:-11:19:31 % in autumn 2006 and 35:0:26:39 % in spring 2007 (Kanduč et al., 2008).

Conclusions

The major solute composition of the River Kamniška Bistrica is dominated by HCO_3^-, Ca^{2+} and Mg^{2+}. Concentrations of HCO_3^- ranged from 1.6 mM to 5.6 mM in main channel and from 2.6 to 5.5 mM in tributaries. The majority of River Kamniška Bistrica system was supersaturated or near equilibrium with respect to calcite/dolomite in all sampling seasons. According to the calculated pCO_2 values, the river is source of CO_2 to the atmosphere during all sampling seasons, higher pCO_2 is observed during summer season. Lower alkalinities and higher $\delta^{13}C_{DIC}$ values of -2.7 ‰ were observed in the upper carbonate part of the watershed, while higher alkalinities and more negative $\delta^{13}C_{DIC}$ values of -12.7 ‰ were observed in the central and lower part of the Kamniška Bistrica system.

The major chemical composition of River Sava water is HCO_3^-, Ca^{2+} and Mg^{2+}. Seasonal (spring 2004, late summer 2004 and winter 2005) concentrations of HCO_3^- range from 2.63 to 4.79 mM, while its tributaries have concentrations of HCO_3^- ranging from 0.39 to 6.02 mM. The majority of the River Sava system is supersaturated or at equilibrium (in the upper part of the river flow) with respect to calcite in all sampling seasons. $\delta^{13}C_{DIC}$ values range from -12.7 to -6.3 ‰ and were observed in late summer. The observed differences in pCO_2, alkalinities and $\delta^{13}C_{DIC}$ between the carbonate rock drainages versus mixed lithology watersheds (carbonate and clastic rocks) at downstream locations are the consequence of the soil thickness since carbonate rocks are more resistant to mechanical weathering processes. The partial pressure is lower in the carbonate part of the watershed and higher at downstream locations. Lower alkalinities and higher $\delta^{13}C_{DIC}$ values are observed in the upper carbonate part of the watershed, while higher alkalinities and lower $\delta^{13}C_{DIC}$ values are observed in the central and lower part of the River Sava watershed.

The biogeochemical processes affecting DIC and $\delta^{13}C_{DIC}$ values were quantified by concentration and isotope mass calculations and it can be concluded that the most important biogeochemical processes at the River Sava mouth in order of significance in different sampling seasons are: (1) carbonate dissolution comprising 19.4 % in spring to 25.9 % in late summer, (2) degradation of organic matter comprising 10.8 % in winter to 16.7 % in late summer, while (3) atmospheric exchange comprises 0.8 % in spring to 4.9 % in late summer.

The River Sava in Slovenia has high discharge, low stream photosynthetic activity and represents a river system where among the biogeochemical processes geological factors prevail (carbonate dissolution). Construction of hydroelectric power plants in the central and lower Sava flow in the next five years will affect the carbon cycle, e.g accelerated primary production, degradation of organic matter, degassing of CO_2 from the river. This investigation will also help to evaluate the biogeochemical state of the river after dam constructions.

The major solute composition of River Idrijca water is dominated by HCO_3^-, Ca^{2+} and Mg^{2+}. Seasonal alkalinity concentrations ranged from 3.88 to 4.66 mM, while its tributaries had concentrations of HCO_3^- ranging from 3.09 to 5.10 mM. The majority of the River Idrijca system was supersaturated or near equilibrium with respect to calcite. The biogeochemical processes affecting DIC concentrations and $\delta^{13}C_{DIC}$ (in the range from -10.8 to -6.6 ‰) calculated by mass balance equations showed that the most important biogeochemical processes at the River Idrijca mouth are: carbonate mineral dissolution, degradation of organic matter and atmospheric exchange. The River Idrijca is a river with torrential character, has a high specific discharge and therefore high weathering intensity.

In all three investigated rivers carbonate dissolution and degradation of organic matter are the most important biogeochemical processes in river system, while exchange with atmosphere could be negligible according to mass balance equations.

Acknowledgements

The authors are thankful to Research Agency of Republic of Slovenia, program research groups P1-0143 and P1-0195. The authors are also thankful to previous research projects funded by Research Agency of Republic of Slovenia and ongoing research project L2–6778 (2014–2017). Finally, our sincere thanks go to prof. dr. Jožef Pezdič for introducing us to stable isotopic geochemistry and hydrogeochemistry and for his guidance in the research and pedagogical work.

References

Amiotte Suchet, P. & Probst, J.L. 1993: Modelling of atmospheric CO_2 consumption by chemical weathering of rocks: Application to the Garonne, Congo and Amazon basins. Chem. Geol., 107/3-4: 205-210, doi:10.1016/0009-2541(93)90174-H.

Anderson, S.P., Drever, J.I., Frost, C.D. & Holden, P. 2000: Chemical weathering in the foreland of a retreating glacier. Geochim. Cosmochim. Acta, 64/7: 1173-1189, doi:10.1016/S0016-7037(99)00358-0.

Atekwana, E.A. & Krishnamurthy, R.V. 1998: Seasonal variations of dissolved inorganic carbon and $\delta^{13}C$ of surface waters: Application of a modified gas evaluation technique. Hydrology Journal, 205/3-4: 265-278, doi:10.1016/s0022-1694(98)00080-8.

Barth, J.A.C., Cronin, A.A, Dunlop, J. & Kalin, R.M. 2003: Influence of carbonates on the riverine carbon cycle in an anthropgenically dominated catchment basin: evidence from major elements and stable carbon isotopes in the Lagan River (N. Ireland). Chem. Geol., 200/3-4: 203-216, doi:10.1016/S0009-2541(03)00193-1.

Berner, E.K. & Berner, R.A. 1996: Global environment, water, air, and geochemical cycles. Prentice Hall, Upper Saddle River.

Broecker, W.S. 1974: Chemical oceanography. Harcourt Brace Jovanovich, New York.

Buser, S. 1987: Geological map of Slovenia. In: Vogler D. (ed.): Encyclopedia of Slovenia No. 8, Mladinska knjiga, Ljubljana (in Slovene): 4-416.

Clark, I. & Fritz, P. 1997. Environmental Isotopes in Hydrogeology. New York: Lewis Publishers.

Cole, J.J., Prairie, Y.T., Caraco, N.F., McDowell, W.H., Tranvik, L.J. Striegl, R.G., Duarte, C.M. Kortelainen, P., Downing, J.A., Middelburg, J.J. & Melack, J. 2007. Plumbing the Global Carbon Cycle: Integrating Inland Waters into the Terrestrial Carbon Budget. Ecosystems, 10: 171-184, doi:10.1007/s10021-006-9013-8.

Čar, J. 2010: Explanatory book to the map: geological structure of the Idrija - Cerkno hills. Geological Survey of Slovenia, Ljubljana: 125 p.

Deines, P. 1980: The isotopic composition of reduced organic carbon. In: Fritz P. & Fontes J.C. (eds.): Hanbook of Environmental Isotopic Geochemistry, 1: 329-406, Elsevier, Amsterdam.

Dever, L., Durand, R., Fontes, J. C.H. & Vaicher, P. 1983: Etude pédogénétique et isotopique des néoformations de calcite dans un sol sur craie. Caractéristiques et origins. Geochimica Cosmochimica Acta, 47: 2079-2090.

Fairchild, I.J., Killawee, J.A., Hubbard, B. & Dreybodt, W. 1999: Interactions of calcareous suspended sediment with glacial meltwater: a field test of dissolution behaviour. Chem. Geol., 155: 243-263, doi:10.1016/s0009-2541(98)00170-3.

Fratar, P. 2005: River Flow Regimes of Slovene Rivers and their fluctuations = Pretočni režimi slovenskih rek in njihova spremenljivost. Ujma, 19: 145-153.

Gaillardet, J., Dupré, B., Louvat, P. & Allègre, C.J. 1999: Global silicate weathering and CO_2 consumption rates deduced from the chemistry of large rivers. Chem. Geol., 159: 3-30.

Germ, M., Gaberščcek A. & Urbanc-Berčič, O. 1999: Aquatic macrophytes in the River Sava, Kolpa and Krka. Ichtyos, 16: 23-34.

Gibbs, R.J. 1972. Water chemistry of the Amazon River. Geochim. Cosmochim. Acta, 36: 1061-1066.

Gieskes, J.M. 1974. The alkalinity-total carbon dioxide system in seawater. In: Goldberg, E.D. (ed.): Marine chemistry of the sea, 5: 123-151.

Hrvatin, M. 1998. Discharge regimes in Slovenia. Geografski zbornik, XXXVIII: 60-87.

Huh, Y., Tsoi M.Y., Zaitsev A. & Edmond, J.M. 1998: The fluvial geochemistry of the rivers of Eastern Siberia: I. Tributaries of the Lena River draining the sedimentary platform of the Siberian Craton. Geochim. Cosmochim. Acta, 62:1657–1676.

Jacobson, A.D., Blum, J.D. & Walter, L.M. 2003: Reconciling the elemental and Sr isotope composition of Himalayan weathering fluxes: insights from the carbonate geochemistry of streams. Geochim. Cosmochim. Acta, 66/19: 3417-3429, http://dx.doi.org/10.1016/S0016-7037(02)00951-1

Jähne, B., Heinz, G. & Dietrich, W. 1987: Measurements of the Diffusion Coefficients of sparingly soluble gases in water. J Geophys Res Oceans, 92: 10767-10776.

Kanduč, T. 2006. Hydrogeochemical characteristics and carbon cycling in the Sava River watershed in Slovenia. PhD Dissertation. University of Ljubljana, Ljubljana: 141 p.

Kanduč, T., Szramek, K., Ogrinc, N. & Walter, L.M. 2007: Origin and cycling of riverine inorganic carbon in the Sava River watershed (Slovenia) inferred from major solutes and stable carbon isotopes. Biogeochemistry, 86: 137-154, doi:10.1007/s10533-007-9149-4

Kanduč, T., Kocman, D. & Ogrinc, N. 2008: Hydrogeochemical and stable isotope characteristics of the river Idrijca (Slovenia), the boundary watershed between the Adriatic and Black seas. Aquatic geochemistry, 14: 239-262, doi:10.1007/s10498-008-9035-2.

Kanduč T., Šturm, MB. & McIntosh, J. 2013. Chemical dynamics and evaluation of biogeochemical processes in alpine River Kamniška Bistrica, North Slovenia. Aquatic Geochemistry, 19:323-346, doi:10.1007/s10498-013-9197-4.

Kanduč, T., Samardžija, Z., Mori, N., Jerebic, A., Levačić, J., Kračun, M., Robinson, J.A., Žigon, S., Blažeka, Ž., Kocman, D. 2016: Hydrogeochemical and isotopic characterization of Pesnica River, Slovenia. Geologija, 59/2: 179-192, doi:10.5474/geologija.2016.010.

Levin, I., Kromer, B., Wagenback D. & Münnich, K.O. 1987: Carbon isotope measurements of atmospheric CO_2 at a coastal station in Antartctica. Tellus, 39B: 89-95.

Liu, Z. & Zhao, J. 2000: Contribution of carbonate rock weathering to the atmospheric CO_2 sink. Environmental Geology, 39:1053–1058, doi: 10.1007/s002549900072.

Mechora, Š. & Kanduč, T. 2016: Environmental assessment of freshwater ecosystems of the River Sava watershed and Cerkniško Lake, Slovenia, using the bioindicator species Fontinalis antipyretica: insights from stable isotopes and selected elements. Isotopes Environ. Isotopes in Environmental and Health Studies, 52/3:239-57, doi:10.1080/10256016.2016.1114933

Miyajima, T., Yamada, Y. & Hanba, Y.T. 1995: Determining the stable isotope ration of total dissolved inorganic carbon in lake water by GC/C/IRMS. Limnology Oceanography, 40:994-1000.

Mlakar, I. & Čar, J. 2009: Geological map of the Idrija - Cerkno hills between Stopnik and Rovte 1:25.000. Geological Survey of Slovenia.

Négrel, P. & Lachassagne, P. 2000: Geochemistry of the Maroni River (French Guiana) during the low water stage: implications for water--rock interactions and groundwater characteristics. Journal of Hydrology, 237:212–233, doi: 10.1016/S0022-1694(00)00308-5.

Parkhurst, D.L. & Appelo, C.A.J. 1999: User's guide to PHREEQC (version 2)-a computer program for speciation, batch –reaction, ne-dimensional transport, and inverse geochemical calculations. Water-Resources Investigations Report, 99-4259.

Pezdič, J. 1999: Izotopi in geokemijski procesi (In Slovene). Univerza v Ljubljani, Naravoslovnotehniška fakulteta, Oddelek za geologijo. Univerzitetni učbenik, Ljubljana: 269 p.

Radinja, D., Grbović, J., Povž, M., Zupan, M. & Skoberne, P. 1987: Kamniška Bistrica. In: Javornik, M. (ed.): Encyclopedia Slovenia 4. Mladinska knjiga, Ljubljana, pp 382 (in Slovene).

Raymond, P.A., Zappa, C.J., Butman, D., Bott, T.L., Potter, J., Mulholland, P., Lauersen, A.E., McDowell, W.H. & Newbold, D. 2012: Scaling the gas transfer velocity and hydraulic geometry in streams and small rivers. Limnology Oceanography Fluids Environment, 2: 41-53, doi:10.1215/21573689-1597669.

Reeder, S.W., Hitchon, B. & Levinson, A.A. 1972: Hydrogeochemistry of the surface waters of the Mackenzie River drainage basin, Canada: 1. Factors controlling inorganic composition. Geochim. Cosmochim. Acta, 36:181–192.

Roy, S., Gaillardet, J. & Allegre, C.J. 1999: Geochemistry of dissolved and suspended loads of the Seine River, France: anthropogenic impact, carbonate and silicate weathering. Geochimica Cosmochimica Acta, 63: 1277-1292, doi:10.1016/S0016-7037(99)00099-X.

Sarmiento, J.L. & Sundquist, E.T. 1992: Revised budget for the oceanic uptake of anthropogenic carbon –dioxide. Nature, 356/6370: 589-593.

Schulte, P., Van Geldern, R., Freitag, H., Karim, A., Négrel, P., Petelet-Giraud, E., Probst, A., Telmer, K., Veizer, J. & Barth, J.A.C. 2011: Applications of stable water and carbon isotopes in watershed research: weathering, carbon cycling, and water balances. Earth Science Review, 109: 20-31, doi:10.1016/j.earscirev.2011.07.003.

Spötl, C. 2005: A robust and fast method of sampling and analysis of $\delta^{13}C$ of dissolved inorganic carbon in ground waters. Isotopes Environ Health Stud, 41: 217-221.

Szramek, K., McIntosh, J.C., Williams, E.L., Kanduč, T., Ogrinc, N. & Walter, L.M. 2007: Relative weathering intensity of calcite versus dolomite in carbonate-bearing temperature zone watersheds: carbonate geochemistry and fluxes from catchments within the St. Lawrence and Danube river basin. Geochem Geophys, 8: 1-26, doi:10.1029/2006gc001337.

Zhang, J., Huang, W.W., Létole, R. & Jusserand, C. 1995: Major element chemistry of the Huange (Yellow River), China-weathering processes and chemical fluxes. J Hydrol., 168/1–4: 173-203, doi:10.1016/0022-1694(94)02635-O.

Žlebnik, L. 1971. Pleistocen Kranjskega, Sorškega in Ljubljanskega polja (In Slovene). Geologija, 14: 5–51.

Yang, C., Telmer, K. & Veizer, J. 1996: Chemical dynamics of the "St. Lawrence" riverine system: δD_{H2O}, $\delta^{18}O_{H2O}$, $\delta^{13}C_{DIC}$, $\delta^{34}S_{sulfate}$ and dissolved $^{87}Sr/^{86}Sr$. Geochim. Cosmochim. Acta, 60: 851-866, doi:10.1016/0016-7037(95)00445-9.

Internet resources:

Internet 1: http://srtm.csi.cgiar.org/ (18.10.2016)

Internet 2: http://www.arso.gov.si/en/ (18.10.2016)

Internet 3: http://www.bgr.de/karten/igme5000/igme.htm (18.10.2016)

GEOLOGIJA *60/1*, 27-35, Ljubljana 2017

https://doi.org/10.5474/geologija.2017.002

Groundwater vulnerability to nitrate pollution of alluvial aquifers in Slovenia – Lower Savinja Valley case study

Ranljivost podzemne vode glede na nitratno onesnaženje v aluvialnih vodonosnikih Slovenije – primer Spodnje Savinjske doline

Jože UHAN

Agencija Republike Slovenije za okolje, Vojkova 1b, SI-1000 Ljubljana, Slovenija;
e–mail: joze.uhan@gov.si

Prejeto / Received 29. 9. 2016; Sprejeto / Accepted 24. 4. 2017; Objavljeno na spletu / Published online 9.6.2017

Dedicated to Professor Jože Pezdič on the occasion of his 70th birthday

Key words: groundwater vulnerability, nitrate pollution, weights-of-evidence modelling
Ključne besede: ranljivost podzemne vode, nitratno onesnaženje, modeliranje teže evidenc

Abstract

The article introduced an upgraded approach to assessing the groundwater vulnerability to nitrate pollution. By using the results of field measurements and process-based models outputs, author takes into account effects of nitrogen biogeochemical processes, that were hitherto underestimated in the evaluation schemes. The upgraded methodological self-validated approach to vulnerability assessment in Lower Savinja Valley case study increases reliability and thus effectiveness of decision-making in the water management. This was achieved by using the process-based models outputs in the new pattern classification schemes with the predictions of pollution phenomena. Spatial prediction of groundwater nitrate pollution probability and vulnerability classification of the study area in Lower Savinja Valley was assessed by weights-of-evidence model (WofE). The increased degree of probability for the groundwater contamination with nitrates was determined for 62.5 percent of the aquifer area of the Lower Savinja Valley. About 27 percent of the most nitrate vulnerable areas in Lower Savinja Valley need groundwater nitrate mitigation through land-use measures and public sewage system construction.

Izvleček

Članek predstavlja nadgrajen pristop ocenjevanja ranljivosti na nitratno onesnaženje podzemnih voda. Ob uporabi rezultatov terenskih meritev in izhodov fizikalno zasnovanih modelov avtor upošteva tudi učinke dušikovih biogeokemičnih procesov, ki so bili v dosedanjih ocenjevalnih shemah podcenjeni. Nadgrajen metodološki samopotrditveni pristop ocenjevanja ranljivosti podzemne vode na primeru Spodnje Savinjske doline zvišuje zanesljivost in učinkovitost odločanja pri upravljanju voda. V ta namen so bili izhodi procesno zasnovanih modelov uporabljeni v novih prostorskih klasifikacijskih shemah, ki omogočajo napoved verjetnosti pojava onesnaženja. Z modelom teže evidenc WofE je bila ocenjena verjetnost pojava z nitratom onesnažene podzemne vode v študijsko izbranem aluvialnem vodonosniku. Povišana stopnja verjetnosti onesnažene podzemne vode z nitratom je bila ugotovljena na 62,5 odstotkih območja vodonosnika Spodnje Savinjske doline. Na okoli 27 odstotkih najbolj ranljivih območij Spodnje Savinjske doline so za zmanjšanje onesnaženosti podzemne vode z nitrati potrebni ukrepi na področju rabe prostora in izgradnje sistema odvodnje komunalne odpadne vode.

Introduction

Groundwater vulnerability maps are an important tool of the water management decision-making process. Information on groundwater vulnerability has been required by the Nitrate Directive (Official Journal of the European Communities, 1991b) and the Urban Waste Water Directive (Official Journal of the European Communities, 1991a) for nitrate pollution management and by the Water Framework Directive (Official Journal of the European Communities, 2000) for programme-of-measures planning. The Nitrate Directive initiated nitrate vulnerable zones as a land zonation for action plan implementation. The WFD operative programme of measures requires identification of the potentially vulnerable priority areas within groundwater bodies for cost-effective measures planning. Most of the previous groundwater vulnerability assessments used a variety of parametric point count methods with a relative rating for the potential of groundwater contamination, e.g. the DRASTIC index, developed as a linear combination of some of the intrinsic properties of aquifers (Aller et al., 1987) or the SINTACS index, adapted to conditions in the Mediterranean region (Civita, 1990). These methods require validation with field measurements, such as a tracer test, groundwater residence studies or investigation of actual pollution incidents. Gogu and Dassargues (2000) identified the integration of results from process-based models in vulnerability mapping techniques as a new research challenge in groundwater vulnerability assessment.

Groundwater nitrate pollution in Slovenian alluvial aquifers has been a major concern in recent years, and about 37 percent of the groundwater in these aquifers has poor chemical status according to WFD criteria, most frequently due to a high concentration of nitrate (Cvitanič et al., 2010). Process-based modelling outputs of groundwater recharge, groundwater flow velocity and nitrate leached from the soil profile in the Lower Savinja Valley aquifer with poor chemical status are available. With the use of statistical probabilistic classification methods, field-verified groundwater nitrate vulnerability was defined and interpreted with the help of surface-water and groundwater isotopic composition. The aim of this study was to assess the spatial prediction of the probability for increased groundwater nitrate concentration in order to plan the groundwater nitrate reduction measures and optimize the programme for monitoring the effects of these measures.

Study area

The Lower Savinja Valley, an area of about 80 square kilometres in Central Slovenia, was selected for this study of groundwater vulnerability to nitrate pollution. The area is situated in the tectonic trench between Kamnik-Savinja Alps on the north and "Posavje fault" tectonic system on the south. Lower Savinja Valley is a tectonic depression, filled with alluvial sediments from Pliocene, Pleistocene and Holocene period. The shallow unconfined Lower Savinja Valley aquifer consists of low permeable Pliocene sediments filling a Miocene depression. On top of the Pliocene sediments are deposited Pleistocene and Holocene layers (Buser, 1979), mainly gravel and sand with some interbedded conglomerate and clay intercalations (Uhan, 2011). The average thickness of middle- to low-permeable Pleistocene (K = $2.0 \cdot 10^{-5}$ m/s to $2.0 \cdot 10^{-4}$ m/s) and high-permeable Holocene sediments (K = $1.1 \cdot 10^{-3}$ to $1.1 \cdot 10^{-2}$ m/s) is up to 30 metres (Käss et al., 1976). Shallow eutric fluvisoils are prevalent on the sandy-gravely alluvium of the lowest terrace along the Savinja River (Fig. 1). Further away from the river, higher terraces on both sides are covered by variously deep eutric cambisoil. The northern part of the valley is covered with low-permeable eutric gleysoil (PKS, 2007). The Lower Savinja Valley aqui-

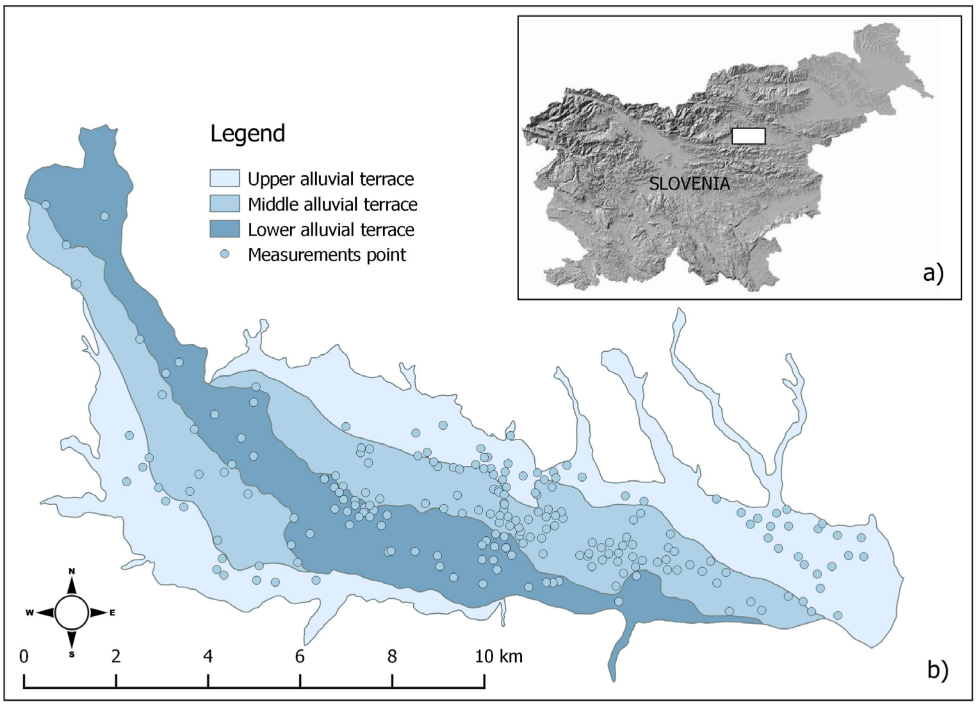

Fig. 1. a) Location of the Lower Savinja Valley study area and b) map of quaternary alluvial terraces with measurements points.

fer is alluvial lowland area, mainly recharged directly by precipitation from surface, and locally by infiltration from surface streams. The average annual precipitation is about 1100 mm and the surface runoff coefficient is very low. The groundwater table in the Lower Savinja Valley aquifer is shallow. According to the national groundwater monitoring network during the period 1986 - 2005, average depth to the groundwater is from 0.7 to 7.3 metres. Amplitude of the groundwater level is in the range of 1.4 m to 7.5 m.

The Lower Savinja Valley aquifer provides about five percent of the total renewable groundwater quantities of all Slovenian alluvial aquifers (Andjelov, 2009). An important part of Lower Savinja Valley regional water demand is covered by pumping groundwater from the alluvial aquifers of the plain, where, even a decade ago, conflicts of interest occurred among the local population due to agricultural activities. The region of Lower Savinja Valley is primarily renowned as the "valley of hops", with intensive hops production. One half of the Lower Savinja Valley aquifer area (50.4 %) is in use for agricultural purposes (20.9 % is pastures, 18.5 % fields and gardens, 8.5 % hops etc.), and 34 percent of the total area is urbanized (CEC, 1994). The sewage system is still in the process of construction in areas with highly dispersed urbanisation.

Recent analysis of national groundwater monitoring data from Lower Savinja Valley in the period 2006 - 2008 shows poor chemical status of groundwater (Cvitanič et al., 2010). The trend of nitrate concentration is statistically insignificant, showing no groundwater quality improvement. The nitrate concentration is higher than the EU maximum allowable concentration 50 mg/l for the drinking water limit value (Official Journal of the European Communities, 1980) in many wells and boreholes, including the main drinking water pumping station. A growing need exists for a more detailed delineation of the aquifer, and for spatial prediction of the probability for increased groundwater nitrate concentration in order to optimize the groundwater monitoring programme and the programme of measures.

Data and methods

A campaign of field measurements on a monthly basis was carried out in the period between 2008 and 2009. Multiprobe ion-specific electrodes with ±2 mg/l-N were controlled by a set of groundwater samples for laboratory nitrate determination using ion chromatography (ISO 10304-1:2007). Accuracy for the in-situ measurements of groundwater temperature, electrical conductivity, dissolved oxygen, pH and redox potential was ±0.1°C, ±0.001 mS/cm, ±0.2 mg/l, ±0.2 and ±20 mV respectively. Isotope information as interpretative support in the delineation of nitrate vulnerable zones was collected by seasonal sampling and determination of $\delta^{15}N$, $\delta^{15}N\text{-}NO_3^-$ and $\delta^{13}C$-DIC in selected surface flows and groundwaters during the period 2008 - 2009 (Uhan, 2011).

Monthly measurements of groundwater temperature averaged at 11.9 °C with the range of 9.7 and standard deviation of 2 °C. Electrical conductivity was in the range of 719 mS/cm with the 704.4 and 139.8 mS/cm as the average and the standard deviation respectively. The average of groundwater pH value was 7.2 with the range of 5.3 and standard deviation of 0.3. The groundwater nitrate concentration varied considerably from 0.8 to 119.9 mg/l with average of 46.4 and standard deviation of 25.8 mg/l. According to our analysis of variance (Uhan et al., 2009), most of the variance in nitrate concentrations in groundwater of Lower Savinja Valley was due to spatial variation. Hence, the field measurements have been extended to 224 randomly chosen groundwater nitrate monitoring locations (Fig. 1b).

Monitoring sites have been classified for further analysis into two groups on the basis of distribution of groundwater nitrate concentration with 20 mg/l as a threshold value. The threshold value to separate background and anomalous nitrate concentrations is necessary to be selected on the basis of distribution characteristics and not after the pre-established values, such as the EU threshold value or trigger value for uprising trends. The threshold value for groundwater nitrate vulnerability assessment in Lower Savinja Valley has been identified from the cumulative probability plot as the inflection point value (Panno et al., 2006; Masetti et al., 2009). The threshold value, adjusted to 20 mg/l in Lower Savinja Valley case study, defined as the cumulative probability plot inflection point, is interpreted to represent "anthropogenic impact" concentration of nitrate in groundwater (Uhan, 2011).

Among the different statistical approaches for pattern classification, including artificial neural networks and neuro-fuzzy classification systems, weights-of-evidence (WofE) was selected as the method with the highest prediction accuracy in the Lower Savinja Valley groundwater nitrate vulnerability case study. The WofE modelling technique (Bonham-Carter et al., 1988), as a part of the Arc Spatial Data Modeller extension (Kemp et al., 2001) implemented in ArcView GIS, is a data-driven method which combines known occurrences of phenomenon (training points) with available spatial data (predictor evidence) in a predictive response (phenomena occurrences conditional probability map). The WofE technique is based on the Bayesian idea of phenomena occurrences probability before (prior probability) and after consideration of any predictor evidence (posterior probability). The prior probability of the phenomena *P(D)* is the relation between the number of unit cells containing an occurrence (*D*) and total number of unit cells in the study area (*T*):

$P(D) = D/T$, expressed as odds by:

$$O(D) = \frac{P(D)}{1 - P(D)} = \frac{D}{T - D}$$

The probability of new phenomena on the basis of predictor evidence present (B) or absent ($\overline{B}$) is, after the Bayesian theorem, expressed as a posterior probability:

$$P(D|B) = P(D)\frac{P(B|D)}{P(B)} \quad , \quad P(D|\overline{B}) = P(D)\frac{P(\overline{B}|D)}{P(\overline{B})}$$

Prior and posterior probability of the *j*-th predictor map can be measured by positive (W^+) and negative weights (W^-), which indicate the association between a phenomena and a prediction pattern:

$$W_j^{\,+} = ln\frac{P(B_j/D)}{P(B_j/\overline{D})} \quad , \quad W_j^{\,-} = ln\frac{P(\overline{B}_j/D)}{P(\overline{B}_j/\overline{D})}$$

The difference between weights defines the contrast ($C=W^+-W^-$), which is the overall measure of spatial association between the training points and evidential theme. The contrast was used as a parameter for assessment of the pattern as a predictor. Absolute weights values under 0.5 are mildly predictive; between 0.5 and 1 are moderately predictive; and values above 1 are strongly predictive (Kemp et al., 2001).

Weights-of-Evidence modelling

After extensive sensitivity analysis of the available evidential themes, the outputs of three empirical/numerical models have been used as evidential themes for prediction of groundwater nitrate pollution probability and vulnerability classification of the study area: long-term groundwater recharge (Fig. 2a), nitrogen load in seepage water (Fig. 2b) and groundwater flow velocity (Fig. 2c).

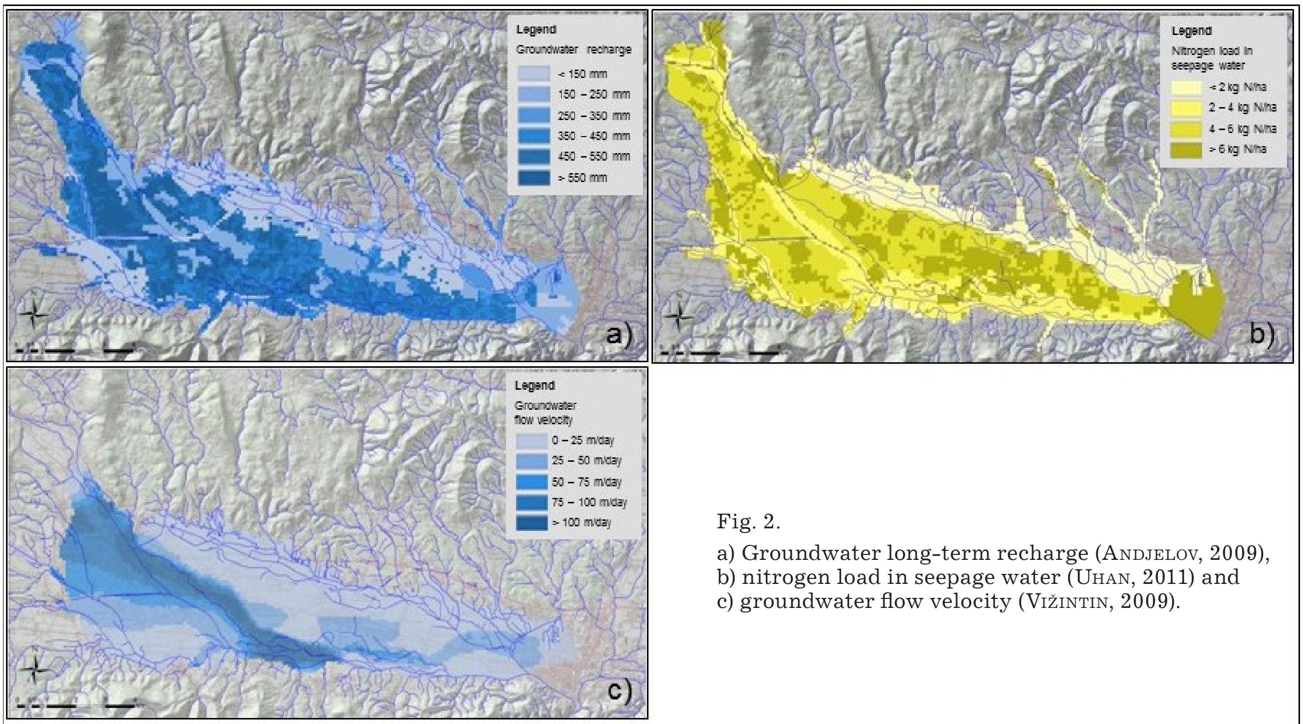

Fig. 2.
a) Groundwater long-term recharge (Andjelov, 2009),
b) nitrogen load in seepage water (Uhan, 2011) and
c) groundwater flow velocity (Vižintin, 2009).

The long-term groundwater recharge of the Lower Savinja Valley aquifer has been modelled with the GROWA water-balance model (Kunkel & Wendland, 2002) using high-resolution digital data of geology, topography, soil, land use, surface waters and climate. Real evapotranspiration was calculated according to the method of Renger and Wessolek (1996), using the national meteorological monitoring database. In order to determine groundwater recharge, a runoff separation was performed. The model was validated using the national hydrological monitoring database, and the Nash-Sutcliff model efficiency coefficient 0.79 indicated good simulation (Andjelov, 2009). The 2008 annual average of groundwater recharge in Lower Savinja Valley was about 320 millimetres.

The nitrogen load in seepage water in Lower Savinja Valley was modelled with the De-Nitrification-DeComposition biogeochemical model (DNDC), developed as a field-scale, process-based, mechanistic model of N and C dynamics in agroecosystems (Li et al., 1992). DNDC consists of the six sub-models for soil climate, crop growth, decomposition, nitrification, denitrification, and fermentation. The six interacting sub-models include the fundamental factors and reactions, which integrate carbon and nitrogen cycles into a computing system. Using the data of climate, soil and use lande of Lower Savinja Valley, nine simulations for 2008 were performed based on the different scenario and combinations of soils and crops. Nitrogen leaching rates for the year 2008 modelled by DNDC in Lower Savinja Valley are in range from 1.7 to 36.9 kilograms of nitrogen per hectare. The comparison of the DNDC / GLEAMS model results for Latkova vas field experiment from year 2000 indicate the adequacy of DNDC model use in further vulnerability studies of shallow alluvial aquifers.

Groundwater flow velocity has been calculated through hydraulic potentials with the numerical solution of the diffusion equation, estimated with the finite element subsurface flow and transport simulation system FEFLOW (Diersch, 2009). The groundwater model of Lower Savinja Valley modelled a two-layer aquifer with one water table (Vižintin, 2009). The values of hydraulic conductivity of Holocene sediments range from $8 \cdot 10^{-3}$ m/s to $5 \cdot 10^{-2}$ m/s and the values of hydraulic conductivity of Pleistocene sediments are to be found around 10^{-4} m/s. A structural palaeodepression is taken into consideration north of the present bed of the river Savinja, which represents its former riverbed with increased hydraulic conductivity. Modelled groundwater flow velocity was in the range of up to 25 metres per day in the major part of the aquifer, increasing to 100 metres a day in the zones of preferential groundwater flows (Vižintin, 2009).

The output data layers of the above mentioned models have been generalized and uniformly used as input in weights-of-evidence modelling for delineation of relative groundwater nitrate vulnerable zones as a response theme map (Fig. 3).

Results and discussion

The training data set in the Lower Savinja Valley aquifer consists of data from 170 groundwater wells and piezometers with a concentration of nitrate above the threshold value. The measurement locations with a concentration higher than 20 mg NO_3^- per litre of groundwater have been considered as training points. The spatial association between the training data points and the evidential theme classes has been initially calculated as contrast (*C*), which combines the effects of the positive and negative weights ($C=W^+-W^-$). Due to a relatively small number of wells and piezometers with nitrate pollution, evidential themes with many classes result in noisy and unreliable estimates of weights. It is these advantageous to generalize and simplify themes in these cases (Bonham-Carter et al., 1989). Evidential themes in Lower Savinja Valley have been generalized with the maximization of the contrasts, which resulted in: six classes for groundwater recharge, four classes for nitrogen load and five classes for groundwater flow velocity. According to the calculated confidence value, the most important contribution to the final response theme was assessed for the groundwater recharge evidential theme, followed by the nitrogen load evidential theme. High values (> 95 %) of the ratio between the posterior probability and its standard deviation in the 97 % of the modeled area indicate that the uncertainty is relatively small compared to the probability value itself. Conditional independence among the evidential themes used in the model, as an important assumption of the WofE model was calculated at 0.93, being within the range 1±0.15 that generally indicates no dependence amongst evidential themes (Baker et al., 2007).

Evidential themes, representing groundwater recharge, nitrogen load and groundwater flow velocity, were applied to generate the response theme with posterior probability values ranging from 0.00135 to 0.0997. The response theme values describe the relative probability that a 100×100 metre spatial unit will have a groundwater nitrate concentration higher than the training points threshold value of 20 mg/l with regard to the prior probability value of 0.0216. Based on the definition of the training point, higher posterior probability values correspond with more groundwater vulnerable cells and lower posterior probability values correspond to less vulnerable areas. The highest probability of groundwater nitrate vulnerability zones has been found to be generally in the southeastern part of the Lower Savinja Valley aquifer.

The WofE posterior probability response theme of the Lower Savinja Valley aquifer was separated into three classes of relative nitrate vulnerability based on the distinction in a chart of the cumulative study area vs. posterior probability values. The vulnerability class breaks were defined by selecting discontinuity in the graph of posterior probability vs. cumulative percent of the modelled area, where was a significant increase in probability detected: 0.022 and 0.034. Higher posterior probability values correspond with more vulnerable areas, based on the definition of training. The most sensitive area has been mostly designated within the lower and middle alluvial terrace of Lower Savinja Valley. A significant part of the drinking water protection areas is most vulnerable to groundwater nitrate pollution with high risk due to groundwater nitrate transport in the saturated zone from upstream sites of the aquifer.

The parametric point count methods are generally not able to describe and analyse important physical processes, such as nitrification/denitrification and nitrate dilution in the aquifer (Debernardi et al., 2008). The knowledge of geochemical processes and pollution sources is necessary for interpretation of the groundwater vulnerability results and the isotopic signature of nitrate in groundwater is valuable evidence (Uhan, 2011). Correlation between the groundwater nitrate concentrations and isotope $\delta^{15}N$ in groundwater nitrate suggested that part of the aquifer was influenced by denitrification, especially at measurement points in the northern heavy soils area of the aquifer. In these areas, decreased dissolved oxygen was measured and the model assessed the lowest groundwater nitrate posterior probability. According to Kendall (1998) ranges of $\delta^{15}N$ values for the major sources of nitrogen in the hydrosphere, the isotope $\delta^{15}N$ in Lower Savinja Valley groundwater nitrate suggests predominant soil (cultivation sources) and/or manure/septic waste nitrate sources. The range of $\delta^{15}N\text{-}NO_3^-$ isotope values in the groundwater of Lower Savinja Valley is between +5.11 ‰ and + 21.90 ‰, which falls inside the range, found in areas with comparable hydrogeological setting and land use in the northeastern part of Slovenia (Pintar, 1996; Pezdič, 1999). The $\delta^{15}N\text{-}NO_3^-$ isotope values in samples from rivers in Lower Savinja Valley were ranged between +3 ‰ and +13 ‰ and grouped together with some groundwater samples from locations where the hydrological impact of the surface water on the groundwater flow regime was significant. The $\delta^{15}N\text{-}NO_3^-$ and $\delta^{13}C$-DIC relation reflects the importance of internal and external

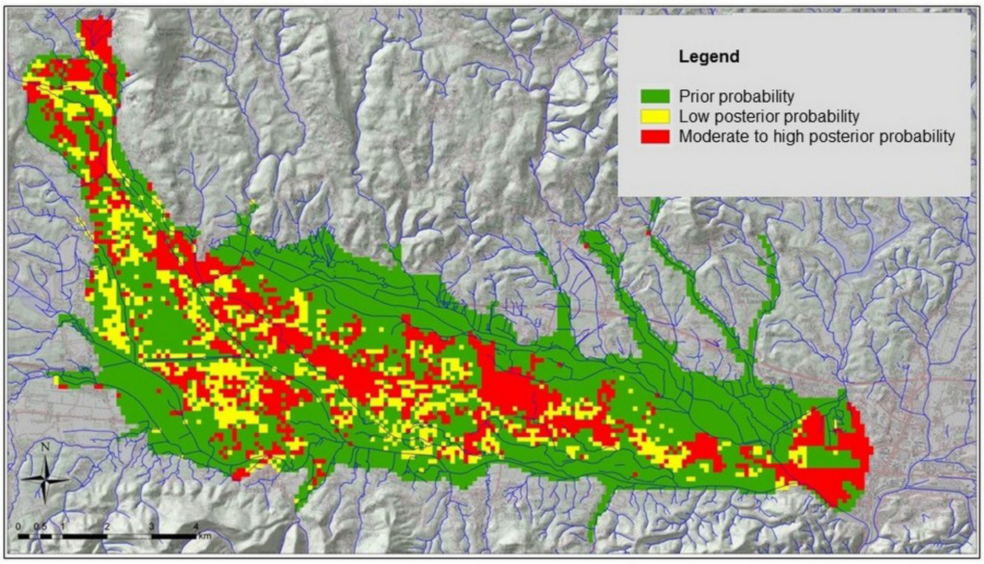

Fig. 3. Map of relative groundwater nitrate vulnerability assessed by WofE probability approach.

sources of dissolved carbon and nitrogen and the degree of processes in the aquifer. The shift in δ^{13}C-DIC toward more negative values was indicative of an isotopically light carbon source as oxidation of organic carbon. The isotope information of predominant soil and manure/septic waste nitrate origin, associated with other local physical and chemical boundary conditions and land use data, offers an interpretative support in the delineation of nitrate vulnerable zones (Uhan, 2011; Uhan et al., 2011a; 2011b).

Conclusions

The model outputs of long-term groundwater recharge, nitrogen load in seepage water and groundwater flow velocity were found to be the most relevant evidential themes for the groundwater nitrate vulnerability study of the Lower Savinja Valley aquifer. Through the application of these process-based model results and groundwater field measurements, the efficiency of probability classification weights-of-evidence (WofE) approach to provide verified groundwater nitrate vulnerable maps was tested. The study highlights the superiority of the WofE model over the parametric point count relative rating approaches. The WofE model results show the highest prediction accuracy and the response theme very well illustrates groundwater vulnerability potential as a posterior probability for increased groundwater nitrate concentration. WofE model generation is dependent upon a training dataset and the results in the self-validation model output as a probability map, displayed in classes of relative vulnerability. About 27 percent of the most nitrate vulnerable areas in Lower Savinja Valley need groundwater nitrate mitigation through land-use measures and public sewage system construction.

The lowest probability of groundwater nitrate vulnerability was determined in the areas with indicated denitrification processes. Field measurements and isotope analysis of groundwater in these parts of Lower Savinja Valley aquifer revealed anoxic conditions. The isotope information of predominant soil and manure/septic waste nitrate origin, associated with other local physical and chemical boundary conditions and land use data, offered interpretative support in the delineation of nitrate vulnerable zones. To achieve a more precise nitrate source or mixing sources determination, more complex isotopic composition would be needed.

The methodology outlined in this study for nitrate contaminant vulnerability analysis, using process-based models and the statistical classification method, can be applied to other areas with a similar hydrogeological setting to get a better characterization of the nature of the contamination. The present study again underlines the importance of redox conditions and denitirification processes for regional groundwater nitrate distribution. The results, obtained in this case study, lead us to envisage additional monitoring programs, focused on a field measurements technique and water sampling for isotopes. In the future, an extensive field groundwater profile measurement program will be of great importance in order to be able to identify contamination sensitivity of the aquifer throughout its vertical extent and to optimize the groundwater protection management strategy.

Acknowledgements

Author gratefully dedicates this article to his PhD advisor, Full Professor Jože Pezdič, PhD, who greatly contributed to the successful completion of this research study through both his scientific as well as pedagogical dimensions.

This study was supported by the Slovenian Environment Agency and represents part of the Ph.D. research work. The author would like to thank Vlado Savić, Janja Turšič and Mišo Andjelov for their essential support during this study. Many thanks to Katherine Artzner for language review.

References

Andjelov, M. 2009: Modeliranje napajanja vodonosnikov za oceno količinskega stanja podzemnih voda v Sloveniji v letu 2006. 20. Mišičev vodarski dan – zbornik referatov, 126-130.

Aller, L., Bennet, T., Lehr, J.H., Petty, R.J. & Hackett, G. 1987: DRASTIC: A Standardized System for Evaluating Ground Water Pollution Potential Using Hydrogeological Settings. U.S. Environmental Protection Agency, Washington: 622 p.

Baker, A.E., Wood, A.R & Cichon, J.R. 2007: The Marion County Aquifer Vulnerability assessment. Marion County Project No. SS06-01: 42 p.

Bonham-Carter, G.F., Agterberg, F.P. & Wright, D.F. 1988: Integration of geological datasets for gold exploration in Nova Scotia. Photogrammetry and Remote Sensing, 54: 1585-1592.

Bonham-Carter, G.F., Agterberg, F.P. & Wright, D.F. 1989: Weights of evidence modelling: a new approach to mapping mineral potencial. In: Agterberg, F.P. & Bonham-Carter, G.F. (eds.): Statistical application in the earth sciences. Geological Survey of Canada: 171-183.

Buser, S. 1979: Osnovna geološka karta SFRJ = Basic geological map of SFRY 1:100.000. Tolmač lista Celje – Explanatory Book to the sheet Celje: L 33-67. Zvezni geološki zavod, Beograd: 72 p.

Civita, M. 1990: La valutazione della vulnerabilitŕ degli acquiferiall'inquinamento - Assessment of aquifer vulnerability to contamination. Proc 1st Conv. Naz. Protezione e Gestione delle Acqe Sotterranee: Metodologie, Technologie e Obiettivi, Marano sul Panaro, 3: 39-86.

CLC 2000: Geografski informacijski sistem ARSO – Geographic information system ARSO. Internet: http://gis.arso.gov.si/geoportal (6. 11. 2010)

Cvitanič, I., Dobnikar Tehovnik, M., Gacin, M., Grbović, J., Jesenovec, B., Kozak-Legiša, Š., Krajnc, M., Kuhar, U., Mihorko, P., Poje, M., Remec-Rekar, Š., Rotar, B., Sever, M., Sodja, E., Andjelov, M., Mikulič, Z., Pavlič, U., Savić, V., Souvent, P., Trišič, N. & Uhan, J. 2010: Vode v Sloveniji: ocena stanja voda za obdobje 2006-2008 po določilih okvirne direktive o vodah – Waters in Slovenia: Status assessment for the period 2006-2008 according to the Water Framework Directive. Ministrstvo za okolje in prostor, Agencija RS za okolje, Ljubljana: 62 p.

Debernardi, L., Deluca, D.A. & Lasagna, M. 2008: Correlation between nitrate concentration in groundwater and parameters affecting aquifer intrinsic vulnerability. Environmental Geology, 55/3: 539–558, doi:10.1007/s00254-007-1006-1.

Diersch, H-J. 2009: FEFLOW 5.4 Finite element subsurface flow and transport simulation system. Users manual, WASY Software, Berlin: 202 p.

Gogu, C. & Dassargues, A. 2000: Current trends and future challenges in groundwater vulnerability assesment using overlay and index methods. Environmental Geology, 39/6: 549-559, doi:10.1007/s002540050466.

ISO 10304-1 2007: Water quality - Determination of dissolved anions by liquid chromatography of ions - Part 1: Determination of bromide, chloride, fluoride, nitrate, nitrite, phosphate and sulfate. ISO 10304-1:2007.

Käss, W., Drobne, F. & Bukvič, B. 1976: Markierung unterirdischer Wässer Untersuchungen in Slowenien 1972-1975. B. Markierung von Porengrund-wässer, 1. Untersuchungen im Quartär des Savinja Tals. Third International Symposium of Underground Water Tracing. Graz: 219-238.

Kemp, L.D., Bonham-Carter, G.F., Raines, G.L. & Looney, C.G. 2001: Arc-SDM: Arcview extension for spatial data modelling using weights of evidence, logistic regression, fuzzy logic and neural network analysis. Internet: http://www.ige.unicamp.br/sdm/ (10. 2. 2008).

Kendall, C. 1998: Tracing nitrogen sources and cycling in catchments. In: Kendall, C. & Mcdonnell, J.J. (eds.): Isotope tracers in catchment hydrology. Elsevier: 519-576.

Kunkel, R. & Wendland, F. 2002: The GROWA98 model for water balance analysis in large river basins – the river Elbe case study. Journal of Hydrology, 259: 152-162.

Li, C.S., Frolking, S. & Frolking, A.T. 1992: A Model of Nitrous Oxide Evolution From Soil Driven by Rainfall Events: 1. Model Structure and Sensitivity. Journal of Geophysical Research, 97/D9: 9759-9776.

Masetti, M., Sterlacchini, S., Ballabio, C., Sorichetta, A. & Poli, S. 2009: Influence of threshold value in the use of statistical methods for groundwater vulnerability assessment. Science of the Total Environment, 407: 3836-3846.

Official Journal of the European Communities, 1980: Direktiva Sveta 80/778/EGS z dne 15. julija 1980 o kakovosti vode, namenjene za prehrano ljudi = Council Directive of 15 July 1980 relating to the quality of water intended for human consumption. Official Journal of the European Communities, L 229: 11–29.

Official Journal of the European Communities, 1991a: Direktiva Sveta ES 91/271/EEC z dne 21. maj 1991 o čiščenju komunalne odpadne vode = Council Directive 91/271/EEC of 21 May 1991 concerning urban wastewater treatment. Official Journal of the European Communities, L 135: 40–52.

Official Journal of the European Communities 1991b: Direktiva Sveta ES 91/676/EEC z dne 12. decembra 1991 o varstvu voda pred onesnaževanjem z nitrati iz kmetijskih virov = Council Directive 91/676/EEC of 12 December 1991 concerning the protection of waters against pollution caused by nitrates from agricultural sources. Official Journal of the European Communities, L 375: 1–8.

Official Journal of the European Communities 2000: Direktiva Evropskega parlamenta in Sveta ES 2000/60/EEC z dne 23. oktobra 2000 o določitvi okvira za ukrepe Skupnosti na področju vodne politike = Directive 2000/60/EC of the European Parliament and of the Council of 23 October 2000 establishing a framework for Community action in the field of water policy. Official Journal of the European Communities, L 327: 1–73.

Panno, S.V., Kelly, W.R., Martinsek, A.T. & Hackley, K.C. 2006: Estimating background and threshold nitrate concentrations using probability graphs. Ground Water, 44/5: 697-709, doi:10.1111/j.1745-6584.2006.00240.x

Pezdič, J. 1999: Izotopi in geokemijski procesi = Isotopes and gechemical processes. Naravoslovnotehniška fakulteta, Oddelek za geologijo, Ljubljana: 269 p.

Pintar, M. 1996: Vpliv kemijske dejavnosti na koncentracijo nitratov in atrazina v vodah Apaškega polja = Impact of agricultural activities on the concentrations of nitrate and atrazine in the waters of Apaško polje. Magistrska naloga. Univerza v Ljubljani, Biotehniška fakulteta, Ljubljana: 106 p.

PKS 2007: Pedološka karta Slovenije – Pedological map of Slovenia. Ministrstvo za kmetijstvo, gozdarstvo in prehrano. Internet: http://rkg.gov.si/GERK/ (10. 2. 2008).

Renger, M. & Wessolek, G. 1996: Berechnung der Verdunstungsjahressummen einzelner Jahre. DVWK-Merkblätter zur Wasserwirtschaft, 238: 47 p.

Uhan, J., Pezdič, J., Savić, V., Andjelov, M. & Turšič, J. 2009: Hidrogeološki faktorji prostorske in časovne porazdelitve nitrata v podzemni vodi Spodnje Savinjske doline. Geološki zbornik, 20: 177-182.

Uhan, J. 2011: Ranljivost podzemne vode na nitratno onesnaženje v aluvialnih vodonosnikih Slovenije = Groundwater vulnerability to nitrate pollution of alluvial aquifers in Slovenia. Doktorska disertacija. Univerza v Ljubljani, Naravoslovnotehniška fakulteta, Oddelek za geologijo, Ljubljana: 163 p.

Uhan, J., Brilly, M., Pintar, M., Vižintin, G., Trček, B. & Pezdič, J. 2011a: The impact of anoxic conditions on regional groundwater nitrate distribution and vulnerability assessment. International conference: 19th to 21st September 2011, South Africa, Pretoria: 1 p.

Uhan, J., Lojen, S., Pintar, M. & Pezdič, J. 2011b: Groundwater nitrate sources in alluvial aquifers: Isotope case study in Savinja Valley (Slovenia). In: Deménz, A. & Fóriys, I. (eds.): Isotope Workshop XI, Budapest, Central European Geology, 54/1-2: 29-33, doi:http://dx.doi.org/10.1556/CEuGeol.54.2011.1-2.4.

Vižintin, G. 2009: Nestacionarni 3D model toka podzemne vode na Spodnjesavinjskem polju – Nonstationary 3D groundwater flow model for Lower Savinja Valley. Univerza v Ljubljani, Naravoslovnotehniška fakulteta, Oddelek za geotehnologijo in rudarstvo: 43 p.

GEOLOGIJA *60/1*, 37-47, Ljubljana 2017
https://doi.org/10.5474/geologija.2017.003

Water retention properties of stiff silt

Retencijske lastnosti trdnih meljev

Barbara LIKAR[1], Vikica KUK[2] & Karmen FIFER BIZJAK[1]

[1]Barbara Likar, ZAG, Dimičeva ul. 12, SI-1000 Ljubljana, Slovenia; e-mail: barbara.likar@zag.si
[2]Vikica Kuk, Žegar 33, SI-3262 Prevorje, Slovenia; e-mail: vikica.kuk@gmail.com
[1]Fifer Bizjak Karmen, ZAG, Dimičeva ul. 12, SI-1000 Ljubljana, Slovenia; e-mail: karmen.fifer@zag.si

Prejeto / Received 9. 5. 2016; Sprejeto / Accepted 20. 4. 2017; Objavljeno na spletu / Published online 9.6.2017

Dedicated to Professor Mihael Ribičič on the occasion of his 70th birthday

Key words: stiff sandy silt, suction, Bishop - Wesley triaxial cell, water retention curve, potentiometer WP4C
Ključne besede: Trden peščeni melj, sukcija Bishop – Wesley triaksialna celica, retencijska krivulja, potenciometer WP4C

Abstract

Recent research into the behaviour of soils has shown that it is in fact much more complex than can be described by the mechanics of saturated soils. Nowadays the trend of investigations has shifted towards the unsaturated state. Despite the significant progress that has been made so far, there are still a lot of unanswered questions related to the behaviour of unsaturated soils. For this reason, in the field of geotechnics some new concepts are developed, which include the study of soil suction.

Most research into soil suction has involved clayey and silty material, whereas up until recently no data have been available about measurements in very stiff preconsolidated sandy silt. Very stiff preconsolidated sandy silt is typical of the Krško Basin, where it is planned that some very important geotechnical structures will be built, so that knowledge about the behaviour of such soils at increased or decreased water content is essential.

Several different methods can be used for soil suction measurements. In the paper the results of measurements carried out on very stiff preconsolidated sandy silt in a Bishop - Wesley double-walled triaxial cell are presented and compared with the results of soil suction measurements performed by means of a potentiometer (WP4C). All the measurement results were evaluated taking into account already known results given in the literature, using the three most commonly used mathematical models. Until now a lot of papers dealing with suction measurements in normal consolidated and preconsolidated clay have been published. Measurements on very stiff preconsolidated sandy silt, as presented in this paper were not supported before.

Izvleček

Zadnje geomehanske raziskave zemljin kažejo na to, da je njihovo obnašanje veliko bolj kompleksno, kot se to lahko opiše z modeli za saturirane zemljine. Danes se trend raziskav nagiba v področje nesaturiranih materialov. Kljub velikim premikom na tem področju ostaja še vedno veliko vprašanj povezanih z obnašanjem materialov v nesaturiranem območju, zato so se v geotehniki uveljavili novi koncepti modelov, ki vključujejo študij sukcije.

Večina preiskav sukcije je osredotočenih na normalno konsolidirani glineni ali meljni material, medtem ko rezultatov preiskav v trdnem, prekonsolidiranem peščenem melju, po dosedaj znanih podatkih, ni objavljenih. Trdni, prekonsolidirani peščeni melj je tipičen za Krško kotlino, kjer se bodo gradili večji geotehnični objekti, in je poznavanje sukcije materiala ob povišanju vlage v njem bistvenega pomena.

Za meritev sukcije je bilo uporabljenih več različnih metod. V članku so predstavljeni rezultati meritve sukcije trdnega peščenega melja v Bishop - Wesley dvostenski triosni celici in primerjava z rezultati meritev sukcije v potenciometru (WPC4). Rezultati so potrjeni z matematičnimi modeli, ki so v tovrstni literaturi najbolj poznani. Rezultati raziskav predstavljajo prispevek k poznavanju obnašanja prekonsolidiranega trdnega peščenega melja v nesaturiranih pogojih.

Introduction

Recent research into the behaviour of soils has shown that it is in fact much more complex than can be described by the mechanics of saturated soils. The general field of soil mechanics can be sub-divided into that part which deals with saturated soils and that part which deals with unsaturated soils. Nowadays the trend of investigations has shifted towards the unsaturated state. Despite the significant progress that has been made so far, there are still a lot of unanswered questions related to the behaviour of unsaturated soils. This refers in particular to the changes in volume and strength which occur in the soil. Under certain conditions soils may behave very unpredictably, either through a rapid increase in their volume (swelling) or by (structural) collapse. For this reason, in the field of geotechnics some new concepts, which include the study of soil suction, are now being introduced.

Several methods for measuring soil suction are known, i.e. measurements with a stick tensiometer, with a potentiometer, with a pressure plate extractor and filter paper. These methods can provide reliable information at both high and very low suctions, whereas in the intermediate zone measurements can be unreliable.

This deficiency can be remedied by using of the Bishop - Wesley double-walled triaxial cell, which can provide very precise measurements of changes which occur in the volume of water and air in the pores.

In geotechnical engineering, soil suction is an important parameter which is used in the design and construction of buildings, roads, tunnels, hydropower dams, and deep excavations, as well as for the construction of sealing layers and covers for surface waste deposits, and elsewhere. Suction also needs to be studied in the case of landslides. Numerous research projects have been performed, including geotechnical and environmental aspects, in connection with waste disposal and ground pollution. Special attention has been focused on the question of the swelling of soils after compaction into sealed layers for the covering of radioactive waste deposits (Umedera et al., 1996; Delage, 2002).

Numerous authors have also studied the impact of soil suction on the triggering of landslides in unsaturated soils (Tofani et al., 2006; Lu & Godt, 2008; Godt et al., 2009), some of them (Ng et al., 2003; Springman, 2011) with the help of artificially caused precipitation.

In recent years quite a lot of research has been performed in Slovenia, too, in connection with various geotechnical structures (Maček et al., 2006; Petkovšek, 2006, Maček, 2006). Based on the results of the laboratory investigations (Petkovšek, 2006), the favourable impact of soil suction on the strength characteristics of bentonite, very stiff clay (i.e. „Sivica“), and flysch material was determined. Apart from laboratory tests, in situ soil suction measurements have been performed in Slovenia, since 2004, on the Lenart - Cogetinci - Vučja vas motorway section, where an embankment of swelling clay was stabilized by lime (Petkovšek, 2008) and the effect of soil suction on the stability of the large Slano blato landslide was examined by Maček (2012).

Until now lot of papers dealing with suction measurements in normal consolidated and preconsolidated clay have been published, but no such measurements on very stiff preconsolidated silt, as it is found in the Krško Basin, are mentioned. Since several important geotechnical structures will be built in this area, it was necessary to carry out more detailed measurement of the soil suction occurring in this material.

Background

The soil suction has been defined as the energy level of the pore water in soils (Suescun Florez, 2010). It is the result of the adsorption of water onto mineral grains, together with a capillary phenomenon and the osmotic effects of the salt in the pore water. It can also be labelled as a measure of the energy that attracts water into the structure of the soil, or keeps it there. It is perceived as a tensile stress of the water in the soil, or as a negative pore water pressure (Marshall & Holmes, 1988).

Three types of soil suction are known: matrix suction, osmotic suction, and total suction. Total soil suction is defined as the sum of the matrix suction and the osmotic suction, and is written as:

$$\psi = (u_a - u_w) + \pi \qquad (1)$$

Where: ψ is the total suction, $(u_a - u_w)$ is the matrix suction, and π is the osmotic suction.

From Equation (1) it can be seen that the matrix suction is defined as the difference between the pore pressure of air (u_a) and the pore pressure of water (u_w). It is in fact defined as the energy which is needed to remove water from the soil matrix or from its structure, without any changes to the physical state of the water. Matrix suction occurs as a result of the capillary phenomenon, the soil structure, and the adsorption of water onto the mineral grains (Bulut et al., 2001). Osmotic suction (π) is a consequence of the concentration of salt dissolved in the water, and is independent of the pressure.

If it is assumed that the osmotic suction is zero, then the change in total suction equals to the change in the matrix suction.

$$\psi = (u_a - u_w) \tag{2}$$

Suction can be expressed per unit volume, mass or weight. The unit expressed per unit volume is given in pascals (Pa), bars (bar), or atmospheres (atm).

The soil-water characteristic curve (SWCC)

The soil-water characteristic curve, sometimes referred to as a „water retention curve“, is a curve which describes the relationship between the suction and the water content, so that it predicts the behaviour of soil in the drying phase (i.e. desaturation) and the wetting phase (i.e. saturation). The shape of the water retention curve depends on many factors, from the density of the soil, its adsorption capacity, the size of the pores in the soil, whether the soil is in a drying or wetting phase, and also on the mathematical model used for the calculation of the retention curve. In most cases, the water retention curve, which covers a range between 0 and 10^6 kPa, has a characteristic „S“ shape (Fredlund & Xing, 1994). Since suction values can be very high, retention curves are usually presented as graphs on a logarithmic scale.

A typical water retention curve is shown in Figure 1, where three identifiable sections can be observed: the saturation zone, the desaturation zone, and the residual zone. Two changes in the slope can also be seen, one at the point of air entry and the other at the point of residual water content. The soil is completely saturated in the saturation zone, where the suction is too small to drain the pores. Between the air-entry value and the point of residual water content there is a desaturation zone. This is the zone where the water in the pores is increasingly displaced by air. Within this zone, the suction is higher than the suction at the air entry value (Kayadelen et al., 2007). The air entry value is the point where the large pores begin to be drained due to the increase of suction (Fredlund et al., 2011), as air enters them. The residual zone is an area where the transport of water in the soil is only possible by means of water vapour.

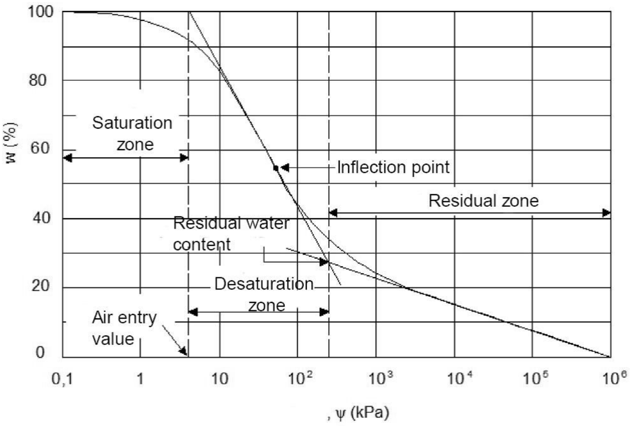

Fig. 1. A typical retention curve (SWCC: soil-water characteristic curve) (after Fredlund et al., 2011 and Kayadelen et al., 2007).

The water retention curves could represent the drying phase (desaturation) or the rewetting phase (saturation). In the paper the results for the drying phase will be presented.

Mathematical models for water retention curves

Various authors have suggested different empirical equations and mathematical models for water retention curves. They can be defined as a function of the suction depending on the degree of saturation, or on the normalized water content. The following models are most frequently used, in which the water retention curve is expressed as a function of the volumetric (i.e. normalized) water content.

Brooks & Corey (1964):

$$\begin{cases} \theta(\psi) = \theta_{sat} & \psi < \psi_{ae} \\ \theta(\psi) = \theta_{sat}\left(\dfrac{\psi}{a}\right)^{-n} & \psi \geq \psi_{ae} \end{cases} \tag{3}$$

where: a and n are the fitting parameters determined by the method of minimum square roots,

ψ is the soil suction, θ_R is the residual water content, θ_{sat} is the volumetric water content at complete saturation, and ψ_{ae} is the air-entry value .

Brooks and Corey (1964) divided the equation into two parts. In the first part the suction is smaller than the air-entry value, whereas in the second part it is greater than the air entry value (Fredlund et al, 2011).

Fredlund & Xing (1995):

$$\theta = \left[1 - \frac{ln\left(1 + \frac{\psi}{\psi_R}\right)}{ln\left(1 + \frac{10^6}{\psi_R}\right)}\right] \cdot \left[\frac{\theta_{sat}}{\left(ln\left(e + \left(\frac{\psi}{a}\right)^n\right)\right)^m}\right] \quad (4)$$

where: θ_{sat} is the volumetric water content at complete saturation, ψ is the soil suction, ψ_R is the soil suction at the residual water content, and a, n, and m are curve-fitting parameters.

van Genuchten (1980):

$$\Theta_n = \frac{\theta - \theta_R}{\theta_{sat} - \theta_R} = \frac{1}{\left[1 + \left(\frac{\psi}{a}\right)^n\right]^m} \quad (5)$$

where: θ_R – is the residual volumetric water content, and a, n, and m are curve-fitting parameters.

Soil suction retention curves were in the presented paper calculated by using the described mathematical models. The function parameters were determined in Excel by using the Least Squares Method, and the retention curves which best fitted with the measured values were defined.

Experimental techniques

Several different methods can be used for soil suction measurements. In the paper the results of measurements carried out on very stiff sandy silt in a Bishop - Wesley double-walled triaxial cell are presented and compared with the results of soil suction measurements performed by means of a potentiometer (WP4C).

Soil suction measurements using a Bishop-Wesley double-walled triaxial cell

The double wall triaxial cell is an improved traditional triaxial cell. Its advantage lies in its double wall cell, which provides constant conditions and thus enables the performance of accurate measurement of the changes which occur in the sample's volume. In conventional triaxial systems water can enter into the saturated sample, or can be pumped out of it. At the same time the air pressure in the sample can be changed, which could influence to the volume expansion of the sample.

On the other hand, in the double wall triaxial cell, the same cell pressure inside and outside the cell ensures that the volume changes of the water in the inner cell is only the consequence of changes in the volume of the sample and not due to external influences (e.g. changes in the cell volume due to the water temperature). These changes lead to changes in the volume of water in the outer cell, which provides constant conditions for the internal chamber.

The double wall triaxial cell ensures accurate measurement of matric suction within the range from 0 to 1500 kPa, depending on which porous plate is used.

The main parts of the double triaxial cell are (Fig. 2):

- a base pedestal on which the sample is placed,
- an inner cell and outer cell that are both cylindrical in shape and, after installation, are filled with water,
- a vertical force transducer together with a hydraulically powered system for vertical loading,
- a pore pressure transducer,
- an axial displacement transducer,
- a pressure gauge in the lower chamber,
- 5 electromechanical volume pressure controllers (VPC) for measuring and setting the air and water pressures and for measuring the volume changes,
- a coarse porous disk
- a porous plate with high air-entry value (a HAEPD: high air entry porous disk).

The entire system is computer-controlled, with corresponding acquisition and storage facilities.

The method of measurement of soil suction in the double-walled triaxial cell is designed in such a way that the sample is pressurized by air and water, i.e. by suction (Figure 3). The volume change at which equilibrium is established in the soil sample is measured. Depending on the volume change of the sample at certain controlled

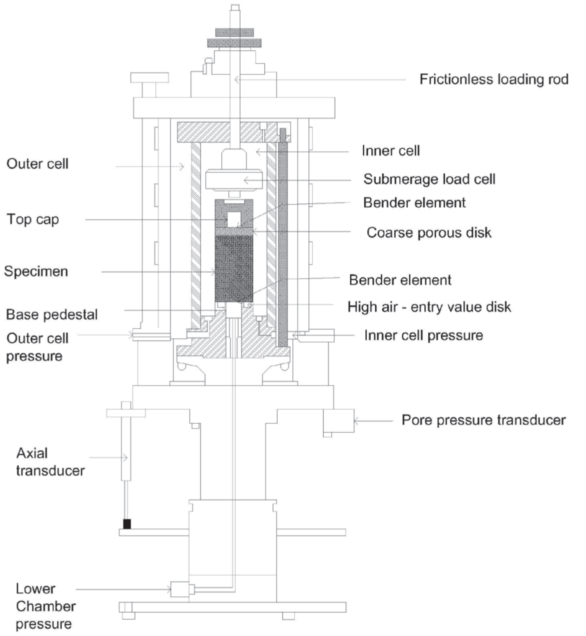

Fig. 2. The Bishop-Wesley double-walled triaxial cell.

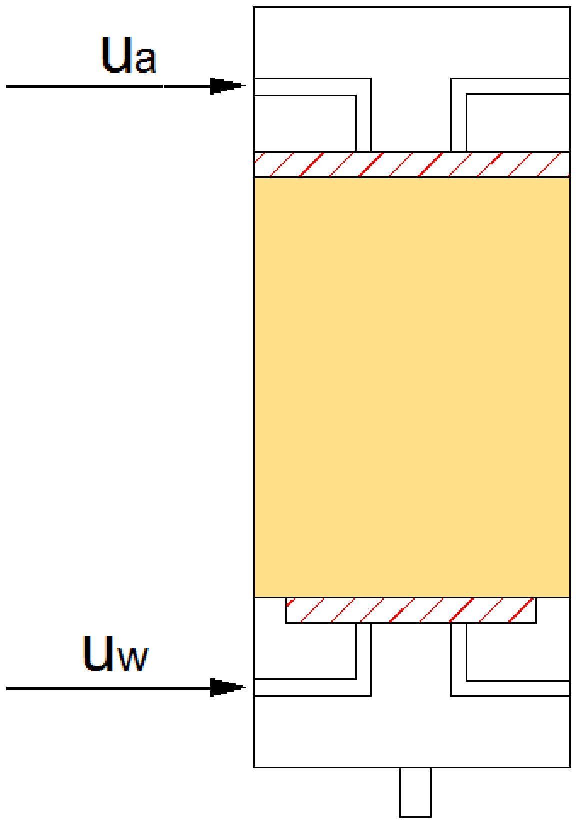

Fig. 3. Pressurizing the sample with an air pore pressure air (ua) and a water pore pressure (uw) (net effective stress controlled stage).

suction, information about the water content of the soil as a function of suction can be obtained by back analysis. Under controlled effective net stress state (suction stage) the change in the volume of the pore water and in the volume of the pore air are measured by volume measuring devices. With the use of appropriate equations the change in the volume of the pore water is calculated as the result of suction.

When measuring suction using the Bishop - Wesley double-walled triaxial cell, the volume change of the pore water is calculated, for each of the suction stages, from the obtained data. The last measured level of the volume change for a given suction stage is taken into account in the calculations. When the values of the volume change are known for each suction stage, then the volumetric and gravimetric moisture content are calculated, as well as the degree of saturation.

Soil suction measurements using a potentiometer (WP4C)

Soil suction was also measured by means of a WP4C (Fig. 4). This particular kind of potentiometer is a device for measuring water potential using a chilled mirror. The device is easy to handle, and measurements are carried out quickly and fairly accurately. The measurement range for suction is between 0 and 300 MPa, and its accuracy is ± 0.05 MPa over the measurement range between 0 and 5 MPa, and 1 % over the range between 5 and 300 MPa. The accuracy of the device also depends on proper calibration of the instrument and on the ambient temperature at which measurements are performed.

Fig. 4. The WP4C potentiometer.

The potentiometer works by measuring suction on the principle of the relative humidity in the air. The specimen is inserted into the machine into the sealed chamber, which is equipped with sensors, a mirror, and a ventilator. The sensors measure the temperature of the mirror, and the ambient temperature. The temperature of the mirror is precisely measured by means of a laser beam, which operates on the principle of the Peltier effect, in which a photo-detector operates by precisely detecting the point at which condensation occurs on the mirror for the first time. The potentiometer directs the light beam onto the mirror so that it is reflects into the photo-detector. When condensation occurs on the mirror, the photo-detector senses the change, and at the same time the thermocouple in the mirror records the temperature at which condensation has occurred. At the point of equilibrium the water potential of the air in the chamber is equal to the potential of the water in the sample. Soil suction is then determined according to Equation 10 (WP4C, 2013).

$$\Psi = \frac{RT}{M} * ln\frac{p}{p_0} \qquad (10)$$

where: Ψ is the water potential, R is the gas constant, T is temperature in the sample in Kelvin, M is thermolecular mass of the water, p is the pore pressure of the air, and p_o is the vapour pressure at the temperature of the sample.

Experimental results

The goal of the suction measurements was to determine the value of suction of very stiff preconsolidated sandy silt in the Krško Basin, where it is expected that some large geotechnical structures will be built in the next few years. The suction measurements were performed in the above-mentioned Bishop-Wesley double-walled triaxial cell (sample V1) and potentiometer (sample V2).

Soil studied

The stiff sandy silt (sample V1) which was studied in the Bishop-Wesley double-walled triaxial cell was similar but not identical to the sandy silt (sample V2) which was used for the measurements in the potentiometer. However, using both measurement methods it was possible to compare data obtained by means of two different suction measurement techniques.

The soil physical parameters are presented in Table 1. The results of the granulometric analysis showed that samples V1 and V2 can be classified as sandy silt (saSi) according to the standard SIST EN ISO 14688-1, and silt (ML) according to the standard JUS U.B1.00.

Water retention curves

The measured data of the sandy silt sample V1 are shown in Figure 5, where the retention curves were calculated by using the van Genuchten, Brooks and Corey, and Fredlund and Xing. With the Bishop-Wesley double-walled triaxial cell the suction is measured in the volumetric water content.

From the retention curves it can be seen that the air-entry value for sandy silt V1 (ψ_{ae}) occurs at a suction of 40 kPa. The suction which corresponds to the natural gravimetric water content of the sample (i.e. 27.7 %) amounts to about 3-4 kPa which means that the sandy silt is at natural water content fully saturated. The slope of the curve in the middle section is steep, which means that most of the water in the sandy silt is bound in the capillaries, so that the material is able to release it at low values of suction.

Table 1. The geomechanical characteristics of the sandy silt V1.

Sample	Water content	Density	Dry density	Specific density	Granulometric analysis		
Designation and unit	w (%)	ρ (Mg/m^3)	ρ_d (Mg/m^3)	ρ_s (Mg/m^3)	sand content (%)	silt content (%)	clay content (%)
Sandy silt V1	27,2	1,93	1,58	2,80	33,3	63,8	2,5
Sandy silt V2	25,3	1,99	1,53	2,76	42	57,8	0,2

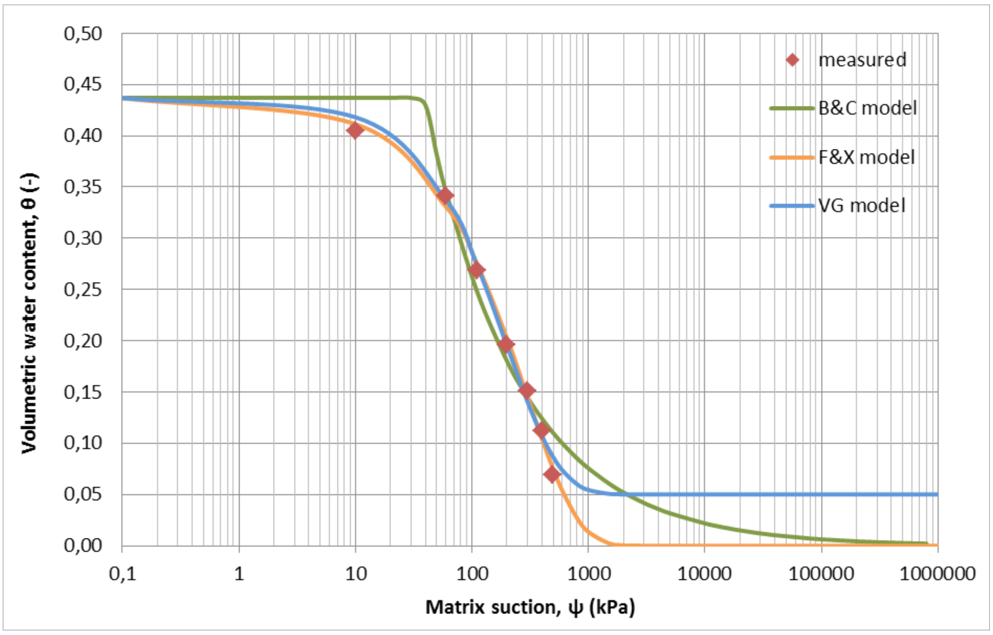

Fig. 5. Comparison of the retention curves obtained by using the different models for the sandy silt sample V1.

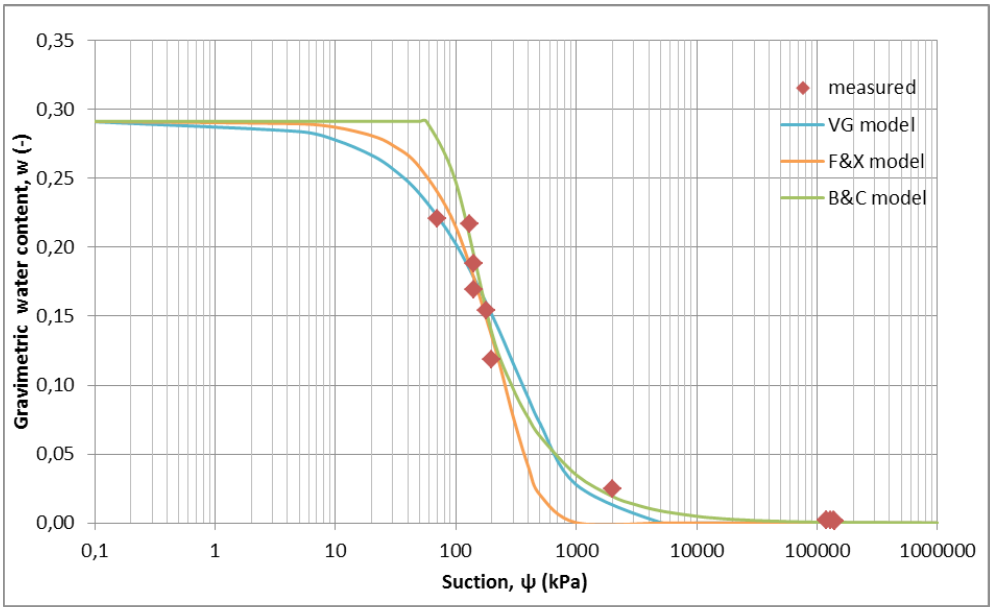

Fig. 6. Comparison of the retention curves obtained by using the different models for the sandy silt sample V2.

The retention curve corresponding to the sandy silt of sample V2 was determined by using the potentiometer (Fig. 6). With the potentiometer suction is measured in the gravimetric water content. The residual moisture point occurs at almost zero water content, at a suction of about 500 kPa, whereas the air-entry point occurs at a suction of 60 kPa. The measured value for the suction at 70 kPa and 22 % of gravimetric water content is questionable, since potentiometer measurements at suctions of up to 100 kPa are inaccurate. The slope of the retention curve is fairly steep. It can be seen that the moisture content decreases very rapidly, even at low values of suction. This indicates that the water between the grains is bonded only in the capillaries, so that the material is able to release it at low values of suction.

Discussion

Soil water retention curves were prepared on the basis of the models proposed by Brooks and Corey, Fredlund and Xing, and van Genuchten.

Based on the comparisons which were made between the different models, we tried to determine which water retention curve best fitted the measured values. From Figures 5 and 6 it can be seen that the measured values fit best when the Fredlund and Xing or van Genuchten model is used. In the case of the Brooks and Corey model, good agreement was observed with the measured values in the middle part of the curve, whereas at low suctions the fit was poorer. A sharp transition curve can be observed at the air-entry point, which makes identification of this point easy.

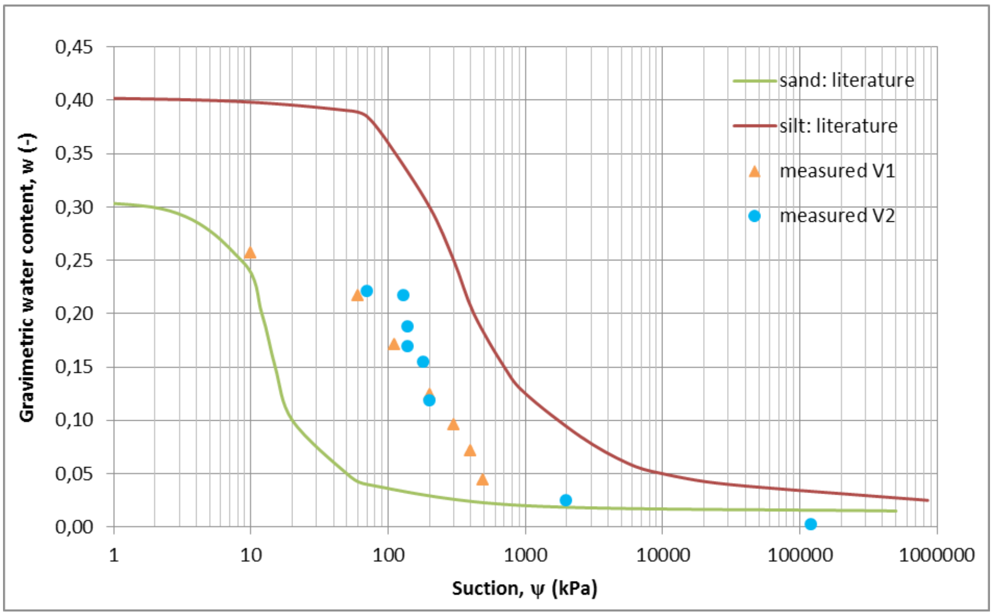

Fig. 7. Comparison of the measured values with data from the literature (the retention curves are according to Fredlund et al., 2011).

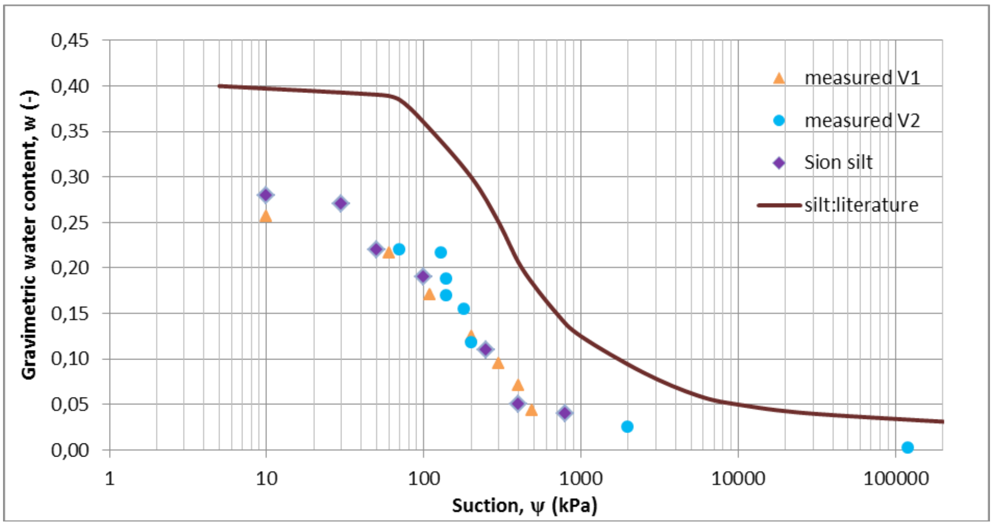

Fig. 8. Comparison of the measured values of sandy silt (samples V1 and V2) with Sion silt and data from the literature (the retention curve is according to Fredlund et al., 2011).

The sharp transition curve is due to the splitting of the model into two parts, where, in the first part of the equation, the moisture content is assumed to be to fully saturated. For this reason in its initial part the curve is flat, whereas in the part from the air-entry point onwards it enters a sharp transition. In the case of the sandy silt V2 the retention curves are located somewhat below the measured values.

Although each type of soil has its own kind of retention curve it is generally considered that various groups of soils have retention curves which are characteristic for them. The measurements results were also checked against data which can be found in the literature. Figure 7 shows the measured values of the retention curves for stiff sandy silt and a typical retention curve for sand and silt. The results of sandy silt V1 and V2 are shifted more in the direction towards retention curves which are typical for sand.

The results were compared with the Sion (Geiser, 1999) silt which is by the structure the most similar material to the Krško valey sandy silt (Table 2). It has a lower percent of sand and the sample was reconstituted before the testing and the consolidated to the primary stress value. If we compare curves of the samples V1 and V2 with the results of the measurements of the Sion silt we can see that there are quite similar in spite of the fact that the samples V1 and V2 are preconsolidated (Fig. 8). The preconsolidation pressure was obtained by the pressuremeter and oedometer tests and it was found that the OCR is approximately 2. From the results we can conclude, that the presonsolidation ratio of samples V1 and V2 is not enough high to have an influence on the level of suction. Higher influence on the results have the sandy component in the silt.

Based on our experiences with testing of stiff silt material we could conclude that each of the

Table 2. The geomechanical characteristics of the Sion silt.

Sample	Liquid limit	Specific density	Granulometric analysis		
Designation and unit	w_l (%)	ρ_s (Mg/m^3)	sand content (%)	silt content (%)	clay content (%)
Sion silt	25,4	2,74	20	72	8

described methods of measurement of soil suction has its advantages and disadvantages. From the point of view of accuracy, the Bishop - Wesley double walled triaxial cell has a big advantage, since very accurate measurements can be made of the changes occurring in the pore water volume and the air volume, and, as well as this, accurate measurements can be performed at low matric suction values. Additionally, the Bishop -Wesley double walled triaxial cell provides constant conditions throughout the duration of the investigation, which reduces the possibility of errors due to the impact of the environment (e.g. temperature changes). The advantage of the cells lies also in the fact that measurements are made on only one of the samples, so that errors due to sample preparation can be avoided. However, in comparison with the potentiometer, the work is much more difficult and requires more knowledge of how to handle with the device, and the measurements are also time-consuming.

Complete investigations in a Bishop - Wesley double-walled triaxial cell, from the sample saturation and consolidation to the measurements of soil suction may last as long as several months, whereas entire measurements in the potentiometer take no longer than a week or two. Apart from making possible faster performance measurements, handling of the potentiometer is much simpler. The disadvantage of the device lies in the fact that the potentiometer does not give good results in the low suction range, and it is also very important to reduce the effect of temperature changes on the soil suction results. The disadvantage of performing measurements with the potentiometer is that the measurements are made on a small amount of the sample having an unknown density, which has a considerable effect on the soil suction values obtained. A small amount of a sample can also increases the possibility for making errors in the measurements. At the same time this might be an advantage, since there is no need for a large amount of the sample for the performance of the measurements.

From the geotechnical point of view, the authors were particularly interested in the matric suction, which has an effect on the stress - strain properties of soils. Matric soil suction can be precisely measured only in a double-walled triaxial cell, whereas in measurement performed with a potentiometer only the total suction is measured, assuming that the osmotic suction is zero.

Conclusions

So far, most research of soil suction has been performed on clay and silt material, whereas measurements of the soil suction of stiff preconsolidated sandy silt have not been performed yet. Very stiff silt is typical of the Krško Basin where, in the future, some very important geotechnical structures will be built. In particular, knowledge is needed about the behaviour of such soil at increased or decreased water content is essential.

In the paper the results of measurements that were carried out on very stiff sandy silt in a Bishop - Wesley double-walled triaxial cell for the very stiff preconsolidated sandy silt are presented, and compared with the results of soil suction measurements performed with a potentiometer (WP4C). Both methods were presented in detail. The results of the measurements were evaluated on the basis of already known results that have been presented in the literature, using the three most commonly used mathematical models which are used for the definition of retention curves.

On the basis of the results of the laboratory tests of unsaturated soils, with an emphasis on measurements of suction in a Bishop - Wesley double-walled triaxial cell and using a potentiometer, it can be concluded that both of these methods of measurements provide useable results. The obtained results are in a good agreement with the results which are already known from the literature, and the models used to describe the soil retention curve fit the measured values very well.

The results were compared with the Sion silt (Geiser, 1999) which is by the structure the most similar material to the Krško valey stiff sandy silt. From the comparison it can be concluded, that the presonsolidation ratio of samples V1 and V2 is not enough high to have an influence on the level of suction. Higher influence has a presence of the sandy component in the silt material.

The disadvantages of most methods for measuring soil suction in the laboratory lie in the inaccurate and unreliable measurements which occur in the low suction range, i.e. up to about 100 kPa. According to the obtained results, the Bishop - Wesley triaxial cell can provide accurate measurement in this range. The specially designed double-walled cell enables accurate measurements of the volume changes which occur in the water and air in the pores, without being affected by outside effects (e.g. changes in temperature) The absolute advantage of this cell lies in the fact that the suction is measured only a single sample, so that the effect of errors in the preparation of the sample, or of its non-homogeneity, can be reduced.

References

Brooks, R.H. & Corey, A.T. 1964: Hydraulic properties of porous medium. Colorado State University (Fort Collins), Hydrology Paper, 37 p.

Bulut, R., Lytton, R. L. &Wray, W. K. 2001: Soil suction measurements by filter paper. Expansive Clay Soils and Vegetative Influence on Shallow Foundations. ASCE Geotechnical Special Publication, 115: 243-261.

Chae, J., Kim B., Park, S. & Kato, S. 2010: Effect of Suction on Unconfined Compressive Strength in Partially Saturated Soils. KSCE Journal of Civil Engineering, 14/3: 281-290, doi:10.1007/s12205-010-0281-7.

Delage, P. 2002: Experimental unsaturated soil mechanics. 3rd International Conference on Unsaturated Soils. Recife: Brazil, 3: 973-996.

Fredlund, D.G. 2006: Unsaturated Soil Mechanics in Engineering Practice. Journal of Geotechnical and Geoenvironmental Engineering, 132/3: 286-321.

Fredlund, D. G. & Rahardjo, H. 1993: Soil mechanics for unsaturated soils. John Wiley and Sons, New York: 521 p.

Fredlund, D.G., Sheng, D. & Zhao, J. 2011: Estimation of soil suction from the soil-water characteristic curve. Canadian Geotechnical Journal, 48/2: 186-198, doi:10.1139/T10-060.

Fredlund, D. G., Vanapalli S. K., Xing, A. & Pufahl D.E. 1995: Predicting the shear strength function for unsaturated soils using the soil-water characteristic curve. Proceeding of the First International Conference on Unsaturated Soils, 1: 63-70,

Fredlund, D. G. & Xing, A. 1994: Equations for the soil-water characteristic curve. Canadian Geotechnical Journal, 31/4: 521-532, doi:10.1139/t94-061.

Geiser, F. 1999: Comportement mechanique d'un limon non sature etude experimentale et modelisation constitutive. Ecole polytechnique federale de Lausanne, These No. 1999, doi:10.5075/epfl-thesis-1942.

Godt, J., Baum, R.L. & Lu, N. 2009: Landsliding in partially saturated materials. Geophysical research letters, 36: 1-5.

Kayadelen, C., Tekinsoy, M.A. & Taşkiran, T. 2007: Influence of matric suction on shear strength behavior of a residual clayey soil. In: Environmental Geology, 53: 891 – 901, doi:10.1007/s00254-007-0701-2.

Lu, N. & Godt, J. 2008: Infinite slope stability under steady unsaturated seepage conditions. Water resources research, 44/11: 1-13, doi:10.1029/2008WR006976

Maček, M. 2006: Sukcija zemljin. Diplomsko delo. Univerza v Ljubljani, Fakulteta za gradbeništvo in geodezijo. Ljubljana: 68 p.

Maček, M. 2012: Vpliv matrične sukcije na pomike plazu Slano blato. Doktorska disertacija. Univerza v Ljubljani, Fakulteta za gradbeništvo in geodezijo. Ljubljana: 210 p.

Maček, M. & Petkovšek, A. 2008: Merjenje zemljinske sukcije v slovenskih geotehničnih laboratorijih. Razprave, 5. posvetovanja slovenskih geotehnikov12. – 16. junij, Nova Gorica. Slovensko geotehniško društvo: 133-142.

Maček, M., Bebar, M. & Petkovšek, A. 2010: Kontrola kakovosti in monitoring nasipov iz glin z uporabo zemljinske sukcije. Zbornik referatov, 10. Slovenski kongres o cestah in prometu, 20. – 22. oktober, Portorož: 891-900.

Marshall, T. J. & Holmes, J. W. 1988: Soil physics. 2nd edition. Cambridge University Press, Cambridge: 374 p.

Mckee, C.R. & BUMB, A.C. 1987: Flow-testing coalbed methane production wells in the presence of water and gas. In SPE Formation Evaluation, December: 599-608.

Murray, E. J. & Sivakumar, N. 2010: Unsaturated soils: a fundamental interpretation of soil behavior. United Kingdom: Wiley-Blackwell: 304 p.

Petkovšek, A. 2006: Vpliv matrične sukcije na trdnostno deformacijske lastnosti zemljin. Doktorska disertacija. Univerza v Ljubljani, Fakulteta za gradbeništvo in geodezijo. Ljubljana: 274 p.

Ng, W.W., Zhan, L.T., Bao, C.G., Fredlund, D.G. & Geong, B.W. 2003: Performace of an unsaturated expansive soil slope subjected to artificial rainfall infiltration. Geotechnique, 53/2: 143-157.

Pereira, J. H. F. & Fredlund, D. G. 2000: Volume change behaviour of collapsible compacted gneiss soil. J. Geotech. Geoenviron. Eng., 126/10, 907–916.

Petkovšek, A. 2008: Zemljinska sukcija - nekaj primerov uporabe v geotehniki = Soil suction - some examples of its application in geotechnical engineering. In: Logar, J. & Petkovšek, A. (eds.): Razprave, 5. posvetovanja slovenskih geotehnikov, Nova Gorica, 12. - 14. junij 2008. Slovensko geotehniško društvo: 283-292.

Pham, H. Q., Fredlund, D. G. & Barbour, S. L. 2005: "A study of hysteresis models for soil-water characteristic curves". Canadian Geotechnical Journal, 42/6: 1548 – 1568, doi:10.1139/t05-071.

Springman, S. M. 2011: Simple slope stability analyses while considering unsaturated behaviour/response. In: Gaberc, A. & Majes, B. (eds.): Zbornik, 12. Šukljetovi dnevi, Ajdovščina, 30. september. Slovensko geotehniško društvo: 5-35.

Suescun Florez, E. A. 2010: Developmenof a suction-controlled resonant column apparatus with self-contained bender elements: Degree of Master of Science in Civil Engineering. The University of Texas, Arlington: 141 p.

Tofani, V., Dapporto, S., Vannocci, P. & Casagli, N. 2006: Infiltration, seepage and slope stability mechanisms during the 20-21 November 2000 rainstorm in Tuscany, central Italy. Journal Geotecnical and Geoenviromental engeenering, 6/6: 1025-1033, doi:10.5194/nhess-6-1025-2006.

Umedera, M., Hyodo, M., Murata, H., Fujiwara, A. & Yasufuku, N. 1996: Effect of suction on the mechanical behaviour of bentonite-sand mixtures. In: Kamon, M. (ed.): Environmental Geotechnics. Rotterdam: Balkema: 169-172.

Van Genuchten, M.T. 1980: A closed-form equation for predicting the hydraulic conductivity of unsaturated soils. Soil Science Society of America Journal, 44: 892-898.

WP4C 2013: Dew Point PotentiaMeter. Operator's Manual. Decagon Device, Inc..

GEOLOGIJA 60/1, 49-60, Ljubljana 2017
https://doi.org/10.5474/geologija.2017.004

Overview of isotopic investigations of groundwaters in a fractured aquifer system near Rogaška Slatina, Slovenia

Pregled izotopskih raziskav podzemne vode v razpoklinskem vodonosnem sistemu na območju Rogaške Slatine

Branka TRČEK[1] & Albrecht LEIS[2]

[1]University of Maribor, Faculty of Civil Engineering, Transportation Engineering and Architecture, Smetanova ulica 17, SI-2000 Maribor, Slovenia; e-mail: branka.trcek@um.si
[2]JR-AquaConSol GmbH, Elisabethstraße 18/II, 8010 Graz, Austria; e-mail: albrecht.leis@jr-aquaconsol.at

Prejeto / Received 15. 11. 2016; Sprejeto / Accepted 9.5.2017; Objavljeno na spletu / Published online 9.6.2017

Dedicated to Professor Jože Pezdič on the occasion of his 70th birthday

Key words: fractured aquifer, mineral waters, environmental isotopes, Rogaška Slatina, Slovenia
Ključne besede: razpoklinski vodonosnik, mineralna voda, naravni izotopi, Rogaška Slatina, Slovenija

Abstract

The isotopic investigations of groundwaters stored in the Rogaška Slatina fractured aquifer system were performed in the periods 1978–1985 and 2007–2011 aiming at answering open questions on the groundwater recharge and dynamics, on connections between different types of aquifers and on solute transport. Environmental isotopes ^{2}H, ^{18}O, ^{3}H, ^{13}C of dissolved inorganic carbon and ^{14}C were analysed in mineral, thermo-mineral and spring waters. Results indicated the source and mechanism of groundwater recharge, its renewability, a transit time distribution, hydraulic interrelationships, the groundwater origin and its evolution due to effects of water-rock interaction. They proved the hypothesis that the Boča massif should be a catchment area of the Rogaška mineral waters. The estimates of the mean residence time of mineral waters in the aquifer system are between 7200 and 3400 years, depending on the location and depth. Thermo-mineral water is the oldest water in the study area with the mean residence time of 14000 years.

Izvleček

V obdobjih 1978–1985 in 2007–2011 so bile izvedene izotopske raziskave podzemne vode, uskladiščene v razpoklinskem vodonosnem sistemu na območju Rogaške Slatine, z namenom, da se odgovori na odprta vprašanja o napajanju podzemne vode in njeni dinamiki, o povezavi različnih vrst vodonosnikov in o prenosu snovi. V mineralnih, termomineralnih in izvirskih vodah smo analizirali ^{2}H, ^{18}O, ^{3}H, ^{13}C v raztopljenem anorganskem ogljiku in ^{14}C. V rezultatih smo opisali vire in mehanizme napajanja podzemne vode, njeno obnovljivost, zadrževalni čas v vodonosniku, izvor in geokemijski razvoj zaradi reakcij s kamninami. Potrdili smo hipotezo, da je masiv Boč napajalno območje Rogaških mineralnih vod, ki se zadržujejo v vodonosniku s povprečnim zadrževalnim časom od 7200 do 3400 let. Le ta je odvisen od lokacije in globine. Termomineralna voda je starejša – njen povprečen zadrževalni čas je 14000 let.

Introduction

Rogaška Slatina is famous by mineral water, which was discovered in this place in the time of ancient Rome. Numerous investigations of the Rogaška groundwaters were subject to balneology and to the larger exploitation quantities (Nosan, 1975), whereas information essential for the definition of the Rogaška aquifer system and for its protection has been still missing. Questions on the groundwater recharge area and dynamics, on connections between aquifers and on solute transport have remained open, which depends on the field geology and structure. The latter is very complicated – three regional faults intersect in this area, which is folded to anticlinal and synclinal folds. The nature of geological structures, their mutual relations and extent have not been explained at a satisfactory level in many parts of the system. With regard to results of previous hydrogeochemical investigations (Nosan, 1973, 1975; Pezdič, 1986, 1997) it was presumed that the Boč massif near Rogaška Slatina is the catchment area of the Rogaška mineral waters, although geological data did not support this hypothesis (Aničić & Juriša, 1984).

Aiming at answering the discussed open questions also the isotopic investigations of groundwaters stored in the Rogaška Slatina fractured aquifer system were performed. The first studies took place in the period 1978–1985 (Pezdič, 1997), while the last studies were performed during a period 2007–2011 (Trček et al., 2010; Trček & Leis, 2011). The isotopic investigations based on the environmental isotopes of H, O and C, which were used as tracers of geological and hydrogeological processes.

The applications of stable isotope ratios of hydrogen and oxygen in groundwater hydrology are based primarily on isotopic variations in precipitation as the predominant groundwater source. After the infiltration of precipitation into the aquifer, only physical processes, such as diffusion, dispersion, mixing and evaporation, alter the groundwater isotopic composition (Clark & Fritz, 1997). The stable isotope content of water may be considered conservative under low-temperature and low-circulation groundwater systems, as long as the relative amount of water involved in chemical reactions remains limited (Clark & Fritz, 1997; Hoefs, 1997). The exchange with oxygen (possibly also hydrogen) bearing minerals of the host rocks is particularly important in geothermal environment. With low reaction rates in low-temperature environments a long time is needed for a significant exchange to take place and equilibrium will generally not be reached (IAEA, 1983). Another process, which may modify the initial stable isotope content of groundwater, is the isotopic exchange with a gas phase which is not initially in equilibrium with the environmental water (e.g. CO_2 or H_2S).

The stable carbon isotope composition of dissolved inorganic carbon ($\delta^{13}C$-DIC) is not a conservative tracer. Nevertheless, the $\delta^{13}C$ can trace the carbon sources and reactions for numerous interacting organic and inorganic species. The isotope ratio $^{13}C/^{12}C$ is an important tool for quantifying the water-rock interactions, identifying the proportion of different CO_2 sources in water, and determining the initial geological settings of the groundwater recharge (Hoefs, 1997; Kendall & McDonnell, 1998).

Groundwater dating is the main field of application of the ^{14}C and ^{3}H radioactive isotopes. Their input source functions, which describe the time-varying global fluxes of isotopes deduced from atmospheric, cosmogenic and anthropogenic production, are well known (Mook, 1980; Hoefs, 1997). The measured activity concentrations are compared with the input functions to get fairly informative age determinations over the past several decades. ^{3}H has a half-life of 12.3 years and is a very applicable tracer for determining spring residence times when recharge processes took place within a timescale of less than 50 years. Groundwaters seldom have more than 50 TU today and are typically in the 5–10 TU range (Criss et al., 2007; Rose, 2007). The recent ^{3}H study (Kovačič, 2015) indicated that Slovene groundwaters could be divided into four categories – groundwaters that are older than 100 years (^{3}H concentration is below the detection limit), groundwaters with the prevailing old component (^{3}H concentration is between 0 and 2.5 TU), groundwaters with the age between 30 and 60 years (^{3}H concentration is on average 8 TU) and recent groundwaters with age up to 15 years (^{3}H concentration is about 6 TU).

On the other hand ^{14}C with a half-life of 5,730 years is applicable for dating groundwaters recharged prior to 1,000–2,000 years (Bajjali et al., 1997) and as old as 30,000 years (Clark & Fritz, 1997).

Study area

The study area with its broader surroundings is geologically one of the most complex parts of Slovenia (Trček et al., 2010). It is the juncture of three major regional fault systems, separating three tectonic units (Figs. 1 and 2). The Boč massif belongs to the Southern Karavanke unit. It borders to the south with the Donat line to the narrow tectonic unit between the Donat line and Šoštanj fault close to which the town of Rogaška Slatina is situated. To the north, the Dravinja fault as part of the Periadriatic line separates the Southern Karavanke unit from the Upper Austro–Alpine unit. The ongoing dextral strike-slip zone along the Lavantal fault and the Šoštanj fault (Fig. 2) associates eastward extrusion of the Eastern Alps as a result of the northward shift and the counter clockwise rotation of the Adria microplate. The complexity of the study area is reflected in a lithological heterogeneity as a result of faulting into many small tectonic blocks, which are relatively displaced and folded (Figs. 1 and 2). Most of the area is composed of massive limestones and dolomites of the Carnian age. They are capping the Boč mountain crest. The Oligocene and Miocene beds, covering the northernmost part of the territory and the lower slopes north of Rogaška Slatina, are composed of alternating sandstones, sands, shaly claystones and marlstones and conglomerates in the lower parts. A wide belt of volcanic rocks (andesite, its tuffs and volcanic breccias) is also present in within these units. The upper part is almost entirely composed of hard and bituminous marlstones (Aničić & Juriša, 1984).

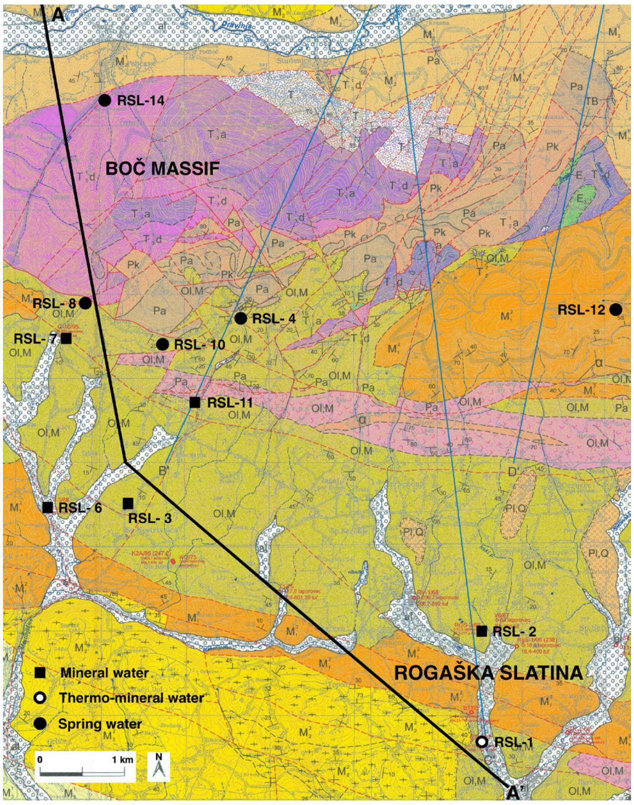

Fig. 1. Study area with locations of boreholes with mineral, thermo–mineral and spring water (Trček et al., 2010).

Sl. 1. Raziskovalno območje z lokacijami vrtin z mineralno, termomineralno in izvirsko vodo (Trček et al., 2010)

Mineral water is stored in fractured layers of the Oligocene tuff covered by the Upper Oligocene and Lower Miocene beds (Figs. 1 and 2). The discussed water belongs to the magnesium-sodium-hydrogen carbonate-sulphate facies. It was exploited from five boreholes that are 24 to 600 m deep (Fig. 1). Donat Mg is the most famous among Rogaška mineral waters. It has the highest mineral content (Tab. 1) and contains more than 1,000 mg/l of Mg. The content of gaseous CO_2 in the water is normally in the range of 2–30 g/l. Gas is practically pure CO_2 with minor share of nitrogen and negligible concentration of oxygen and methane (Pezdič, 1997).

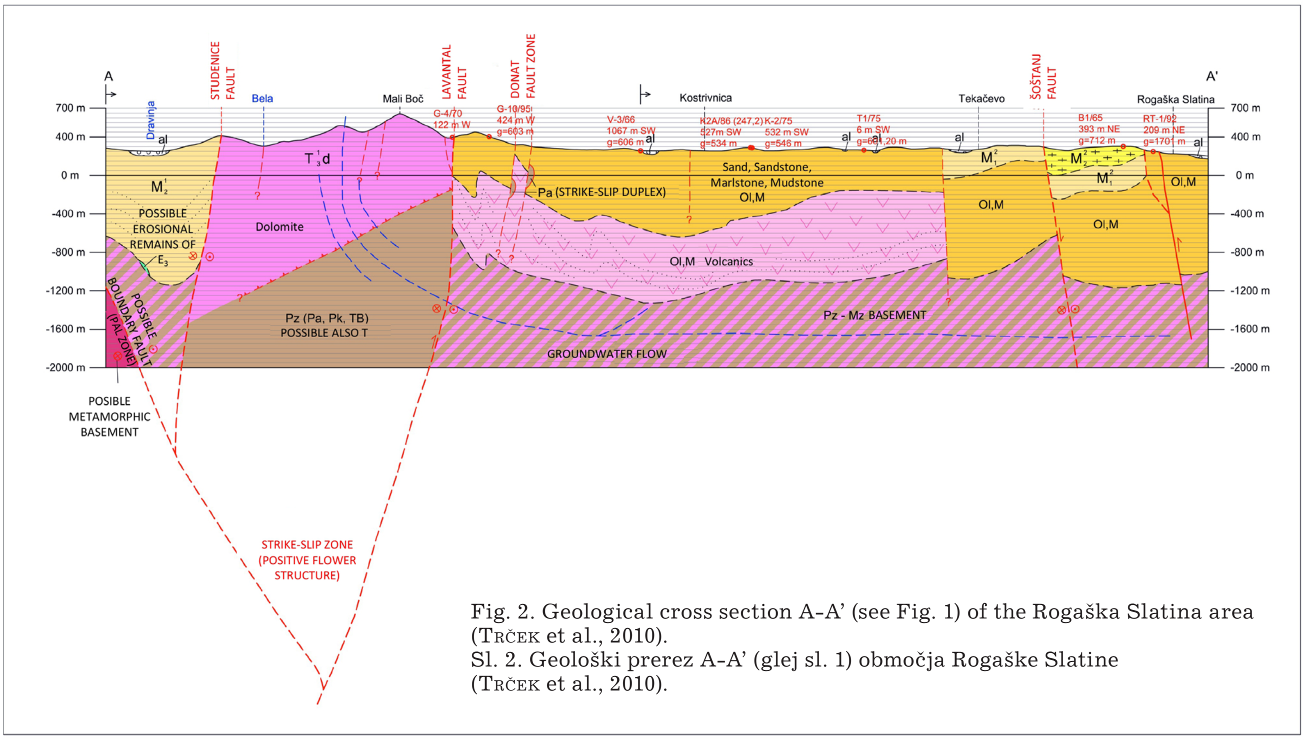

Fig. 2. Geological cross section A-A' (see Fig. 1) of the Rogaška Slatina area (Trček et al., 2010).

Sl. 2. Geološki prerez A-A' (glej sl. 1) območja Rogaške Slatine (Trček et al., 2010).

Table 1. Average values of sampled water discharges (Q), electroconductivity (SEC), mineralisation (M), temperature (T) and pH in the period 2007–2011

Tabela 1. Povprečne vrednosti pretoka vzorčenih vod ter njene elektroprevodnosti (SEC), mineralizacije (M), temperature (T) in pH v obdobju 2007–2011.

	Borehole name	Borehole depth (m)	Q (l/s)	M (g/l)	SEC (μS/cm)	T (°C)	pH
Mineral water	RSL-2	274	0.5	12.75	10999	14.6	6.8
	RSL-3	24	0.2	5.8	5165	11.9	6.4
	RSL-6	606	1	11.8	10539	28.4	6.9
	RSL-7	603	0.4	8.65	8627	15.1	6.5
	RSL-11	170	0.1	8.08	7102	12.0	6.5
Thermo-mineral water	RSL-1	1700	6	6	6418	55.4	7.1
Spring water from limestone	RSL-4	215	2.2		459	12.6	7.1
	RSL-10	130	2.1		379	11.0	7.5
Spring water from dolomite	RSL-8	170	1.4	0.5	570	11.7	7.3
	RSL-14	38	40		481	12.9	7.5
Spring water from sandstone	RSL-12	100	2		382	9.9	7.7

Spring water and thermo–mineral water are also exploited at the study area (Fig. 1, Tab. 1). The former is stored in fractured Triassic carbonate rocks and Miocene sandstones of the Boč massif and the latter in the dolomitized keratophyre at depths between 1,500 and 1,700 m.

The Rogaška mineral waters discharge with a help of a gas lift, thermo–mineral water discharges with a help of a thermo lift, while spring waters of boreholes RSL-4, RSL-8, RSL- 10 and RSL-14 are artesian.

Methods

Isotopic investigations were fundamental for studies of groundwater dynamics and solute transport in aquifers with mineral and spring water and among them. The recent investigations included the monitoring of 5 boreholes with mineral water (RSL-2, RSL-3, RSL-6, RSL-7 and RSL-11), 1 borehole with thermo–mineral water (RSL-1), 2 boreholes with spring water from a limestone (RSL-4, RSL-10), 2 boreholes with spring water from a dolomite (RSL-8, RSL-14) and 1 borehole with spring water from a sandstone (RSL-12; Fig. 1, Tab. 1). Besides the groundwater CO_2 was sampled and also precipitation at altitudes of 340, 530 and 710 m asl. The previous investigations involved only the sampling of mineral waters and spring water from carbonate rocks (Pezdič, 1997).

Recent isotopic analyses of stable isotopes of H and O were made in Laboratory Centre for Isotope Hydrology and Environmental Analytics, Joanneum Research, Graz, Austria. The oxygen isotopic composition ($\delta^{18}O$) of the water was measured by the classic $CO_2 - H_2O$ equilibrium technique (Epstein & Mayeda, 1953) with a fully automated device adapted from Horita et al. (1989) coupled to a Finnigan DELTAplus Mass Spectrometer. Deuterium ($\delta^{2}H$) was measured in a continuous flow mode by chromium reduction using a ceramic reactor slightly modified from Morrison et al. (2001). Stable oxygen and hydrogen isotopic ratios are reported relative to the VSMOW (Vienna-SMOW) standard with an overall precision of 0.1 and 1 ‰, respectively.

The data of H and O stable isotopic composition in precipitation were applied to define the local meteoric waterline (LMWL) of the Rogaška Slatina area. Due to small number of samples (57) the ordinary linear regression analysis was conducted that based on the method of seasonally weighted mean values (Rozanski et al., 1993).

The ^{13}C content was also measured in the Stable Isotope Laboratory of the Institute of Water Resources Management, Joanneum Research, Graz, mass spectrometrically by Thermo Finnigan DELTA^{plus}XP (CF-IRMS). The values are reported as ‰ vs. V-PDB standard with an overall precision of 0.1 ‰.

Measurements of the radioactive isotopes ^3H and ^{14}C were performed in the Isotope laboratory HYDROSYS – Water and Environmental Protection Developing Ltd, Budapest, Hungary. ^3H was measured by counting β-decay events in a liquid scintillation counter (LSC). Values are reported in absolute concentrations as tritium units (TU), where one TU corresponds to one ^3H atom per 10^{18} atoms of hydrogen ^1H or to an activity of 0.118 Bq/kg in water.

^{14}C was measured by the super low level liquid scintillation analyser (PerkinElmer Tri-Carb 3170TR/SL) based on ASTM D6866-06 standard. The values are expressed in pmC (Percent Modern Carbon). Groundwater age (t) is determined using the radioactive decay equation (Eq. 1), employing the pre-industrial baseline ^{14}C activity of the soil CO_2 equal to 100 pmC as an initial concentration and the ^{14}C activity of the DIC (HCO_3^-) measured in the groundwater sample. However, the dissolved C mass balance of groundwaters is altered during the groundwater flow path due to geochemical reactions that take place within the aquifer. In such cases, a factor q is incorporated into the radioactive decay equation to take into account the ^{14}C dilution effect (other than radioactive decay) during the groundwater flow path caused by a dissolution of ^{14}C–free marine carbonates and incorporation of a geogenic ^{14}C–free CO_2 of the magmatic or metamorphic source. The groundwater age is thus determined:

$$t = -8267 \ln\left(\frac{a_t\,{}^{14}C}{q a_0\,{}^{14}C}\right) \qquad \text{(Eq. 1)}$$

where t is groundwater age, $a_0\,{}^{14}C$ is a modern ^{14}C activity in the soil zone (100 pmC), $a_t\,{}^{14}C$ is a ^{14}C activity of DIC in the groundwater sample and q is a dilution factor.

The chemical mass-balance correction (CMB model) has been used to quantify the ^{14}C dilution due to incorporation of ^{14}C–free geogenic CO_2, assuming that the carbonate dissolution in the recharge area evolves under the closed system condition. In such cases the ^{14}C dilution factor of carbonate groundwaters is about 0.5. The subsequent ^{14}C dilution caused by the incorporation of ^{14}C–free geogenic CO_2 and resulting geochemical reactions has been determined as a ratio of the HCO_3^- concentration in the recharge area to the HCO_3^- concentration in samples of mineral and thermos-mineral waters. The HCO_3^- concentration in the recharge area is given as an average value of sampled spring waters that equals to 304 mg/l. The total ^{14}C dilution factor is thus the product of the ^{14}C dilution ensuing in the recharge area (0.5) and the subsequent ^{14}C dilution induced by the incorporation of ^{14}C-free geogenic CO_2.

The first analyses of O, H and C environmental isotopes were made at Institute Jožef Stefan, Ljubljana (Pezdič, 1997). For $\delta^{18}O$ determination from water the classic CO_2 – H_2O equilibrium technique was also applied (Epstein & Mayeda, 1953). Hydrogen gas was prepared by reducing water vapor on hot zinc wool at 400 °C or on zinc granules at 490 °C (Coleman et al., 1982). Precipitated DIC and carbonates reacted with 100 % orthophosphoric acid at 55 °C. Dissolved carbonate species are treated with phosphoric acid to measure just $\delta^{13}C$. The isotopic composition of prepared gaseous compounds (H_2 and CO_2) were measured on the Varian MAT 250 mass spectrometer. Measuring accuracy exceeds ± 0.05 ‰ for oxygen and carbon and ± 0.5 ‰ for hydrogen. Results were given relative to the SMOW standard for oxygen and hydrogen and PDB for carbon.

The tritium content was measured with a liquid scintillation counter at Institute Jožef Stefan, Ljubljana (Pezdič, 1997). Concentrations were given in TU and Bq. The activity of radiogenic carbon (^{14}C) was measured at Rudjer Boikovic Institute in Zagreb using a gas proportional counter. ^{14}C data were presented as % Modern Carbon (pmC) vs. the activity of standard oxalic acid (Ox) formed before the nuclear period with a correction factor of 0.95 (Pezdič, 1997).

Results and discussion

Average values of sampled water discharges, electroconductivity, mineralisation, temperature and pH during a monitoring period 2008–2010 are presented in Table 1. The level of gaseous CO_2 in water is normally in the range 2-30 g/l, but in some areas is as high as 40 g/1 (Nosan, 1973). Gas analysis revealed that the gas is practically pure

CO_2 with a minor share of nitrogen (0.3 %) and negligible concentrations of oxygen and methane (below 0.01 %; Pezdič, 1997).

The relationship between O and H stable isotopic compositions of sampled water is illustrated in Figure 3. The average groundwater O and H isotopic composition approximately equals the weighted average of the precipitation O and H composition as a rule, while surface water is may be enriched more with heavier (more positive) isotopes than precipitation, due to the evaporation process (Clark & Fritz, 1997; Rozanski et al., 1992, 1993; Trček & Zojer, 2010).

Mineral waters have ^{18}O in the range between -12.2 and -10.3 ‰ and δ^2H in the range between -80.5 and -63.9 ‰. The lowest δ values refer to waters with the highest mineralization, RSL-2 and RSL-6, and the highest to water of RSL-3 with the lowest mineralisation (Tab. 1), which reflects mixing processes of older and younger waters (Fig. 3).

The $\delta^{18}O$ and δ^2H values range in spring waters from carbonate rocks is -10.7 to -9.9 ‰ and -78.9 to -65.0 ‰, respectively. It is slightly different and more narrow in spring water from sandstone, -10.9 to -10.6 ‰ and -76.9 to -67.2 ‰, respectively (Fig. 3). The $\delta^{18}O$ and δ^2H of thermo–mineral water is similar to spring water from a dolomite.

Similar $\delta^{18}O$ and δ^2H results were obtained in previous investigations (Pezdič, 1997). Mineral waters had a $\delta^{18}O$ range -11.2 to -9.55 ‰ and a δ^2H range -84.0 to -76.9 ‰, while the parameters ranged in spring waters from carbonate rocks from -10.25 to - 8.19 ‰ and from -78.6 to -63.6 ‰, respectively.

Craig (1961) firstly described the relationship of discussed isotopes in the precipitation by the global meteoric waterline (GMWL, Fig. 3). The local meteoric waterline (LMWL) of the Rogaška Slatina area slightly differs from the GMWL in both the slope and the intercept (Fig. 3). It is a function of temperature during the secondary evaporation as rain falls from a cloud, which results in effects of the isotopic fractionation with respect to the latitude, altitude, and climate. The isotopic composition of precipitation is affected by the season, latitude, altitude, precipitation amount, and distance from the coast (Rozanski et al., 1992, 1993). All sampled waters from recent and previous investigation (Pezdič, 1997) are distributed in the LMWL vicinity. The $\delta^{18}O$ and δ^2H values

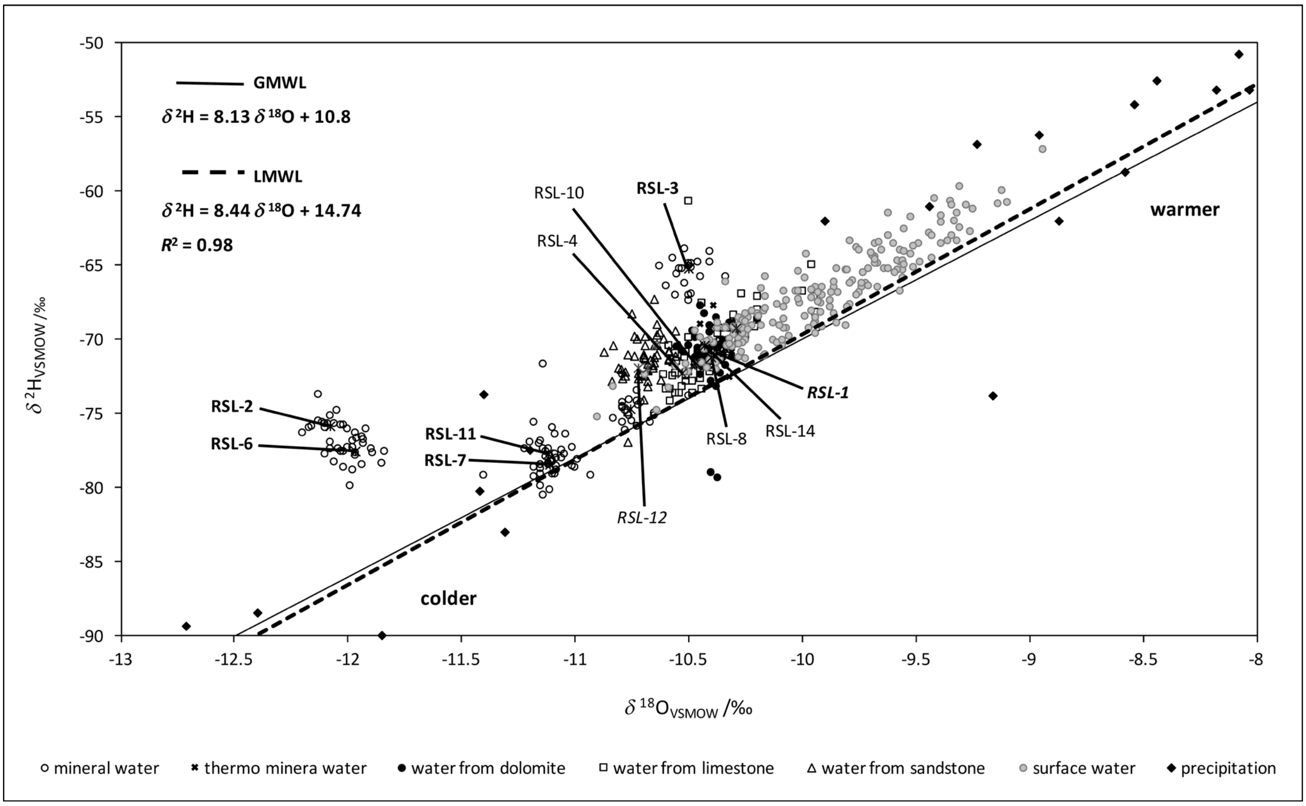

Fig. 3. The relationship between stable oxygen and hydrogen isotopic composition of sampled water in the period 2007-2011.
Sl. 3. Razmerje med sestavo stabilnih izotopov kisika in vodika v vzorčenih vodah v obdobju 2007-2011.

and their distribution indicate that sampled waters are of a meteoric origin, hence the Rogaška fractured aquifer system is recharged with local precipitation. The δ values of mineral waters fall on the same LMWL, but on its lower part with the depleted heavy isotopes (Fig. 3, Pezdič, 1997), which reflects colder climate conditions during the infiltration processes (Clark & Fritz, 1997; Hoefs, 1997; Iaea, 1983). The exception is the shallow RSL-3 mineral water (Tab. 1) that is mixed with surface waters (Figs. 3 and 4). The δ values of mineral waters sampled from RSL-2, RSL-6 and RSL-3 slightly deviate from LMWL (Fig. 3). The level of gaseous CO_2 in these waters is the highest (up to 40 g/1; Nosan, 1973), therefore it is assumed that ^{18}O is depleted due to the exchange of water with the geogenic CO_2 (Clark & Fritz, 1997; Hoefs, 1997; Iaea, 1983).

During the period of previous isotopic investigations (1978–1985) the ^{3}H contents of 1.9 to 176 TU were measured in mineral waters and of 37 to 150 TU in spring waters from carbonate rocks (Pezdič, 1997). The ^{3}H data of investigations in July 2008, when almost three half-lives of ^{3}H has passed, are illustrated in Figure 4. The precipitation had the ^{3}H content of 10.7 TU, which coincides with the summer values measured in Ljubljana (Kovačič, 2015). ^{3}H was not detected in mineral waters from boreholes RSL-6 and RSL-7, hence these waters are not in contact with recent precipitation infiltration. According to Kovačič (2015) mineral waters from boreholes RSL-6 and RSL-7 are older than 100 years. The samples of thermo–mineral and mineral waters from boreholes RSL-1, RSL-2 and RSL-11 contain 0.6 TU or less ^{3}H, which indicates the prevailing old water component (Kovačič, 2015). Evidently the recharge of these groundwaters occurred prior to the 1950s, therefore they are relatively unblemished by human activities. Similar findings were published in previous investigations (Pezdič, 1997).

Groundwater samples from RSL-3, RSL-4, RSL-8, RSL-10, RSL-12 and RSL-14 with tritium contents 4.6 to 9.4 TU (Fig. 4) should contain modern water that infiltrated predominantly after the 1960s, suggesting the vulnerability of these groundwater systems to man–made impacts. According to Kovačič (2015) the mean residence time of spring water of shallower boreholes RSL-10, RSL-12 and RSL-14 (Tab. 1) should be around 15 years, around 30 years for spring water of the deeper borehole RSL-4 and up to 60 years for spring water of the deeper borehole RSL-8. Among listed waters only RSL-3 is mineralized. The water is captured from a depth of 20 m, where it should be mixed with young fresh water. Pezdič (1997) reported that spring waters from carbonate rocks are no more than 15 years old.

During the period 2007–2011 the $\delta^{13}C$ values of the dissolved inorganic carbon varied between -13 and +2 ‰ in sampled groundwater (Figs. 5 and 6). The parameter values between -2 and +2 ‰ are characteristic for groundwaters that are influenced by the volcanic CO_2: RSL-2, RSL-3, RSL-6, RSL-7 and RSL-11 (Clark & Fritz, 1997). These waters are highly mineralized, as it is evidenced in Table 1. The RSL-1 water has lower mineralization, which is reflected in $\delta^{13}C$-DIC values. On the other hand low $\delta^{13}C$ values (-12 to -13 ‰) are typical for spring waters, collected from RSL-4, RSL-8, RSL-10 and RSL-14. According to Clark & Fritz (1997) these values closely resemble the $\delta^{3}C$ content of carbonate groundwater that evolves under a closed system condition.

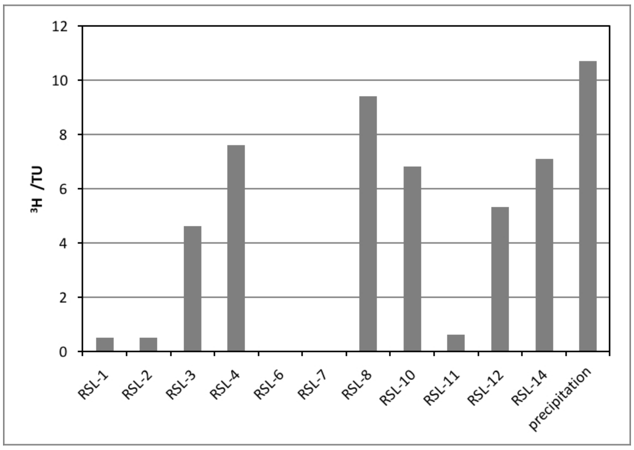

Fig. 4. Tritium concentrations in groundwater and in precipitation of the Rogaška Slatina area in the period 2007–2011.
Sl. 4. Koncentracije tricija v podzemnih vodah in padavinah na območju Rogaške Slatine v obdobju 2007–2011.

During the period 1978–1985 similar $\delta^{13}C$ values were detected in mineral waters, between -3.1 and +3.3 ‰, and between -16.9 and 13.1 ‰ in spring waters of carbonate rocks (Pezdič, 1997).

The main sources of the carbon dissolved in groundwater are soil CO_2, CO_2 of a geogenic origin or a magmatic CO_2 (from deep crustal or mantle sources), carbonate minerals, an organic matter in soils and rocks, fluid inclusions, and methane. Each of these sources has a different carbon isotopic composition and contribute to the totally dissolved carbon in various proportions. In the studied groundwater systems the total dissolved inorganic carbon (DIC) exists practically

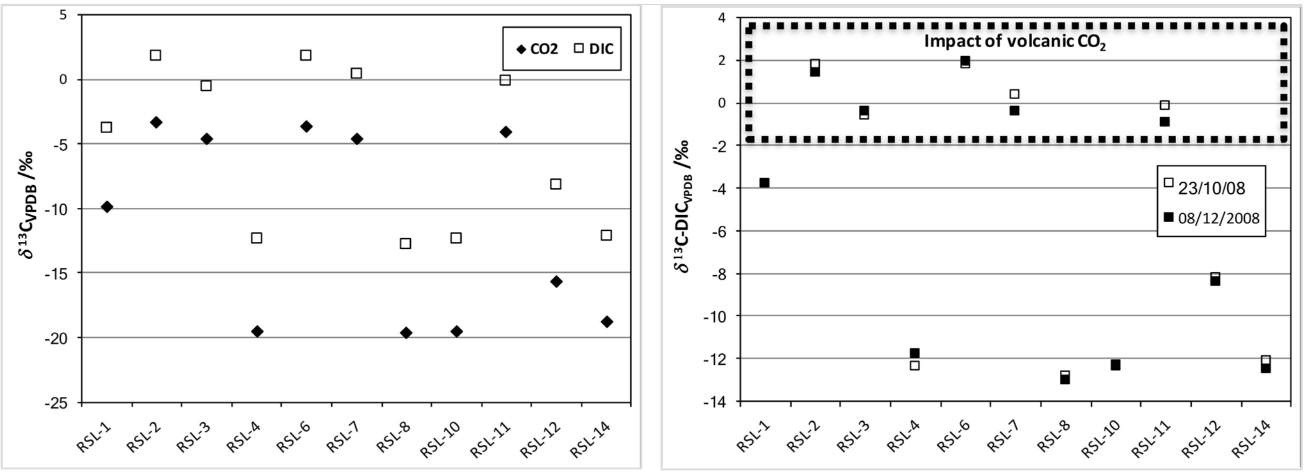

Fig. 5. Stable C isotopic composition of total dissolved inorganic carbon (DIC) in sampled water and its CO_2 in the period 2007–2011.
Sl. 5. Izotopska sestava ^{13}C raztopljenega anorganskega ogljika v vzorčenih vodah in v njihovem CO_2 v obdobju 2007–2011.

all in a HCO_3^- form. The HCO_3^- concentration varies between 224–382 mg/l in groundwater samples from RSL-4, RSL-8, RSL-10, RSL-12 and RSL-14, where the carbonate rocks were dissolute in the reaction with biogenic CO_2 in soil. The HCO_3^- concentration of mineral and thermo–mineral waters from RSL-1, RSL-2, RSL-3, RSL-6, RSL-7 and RSL-11 is increased to about 1950–8280 mg/l (Tab. 2). The hydrochemical composition was most probably altered to a great extent by the incorporation of the geogenic CO_2 influx that originates from a volcanic source (Fig. 5). The average $\delta^{13}C$ of CO_2 in mineral waters is -4.1 ‰ and -9.9 ‰ in thermo–mineral water, respectively. It induced the intensive rock-water interactions and consequently the dissolved solute contents increased significantly. It is well known that the $\delta^{13}C$ is about -25 ‰ in the soil CO_2 (similar to plants), -7 ‰ in the atmospheric CO_2, -8 ‰ to -3 ‰ in the CO_2 originating from the geothermal and volcanic systems and about 0 ‰ in marine carbonate rocks (Kendall & McDonnell, 1998). δ values from -2.0 ‰ to +4.1 ‰, with an average of +2.2 ‰ were analysed in Slovene carbonate rocks

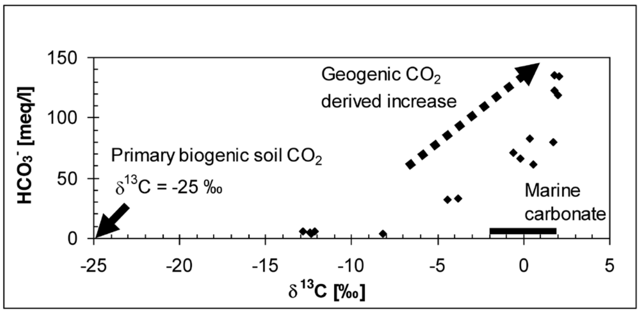

Fig. 6. The relationship between stable C isotopic composition and HCO_3^- concentration in sampled waters in the period 2007–2011.

Sl. 6. Razmerje med izotopsko sestavo ^{13}C in koncentracijo raztopljenega anorganskega ogljik v vzorčenih vodah v obdobju 2007–2011.

(Koceli et al., 2013; Ogorelec et al., 2000). The relationship between $\delta^{13}C$ and HCO_3^- concentration in sampled water is illustrated in Figure 6.

The ^{14}C investigation was done on five groundwater samples of mineral and thermo–mineral waters collected from the boreholes RSL-1, RSL-2, RSL-3, RSL-6 and RSL-7 in 2009. Very low ^{14}C contents, ranging between 0.9 to 1.4 pmC, have been determined (Tab. 2), which reflects very long mean residence times of groundwaters. With the aim to determine the resident time of groundwater according to Equation 1 the geogenic CO_2 was characterised first based on the $\delta^{13}C$ value of the CO_2 gas phase of water samples. The $\delta^{13}C$ values show a very wide spread, between -10 and -3 ‰ (Fig. 5). They are within the range of $\delta^{13}C$ reported in the literature for magmatic CO_2, -12 to -1 ‰ (Truesdell & Huston, 1980; Exley et al., 1986; Rose & Davisson, 1996). Further the chemical mass-balance correction (CMB model) has been used to quantify the ^{14}C dilution due to incorporation of the ^{14}C–free volcanic CO_2, assuming that the carbonate dissolution in the recharge area evolves under a closed system condition. From stoichiometry in such cases the initial ^{14}C concentration (~ 100 pmC) is expected to become diluted for about 50 %. It follows that the ^{14}C dilution factor is about 0.5. The subsequent ^{14}C dilution caused by the incorporation of the ^{14}C–free volcanic CO_2 and the resulting geochemical reactions has been determined as a ratio of the HCO_3^- concentration acquired in the recharge zone to the HCO_3^- concentration in the groundwater samples from RSL-1, RSL-2, RSL-3, RSL-6 and RSL-7. The HCO_3^- concentration acquired in the recharge zone is given as an average value from RSL-4, RSL-8, RSL-10 and RSL-14, which is about 304 mg/l. The ages of sampled mineral waters were calculated employing the total ^{14}C dilution factor, which is the product of the ^{14}C dilution ensuing in the recharge zone (= 0.5) and the subsequent ^{14}C dilution induced by the incorporation of the ^{14}C–free volcanic CO_2.

Table 2. HCO_3^- concentration, stable C isotopic compositions, ^{14}C content, dilution factor q_{total} and age estimates of the mineralized waters and thermos mineral water (RSL-1) sampled in 2009.

Tabela 2. Koncentracije HCO_3^-, izotopska sestava ^{13}C, vsebnost ^{14}C, faktor razredčenja q_{total} in ocena starosti mineralne in termomineralne vode, vzorčene leta 2009.

Sampling point	HCO_3^- (mg/l)	$\delta^{13}C$ (‰)	^{14}C (pmC)	q_{total}	Age (year)
RSL-1	1949.6	-4.37	1.43	0.078	14000
RSL-2	8176.7	2.05	1.23	0.019	3400
RSL-3	3771.0	0.53	0.95	0.040	----
RSL-6	7279.7	1,99	0.88	0.021	7100
RSL-7	4875.5	1,75	1.31	0.031	7200

The estimated ages of mineral waters are listed Table 2. The thermo–mineral water, captured from RSL-1 at depths 1500–1700 m exhibits a considerably high mean residence time – 14000 years, corresponding to the Pleistocene epoch, the Bølling-Allerød interglacial period that lasted from 14700 to 12900 years ago. During this period glaciers almost disappeared in many European mountain ranges, also in the Alps (Palacios et al., 2016; Dielforder & Hetzel, 2014; Hippe et al., 2014; Ivy-Ochs, 2015). The wormer climate during the infiltration process of thermo–mineral water is reflected also in the stable isotopic composition of O and H (Fig. 3).

The mean residence time of mineral waters RSL-6, RSL-7 and RSL-2 is 7200, 7100 and 3400 years, respectively. The first two correspond to the Holocene epoch, the end of the colder Boreal period that lasted from 8600 to 7200 years ago (Roberts, 2014). According to the ^{18}O and ^{2}H isotopic data (Fig. 3) waters from RSL-6 and RSL-2 should be recharged and discharged under similar conditions, but they are captured at different depths (606 and 274 m respectively, Tab. 1) and hence fallow different flow paths, which should result in age differences. It is also worth to note that despite the low ^{14}C concentration in the groundwater sample from RSL-3, no groundwater age was calculated due to the presence of a higher tritium concentration (4.6 TU) in the groundwater sample. Most likely it represents mixing of recent and old groundwater, thus groundwater age dating using ^{14}C is not appropriate.

The ^{14}C was investigated in the RSL-7 mineral water also in 1980s (Pezdič, 1997). A content of 2 pmC was recorded. Two corrections were made to estimate the water mean residence time based on ^{14}C data: a) according to a dilution factor determined as the ratio between the predicted active and measured total DIC (equals to 0.037), which indicated that the mixture had about 3.7 pmC of initial ^{14}C activity (ICA) and measured 2 pmC and b) according to estimation that primary mineral water had become mixed with about 20 % of young meteoric water. The recalculation of values indicated the relative ^{14}C activity of primary RSL-7 mineral water to be approximately 35 pmC. This pointed to an estimated age of about 8000 years, which is compatible with the result of recent investigations.

Conclusions

The results of isotopic investigations of groundwaters in the Rogaška Slatina area performed in the period 1978–1985 (Pezdič, 1997) and 2007–2011 coupled with available information on a physical hydrogeology and a water chemistry help in understanding the source and mechanism of groundwater recharge, groundwater circulation and its renewability, groundwater transit time distribution, hydraulic interrelationships, the groundwater origin and its evolution due to effects of water-rock interaction.

The $\delta^{18}O$ and $\delta^{2}H$ values indicated the meteoric origin of mineral and thermos-mineral waters and proved the hypothesis that the Boč massif near Rogaška Slatina should be a catchment area of the Rogaška mineral waters. They reflected the mixing processes between younger and older waters or mineral and spring waters and hence contributed to the water body vulnerability assessment together with ^{3}H data. The latter pointed out waters that infiltrated predominantly after the 1960s, suggesting the vulnerability of these groundwater systems to man-made impacts.

The estimations of the mean residence time of mineral, thermos-mineral and spring waters based on ^{3}H, $\delta^{13}C$ and ^{14}C data provided additional information on groundwater recharge processes, its renewability and vulnerability. Thermo-mineral water, captured from RSL-1 at depths 1500–1700 m is the oldest water in the study area with the mean residence time of 14000 years. The mean residence time of mineral waters captured at depth around 600 m from RSL-6 and RSL-7 is estimated to 7100 and 7200 years respectively. However, the residence time of mineral water captured at depth around 270 m from RSL-2 is shorter – 3400 years. Nevertheless, the ^{18}O and ^{2}H data indicated that mineral waters from RSL-6 and RSL-2 should be recharged and discharged under similar conditions. Based on ^{3}H data it was estimated that shallow spring waters are around 15 years old, while the age of deeper ones is 30 to 60 years.

The presented findings were integrated with the structural analysis of the study area (Trček et al., 2010; Žibret, 2016). The results improved a conceptual hydraulic model of the Rogaška Slatina fractured aquifer system and are essential to determine the optimal balance between environmental protection and economic use of mineral and spring water resources in the study area.

Acknowledgement

The author would like to acknowledge the Droga Kolinska, Živilska industrija d.d., Slovenian Research Agency and K_{net} Water for the financial support of the researches.

Pregled izotopskih raziskav podzemne vode v razpoklinskem vodonosnem sistemu na območju Rogaške Slatine

(daljši povzetek)

V obdobjih 1978–1985 in 2007–2011 so bile izvedene izotopske raziskave podzemne vode, uskladiščene v razpoklinskem vodonosnem sistemu na območju Rogaške Slatine z namenom, da se odgovori na odprta vprašanja o napajanju podzemne vode in njeni dinamiki, o povezavi različnih vrst vodonosnikov in o prenosu snovi. V mineralnih, termomineralni in izvirskih vodah so se analizirali ^{2}H, ^{18}O, ^{3}H, ^{13}C-DIC in ^{14}C (sl. 1). Mineralna voda je uskladiščena v razpokanih plasteh oligocenskega tufa, ki jih prekrivajo zgornje oligocenske in spodnje miocenske kamnine, izvirska voda pa v razpokanih zgornje triasnih karbonatnih Boča in miocenskih peščenjakih (sl. 1 in 2, tab. 1). Termomineralna voda je zajeta v vrtini RSL-1 na globinah 1500 do 1700 m, v dolomitiziranem keratofirju.

Razmerje med izotopsko sestavo ^{18}O in ^{2}H v vzorčenih vodah na območju Rogaške Slatine je predstavljeno na sliki 3. Lokalna meteorna premica (LMWL) ne odstopa dosti od globalne (GMWL). Vrednosti parametrov, izmerjenih v površinskih in podzemnih vodah, so razporejene v območju, ki ga pokrivajo vrednosti, izmerjene v padavinah. Na podlagi tega in sorodnih rezultatov predhodnih raziskav (Pezdič, 1997) lahko zaključimo, da so vse vzorčene vode meteornega izvora. Na sliki 3 odstopajo nekoliko vrednosti mineralnih vod, vzorčenih na vrtinah RSL-2, RSL-6 in RSL-3. Možnih je več vzrokov: drugačne klimatske razmere v času infiltracije padavin, drugačni pogoji napajanja vodonosnika in izotopska izmenjava s CO_2 v mineralni vodi. Razberemo, katere vode imajo podoben režim napajanja ali podobno napajalno območje. Med mineralnimi vodami je treba izpostaviti podobnost med vodami vzorčnih mest RSL-2 in RSL-6 oziroma RSL-11 in RSL-7. Iz tega sledi, da pripada par najverjetneje istemu vodonosniku. Termomineralna voda vrtine RSL-1 ima podobno izotopsko sestavo ^{18}O in ^{2}H kot dolomitne vode vrtin RSL-8 in RSL-14, kar kaže na podobno nadmorsko višino napajalnih zaledij vodonosnikov.

Rezultati analiz ^{3}H v vzorčenih vodah so prikazani na sliki 4. Mineralne in termomineralne vode vrtin RSL-1, RSL-2, RSL-6, RSL-7 in RSL-11 vsebujejo 0,6 TU ali manj, kar pomeni, da so se napajale pred letom 1960. Po drugi strani lahko sklepamo, da so omenjene vode zavarovane pred antropogenimi vplivi iz površja. Vsebnost ^{3}H v mineralni vodi RSL-3, več kot 4 TU, opozarja da se meša mineralna voda v vrtini z mlajšimi vodami, ki dotekajo s površja. Izvirske vode vrtin RSL-3, RSL-4, RSL-8, RSL-10, RSL-12 in RSL-14 vsebujejo 4,6 do 9,4 TU, kar pomeni, da so mlajše od 60 let. Ocenjujemo, da je starost plitvejših izvirskih vod okoli 15 let, medtem ko so globlje stare med 30 in 60 let.

Na podlagi podatkov $\delta^{13}C$, HCO_3^- in ^{14}C se je določila starost mineralnih in termo mineralnih vod (sl. 5 in 6, tab. 2). Uporabila se je enačba radioaktivnega razpada (enačba 1), ki se ji doda faktor *q*, s pomočjo katerega se upošteva učinek razredčenja ^{14}C zaradi raztapljanja karbonatnih kamenin in geogenega CO_2 (vulkanskega izvora). Izotopska sestava ^{13}C-DIC v vzorčenih vodah je predstavljena na sliki 5. Le ta izpostavlja mineralne vode, ki so pod vplivom vulkanskega CO_2: RSL-2, RSL-3, RSL-6, RSL-7 in RSL-11. Omenjene vode so visoko mineralizirane, kar je evidentirano v tabeli 1. Termomineralna voda RSL-1 ima nižjo mineralizacijo, kar se kaže tudi v vrednosti δ^{13}C-DIC. V izvirskih vodah RSL-4, RSL-8, RSL-10 in RSL-14 so bile izmerjene vrednosti δ^{13}C-DIC med -13 in -14 ‰. Te vrednosti so značilne za zaprt sistem raztapljanja karbonatnih kamnin v območju napajanja vodonosnika.

Za določitev vpliva vulkanskega CO_2 na merjene vrednosti ^{14}C se je uporabil model korekcije kemijske masne bilance (CMB model) ob predpostavki, da poteka proces raztaplanja karbonatnih kamenin v napajanem območju vodonosnika pod zaprtimi pogoji. V takih primerih se upošteva, da se zmanjša začetna koncentracija ^{14}C (~ 100 pmC) za okoli 50 %. Iz tega sledi, da je faktor razredčenja ^{14}C v karbonatnih podzemnih vodah raziskovalnega območja okoli 0,5. Dodatno razredčenje ^{14}C povzroči še vulkanski CO_2. Le-to se je ocenilo s pomočjo razmerja med koncentracijo HCO_3^- v vodah z območja napajanja vodonosnega sistema (karbonatne izvirske vode) in koncentracijo HCO_3^- v mineralnih in termo mineralnih vodah RSL-1, RSL-2, RSL-3, RSL-6 in RSL-7. Za koncentracijo HCO_3^- na območju napajanja vodonosnika z mineralno vodo se je upoštevala povprečna vrednost vzorčenih vod RSL-4, RSL-8, RSL-10 in RSL-14, 304 mg/l.

Opisani podatki in informacije so se upoštevali pri določitvi starosti mineralnih vod, podanih v tabeli 2. Najdaljši zadrževalni čas, 14000 let, je značilen za termomineralno vodo RSL-1, ki je zajeta v globinah 1500-1700 m. Povprečni zadrževalni časi mineralnih vod RSL-6, RSL-7 in RSL-2 so 7200, 7100 oziroma 3400 let. Glede na podatke δ^{18}O in δ^{2}H (sl. 3) imata vodi RSL-6 in RSL-2 isto napajalno območje in pripadata istemu vodonosnemu sistemu, kjer potekajo geokemijske reakcije pod podobnimi pogoji. Ker pa se zajemata obravnavani vodi na različnih globinah, 606 oziroma 274 m, je različen njun zadrževalni čas v vodonosniku. V predhodnih raziskavah je bilo ocenjeno, da je zadrževani čas mineralne vode RSL-7 okoli 8000 let (Pezdič, 1997).

Rezultati izotopskih raziskav so opisali vire in mehanizme napajanja podzemne vode, njeno obnovljivost, zadrževalni čas v vodonosniku, izvor in geokemijski razvoj zaradi reakcij s kamninami. Potrdili so hipotezo, da je masiv Boča napajalno območje Rogaških mineralnih vod, ki se zadržujejo v vodonosniku s povprečnim zadrževalnim časom od 7200 do 3400 let, ki je odvisen od lokacije in globine.

References

Aničić, B. &Juriša, M. 1984: Basic geological map SFRJ, 1:100.000, Sheet Rogatec. Zvezni geološki zavod, Beograd.

Bajjali, W., Clark, I. & Fritz, P. 1997: The artesian thermal groundwaters of northern Jordan: insights into their recharge history and age. J. Hydrol., 192: 355–382, doi:10.1016/S0022-1694(96)03082-X.

Clark, I. & Fritz, P. 1997: Environmental Isotopes in Hydrogeology, Lewis Publishers.

Criss, R. E., Davisson, M. L., Surbeck, H., & Winston, W. E. 2007: Isotopic Techniques. In: Goldscheider, N. & Drew, D. (eds.): Methods in karst hydrogeology, International contribution to hydrogeology 26. Taylor and Francis, London: 123–145.

Coleman, M.L., Shepherd, T.J., Durham, J.J., Rouse, J.E. & Moore, G.R. 1982: Reduction of water with zinc for hydrogen isotope analysis. Anal. Chem., 54/6: 993–995, doi:10.1021/ac00243a035.

Dielforder, A. & Hetzel, R. 2014: The deglaciation history of the Simplon region (southern Swiss Alps) constrained by 10Be exposure dating of ice-molded bedrock surfaces. Quat. Sci. Rev, 84: 26–38, doi:10.1016/j.quascirev.2013.11.008.

Epstein, S. & Mayeda,T. 1953: Variation of O^{18} content of waters from natural sources. Geochimica et Cosmochimica Acta, 4/5: 213–224, doi:10.1016/0016-7037(53)90051-9.

Exley, R.A., Mattey, D.P., Clague, D.A. & Pillinger, C.T. 1986: Carbon isotope systematics of a mantle "hotspot": a comparison of Loihi Seamount and MORB glasses. Earth and Planetary Science Letters, 78/2-3: 189–199, doi:10.1016/0012-821X(86)90060-9.

Hoefs, J. 1997: Stable isotope geochemistry, fourth ed. Springer-Verlag, Berlin-Heidelberg.

Horita, J., Ueda, A., Mizukami, K. & Takatori, I. 1989: Automatic δD and δ^{18}O analyses of multi-water samples using H_2 and CO_2-water equilibration methods with a common equilibration set-up. Appl. Radiat. Isot., 40/9: 801–805, doi:10.1016/0883-2889(89)90100-7.

Hippe, K., Ivy-Ochs, S., Kober, F., Zasadni, J., Wieler, R., Wacker, L., Kubik, P.W. & Schlüchter, C. 2014: Chronology of Lateglacial ice flow reorganization and deglaciation in the Gotthard Pass area, Central Swiss Alps, based on cosmogenic ^{10}Be and in situ ^{14}C. Quat. Geochronol, 19: 14–26, doi:10.1016/j.quageo.2013.03.003.

International Atomic Energy Agency 1983: Isotope techniques in the hydrogeological assessment of potencial sites for the disposal of high-level radioactive wastes. Technical reports series 228, International Atomic Energy Agency, Vienna: 151 p.

Ivy-Ochs, S. 2015: Glacier variations in the European Alps at the end of the last glaciation. Cuadernos de Investigación Geográfica, 41/2: 295–315, doi:10.18172/cig.2750.

Kendall, C. & McDonnell, J.J. 1998: Isotope tracers in catchment hydrology. Elsevier, Amsterdam.

Koceli, A., Kanduč, T. & Verbovšek, T. 2013: Anorganski ogljikov cikel v sistemu tla-kamnina-podzemna voda v kraško-razpoklinskih vodonosnikih. Geologija, 56/2: 219–228, doi:10.5474/geologija.2013.014.

Kovačič, K. 2015: Radioactive isotopes in ground waters of Slovenia. Ph.D. Thesis. University of Nova Gorica Graduate School, Nova Gorica: 127 p.

Márton, E., Fodor, L., Jelen, B., Márton, P., Rifelj, H. & Kevrić, R. 2002: Miocene to Quaternary deformation in NE Slovenia: complex paleomagnetic and structural study. Journal of Geodynamics, 34: 627–651, doi:10.1016/S0264-3707(02)00036-4.

Mook, W.G. 1980: Carbon-14 in hydrogeological studies. In: Fritz, P. & Fontes, J. CH. (eds.): Handbook of Environmental Isotope Geochemistry 1A, The Terrestrial Environment, 75–134.

Morrison, J., Brockwell, T., Merren, T., Fourel, F. & Philips, A.M. 2001. On-line high-precision stable hydrogen isotopic analyses on nanoliter water samples. Anal. Chem., 73/15: 3570–3575, doi:10.1021/ac001447t.

Nosan, A. 1973: Thermal and mineral wells in the Slovenia = Termalni in mineralni vrelci v Sloveniji). Geologija, 16: 6–81.

Nosan, A. 1975: Hydrogeological investigations of mineral waters in Rogaška Slatina from 1952 to 1972. Geological Survey of Slovenia, Ljubljana: 44 p.

Ogorelec, B., Dolenec, T. & Pezdič, J. 2000: Izotopska sestava O in C v mezozojskih karbonatnih kamninah Slovenije - vpliv faciesa in diageneze. Geologija, 42: 171–205, doi:10.5474/geologija.1999.012.

Palacios, D., Gomez-Ortiz, A., Andres, N., Salvador, F. & Oliva, M. 2016: Timing and new geomorphologic evidence of the last deglaciation stages in Sierra Nevada (southern Spain). Quat. Sci. Rev., 150: 110–129, doi:10.1016/j.quascirev.2016.08.012.

Pezdič, J. 1997: Recharge and retention time study of a partly karstified area of Boč (Eastern Slovenia) using hydrogen, oxygen and carbon isotope composition as natural tracers. Isotopes Environ. Health Stud., 33: 293–306, doi:10.1080/10256019708234040.

Roberts, N. 2014: The Holocene, the Environmental History, third edition. John Wiley & sons: 358 pp.

Rose, S. 2007: Utilization of decadal tritium variation for assessing the residence time of base flow. Ground Water, 45/3: 309–317, doi:10.1111/j.1745-6584.2006.00295.x.

Rose, T.P. & Davisson, M.L. 1996: Radiocarbon in Hydrologic Systems Containing Dissolved Magmatic Carbon Dioxide. Science, 273: 1367–1370, doi:10.1126/science.273.5280.1367.

Rozanski, K., Araguds–Araguds, L. & Gonfiantini, R. 1992: Relation between long–term trends of ^{18}O isotope composition of precipitation and climate. Science, 258: 981–985, doi:10.1126/science.258.5084.981.

Rozanski, K., Araguds-Araguds, L. & Gonfiantini, R. 1993: Isotopic patterns in modern global precipitation. In: Swart, P.K., Lohman, K.C., McKenzie, J. & Savin, S. (eds.): Climate change in continental isotopic records–Geophysical monograph 78. American Geophysical Union, Washington, DC: 1–36.

Trček, B., Novak, M., Celarc, B. & Leis, A. 2010: Origin of mineral water from Rogaška Slatina (Slovenia). In: Zuber, A., Kania, J. & Kmiecik, E. (eds.): XXXVIII IAH Congres, Groundwater Quality Sustainability. University of Silesia, Krakow: 1769–1775.

Trček, B. & Zojer, H. 2010: Recharge of springs. In: Krešić, N. & Stevanović, Z. (eds.): Groundwater hydrology of springs: engineering, theory, management, and sustainability. Butterworth-Heinemann: 87–127.

Trček, B & Leis, A. 2011: Isotopic investigations of mineral waters in Rogaška Slatina. In: Groundwater: our source of security in an uncertain future. Papers presented at the international conference incorporating the Biennial Conference of the Ground Water Division (GWD) of the Geological Society of South Africa (GSSA) and Meeting of the International Association of Hydrogeologists (IAH). Beta Products, Pretoria: 8 p.

Truesdell, A.H. & Huston, J.R. 1980: Isotopic evidence on environments of geothermal systems. In: Fritz, P. & Fontes, J. CH. (eds.): Handbook of Environmental Isotope Geochemistry, The Terrestrial Environment, A, 1: 179–226.

Žibret, L. 2016: A contribution to better understanding of structural characteristics and tectonic phases of the Boč region, Periadriatic Fault Zone. Geologija, 59/2: 243–257, doi:10.5474/geologija.2016.015.

GEOLOGIJA *60/1*, 61-75, Ljubljana 2017
https://doi.org/10.5474/geologija.2017.005

Characterization of silicified fossil assemblage from upper Carnian "Amphiclina beds" at Crngrob (central Slovenia)

Značaj okremenjene fosilne združbe zgornjekarnijskih amfiklinskih plasti pri Crngrobu (osrednja Slovenija)

Luka GALE[1,2], Uroš NOVAK[3], Tea KOLAR-JURKOVŠEK[2], Matija KRIŽNAR[4] & France STARE[5]

[1]University of Ljubljana, Faculty of Natural Sciences and Engineering, Department of Geology, Privoz 11, SI-1000 Ljubljana, Slovenia, e-mail: luka.gale@ntf.uni-lj.si
[2]Geological Survey of Slovenia, Dimičeva 14, SI-1000 Ljubljana, Slovenia
[3]Lovšetova ulica 4, SI-1260 Ljubljana-Polje, Slovenia
[4]Slovenian Museum of Natural History, Prešernova 20, SI-1000 Ljubljana, Slovenia
[5]Žabnica 75, SI-4209 Žabnica, Slovenia

Prejeto / Received 29. 9. 2016; Sprejeto / Accepted 28. 2. 2017; Objavljeno na spletu / Published online 9.6.2017

Key words: Slovenian Basin, Southern Alps, Upper Triassic, Tuvalian, diagenesis, chert, silicification, conodonts
Ključne besede: Slovenski bazen, Južne Alpe, zgornji trias, tuval, diageneza, roženec, okremenitev, konodonti

Abstract

The village of Crngrob (central Slovenia) is known to geologists for the silicified fossils found in the thick soil covering the "Amphiclina beds", a Carnian lithostratigraphic unit of the Mesozoic Slovenian Basin. Due to silicification, the assemblage may provide an important insight into Carnian marine life; however, the nature of the fossil assemblage, as well as the timing and mode of silicification are unknown. A detailed sedimentological section, which covers the uppermost part of the "Amphiclina beds" and their transition to the "Bača Dolomite", was recorded at one of the fossil-bearing localities. The section consists of limestone (including bioturbated filament and radiolaria-filament wackestones, laminated filament packstone, bioclast wackestone, peloid packstone, floatstone with intraclasts and bioclasts, and intraclast floatstone and rudstone), marlstone and dolomite. Chert is locally present in nodules or as dispersed silicified patches, giving a speckled appearance to the host rock. According to our interpretation, the deposition of the limestone occurred via hemipelagic settling, turbidite currents and debris flows in a slope-to-basin or outer ramp setting. The composition of the grains (which include green algae fragments, thick-shelled bivalves, corals and solenoporacean algae) clearly points to the allochthonous nature of the material, which was largely derived from shallow-water environments. Fossils, as well as the intraclasts and sometimes the matrix, are locally replaced by chalcedony and granular megaquartz. This type of silicification does not appear to be selective to particular microfacies. As the silicification occurred after the down-slope transport of shells and the deposition of the sediment, the Crngrob fossil assemblage represents a thanatocoenosis or even a taphocoenosis, and it is not representative of autochthonous Carnian associations.

Izvleček

Okolica Crngroba (osrednja Slovenija) je geologom poznana po okremenjenih fosilih, najdenih v preperini, ki prekriva karnijske amfiklinske plasti. Zaradi okremenjenosti bi fosilna združba lahko nosila pomembno paleoekološko vrednost, vendar njen izvor in značaj nista znana, tako kot nista poznani vrsta in čas okremenitve. V okviru raziskave smo na eni od lokalitet, kjer so bili najdeni fosili, posneli sedimentološki profil preko zgornjega dela amfiklinskih plasti in prehoda v baški dolomit. Zaporedje sestavlja menjavanja plasti apnenca (bioturbiranega filamentnega in radiolarijsko-filamentnega wackestona, laminiranega filamentnega packstona, bioklastičnega wackestona, peloidnega packstona, floatstona z intraklasti in bioklasti ter intraklastičnega floatstone do rudstona), laporovca in dolomita. Lokalno se pojavlja roženec v obliki večjih gomoljev ali drobnih, razpršenih zaplat. Glede na našo interpretacijo je sedimentacija potekala na zunanjem delu pobočja ali ob vznožju pobočja, kjer se hemipelagični in deloma pelagični apnenci prepletajo s sedimenti turbiditnih in drobirskih tokov. Gravitacijski tokovi so večino biogenih zrn, kot so zelene alge, debelolupinske školjke, korale in solenoporaceje, prinesli iz plitvomorskih okolij. Fosili, mestoma pa tudi mikritni intraklasti in osnova, so nadomeščeni s kalcedonom in zrnatim megakremenom. Ta vrsta okremenitve ni vezana na posamezen mikrofacies, temveč se pojavlja v vseh apnenčastih in dolomitnih plasteh. Ker je do okremenitve prišlo po prenosu materiala po pobočju navzdol, nabrana fosilna združba ne more predstavljati naravne karnijske življenjske združbe, temveč gre za primer tanatocenoze ali celo za tafocenozo.

Introduction

With the right timing, silicification may provide high-quality preservation of fossils, because it preserves fine-scale morphological details and small, fragile or otherwise rarely fossilized organisms. Silicified fossil assemblages may thus yield a valuable insight into past life (Cherns & Wright, 2009; Mergl, 2010; Butts & Briggs, 2011). A large collection of silicified and/or pyritized (limonitized) centimetre-sized cephalopods (ammonites), brachiopods, bivalves and gastropods, as well as a few large pieces of colonial corals has been assembled through almost 25 years of field work by F. Stare in the vicinity of Crngrob (central Slovenia). This site has raised considerable interest among professional geologists, but the lack of quality exposures has prevented a more detailed analysis. According to previous work (Ramovš, 1981, 1986, 1987, 1998a, b) the fossils derive from black micritic limestone of Tuvalian (Upper Carnian) age, which belongs to the "Amphiclina beds" (Grad & Ferjančič, 1968; Rožič et al., 2015), an informal lithostratigraphic unit of the Slovenian Basin, but no further account of the fossil-bearing beds has been given until now.

A well exposed succession of shale, limestone, marlstone and dolomite at one of the fossil-bearing sites near the village of Crngrob has been discovered during the geological mapping of the area. The section provided an opportunity to document the composition of the uppermost "Amphiclina beds" and to evaluate the nature of the Crngrob fossil assemblage and its potential use in palaeoecological studies of Carnian marine life. We attempted to identify the depositional environment, the diagenetic sequence, the type and relative timing of silicification and/or pyritization, and to characterize the quality of the preservation. This paper also provides the basis for future taxonomic determinations of the Crngrob fossil assemblage.

Geological Setting

The studied area is located in the vicinity of the village of Crngrob in central Slovenia (Fig 1). The geological structure of this area is covered by the Basic Geological Map of Yugoslavia, Sheet Kranj (Grad & Ferjančič, 1968, 1976). A reconnaissance of the area has been carried out by Rožič et al. (2015). Most recently, the leading author of this paper made a detailed map in order to compare the distribution of lithological units with the positions of fossil sites (Fig. 2). Two major tectonic units have been identified. The eastern part of the map belongs to the Tolmin Nappe of the eastern Southern Alps (Placer, 1999, 2008). The oldest lithostratigraphic unit here consists of alternating shale, siltstone, bedded limestone

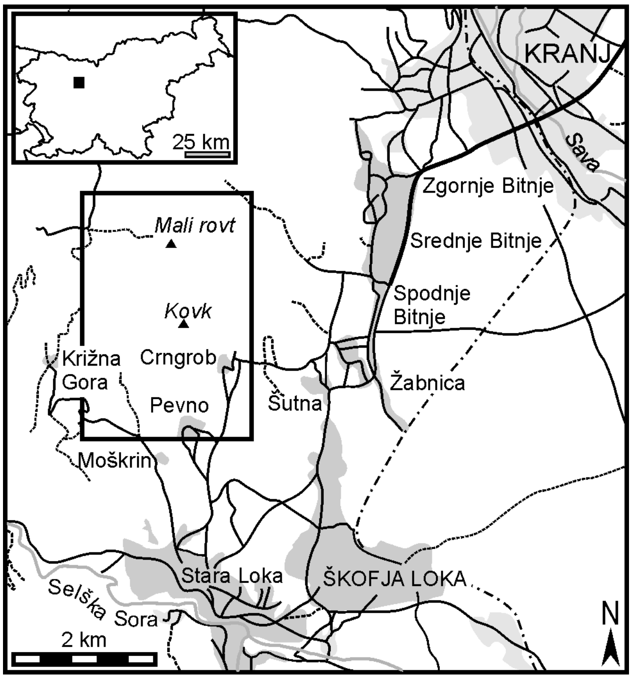

Fig. 1. Location of the studied area. Rectangle shows the area of the geological map in Fig. 2.

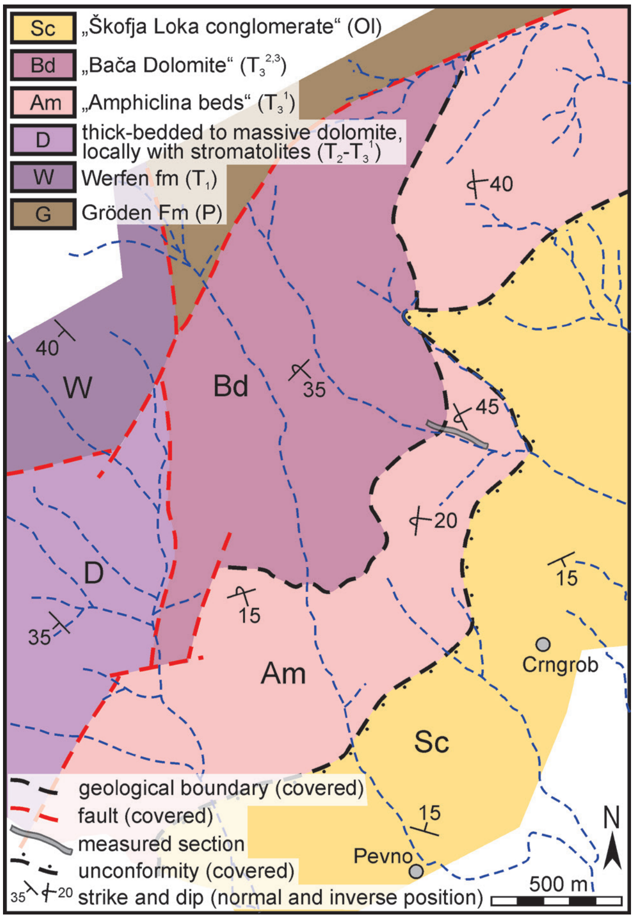

Fig. 2. Simplified geological sketch map of area E of the village of Crngrob (the mapping was performed by one of the authors, L.G.).

and black dolomite, which belong to the "Amphiclina beds" (sensu Turnšek et al., 1982; Buser, 1986). The "Amphiclina beds" grade into the Norian-Rhaetian "Bača Dolomite" (i.e., bedded dolomite with chert). Both are considered to have been deposited in the deeper marine Slovenian Basin (Cousin, 1981; Buser, 1986, 1989, 1996), a marine intraplatform trough situated at the western passive continental margin of the Neotethys Ocean (see the palaeogeographic reconstruction in Haas et al., 1995). To the east, the "Amphiclina beds" are unconformably overlain by uppermost Eocene-lower Oligocene conglomerates. To the west, the "Amphiclina beds" and the "Bača Dolomite" are in fault contacts with red quartz sandstone (the Permian Gröden Formation), marly limestone, carbonate siltstone and marlstone with mica (the Lower Triassic Werfen Formation), and Triassic thick-bedded to massive dolomite with some stromatolites, all of which belong to the External Dinarides tectonic unit (Placer, 1999, 2008). A reconnaissance of the area (Fig. 2) shows that the silicified fossils derive only from the "Amphiclina beds".

Methods

The fossil-bearing succession was recorded along a forest road (Figs. 1-2) at one of the fossil-bearing sites. From this section, 26 samples were collected. An additional 10 samples, which were silicified to various degrees, were collected from debris approximately 130 m to the SW after the lateral continuity of the beds had been verified. For optical microscope analysis, 40 thin sections of sizes 47×28 mm and 75×49 mm were prepared. Selected thin sections were stained with Alizarin Red S. Microfacies (MF) types were named according to the terminology of Dunham (1962) and Embry and Klovan (1971). The quartz terminology used here follows that of Maliva and Siever (1988). Grain proportions were determined by counting 300 random points per section using JMicroVision v.1.2.7 software (© 2002-2008 Nicholas Roduit). Cathodoluminescence (CL) was performed using a cold cathode CITLCL8200/MK4 (Technosyn, Cambridge) at a voltage of 16 kV and a current of 300-450 mA. Neither filters nor standards were used for image calibration. In addition to sedimentological samples, nine composite conodont samples with an average weight of approximately 2 kg were collected and treated with acetic acid. Following this treatment, the conodont elements were hand-picked for determination. The conodont elements were photographed with a JEOL JSM 6490 LV Scanning Electron Microscope. The Conodont Alteration Index (CAI) was determined according to Epstein et al. (1977).

Description of section

The studied section (46°12´22.59´´N, 14°18´12.68´´E) is located in the upper part of the "Amphiclina beds", and extands to the contact with the "Bača Dolomite" (Figs. 3, 4). The recorded beds are underlain by shale and siltstone, whereas the dominant lithology in the section is bedded limestone (locally dolomitized), which is interbedded with marlstone. Several MF types were identified within the limestone beds (see Table 1 for a detailed description).

Wackestone (MF 1 and 3) is bioturbated and mostly thin- to medium-bedded. Some thicker beds display amalgamation, with wavy intercalations of marl. Thin-shelled bivalves (filaments) and radiolaria are common fossils (Fig. 5.1-5.2). In a few beds, filaments form a packstone texture, with shells oriented concordant to the bedding plane (MF 4; Fig. 5.3). Small ammonites were found in larger amounts in a few beds. Wackestone containing mollusc fragments and lacking radiolarian fossils and filaments was identified among the samples from the debris (MF 2; Fig. 5.4). Thin- to medium-thick bedded peloid packstone (MF 5) is present, though less common. Some beds are normally graded and/or display parallel laminae. Bioclasts are subordinate to peloids; in addition to filaments, ammonites and *Tubiphytes*-like microproblematica, fragments of mollusc shells, geniculi of dasyclad green algae and benthic foraminifera were also found. Thin- to medium-bedded floatstone with intraclasts and bioclasts (MF 6; Fig. 5.5-5.8) is characterized by a chaotic texture, with clasts floating in a wackestone or packstone matrix containing thin-shelled bivalves and radiolaria, as well as very rare abraded ooids. Besides intraclasts that are identical in composition to those seen in MF types 1-5, rare fragments of corals, sponges, dasyclad and solenoporacean algae appear among the larger particles. Thin-shelled bivalves are oriented with their convex sides upwards. Floatstone sometimes sharply overlies filament wackestone and grades into peloid packstone. Limestone beds were subject to slumping, resulting in disrupted beds up to 120 cm thick, with angular to rounded wackestone intraclasts kneaded into the marly matrix (MF 7 in Table 1; Fig. 5.9).

Table 1. Microfacies types of the uppermost "Amphiclina beds" at Crngrob.

Microfacies type	Short description	Figures
1 - Bioturbated filament wackestone	Filaments represent 80 % of grains. Subordinate are putative calcified radiolarian, calcite sponge spicules and echinoderm plates.	Fig. 5.1
2 - Bioturbated radiolaria-filament wackestone	Radiolaria prevail over sparse filaments and very rare echinoderms plates, nodosariid foraminifers and juvenile ammonites.	Fig. 5.2
3 - Laminated filament packstone	Filaments (50 % of thin section area) are concordant with the bedding and oriented with their convex sides up or down. The space between filaments is filled with dense wackestone consisting of 40 % pellets and rare (2 %) radiolaria. Calcite cement often fills shielded sites below and between the valves.	Figs. 5.3
4 - Bioclast wackestone	Bioclasts (20 %) are randomly distributed within microsparitic matrix. Mollusc shell fragments represent 10 %, small ammonites 6 %, and echinoderms 3 % of the clasts. Gastropods and ostracods are very rare. With the exception of the ostracods, the bioclasts are replaced by drusy mosaic spar. Some larger bivalve shells show signs of bioerosion and/or endolitization. The patches of drusy mosaic spar (8 % of the area) indicate that part of the micritic matrix was probably winnowed away.	Fig. 5.4
5 - Peloid packstone	Grains are arranged in crude laminae and are sorted by size. Some laminae indicate normal grading. Elongated grains are sometimes aligned with the bedding, but this appears to be mostly due to compaction. Peloids predominate among grains. They range from 0.05 mm to over 1 mm in size. They are ellipsoidal to elongated and angular to well rounded. The smaller ones display only micritic interiors, whereas internal layering may be observed in the larger grains. Due to the presence of *Tubiphytes*-like microproblematica (1.5 % of the area), some of the peloids probably originated as microbialite intraclasts. Mollusc fragments represent 5-10 % of the area, and echinoderm plates up to 5 %. Geniculi of dasyclad green algae, gastropods, brachiopods, "spherulites", juvenile ammonites, ostracods, microproblematica *Thaumatoporella parvovesiculifera* (Raineri) and benthic foraminifera (*Decapoalina schaeferae* (Zaninetti, Altiner, Dager & Ducret), *Palaeolituonella meridionalis* (Luperto), *Duotaxis* sp., *Reophax* sp., Duostominidae, and nodosariid Lagenida) are very rare. Thin-shelled bivalves ("filaments") may be locally present. They are oriented with their convex sides upwards, and blocky spar sometimes fills the spaces beneath the valves.	
6 - Bioclast-intraclast and intraclast-bioclast floatstone	Clasts larger than 2 mm represent 30 % of the area (note that some compaction likely occurred), while wackestone or packstone matrix fills the remaining volume. The distribution of large clasts seems chaotic, although some alignment parallel to the bedding may be present that is due to compaction. Most are intraclasts with subangular edges and correspond to MF 1-5. Rrecrystallized sponges (up to 3 cm large fragments) are rarer, as are partly broken bivalve and brachiopod shells, corals, ammonites, solenoporacean algae and presumed genicules of dasyclad algae. Some large echinoderm plates and fragmented gastropods may also be counted among the largest grains. Within the wackestone matrix, some filaments, echinoderm plates, calcified or pyritised radiolaria, gastropods, and foraminifera (*Aulotortus sinuosus* Weynschenk, *Diplotremina subangulata* Kristan-Tollmann, ?*Duostomina biconvexa* Kristan-Tollmann, "*Trochammina*" *almtalensis* Koehn-Zaninetti, *Variostoma pralongense* Kristan-Tollmann, *Reophax* sp., Duostominidae, and nodosariid Lagenida) are present. A similar association of grains is present within the packstone matrix, together with peloids, microbialite aggregate grains, calcimicrobes, *Tubiphytes*-like microproblematica, fragments of *Thaumatoporella parvovesiculifera* (Raineri), ostracods, and occasional abraded ooids.	Figs. 5.5-5.8
7 - Intraclast floatstone and rudstone	Angular to subrounded clasts are up to 16 mm in size and represent up to 60 % of the thin-section area. Mudstone, "calcisiltite" (with small sparitic fragments and nodosariid lagenid foraminifera), wackestone with thin-shelled bivalves, and wackestone with microbialite fragments and echinoderm plates are seen. The interstitial space is filled with dolomitized matrix. Rarely, echinoderm plates can be found.	Fig. 5.9

Diagenesis

Although different lithologies constitute the sequence, it appears that diagenetic processes did not act selectively on the individual MF types: neomorphism, silicification, and precipitation of ferrous dolomite were detected in wackestone, as well as in floatstone. However, due to the larger number of aragonitic shells and intraclasts, these diagenetic processes seem to be most common in floatstone.

Micrite, commonly recrystallized into microspar (which shows speckled luminescence under CL), is the main supporting medium in all MF types. Early mosaic calcite in places fills vugs and intragranular spaces (Fig. 6.1) in bioclastic wackestone. Bladed spar has also been observed within a brachiopod interior in peloid packstone. Compaction of the sediment is evident from flattened peloids, sometimes wrapped around echinoderm plates, puzzle-like breakage of bivalve or other shells, and alignment of the filaments within bioturbations, as well as outside them. Pyrite crystals are present in the matrix and in micritic intraclasts. In thin section 654b (laminated filament packstone), radiolaria appear to be pyritized within a thin strip of sediment (Fig. 6.2). They preserve many details of their tests, in contrast to more common calcified specimens. In one case, pyrite also crystallized on the bivalve shell, pre-dating the precipitation of ferrous dolomite. In other cases, however, well-formed and relatively large pyrite crystals cross-cut blocky spar or calcite veins. Relatively early changes further incorporate replacement of aragonite with drusy mosaic calcite through the complete dissolution of aragonitic bioclasts (thick-shelled bivalves, gastropods, ammonites, sponges, corals) and the formation of moulds (Figs. 6.3-6.4).

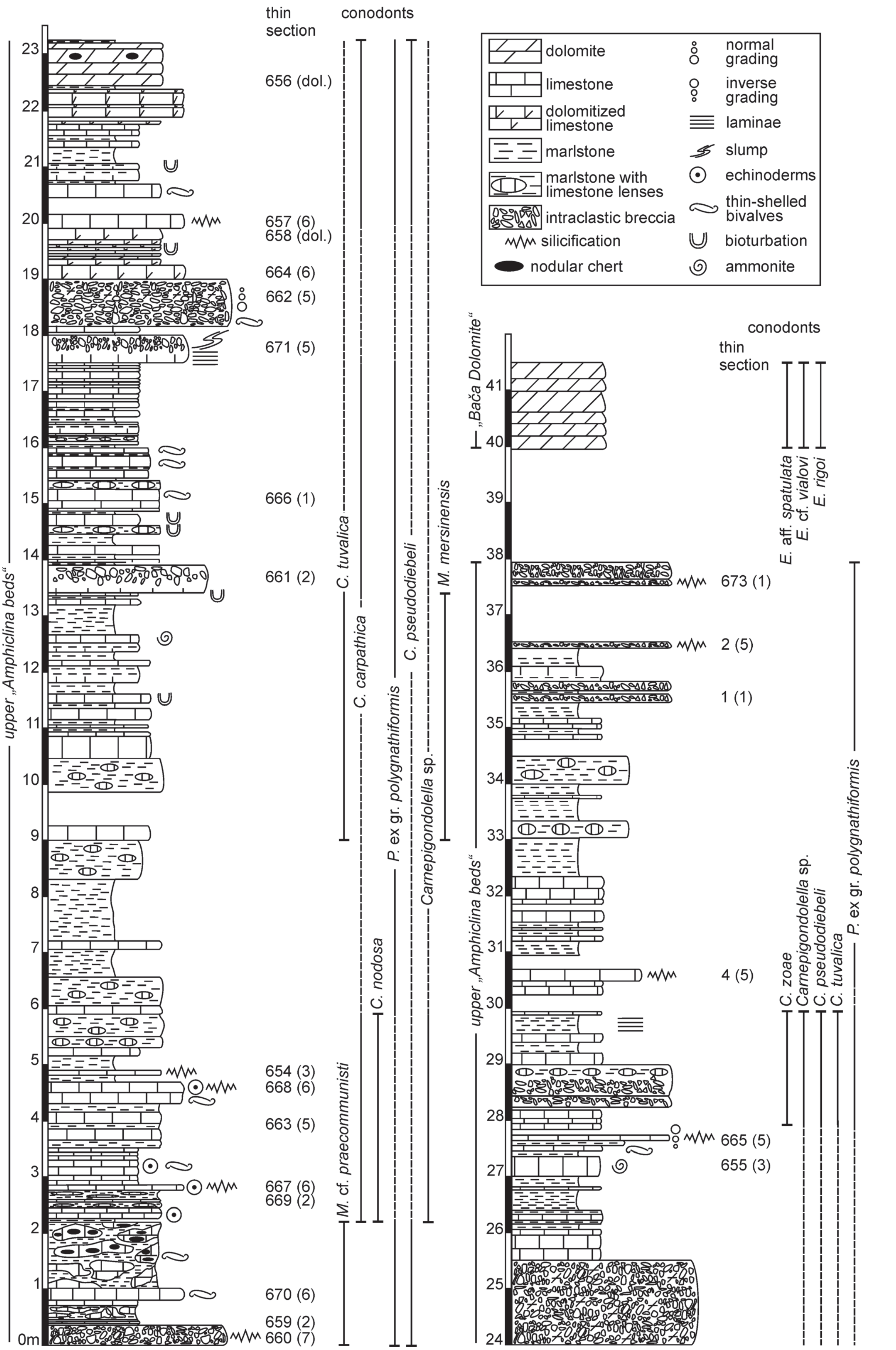

Fig. 3. Presentation of the recorded section. Numbers in brackets refer to MF type (see Table 1). Other samples (for additional study of the silicification) were collected ex situ. Abbreviations: *C- Carnepigondolella, E- Epigondolella, M- Metapolygnathus, P- Paragondolella*.

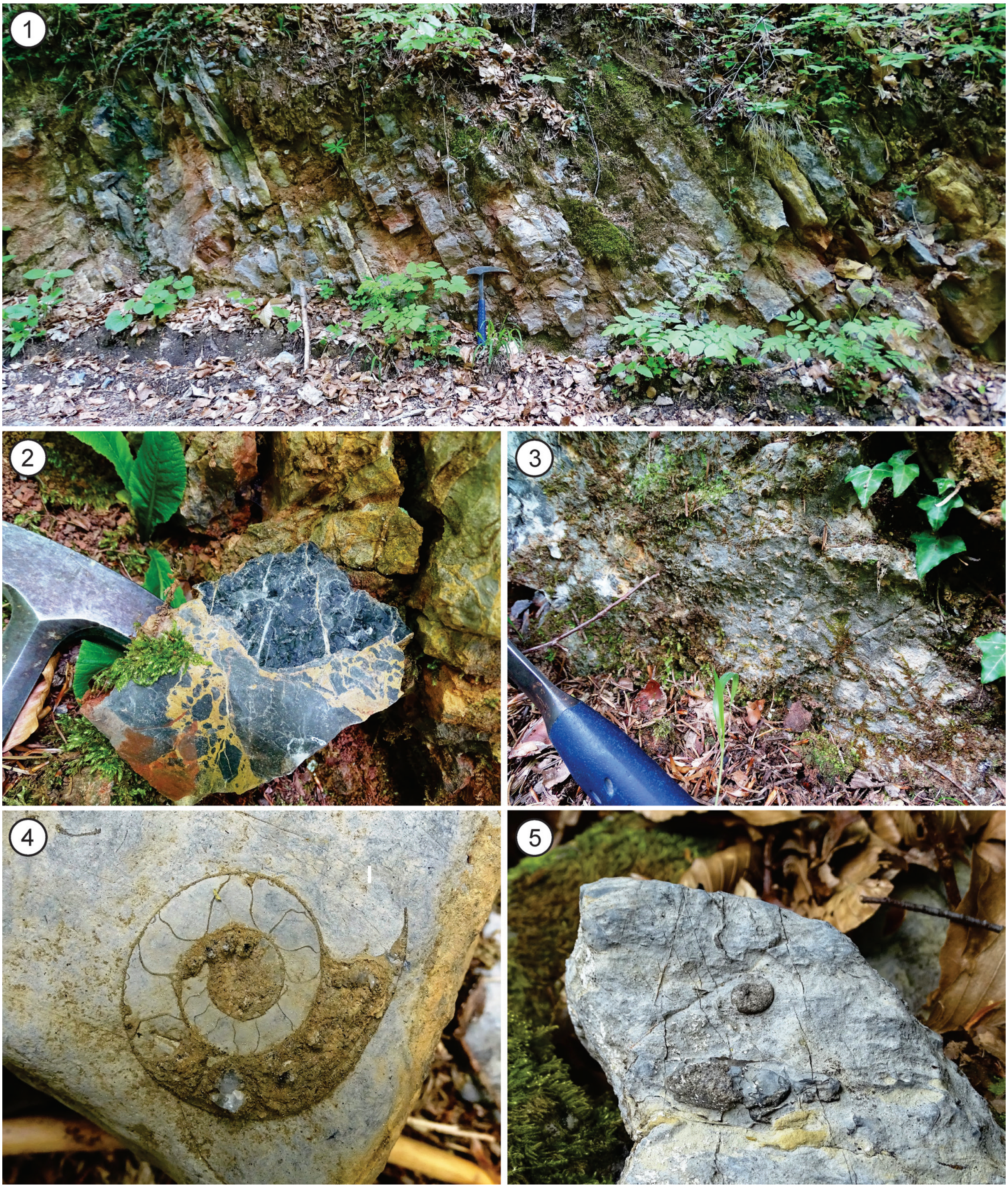

Fig. 4. Field photographs of the recorded section of the uppermost "Amphiclina beds". 4.1- Part of the recorded section. Beds are in overturned position. 4.2- Intraclastic floatstone to rudstone. Note the black chert, which substitutes for most of one clast (a thin strip of limestone remains on the outer side of the clast). 4.3- Selective silicification, giving a "mottled" appearance to the rock. 4.4- An at least partly silicified ammonite, approximately 2.5 cm in size. 4.5- Small silicified ammonites. The larger ammonite is approximately 5 cm in diameter.

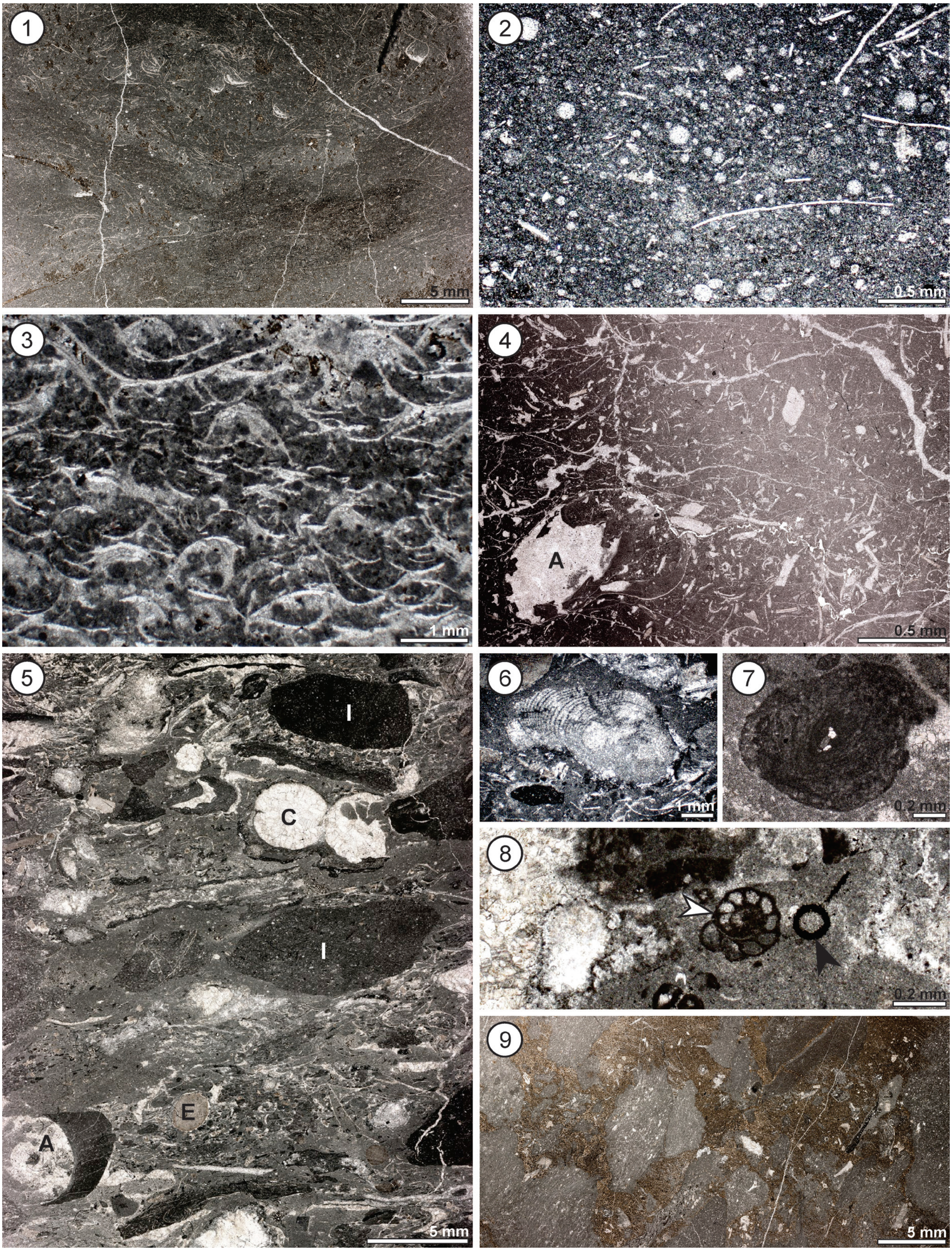

Fig. 5. Microfacies types of the uppermost "Amphiclina beds" at Crngrob.

5.1- Bioturbated filament wackestone. Thin section 666. 5.2- Bioturbated radiolaria-filament wackestone. Thin section 659. 5.3- Laminated filament packstone. Thin section 654b. 5.4- Bioclast wackestone. A: ammonite. Thin section 652. 5.5- Bioclast-intraclast and intraclast-bioclast floatstone. C: corals; E: echinoderm; A: ammonite (as part of an intraclast); I: intraclasts. Thin section 672a. 5.6- Fragment of solenoporacean red algae. Intraclast-bioclast floatstone. Thin section 672e. 5.7- *Tubiphytes* sp. Intraclast-bioclast floatstone. Thin section 672c. 5.8- Duostominid foraminifera (white arrowhead) and pyritized radiolaria (black arrowhead). Bioclast-intraclast or intraclast-bioclast floatstone. Thin section 672h. 5.9- Intraclast floatstone and rudstone. Thin section 660.

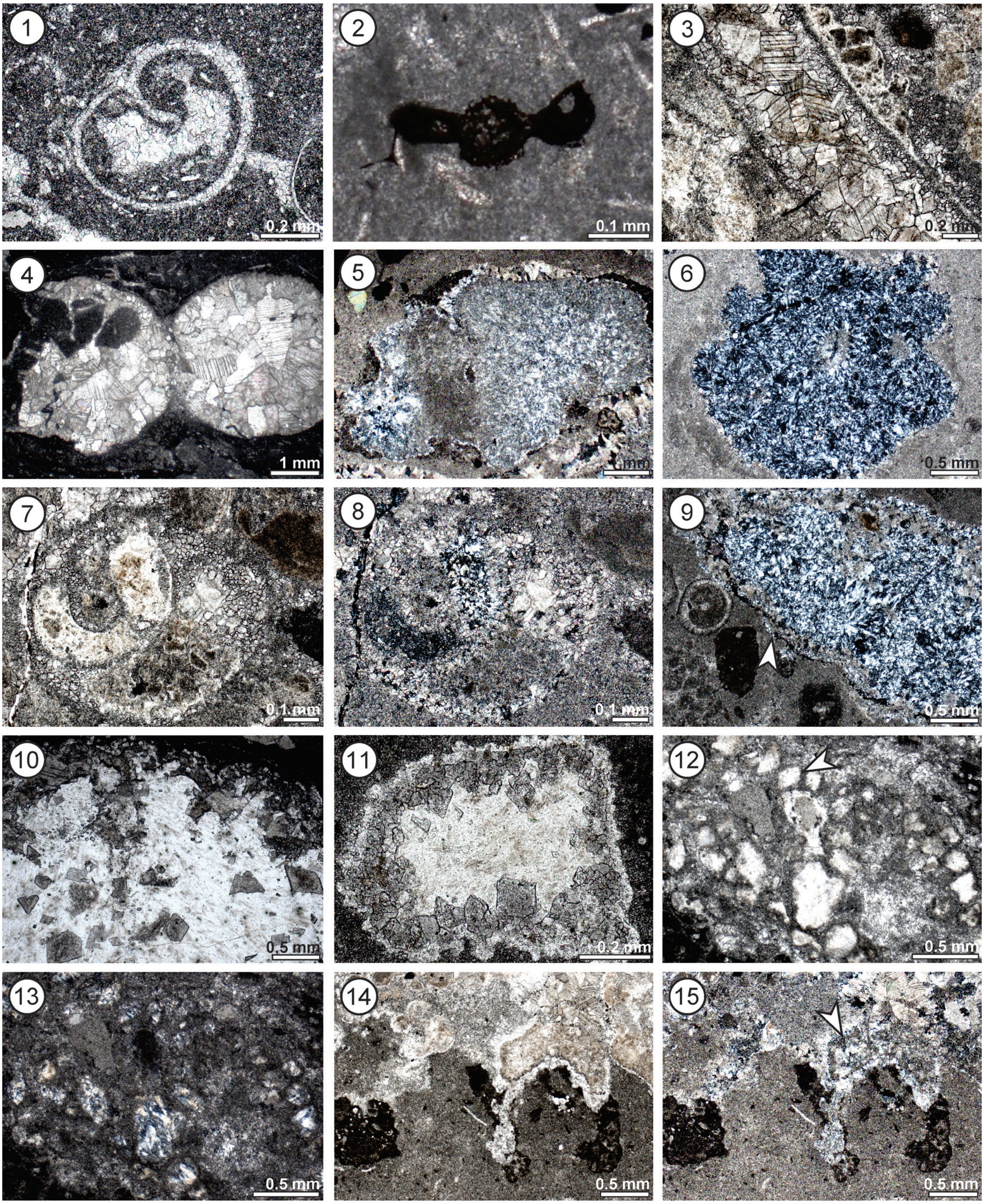

Fig. 6. Diagenetic features of the uppermost "Amphiclina beds" at Crngrob. 6.1- Mosaic spar, partly infilling the interior of a gastropod. Micrite (automicrite?) clings to the inner wall of the shell. Thin section 652. 6.2- Pyritized radiolarian and small sponge spicules. Thin section 654b. 6.3- Neomorphism of a bivalve shell. Thin section 653. 6.4- Neomorphism of corals. Thin section 672a. 6.5- Replacement of a probable micritic intraclast by chalcedony. Thin section 672h. 6.6- Silicification of an echinoderm plate. Thin section 653. 6.7- Partial silicification of a gastropod. Note that the chert infills the interior of the gastropod and partly replaces its shell. Thin section 653. 6.8- Same view under crossed Nicols. 6.9- Silicification front (arrowhead). Note the adjacent gastropod, which is not yet silicified. Thin section 653. 6.10-6.11- Void-filling chert. Note the rhombic carbonate crystals lining the wall of the void. Chips of crystals are included within the chert. Thin sections 667b and 653. 6.12- Chert, replacing some particles, including presumably rhombic crystals. Thin section 668b. 6.13- Same view under crossed Nicols. 6.14-6.15- Silicification front. Note the large rhombic crystal replaced by chalcedony that is seen under crossed Nicols (Fig. 6.15). Thin section 672h.

Spherulitic chalcedony and granular megaquartz locally replace the micritic matrix, gastropods, thick-shelled bivalves, echinoderms (excluding the surrounding syntaxial calcite cement), brachiopods, calcimicrobes, some intraclasts and even lagenide foraminifera (Figs. 6.5-6.9). Microstructure-controlled replacement of brachiopod shells by chalcedony has also been observed, while microbial crusts are often the sites of precipitation of quartz euhedra. Chalcedony may enclose rhombic carbonate crystals and/or infill the remaining internal parts of the voids, which are lined with large rhombic crystals of a carbonate mineral (Figs. 6.10-6.11). These rhombic crystals may be partly shattered, with chips incorporated into the chert. Rarely, chalcedony appears to replace the rhombic crystals (Figs. 6.12-6.15). In sample 654b, silicification has affected some or part of the laminae with higher porosity: it appears to stop at the contact with more matrix-rich lamina (Fig. 7.1). Ferrous dolomite in large crystals substitutes for the matrix between filaments in other parts of the thin section (Fig. 7.2). Ferrous dolomite locally fills gastropod (Fig. 7.3), ammonite (Figs. 7.4-7.5), and thick-shelled bivalve shells (Fig. 7.6), especially in bioclast-intraclast and intraclast-bioclast floatstone. The infill may be partial (in which case the other part of the mould is being filled by drusy mosaic calcite) or complete. Ferrous dolomite is also found within veins (Fig. 7.7). Under CL, bright orange, dull red and non-luminescent bands are seen in clearly zoned crystals. The non-luminescent clear mosaic or blocky calcite post-dates ferrous dolomite; the calcite fills the remaining space (Fig. 7.8). In one sample, the clear blocky spar forms patches within the micritic matrix (Fig. 7.9). In rare cases, the clear spar fills veins. The relationship with chert is unresolved. Another generation of megaquartz, which is reflected by crystals more than 1 mm in size, occurs rarely in veins or fills the spaces between the clear spar crystals (Fig. 7.10).

Some samples are completely dolomitized, and dolomitization may have taken place contemporary with selective replacement of fossils by ferrous dolomite (the timing of dolomitization is currently not resolved). Different types of pervasive dolomitization can be distinguished, hinting at different generations of dolomite. Sedimentary structures are sometimes still preserved, due to the different colours, shapes and sizes of the dolomite crystals. Smaller euhedral to subhedral crystals with brownish outer rims (which are enriched in Fe) seem to preferentially substitute for the micritic matrix (Fig. 7.11). Under CL, they exhibit dark red luminescence with thin bright yellow bands. The second type of dolomite is represented by lighter and larger subhedral crystals (Fig. 7.12), which emit very weak, dark red luminescence. Some veins are also filled with dolomite. Calcite veins cut through all other diagenetic phases. The exception may be the second generation of megacrystalline quartz, for which the relationship with the calcite veins could not be determined.

Age of the studied succession

Conodont biostratigraphy

The Colour Alteration Index (CAI) of the recovered conodont elements (some of which are shown in Fig. 8) is 5 and/or slightly above 5, demonstrating strong alteration and even a low grade of metamorphism (see Kovacs & Arkai, 1987; Sudar & Kovacs, 2006; Kovacs et al., 2006).

The conodont fauna from the uppermost "Amphiclina beds" is dominated by the elements *Paragondolella* ex gr. *polygnathiformis* (Budurov & Stefanov) and *Carnepigondolella* with the representatives: *Carnepigondolella* aff. *carpathica* (Mock), *C. nodosa* (Hayashi), *C. pseudodiebeli* (Kozur), *C. tuvalica* Mazza et al., *Carnepigondolella zoae* (Orchard), *Carnepigondolella* sp., in association with *Metapolygnathus mersinensis* (Moix et al.) and *M.* cf. *praecommunisti* Mazza et al. As a direct forerunner of *Metapolygnathus*, the genus *Paragondolella* can be distinguished by the terminal or subterminal position of the basal pit (Kozur, 2003). Some specimens of *Paragondolella* reveal transitional features towards the genus *Metapolygnathus*, with a prolonged keel behind the basal pit. This feature is consistent with observations of Mazza et al. (2012). The genus *Paragondolella* is confined to the Carnian, whereas *Metapolygnathus* ranges from the Late Carnian to the basal Norian. The species *M. praecommunisti* has not yet been documented from Slovenia, but its successor, *M. communisti* Hayashi has been reported from the Late Carnian-Early Norian fauna of the Martuljek Group in the Julian Alps (Celarc & Kolar-Jurkovšek, 2008). *Carnepigondolella* is characterized by a weak ornamentation on the platform margins and by a subterminal basal pit (Kozur, 2003). This genus is a marker of the Upper Carnian that also occurs rarely in the Lower Norian and is regarded as the forerunner of *Epigondolella*.

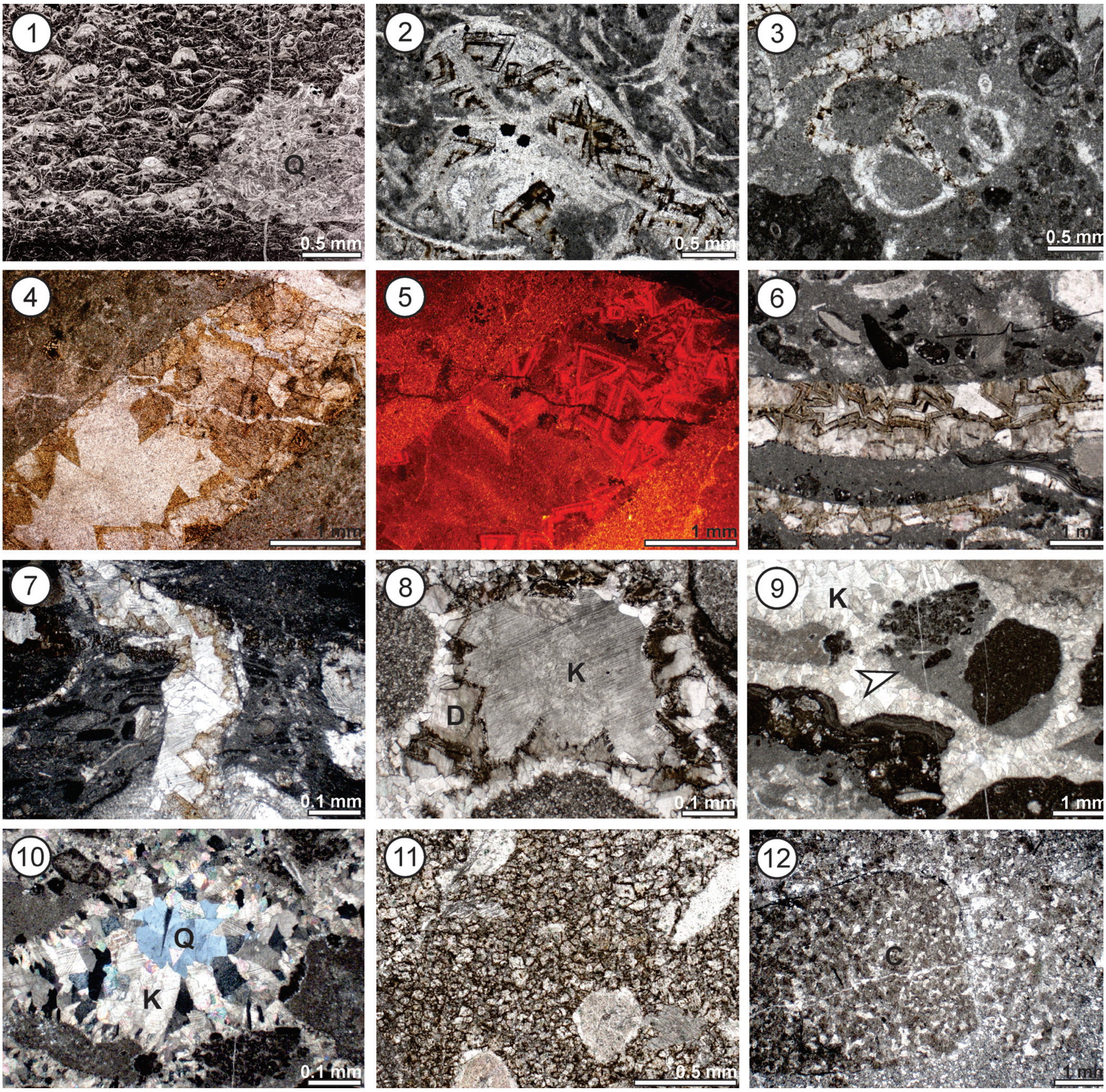

Fig. 7. Diagenetic features of the uppermost “Amphiclina beds” at Crngrob. 7.1- Partial silicification of the radiolarian-filament packstone. Note the sharp lower boundary of the chert (Q), which follows a lithological boundary with a greater amount of micritic matrix. Thin section 654b. 7.2- Ferrous dolomite between bivalves. Thin section 654b. 7.3- Replacement of a gastropod shell by ferrous dolomite. Thin section 672c. 7.4- Ferrous dolomite filling the dissolved shell of an ammonite. Thin section 667c. 7.5- Same view under CL. 7.6- Ferrous dolomite filling dissolved bivalve shells. Shells are fragmented. Thin section 672c. 7.7- Vein-filling ferrous dolomite. Thin section 667b. 7.8- Blocky calcite (K) filling the interior of the void lined by ferrous dolomite (D). Thin section 672i. 7.9- Blocky calcite (K) precipitated after partial dissolution of the matrix (arrowhead). Thin section 672h. 7.10- Megaquartz (Q) interior to the blocky calcite (K). Thin section 672h. 7.11- Subhedral to euhedral dolomite crystals. Note the brownish colour of the outer rim. Large, undolomitized grains are echinoderm plates. Thin section 660. 7.12- Subhedral dolomite. Note the ghostly image of the clast (C), suggesting a former floatstone texture. Thin section 672g.

Fig. 8. Conodont elements from the uppermost “Amphiclina beds” (8.1-8.6) and the lowermost “Bača Dolomite” (8.7-8.8). 8.1- *Carnepigondolella tuvalica* Mazza et al., sample GeoZS 5661. 8.2- *Carnepigondolella zoae* (Orchard), sample GeoZS 5661. 8.3-8.4- *Paragondolella* ex gr. *polygnathiformis* (Budurov & Stefanov), samples GeoZS 5540 and 5539. 8.5-8.6- *Carnepigondolella* aff. *carpathica* (Mock), sample GeoZS 5660. 8.7- *Epigondolella rigoi* Noyan & Kozur, sample GeoZS 5643. 8.8.- *Epigondolella* cf. *vialovi* (Buryi), sample GeoZS 5643.


1a
1b
1c
2a
2b
2c
200 µm
3a
3b
3c
4a
4b
4c
5a
5b
5c
6a
6b
6c
7a
7b
7c
8a
8b
8c

Among the *Carnepigondolella* species that were identified, the presence of *C. tuvalica* and *C. zoae* that occur in the Late Tuvalian is important. The measured uppermost part of the "Amphiclina beds" is thus Tuvalian in age.

A single sample from the "Bača Dolomite" yields a small but significant fauna. It is marked by the exclusive presence of *Epigondolella* that reveals a more reduced platform, allowing development of a free blade. This genus is characteristic of the Norian, but it had already appeared in the Late Tuvalian. Several morphogenetic lineages are recognized from the period of their rapid evolution (Orchard, 2007). The co-occurrence of the species *E.* aff. *spatulata* (Hayashi), *E. rigoi* Noyan & Kozur, and *E.* cf. *vialovi* (Buryi) defines the Lacian age of the sample. Norian epigondolellids are known to occur extensively in Slovenia (Kolar-Jurkovšek, 1991; Buser et al., 2008), and a similar fauna was recently documented from the Lower Norian strata of the Martuljek Group in the Julian Alps (Celarc & Kolar-Jurkovšek, 2008).

Foraminifera

Concerning foraminifera, the following taxa (listed alphabetically) were identified in thin sections of bioclast-intraclast/intraclast-bioclast floatstone and in peloid packstone: *Aulotortus sinuosus* Weynschenk, ?*Decapoalina schaeferae* (Zaninetti, Altiner, Dager & Ducret), *Diplotremina subangulata* Kristan-Tollmann, ?*Duostomina biconvexa* Kristan-Tollmann, *Duotaxis* sp., *Palaeolituonella meridionalis* (Luperto), *Reophax* sp., "*Trochammina*" *almtalensis* Koehn-Zaninetti, *Variostoma pralongense* Kristan-Tollmann. Undetermined Duostominidae and nodosariid Lagenida were also recognized. Neither species provides a detailed stratigraphic range. It should be noted, however, that the range of *Decapoalina schaeferae*, which was previously known from Norian and Rhaetian strata (Gale et al., 2013), should be extended to the Late Tuvalian.

Discussion

Depositional model

Concerning sedimentation, three types of sediments can be distinguished in the observed section. The bioturbated filament wackestone, radiolaria-filament wackestone and laminated filament packstone are interpreted as hemipelagic/pelagic sediments. The concordant position of thin-shelled bivalves in the latter may be due to redeposition out of suspension, compaction, or the presence of weak bottom currents (Kidwell & Bosence, 1991). Traces of bioturbation suggest oxygenated bottom conditions. The presence of radiolaria, ammonites, and thin-shelled bivalves suggests an open-marine environment (Flügel, 2004). The bioclast wackestone and peloid packstone are interpreted as distal turbidites, or as the result of some other gravitational current transport mode. This is supported by the presence of normal grading and laminae in peloid packstone and the presence of grains derived from within the photic zone (green algae, bioerosion on bivalve shells, foraminifera *Decapoalina schaeferae*, *Palaeolituonella meridionalis*).

The chaotic distribution of clasts floating in slightly convoluted (fluid) matrix suggests that the bioclast-intraclast and intraclast-bioclast floatstone formed via debris flows. Grains are again partly derived from shallow water (corals, solenoporaceans, green algae, and the foraminifera *Aulotortus sinuosus*), but some micritic intraclasts represent mud chips torn from the sea bottom, and fossils found within the matrix (radiolaria, filaments) represent open-marine biota. The intraclast floatstone to rudstone might alternatively represent a debris flow deposit with a predominance of basin-derived clasts, or a slump conglomerate/breccia.

This facies association suggests the slope to toe-of-slope setting, or the outer ramp environment (Flügel, 2004).

Timing of silicification of fossils

Although we could clearly distinguish between the megaquartz that post-dates the blocky spar from the chalcedony, which replaces fossils, we are not able to confidently assign the silicification of fossils to the early or late stages of diagenesis. The ammonites, gastropods and bivalves, which were originally made up of aragonite (Flügel, 2004), were probably already replaced by low-Mg calcite spar when silicification occurred. They are replaced alongside low-Mg calcite calcimicrobes, brachiopods and lagenide foraminifera, as well as high-Mg calcite echinoderms (Flügel, 2004). Chalcedony usually replaces only parts of fossils and is not always confined to the fossils itself. As seen in Figure 6.9, silicification did not extend to the gastropod immediately adjacent to the progressing silicification front. The silicification thus clearly post-dates deposition of the sediment. Furthermore, the presence of rhombic crystals lining some vugs filled with chalcedony, seemingly shattered and broken-off rhombic crystals, and rhombic crystals replaced by silica suggest that the chalcedony precipitated after the vug-lining spar.

The silicification in the "Amphiclina beds" might be somewhat similar to the late diagenetic silicification that selectively affected clasts in conglomerates of the Upper Jurassic Toril Formation in the Bethic Mountains of Spain (Bustillo & Ruiz-Ortiz, 1987). Bustillo and Ruiz-Ortiz (1987) additionally recorded nodule- and bed-producing early diagenetic silicification that was restricted to the Ta (partly), Tb and Tc parts of the intercalated turbidite beds. The rare nodular chert in the recorded part of the "Amphiclina beds" may indeed be early diagenetic, as shown by the presence of chert clasts in rudstone shown in Figure 4.2 (which is similar to the nodular chert in the Norian-Rhaetian "Bača dolomite"; D. Skaberne, pers. com. 2009). In the case of the silicified fossils, however, there seems to be no preference for lithology, as the same type of clasts may be silicified in both bioclast-intraclast floatstone and hemipelagic sediments. The impression that silicification is confined to certain lithologies is solely a consequence of the greater amount of calcareous bioclasts in bioclast-intraclast and intraclast-bioclast floatstone. Therefore, rather than arguing for lithological control over the silicification of fossils, we suggest that all the investigated types of limestone acted similarly during the burial diagenesis, which can be attributed to the largely homogenous permeability of the matrix-rich sediment.

Conclusions

The uppermost 38 m of the "Amphiclina beds" were sampled at Crngrob in order to define the origin of the silicified fauna, the nature of the assemblage and the timing of silicification. The section exposes limestone, dolomite and marlstone of Tuvalian age. Within the limestone, seven microfacies types were determined. Bioturbated filament wackestone, bioturbated radiolaria-filament wackestone and laminated filament packstone represent hemipelagic sediments. Peloid packstone and bioclast wackestone were deposited from distal turbidite flows. Bioclast-intraclast and intraclast-bioclast floatstone represent the debris-flow microfacies, while intraclast floatstone and rudstone are interpreted as debris-flow deposits or as slump breccias. The sediments were deposited in the slope to toe-of-slope setting or in the outer ramp setting (Flügel, 2004). A complex diagenetic history has been partly resolved. Early diagenesis involved compaction of the sediment and replacement of aragonite with drusy mosaic calcite. Local selective silicification affected the fossils, as well as some of the intraclasts and even parts of the matrix. Silicification (replacement by chalcedony and megaquartz) was detected in all of the limestone types, but it is most evident in bioclast-intraclast and intraclast-bioclast floatstone, where the majority of the larger fossils are found. Because the silicification occurred after deposition of the sediment, and because the fossils are partly derived from shallow-water environments, the Crngrob silicified fossil assemblage represents a biased thanatocenosis or even a taphocenosis, and it is not an autochthonous Carnian fossil association. Ferrous dolomite, sometimes associated with veins, locally replaces non-silicified or partly silicified fossils and matrix. Clear mosaic or blocky calcite postdates ferrous dolomite. Some samples are completely dolomitized. Two types of dolomitization are suggested by the different sizes, shapes, and colours of the dolomite crystals, and the original texture of the sediment is sometimes preserved. The timing of dolomitization has not been resolved.

Acknowledgements

The field work and preparation of samples were financially supported by the Slovenian Research Agency (Programme Number P1-0011). We thank the technical staff of the Geological Survey of Slovenia (Marija Petrović and Mladen Štumergar) and the Faculty of Natural Sciences and Engineering (Ema Hrovatin and Miran Udovč) for the preparation of thin sections and conodont samples. We also thank Bojan Otoničar from the Karst Reseach Institute in Postojna, who gave us access to the cathodoluminescence equipment and a brief tutorial. Conodont elements were photographed with the kind help of Miloš Miler at the Geological Survey of Slovenia. Andrej Novak helped with some of the field work. Communication on conodonts with Michele Mazza (Milano, Italy) is acknowledged. We are also grateful to the reviewers of the manuscript, Mirijam Vrabec, Boštjan Rožič and Dragomir Skaberne for their constructive comments.

References

Buser, S. 1986: Explanatory book for Basic geological map SFRY 1:100.000, Sheets Tolmin and Videm (Udine): L 33-64. Federal Geological Survey, Beograd: 103 p.

Buser, S. 1989: Development of the Dinaric and the Julian carbonate platforms and of the intermediate Slovenian Basin (NW Yugoslavia). Boll. Soc. Geol. Ital. 40: 313-320.

Buser, S. 1996: Geology of Western Slovenia and its paleogeographic evolution. In: Drobne K., Goričan, Š. & Kotnik, B. (eds.): International workshop Postojna '96: The role of impact processes and biological evolution of planet Earth. Research Institute of Slovenian Academy of Sciences and Arts, Ljubljana: 111-123.

Buser, S., Kolar-Jurkovšek, T. & Jurkovšek, B. 2008: The Slovenian Basin during the Triassic in the Light of Conodont Data. Boll. Soc. Geol. It. (Ital. J. Geosci.), 127: 257-263.

Bustillo, A. M. & Ruiz-Ortiz, A. P. 1987: Chert occurrences in carbonate turbidites: examples from Upper Jurassic of the Betic Mountains (southern Spain). Sedimentology, 34: 611-621.

Butts, S. H. & Briggs, D. E. G. 2011: Silicification through time. In: Allison, P. A. & Bottjer, D. J. (eds.): Taphonomy: Process and bias through time. Springer Science and Business Media B.V., Topics in Geobiology, 32: 411-434.

Celarc, B. & Kolar-Jurkovšek, T. 2008: The Carnian-Norian basin-platform system of the Martuljek Mountain Group (Julian Alps, Slovenia): progradation of the Dachstein carbonate platform. Geol. Carpathica, 59: 211-224.

Cherns, L. & Wright, V. P. 2009: Quantifying the impacts of early diagenetic aragonite dissolution on the fossil record. Palaios, 24: 756-771.

Cousin, M. 1981: Les rapports Alpes-Dinarides; Les confins de l'Italie et de Yougoslavie. I. Soc. Géol. Nord, 5: 521 p.

Dunham, R. J. 1962: Classification of carbonate rocks according to depositional texture. In: Han, W. E. (ed.): Classification of carbonate rocks, A symposium. Amer. Ass. Petrol. Geol. Mem. : 108-121.

Embry, A.F. & Klovan, J.E. 1971: A late Devonian reef tract on northeastern Banks Island, N.W.T. Bull. Canad. Petrol. Geol. 19: 730-781.

Epstein, A.G., Epstein, J.B. & Harris, L.D. 1977: Conodont color alteration – An index to organic metamorphism. U.S. Geol. Surv. Prof. Pap., 995: 1-27.

Flügel, E. 2004: Microfacies of carbonate rocks: Analysis, interpretation and application. Springer-Verlag, Berlin: 976 p.

Gale, L., Rettori, R., Martini, R. & Rožič, B. 2013: *Decapoalina* n. gen. (Miliolata, Milioliporidae; Late Triassic), a new foraminiferal genus for "*Sigmoilina*" *schaeferae*. Boll. Soc. Paleontol. It., 52: 81-93.

Grad, K. & Ferjančič, L. 1968: Basic geological map SFRY 1:100.000, Sheet Kranj. Federal Geological Survey Beograd.

Grad, K. & Ferjančič, L. 1976: Explanatory book for Basic geological map SFRY 1:100.000, Sheet Kranj: L 33-65. Federal Geological Survey, Beograd: 70 p.

Haas, J., Kovács, S., Krystyn, L. & Lein, R. 1995: Significance of Late Permian-Triassic facies zones in terrane reconstructions in the Alpine-North Pannonian domain. Tectonophysics, 242: 19-40.

Kidwell, S.M. & Bosence, D.W.J. 1991: Taphonomy and time-averaging of marine shelly faunas. In: Allison, P.A. & Briggs, D.E.G. (eds.): Taphonomy: Releasing the Data Locked in the Fossil Record. Topics in Geobiology. Plenum Press, New York, 9: 115–209.

Kolar-Jurkovšek, T. 1991: Microfauna of Middle and Upper Triassic in Slovenia and its biostratigraphic significance. Geologija, 33: 21-170.

Kovács, S. & Arkai, P. 1987: Conodont alteration in metamorphosed limestones from the northern Hungary, and its relationship to carbonate texture, illite – crystallinity and vitrinite reflectance. In: Austin, R.L. (ed.): Conodonts: Investigative Techniques and Applications. British Micropaleontol. Soc. Series, Ellis Horwood Ltd., Chichester: 207-229.

Kovács, S., Rálisch-Felgenhauer, E. & Bóna, J. 2006: Conodont colour alteration related to a half-graben structure: an example from the Mesozoic of the Mecsek and Villány Hills area (Tisza, Megaunit, Southern Hungary). Geol. Carpathica, 57: 257-268.

Kozur, H.W. 2003: Integrated ammonoid, conodont and radiolarian zonation of the Triassic. Hallesches Jb. Geowiss., B25: 49-79.

Maliva, R.G. & Siever, R. 1988: Mechanism and controls of silicification of fossils in limestones. J. Geology, 96: 387-398.

Mazza, M., Rigo, M. & Gullo, M. 2012: Taxonomy and biostratigraphic record of the Upper Triassic conodonts of the Pizzo Mondello section (western Sicily, Italy), GSSP candidate for the base of the Norian. Riv. Ital. Paleont. Strat., 118: 85-130.

Mergl, M. 2010: Silicification of fossils in the Silurian and Devonian of the Barrandian, Czech Republic. J. Nat. Mus. (Prague), Nat. Hist. Ser., 179/13: 139-145.

Orchard, M.J. 2007: Conodont lineages from the Carnian-Norian boundary at Black Bear Ridge, Northeast British Columbia. In: Lucas, S.G. & Spielmann, J.A. (eds.): The global Triassic. New Mexico Museum of Natural History and Science, Bull., 41: 321-330.

Placer, L. 1999: Contribution to the macrotectonic subdivision of the border region between Southern Alps and External Dinarides. Geologija, 41: 223-255, doi:10.5474/geologija.1998.013.

Placer, L. 2008: Principles of the tectonic subdivision of Slovenia. Geologija, 51/2: 205-217, doi:10.5474/geologija.2008.021.

Ramovš, A. 1981: Zanimive triasne okamnine v obzidju crngrobske cerkve. Loški razgledi, 28: 271-275.

Ramovš, A. 1986: Pelagische obertriadische (karnische) Kalksteine im Gebiet von Škofja Loka. Loški razgledi, 33: 111-114.

Ramovš, A. 1987: Obertriassische (oberes Tuval) Kalke oberhalb von Crngrob. Loški razgledi, 34: 77-78.

Ramovš, A. 1998a: Amoniti na loškem ozemlju. Loški razgledi, 45: 11-14.

Ramovš, A. 1998b: Conodonten-Stratigraphie der Obertrias von Slowenien Ergebnisse eigener Untersuchungen. Geologija, 40: 223-232, doi: 10.5474/geologija.1997.009.

Rožič, B., Gale, L., Oprčkal, P., Švara, A., Udovč, J., Debevec, G., Popit, T., Vrabec, M. & Šmuc, A. 2015: Stratigrafski in strukturni pomen kamnin Slovenskega bazena pri Škofji Loki. In: Rožič., B. (ed.): Razprave, poročila = Treatises, reports / 22. posvetovanje slovenskih geologov = 22nd Meeting of Slovenian Geologists. Geološki zbornik, 23: 171-175.

Sudar, M. & Kovacs, S. 2006: Metamorphosed and ductile deformed conodonts from Triassic limestones situated beneath ophiolite complexes: Kopaonik Mountain (Serbia) and Bükk Mountains (NE Hungary) – a preliminary comparison. Geol. Carpathica, 57: 157-176.

Turnšek, D., Buser, S. & Ogorelec, B. 1982: Carnian coral-sponge reefs in the Amphiclina beds between Hudajužna and Zakriž (western Slovenia). Razprave IV razreda SAZU, Ljubljana: 1-48.

GEOLOGIJA *60/1*, 77-85, Ljubljana 2017
https://doi.org/10.5474/geologija.2017.006

Early Miocene decapod *Retropluma slovenica* Gašparič & Hyžný, 2014 from Govce beds of Tunjice Hills (Central Slovenia)

Spodnjemiocenska rakovica *Retropluma slovenica* Gašparič & Hyžný, 2014 iz govških plasti Tunjiškega gričevja

Rok GAŠPARIČ[1,2] & Matija KRIŽNAR[3]

[1]Oertijdmuseum De Groene Poort, Bosscheweg 80, 5293 WB Boxtel, the Netherlands; e-mail: rok.gasparic@gmail.com
[2]Ljubljanska cesta 4j, SI-1241 Kamnik, Slovenija; e-mail: rok.gasparic@gmail.com
[3]Prirodoslovni muzej Slovenije, Prešernova 20, SI–1001 Ljubljana, Slovenija; e-mail: mkriznar@pms-lj.si

Prejeto / Received 5. 10. 2016; Sprejeto / Accepted 1. 3. 2017; Objavljeno na spletu / Published online 9.6.2017

Key words: Decapoda, Miocene, Govce beds, Central Paratethys, Slovenia
Ključne besede: deseteronožci, miocen, govške plasti, Centralna Paratetida, Slovenija

Abstract

Increasing reports of genus *Retropluma* Gill, 1894 from the siliciclastic sediments of South-East Europe demonstrate the abundance and preferred habitat of this genus in Miocene seas of Central Paratethys. In the present paper we report new specimens of decapod *Retropluma slovenica* Gašparič & Hyžný, 2014, which extend the known palaeogeographic and stratigraphic distribution of the species to the western borders of Slovenian Basin of the Central Paratethys. The described specimens originate from the Early Miocene locality of Rovček in the Tunjice Hills in Slovenia and exhibit associated preservation, characteristic for endobenthic infaunal mode of living.

Izvleček

Vse več najdb rakovice rodu *Retropluma* Gill, 1894 v klastičnih kamninah jugovzhodne Evrope kaže na to, da so bile v miocenskem morju Paratetide pogostejše kot smo doslej predvidevali. V članku predstavljamo nove najdbe rakovice *Retropluma slovenica* Gašparič & Hyžný, 2014, ki dopolnjujejo naše poznavanje paleogeografske in stratigrafske razširjenosti vrste do najbolj zahodnih delov Slovenskega bazena v miocenskem morju Centralne Paratetide. Opisani so primerki iz spodnjemiocenskih govških plasti iz nahajališča Rovček v Tunjiškem gričevju. Primerki so ohranjeni s povezanimi okončinami, kar je značilno za rakovice, ki so se vkopavale v podlago.

Introduction

The he rich palaeontological diversity of Tunjice Hills is known already from the early 19th century. Most fossiliferous strata in the region are Early and Middle Miocene beds, which were investigated by Austro-Hungarian geologists and amateur naturalists of the era (Fuchs, 1875; Hilber, 1888). One of most important researchers of the region was a local priest Simon Robič who collected fossils in his daily walks through the woods and creeks of Tunjice Hills (Žalohar & Hitij, 2014). His collection, stored in Natural History Museum of Slovenia consists of about 135 fossil specimens, among others also fossil crabs *Tasadia carniolica* (Bittner 1884) from *locus typicus* within Laško Formation beds in Košiše, which are common fossils in the region. Despite frequented finds of *T. carniolica* in Middle Miocene layers of Tunjice Hills, other occurrences of fossil decapods are unusually rare. The oldest are the remains of crabs from Early Miocene beds south of Tunjice village in Rovček creek. Rare specimens of *Chaceon sp.* and *Homarus sp.* (Križnar & Preisinger, 2008; Gašparič & Brajkovič, 2016) occur in concretions in Early Miocene claystones. The age of fauna, containing also *Teredo*-bored wood remains, is questionable and concretions could have been reworked from older (Oligocene) strata (Gašparič & Brajkovič, 2016).

Herein we present new findings of *Retropluma slovenica* Gašparič & Hyžný, 2015 from Early Miocene clastic sequence of Rovček creek in Tunjice Hills. The family Retroplumidae Gill, 1894 consists of nine genera of brachyuran crabs, seven of which have exclusively fossil representatives (De Grave et al., 2009; Khodaverdi et al., 2016). The two extant genera, *Retropluma* and *Bathypluma* de Saint Laurent, 1989, occur in the Indo-Pacific and have been reported from muddy or sandy bottoms in the depths ranging from 70 to 600 m (McLay, 2006).

Geology and stratigraphy of the localities

Tunjice Hills belong to the westernmost part of the Tunjice Syncline of the Sava Folds (Placer, 1999, 2008).

Cenozoic sequence of Tunjice Hills starts with few meters of Oligocene conglomerates alternating with beds of sandstones. These are followed by grey clays and a basal conglomerate horizon of fluvial origin. Oligocene layers end with a thick horizon of grey marine clay sequence, which at its top alternates with individual lenses of fine grained clastic rocks, particularly loose sands, and conglomerates (Žalohar & Zevnik, 2006; Gašparič & Brajković, 2016).

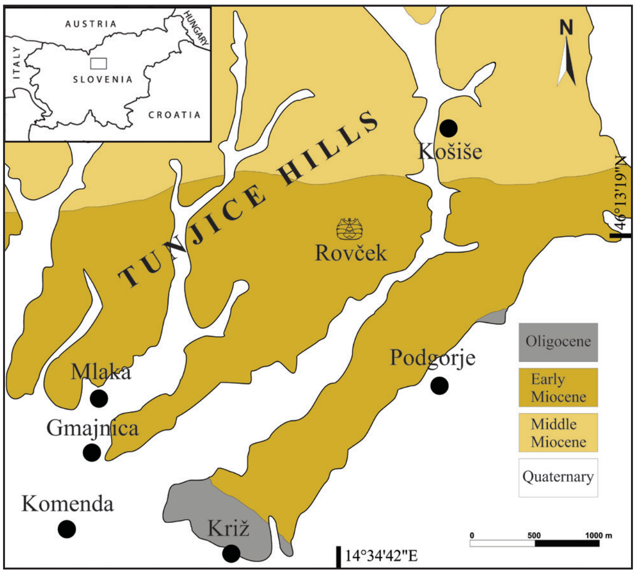

Fig. 1. Simplified geological map of the Tunjice Hills (modified after: Žalohar & Zevnik, 2006). Locality of Retropluma slovenica specimens, Rovček creek, is marked on the map.

Oligocene strata are discordantly overlain with Early Miocene Govce Formation. Lithologies of Govce Formation sequence starts with deposition of clays with lenses of sand and sandstones but it mostly consist of interchanging of conglomerates, sandstones, and fine-grained marls and clays. Succession of retrogradational and progradational sequences implies alternation of deepening and shallowing cycles (Vrabec, 2000). According to Žalohar & Zevnik (2006) Govce Formation layers consist of three separate members: the Lower Govce Member, the Middle Govce Member and the Upper Govce Member. The Lower Govce Member is represented by the succession of alternating beds of clay, siltstones, sandstone, and conglomerate. Middle Govce Member consists mainly of greenish (Glauconite rich) and brownish sandstones and marls. The Upper Govce Member begins with conglomerate, sandstones, sandy siltstones and ends with loose sands. The Rovček section, where the described specimens originate from is part of the Upper Govce Member. Total thickness of Govce beds is between 350 to 450 m (Premru, 1983).

The Early Miocene sediments in Tunjice Hills are followed, after an unconformity, by Laško Formation of Middle Miocene (Badenian). The Middle Miocene strata consist of sandstones, marls, and marly limestones, which are rich in marine macrofossil remains. In the upper part of Laško beds we recognize increasing terrestrial influence and a transition to the Sarmatian Dol Formation beds (Vrabec et al., 2014). The layers of Dol Formation are the youngest lithostratigraphic unit of Tunjice Hills. Characteristic horizons are cerithiid sandstone and Coprolitic horizon. Fossil fauna indicates marine environment still connected with Central Paratethys (Horvat, 2003). Upper most parts Dol Formation show renewed shallowing of the environment, fresh water influx and periodic tectonic isolation of the Tunjice basin (Žalohar & Hitij, 2014).

Material and methods

The studied material consists of 5 specimens of *Retropluma slovenica*. Original cuticle of specimens is lacking, so structures are preserved as impressions in fine grained brownish sandy siltstones. Following specimens were studied: an almost complete articulated specimen (Inv. No. RGA/SMNH 1500, part and RGA/SMNH 1501, counterpart), a partial articulated specimen (Inv. No. RGA/SMNH 1502, part and RGA/SMNH 1503, counterpart), a complete articulated specimen (Inv. No. RGA/SMNH 1504, part and RGA/SMNH 1505, counterpart), an isolated carapace (Inv. No. RGA/SMNH 1506), and an isolated cheliped (Inv. No. RGA/SMNH 1507). All specimens were photographed, measured and studied using computer programmes (CoreDRAW

X5, Adobe Photoshop CC and Statistica). Photographs were taken with digital camera Nikon D810 under low angle light source conditions.

Abbreviations

RGA/SMNH - Slovenian Museum of Natural History, Ljubljana, Slovenia (R. Gašparič Collection)

Systematic description

The higher systematics used herein follows De Grave et al. (2009).

Superfamily **Retroplumoidea** Gill, 1894

Family **Retroplumidae** Gill, 1894

Genus ***Retropluma*** Gill, 1894

Type species. *Archaeoplax notopus* Alcock & Anderson, 1894, by monotypy.

Retropluma slovenica Gašparič & Hyžný, 2014
(Plate 1. A–H)

2014 *Retropluma slovenica* Gašparič & Hyžný; p. 141–166, Figs. 18–21
2015 *Retropluma slovenica* Gašparič & Hyžný – Hyžný et al.; pp. 147, Fig. 5, A–F

Description

The studied specimens exhibit subrectangular carapace, about 1.20 times wider than long, maximum width at the level of median carina.

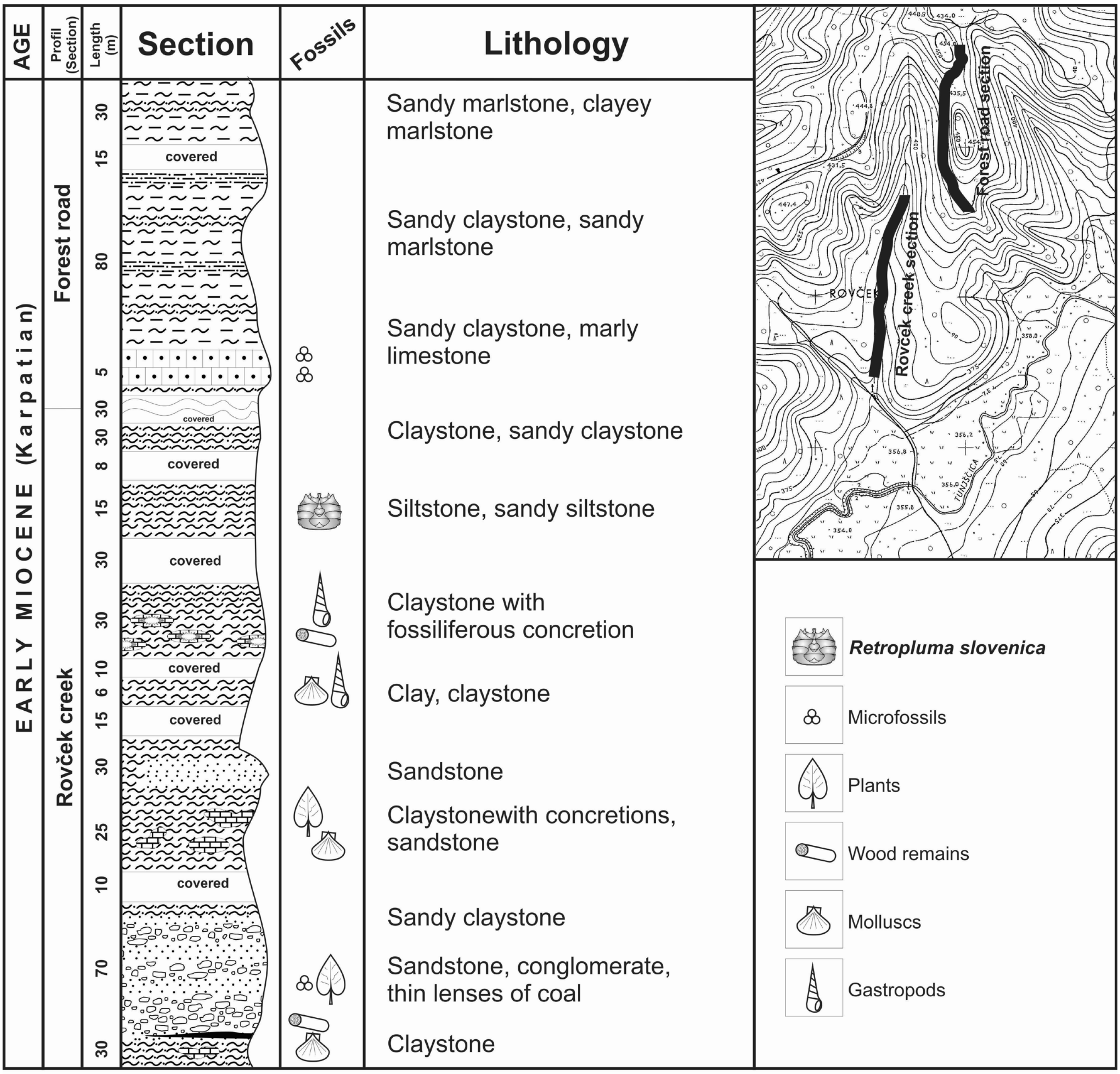

Fig. 2. A detailed lithostratigraphic section of Rovček creek locality with Early Miocene marine layers from where the described specimens were recovered.

Carapace partially deformed and flattened, but appears transversely slightly convex and longitudinally nearly flat (Pl. 1F). Rostrum long, with concave sides and wider distally (Pl. 1A). Orbital margin sinuous with well-developed anterolateral tooth, pointing by some degrees outward; the supraorbital tooth is present, but poorly preserved (Pl. 1E). Long anterolateral margin, concave till anterior carina. Lateral and posterior margins convex, with well-developed concave re-entrant for reduced fifth pereiopod at the posterolateral part.

Dorsal carapace is adorned with three transverse carinae, forming blunt projections at intersection with lateral carapace margin (Pl. 1A, C). Anterior carina almost straight, slightly downwards curved in last third toward lateral margin. Median carina strongly developed at flanks only, interrupted by urogastric region. Posterior carina sinuous and well formed. Dorsal carapace surface is pitted and finely granulose.

The mesogastric region pointedly pentagonal continuing over anterior carina in a long anterior process, ending behind the rostrum. All sides of mesogastric region are concave and posterior border is divided into two lobes. Protogastric regions are not clearly delimited from hepatic region, forming a sub-rectangular shape, which is intersected by the anterior carina (Pl. 1D). The urogastric region is well defined and recognized as a crescent shape; its posterior border is defined by the cervical groove. The cardiac region is large and well formed; its posterior margin is long and concave and the whole cardiac region is divided by the posterior carina. The intestinal region is wide and narrow, with concave anterior margin and straight lateral margin (Pl. 1G). The branchial regions are less defined, elongated and sub rectangular in outline (Pl. 1C). Male sternal plate round in outline sternites 7–5 long, overlapping, with squarer termination. Sternite 8 reduced and covered by pleon.

Male pleon narrow; somite 2 wide and narrow; somites 3–5 fused; male pleon narrows significantly after somite 3, lateral margins of fused 3–5 segment concave, narrowest between somites 4 and 5, slightly widening distally. Somite 6 almost as wide as long with rounded anterior corners and pronounced transverse crest. Telson narrow and longest, with rounded termination (Pl. 1A, B).

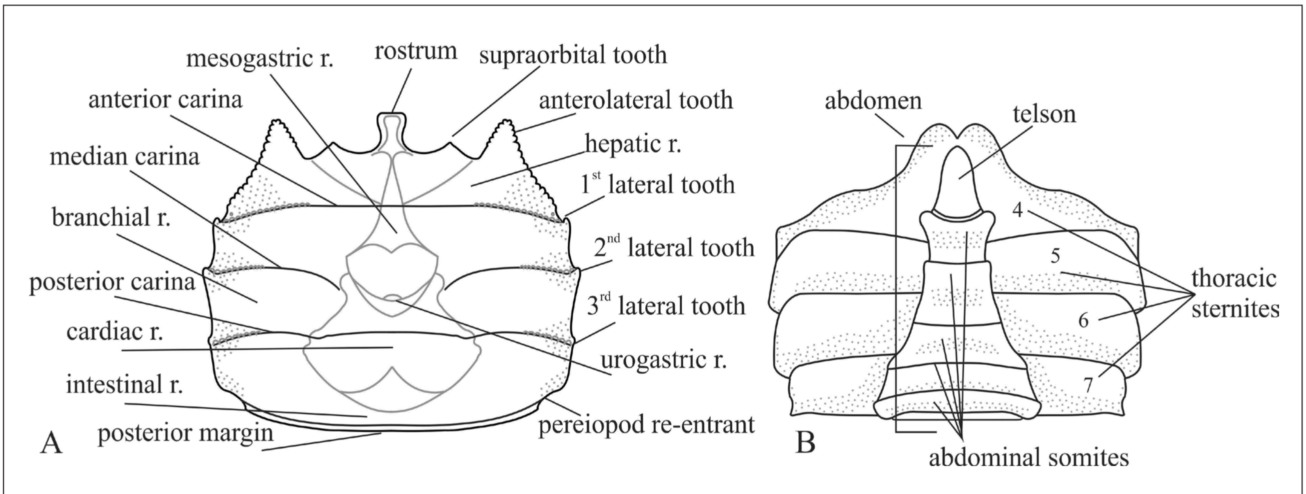

Fig. 3. Descriptive terminology used in the text showing dorsal (A) and ventral morphology (B) of retroplumid crab (modified after: Gašparič & Hyžný, 2014).

PLATE 1

Retropluma slovenica Gašparič & Hyžný, 2014. A – RGA/SMNH 1500, complete associated ventral carapace with chelipeds, male; B – RGA/SMNH 1501, complete associated ventral carapace with chelipeds, male; C – RGA/SMNH 1502, complete dislocated carapace showing abdomen and dorsal carapace, male; D – RGA/SMNH 1503, complete dislocated carapace showing abdomen and dorsal carapace, male; E – RGA/SMNH 1504, partial associated dorsal carapace; F – RGA/SMNH 1505, partial associated dorsal carapace; G – RGA/SMNH 1506, partial imprint of dorsal carapace; H – RGA/SMNH 1507, left cheliped without dactylus. Scale bars A – G are 10 mm, scale bar in H is 5 mm.

PLATE 1

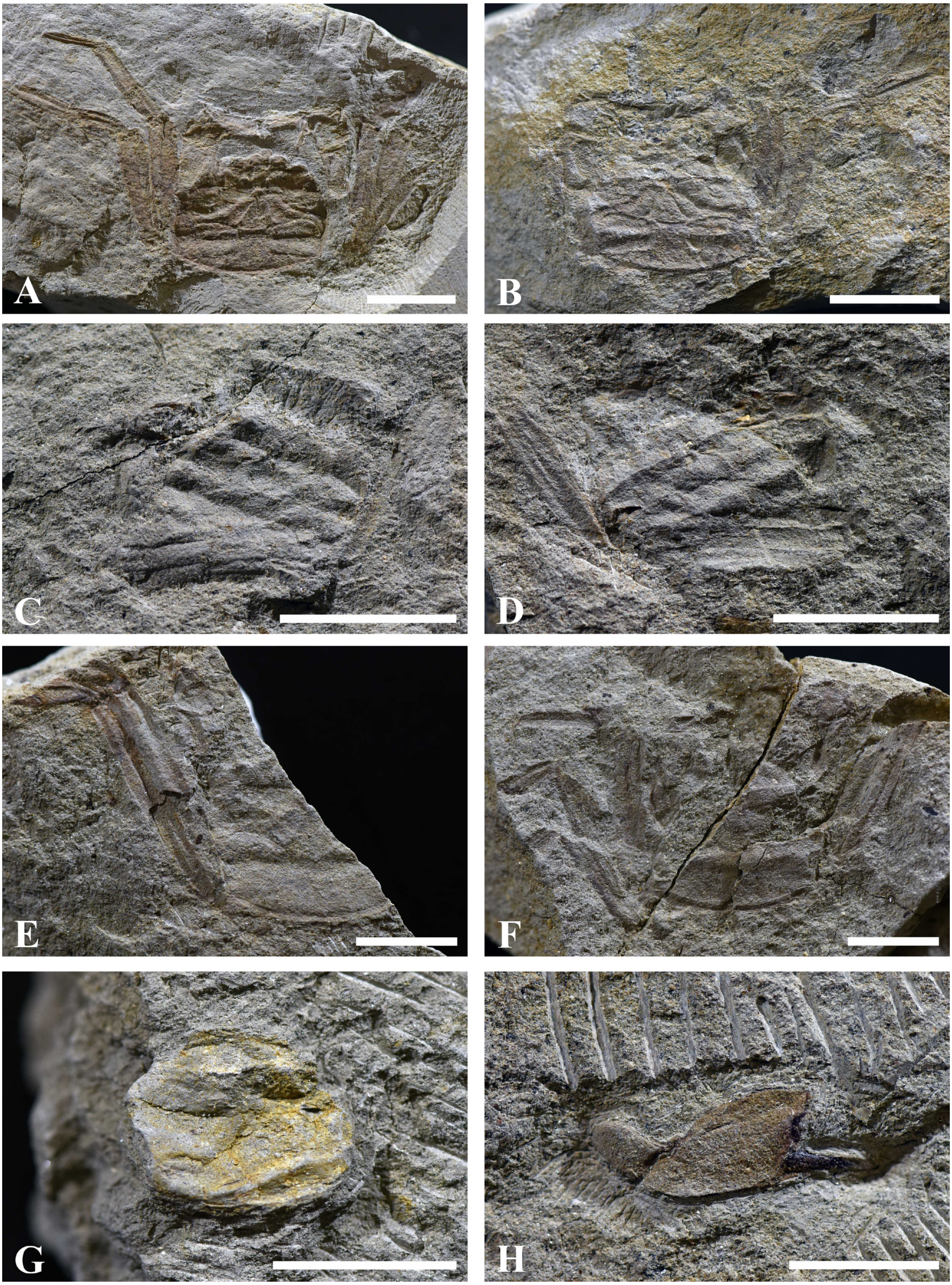

Chelipeds long and appear equally big (Pl 1A); propodus and dactylus curved, narrowing distally and with smooth surface (Pl. 1H). Pereiopods 2–4 long and slender; surface finely granulose and flattened, ending in blade-like dactyli; third pereiopod longest. Fifth pereiopod strongly reduced (Pl. 1A, E), thin and fragile.

Palaeoecology and environment

Despite the study of extant representatives, several ecological and behaviouristic aspects of crabs from genus *Retropluma* are still undefined, mostly due to the deep sea environments which they preferentially inhabit. De Saint Laurent (1989) and McLay (2006) report the occurrences of extant specimens from deep-water muddy bottom waters of up to 470 m. Similarly it can be inferred that fossil representatives have been adapted to the soft muddy or sandy bottoms on inner to outer continental shelves (Gašparič & Hyžný, 2015). As Paleogene species are known also from shallower water settings (Beschin et al., 1996; Hyžný & Müller, 2010; Khodaverdi et al., 2016), it can be concluded that the deeper water habitation preference, with depth interval of 100–450 m, was developed by the Neogene representatives of genus *Retropluma*.

Extant retroplumids spend most of the time buried in soft substrate (Ahyong, 2008), exposing only the most posterior part of the carapace with reduced setose fifth pereiopods, which possibly have a sensory function (McLay, 2006). Known fossil retroplumid material has so far been found exclusively in fine grained clastic rocks, which exhibit relatively fast sedimentation rates (Fraaije et al., 2005; Hyžný, 2011). This supports the hypothesis, that most of the fossil remains represent an endobenthic infaunal community that spent most of the time already buried in the sediment, which enhanced the preservation potential of otherwise fragile retroplumid cuticle.

Palaeobiogeography

The Eocene has been considered as a time of high evolution within the decapoda (Schweitzer & Feldmann, 2001). This can be also concluded for the retroplumids, which show high diversity in Eocene Tethys Ocean, with six different genera and two species of *Retropluma* Gill, 1894 known from Eocene strata of Europe (Vía Boada, 1959; Beschin et al., 1996; Artal et al., 2006, 2013; van Bakel, et al. 2010; Hyžný & Müller, 2010; Gašparič & Hyžný, 2015). It was also observed that many taxa which evolved during this period were endemic to their regions of origin (Feldmann et al., 2010).

Retropluma is considered of Tethyan origin, as the oldest species *Retropluma gallica* Artal, van Bakel & Castillo, 2006 appeared in strata from Early Eocene of France (Artal et al., 2006). Genus survived in the Mediterranean until the Pliocene and Pleistocene with *R. craverii* known from Italy (Crema, 1895; Baldanza et al., 2013). The Miocene occurrences comprise of *Retropluma slovenica* from Early Miocene of Slovenia (Gašparič & Hyžný, 2015) and Middle Miocene of Slovakia (Hyžný et al., 2015), *Retropluma borealis* from Late Miocene of Denmark (Fraaije et al., 2005), and *Retropluma laurentae* from Late Miocene of Sabakh, Borneo (Collins et al., 2003). The genus is represented today by seven species of Indo-Pacific and North-Western Pacific distribution (McLay, 2006).

Conclusions

New findings of *Retropluma slovenica* Gašparič & Hyžný, 2014 from Early Miocene siliciclastic sequence of Rovček creek in Tunjice Hills represents an important report, which further enhances our knowledge of Early Miocene decapod communities in Paratethys of Slovenia. The species was previously known from a single Early Miocene locality on northern slopes of Pohorje mountain range, so the new locality expands the geographical distribution of the species to the western part of Slovenian Basin of Paratethys which was in Early Miocene very close to the Mediterranean and most likely connected to it through the Slovenian corridor. As genus *Retropluma* is missing from the Miocene of Mediterranean, but occurs in its Pliocene and Pleistocene strata, it is likely the genus was reintroduced in the Mediterranean from Paratethys before the marine connection between both realms closed in Late Miocene.

Further we conclude that all fossil representatives of genus *Retropluma* shared the extant species preference for inhabiting a wide range of siliciclastic environments of outer continental shelves. As part of infaunal community they have a good preservation potential and are therefore likely to exhibit a robust fossil record.

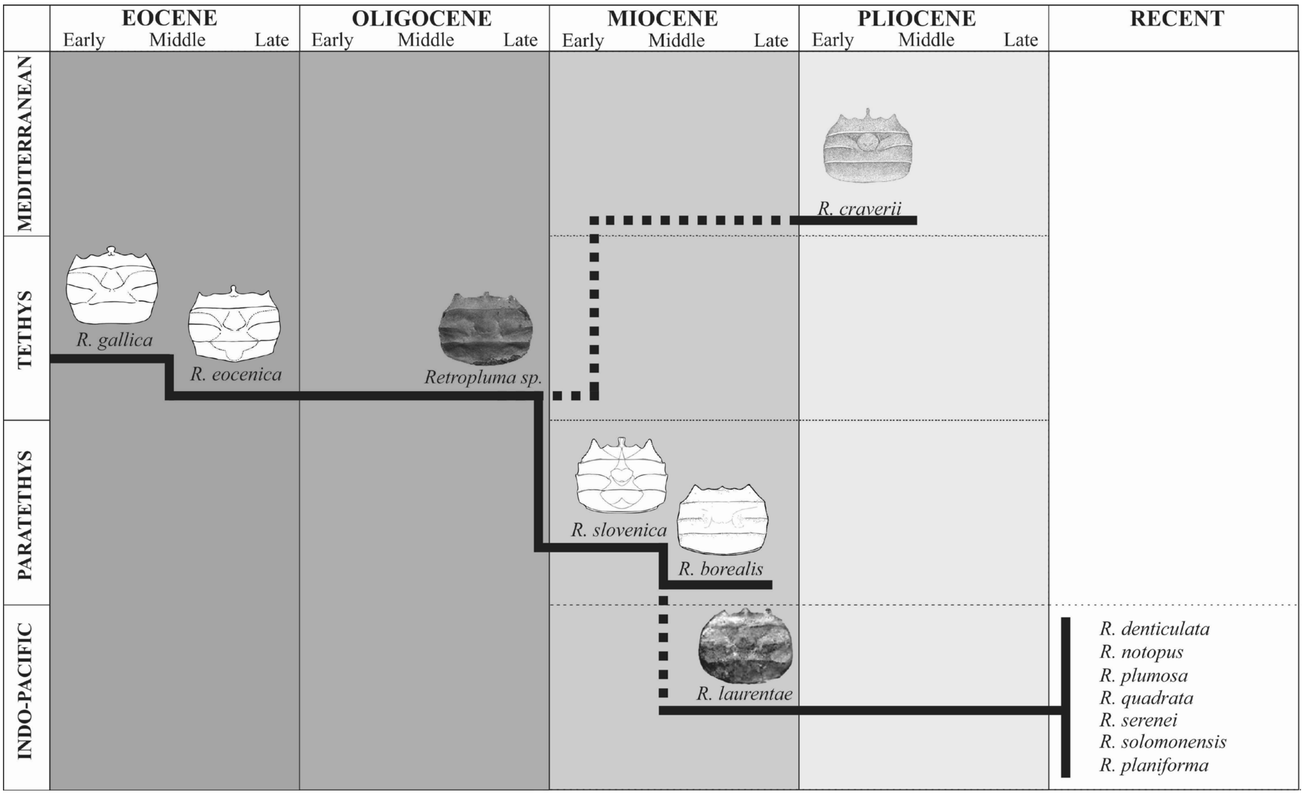

Fig. 4. Temporal and spatial distribution of fossil and extant species of *Retropluma* Gill, 1894.

Acknowledgements

We wish to thank Mojca Potočnik for access to the relevant fossil material, Rok Brajković for providing additional information on stratigraphy and Andreja Žibrat Gašparič for thoroughly proofreading our manuscript.

References

Ahyong, S. T. 2008: Deepwater crabs from seamounts and chemosynthetic habitats off eastern New Zealand (Crustacea: Decapoda: Brachyura). Zootaxa, 1708: 1–72.

Alcock, A. & Anderson, A. R. 1894: Natural History notes from H. M. Indian Marine Survey Steamer "Investigator", Commander C.F. Oldham, R.N., commanding. Series II, No. 14. An account of a recent collection of deep-sea Crustacea from the Bay of Bengal and Laccadive Sea. Journal of the Asiatic Society of Bengal, 63: 141–185.

Artal, P., Bakel, B. W. M. Van & Castillo, J. 2006: *Retropluma* Gill, 1894 (Crustacea, Decapoda) from the Eocene of the eastern Pyrenees (Spain, France). Cainozoic Research, 5: 65–71.

Bakel, B. W. M. Van, Artal, P., Fraaije, R. H. B. & Jagt, J. W. M. 2010: *Loerenthopluma danielae*, A new crab (Decapoda, Brachyura, Retroplumidae) from the Lower Eocene of Northwest Belgium. In: Castro, P. et al. (eds.): Brachyura: A Homage to Danièle Guinot. Studies on Brachyura, 41–49.

Baldanza, A., Bizzarri, R., Famiani, F., Garassino, A., Hyžný, M. & Pasini, G. 2013: The bathyal decapod crustacean community from the Poggio i Sodi quarries (Siena Basin, Tuscany, Italy). Boletín de la Sociedad Geológica Mexicana, 65/2: 335–353.

Beschin, C., Busulini, A., De Angeli, A. & Tessier, G. 1996: Retroplumoidea (Crustacea, Brachyura) nel Terziario del Vicentino (Italia settentrionale). Lavori – Società Veneziana di Scienze Naturali, 21: 83–102.

Bittner, A. 1884: Beiträge zur Kenntniss Tertiärer Brachyuren Faunen. Denkschriften der Akademie der Wissenschaften, Mathematik und Naturwissenschaften. Cl., 48/2: 3–18 (15-30).

Collins, J. S. H., Lee, C. & Noad, L. 2003: Miocene and Pleistocene crabs (Crustacea, Decapoda) from Sabah and Sarawak. Journal of Systematic Palaeontology, 1/3: 187–226.

Crema, C. 1895: Sopra alcuni decapodi terziario del Piemonte. Atti della Reale Accademia di Scienze di Torino, 30: 664–681.

De Grave, S., Pentcheff, N. D., Ahyong, S. T., Chan, T. Y., Crandall, K. A., Dworschak, P. C., Felder, D. L., Feldmann, R. M., Fransen, C. H. J. M., Goulding, L. Y. D., Lemaitre, R., Low, M. E. Y., Martin, J. W., Ng, P. K. L., Schweitzer, C. E., Tan, S. H., Tshudy, D. & Wetzer, R. 2009: A classification of living and fossil genera of decapod crustaceans. The Raffles Bulletin of Zoology, Supplement, 21: 1–109.

De Saint Laurent, M. 1989: La nouvelle superfamille des Retroplumoidea Gill, 1894 (Decapoda, Brachyura): systématique, affinités et évolution. In: Résultats des Campagnes Musorstom, 5 Mémoire du Muséum national d'Histoire naturelle, 144: 103–179.

Feldmann, R. M., Schweitzer, C. E. & Encinas, A. 2010: Neogene Decapod Crustacea from southern Chile. Annals of Carnegie Museum, 78/4: 337–366.

Fuchs, T. 1875: Die Tertiarbildungen von Stein in Krain. Verh. der k. k. Geol., 48–49.

Fraaije, R. H. B., Hansen, J. & Hansen, T. 2005: Late Miocene decapod fauna from Gram, Denmark. Palaeontos, 7: 51–61.

Gašparič, R. & Brajkovič, R. 2016: New Miocene decapod crustaceans from Tunjice Hills (Central Slovenia). 6th Symposium on Mesozoic and Cenozoic Decapod Crustaceans, Villers sur Mer, 30–34.

Gašparič, R. & Hyžný, M. 2014: An early Miocene deep-water Decapod Crustacean Faunule from the slovenian part of the Styrian Basin and its palaeoenvironmental and palaeobiogeographical significance. Papers in Palaeontology, 1/2: 141–166, doi:10.1002/spp2.1006.

Gill, T. 1894: A new bassalian type of crabs. American Naturalist, 28: 1034–1045.

Hilber, V. 1881: Ueber das Miocän, insbesondere das Auftreten sarmatischer Schichten bei Stein in Krain. Jb. Geol. R. A., 31: 473-478.

Horvat, A. 2003: Upper Badenian diatom paleoecology of the western part of Central Paratethys. Geologija, 46/2: 251–262, doi:10.5474/geologija.2003.022.

Hyžný, M. 2011: Synopsis of fossil decapod crustaceans from Slovakia (Western Carpathians). Neues Jahrbuch für Geologie und Paläontologie Abhandlungen, 260: 165–171.

Hyžný, M. & Müller, P. M. 2010: Loerenthopluma Beschin, Busulini, De Angeli & Tessier, 1996 (Decapoda: Brachyura: Retroplumidae) from the Oligocene of Hungary. Atti della Società italiana di Scienze naturali e del Museo civico di Storia naturale in Milano, 151/2: 129–140.

Hyžný, M., Hudáčková, N. & Szalma, Š. 2015: Taphonomy and diversity of Middle Miocene decapod crustaceans from the Novohrad-Nógrad Basin, Slovakia, with remarks on palaeobiography. Acta Geologica Slovaca, 7/2: 139–154.

Khodaverdi Hassan-vand, M., Bahrami, A., Yazdi, M., Ossó, À., Safari, A., Martínez, J. L. & Vegad, F. J. 2016: Occurrence of Retrocypoda almelai Via Boada, 1959 (Decapoda: Retroplumidae) in the Eocene of Central Iran. Paleontología Mexicana, 5/1: 21–31.

Križnar, M. & Preisinger, D. 2008: Rak *Coeloma* iz govške formacije Tunjiškega gričevja. Kamniški zbornik, 19: 335–338.

Mclay, C. L. 2006: Retroplumidae (Crustacea, Decapoda) from the Indo-Malayan archipelago (Indonesia, Philippine) and the Melanesian arc islands (Solomon Islands, Fiji and New Caledonia), and paleogeographical comments. In: Richer de Forges B. & Justine J. L. (eds.): Tropical Deep-Sea Benthos, 24. Mémoires du Muséum national d'Histoire naturelle 193: 375–391.

Placer, L. 1999: Strukturni pomen Posavskih gub = Structural meaning of the Sava folds. Geologija, 41: 191–221, doi:10.5474/geologija.1998.012.

Placer, L. 2008: Principles of the tectonic subdivision of Slovenia = Osnove tektonske razčlenitve Slovenije. Geologija, 51/2: 205–217, doi:10.5474/geologija.2008.021.

Premru, U. 1983: Osnovna geološka karta SFRJ 1:100.000. Tolmač za list Ljubljana. Zvezni geološki zavod Beograd, Beograd: 69 p.

Schweitzer, C. E. & Feldmann R. M. 2001: Differentiation of the fossil Hexapodidae Miers, 1886 (Decapoda: Brachyura) from similar forms. Journal of Paleontology, 75: 330–345.

Vía Boada, L. 1959: Décapodos fósiles del Eoceno español (Resumen - avance de la tesis doctoral). Boletin del Istituto Geológico y Minero de España, 70: 313–402.

Vrabec, M. 2000: Govški peščenjak v profilu Doblič (govška formacija - govške plasti): Diplomsko delo. UL NTF, Oddelek za geologijo, Ljubljana: 142 p.

Vrabec, M., Brajković, R. & Skaberne, D. 2014: Sedimentološke značilnosti terciarnih kamnin Tunjiškega gričevja. In: Rožič, B., Verbovšek, T., Vrabec, M. (eds.): Povzetki in ekskurzije, 4. slovenski geološki kongres, Ankaran 8.-10. oktober 2014. Naravoslovnotehniška fakulteta, Ljubljana: 75-76.

Žalohar, J. & Hitij, T. 2014: Fossil seahorses and other biota from the Tunjice Konservat-Lagerstätte, Slovenia. Faculty of Life Sciences, University of Machester, Manchester: 176 p.

Žalohar, J. & Zevnik, J. 2006: Miocenske plasti v Tunjiškem gričevju. Kamniški zbornik, 18: 289–301.

GEOLOGIJA *60/1*, 87-97, Ljubljana 2017

https://doi.org/10.5474/geologija.2017.007

Novo najdišče pleistocenske sesalske favne v kamnolomu pri Črnem Kalu (Primorska, Slovenija) ter problematika zaščite in ohranjanja najdišč v kamnolomih

New Pleistocene mammal site in Črni Kal quarry (Primorska region, Slovenia) with discussion on problems of protection and preservation of fossil sites in quarries

Matija KRIŽNAR[1] & Davorin PREISINGER[2]

[1]Prirodoslovni muzej Slovenije, Prešernova 20, SI-1000 Ljubljana, Slovenija; e-mail: mkriznar@pms-lj.si
[2]Kajuhova ulica 34, SI-4000 Kranj, Slovenija; e-mail: davorin.preisinger@gmail.com

Prejeto / Received 29. 9. 2016; Sprejeto / Accepted 1. 3. 2017; Objavljeno na spletu / Published online 9.6.2017

Ključne besede: Črni Kal, pleistocen, pleistocenski sesalci, gozdni nosorog, kamnolom, geološka dediščina
Key words: Črni Kal, Pleistocene, Pleistocene mammals, Merck's rhinoceros, Quarry, geoheritage

Izvleček

Kamnolom pri Črnem Kalu je s svojim delovanjem razkril več najdišč pleistocenskih sesalcev, med katerimi v tem prispevku predstavljamo najnovejše najdišče, ki je bilo leta 2016 razkrito v severnem delu kamnoloma. Najdišče predstavlja s sedimenti zapolnjeno brezno ali razširjeno špranjo, kjer se je na dnu ohranila plast kostne breče. V preliminarni analizi smo lahko potrdili prisotnost gozdnega (Merckovega) nosoroga in trenutno še nedoločenih jelenov in zveri. S problematiko, ki spremlja odkrivanje in dokumentiranje podobnih najdišč v še delujočih kamnolomih, predstavljamo tudi nekaj smernic, predlogov in pomislekov glede reševanja paleontološke dediščine, ki temelji na rednem terenskem delu, poimenovanju najdišč in ustreznem dokumentiranju in sodelovanju z lastniki kamnolomov.

Abstract

The Črni Kal quarry has been known for decades for fossils of Pleistocene mammal preserved in sinkholes or karst fissures fillings. We present some of the new fossil material discovered in the northern part of the quarry in 2016. The new site is an expanded karst fissure or cave filled with flowstone rubble and fine grained sediments with only one layer of bone breccia. The preliminary results of the analysis of fossil vertebrate remains show the presence of Merck's rhinoceros, currently unidentified species of deer and fragmented teeth of carnivores. Furthermore, we discuss some problems in documenting, protecting and preserving of Pleistocene fossil vertebrate sites in quarries in Slovenia.

Uvod

Območje severno od vasi Črni Kal sestavljajo predvsem alveolinsko–numulitni apnenci, ki so močno zakraseli. Tako lahko že na površini opazujemo manjše vrtače, v cestnih usekih tudi erozijsko razširjene razpoke, manjša brezna in celo jame. Kamnolom pri Črnem Kalu je kot paleontološko in arheološko najdišče znano že od leta 1955, ko so v sedimentih zasute jame našli številne ostanke pleistocenske favne (Brodar S., 1958; Rakovec, 1958). S širitvijo kamnoloma so dokaj pogosto odpirali tudi druge kraške strukture, ki pa so redko vsebovale ostanke pleistocenskih živali. Šele konec prejšnjega stoletja so bila odkrita nekatera nova najdišča v vzhodnem in južnem delu kamnoloma (Jamnik et al., 2013). Novo najdišče, ki ga predstavljamo tukaj je bilo odkrito ob napredovanju del na severni strani kamnolomu. Najdišče predstavlja brezno, v celoti zapolnjeno s sedimenti, med katerimi je tudi približno 40 cm debela plast kostne breče.

V drugem delu prispevka se osredotočamo na problematiko zaščite in ustrezne dokumentacije naravne in kulturne dediščine v kamnolomih. Na problematiko uničevanja, tako geotopov kot paleontološke dediščine, sta prav na primeru kamnoloma Črni Kal opozorila že Pavlovec in Poharjeva (1997; 2000). Pavlovec in Pohar (1997) sta tudi že navedla nekatere zgoraj omenjene naloge, ki pa jih po našem mnenju morajo izvajati odgovorne institucije s tega področja, seveda v primerni obliki sodelovanja z lastniki (upravljavci) kamnolomov in drugo zainteresirano javnostjo (zbiralci, naključni obiskovalci, jamarji). S problematiko novo odkritih jam ter drugih kraških pojavov in njihove zaščite v kamnolomih (predvsem delujočih) se je ukvarjala tudi Zupan Hajna (2011), ki se navezuje tudi na nekatere najdbe fosilnih ostankov pleistocenskih sesalcev v kamnolomih.

Pregled in stanje do sedaj odkritih najdišč v kamnolomu Črni Kal

Črnokalski kamnolom je kot sklop najdišč pleistocenske favne in tudi kot arheološko najdišče znano že od prvih del v kamnolomu. Leta 1955 so pri začetnih delih na čelu kamnoloma (sl. 1) odkrili s pleistocenskimi sedimenti zapolnjeno vodoravno jamo (rov), ki so jo sistematično raziskali v oktobru in novembru leta 1955 (Brodar S., 1958; Jamnik et al., 2013). Pri izkopavanjih so v profilu pleistocenskih sedimentov razkrili 20 plasti skupne debeline okoli 8 m, med katerimi je bila ena (plast 10) identificirana kot kulturna plast z najdbo paleolitskega strgala (Brodar S., 1958, 363). V paleontološkem pogledu so skoraj vse plasti vsebovale ostanke pleistocenskih sesalcev. Od sesalcev so odkopali največ ostankov jamskega medveda *Ursus spelaeus* Rosenmüller, prisotni pa so bili še ostanki drugih večjih sesalcev: jelena *Cervus elaphus* Linné, srne *Capreolus capreolus* (Linnaeus) in *Capreolus* cf. *süssenbornensis* Kahlke, nosoroga *Dicerorhinus kirchbergensis* (Jäger), tura *Bos primigenius* (Bojanus), kozoroga *Capra ibex prisca* (Linnaeus), lisice *Vulpes vuples* (Linnaeus), jamske hijene *Crocuta spelaea* (Goldfuss), jamskega leva *Panthera spelea* (Goldfuss), volka *Canis lupus* Linnaeus (Rakovec, 1958; Dietrich, 1958; Brodar M. & Osole, 1979). Danes je najdišče vidno v zelo omejenem obsegu, saj ga je delno uničila izdelava ceste in napredovanje del v kamnolomu (sl. 2, A). V tem profilu je bilo leta 2009 po naključju odkrito še eno paleolitsko orodje, ki so ga proučili Jamnik s sodelavci (2013), in hkrati analizirali in dokumentirali še preostali in ohranjeni del Brodarjevega najdišča (»Brodarjev profil« po Jamnik et al., 2013).

Širitev in nadaljnja dela v kamnolomu so pogosto odpirala tudi manjša brezna in zasute vrtače, ki običajno niso bila dokumentirana, oziroma niso bila ustrezno nadzirana in proučevana. Šele v letih 1995 – 2002 so se ponovno pojavila posamezna najdišča, ki so vsebovala tudi ostanke pleistocenskih sesalcev. Pavlovec in Poharjeva (1997) sta prvič prikazala novo najdišče na takratni zgornji etaži kamnoloma (Pavlovec & Pohar, 1997, sl. 3) v severovzhodnem delu kamnoloma, od koder omenjata ostanke rastlinojedcev, med katerimi je bilo najdeno tudi rebro ledenodobnega nosoroga (? *Dicerorhinus* sp.) z vrezninami antropogenega izvora. Isto najdišče (sl. 2, C- E),

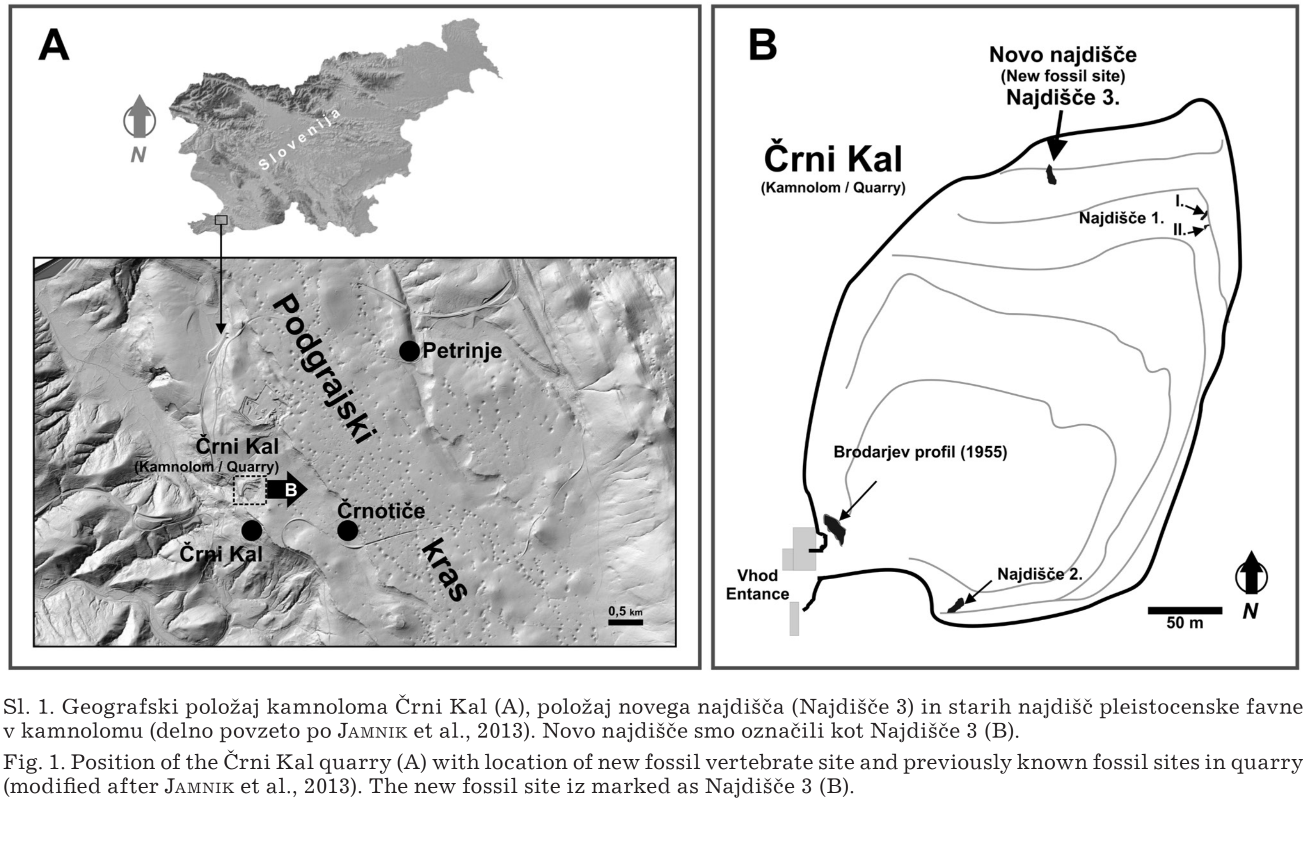

Sl. 1. Geografski položaj kamnoloma Črni Kal (A), položaj novega najdišča (Najdišče 3) in starih najdišč pleistocenske favne v kamnolomu (delno povzeto po Jamnik et al., 2013). Novo najdišče smo označili kot Najdišče 3 (B).

Fig. 1. Position of the Črni Kal quarry (A) with location of new fossil vertebrate site and previously known fossil sites in quarry (modified after Jamnik et al., 2013). The new fossil site iz marked as Najdišče 3 (B).

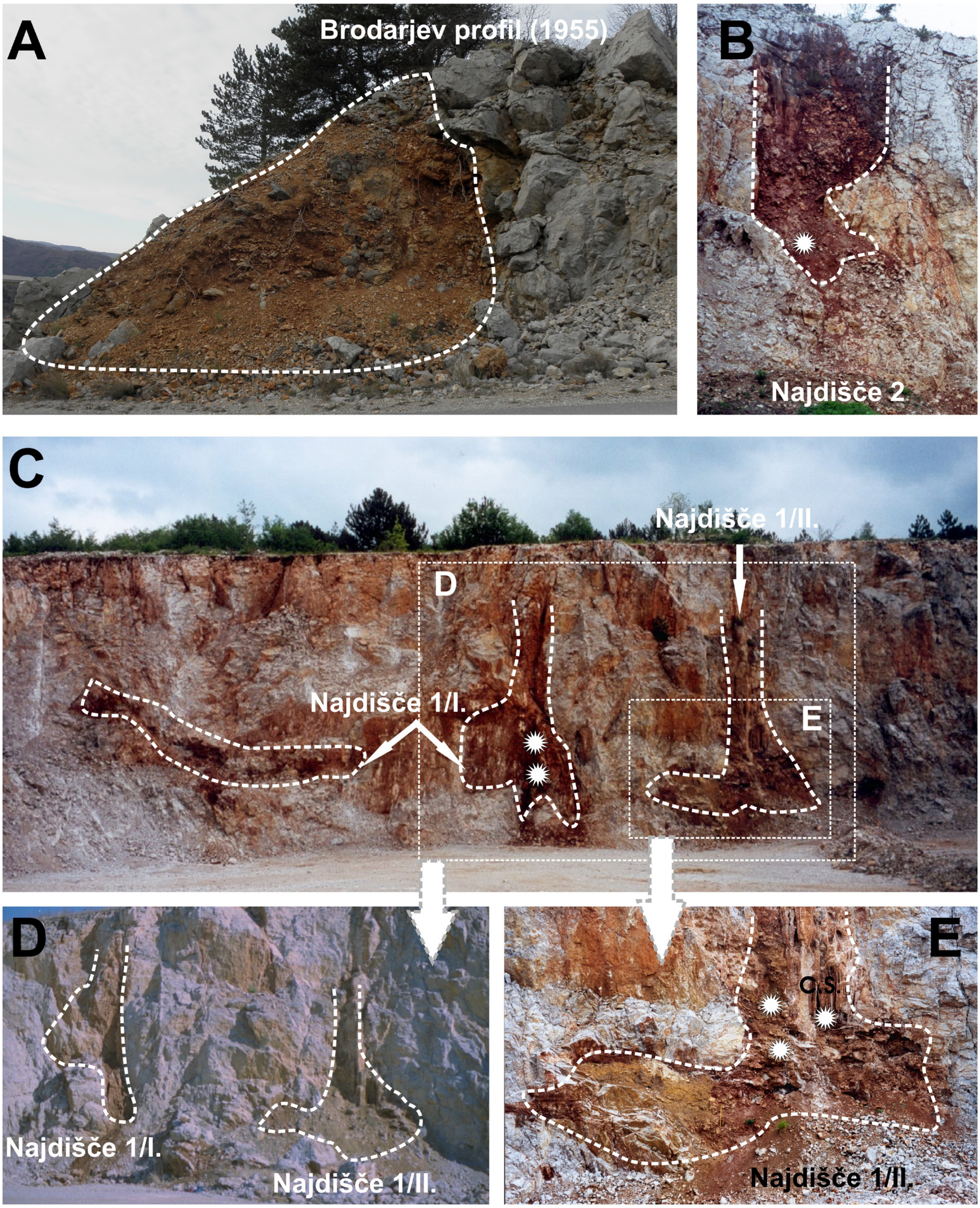

Sl. 2. Pregled dokumentiranih najdišč pleistocenskih sesalcev v kamnolomu Črni Kal. A – ostanek najdišča »Brodarjev profil« (situacija leta 2013), B – Najdišče 2 (situacija leta 2001), C – širše območje Najdišča 1 (situacija leta 2001), D – delno zasuto Najdišče 1-, brezni 1/I. in 1/II. (situacija leta 1997), E – odkopano Najdišče 1 II. (situacija leta 2001). Z zvezdicami so označeni položaji nakopičenj ostankov pleistocenske favne. Fotografije: M. Križnar.

Fig. 2. Views on documented Pleistocene localities in Črni Kal quarry. A – remains of Pleistocene cave sediments on »Brodar section« site, known after paleontological and archeological content (situation in 2013), B – Najdišče 2 (situation in 2001), C – wider area of Najdišče 1 (situation in 2001), D – partially covered site Najdišče 1, I. and 1 II. (situation in 1997), E – open site Najdišče 1 II. (situation in 2001). With asterisk are marked most rich accumulations of vertebrate remains. Photo: M. Križnar.

sestavljeno iz vsaj dveh zasiganih brezen (1/I in 1/II), od koder so tudi opisali pleistocensko favno (jelen *Cervus* cf. *elaphus* Linnaeus, srna *Capreolus capreolus* (Linnaeus), lisica *Vulpes* sp., nosorog *Stephanorhinus* sp., ostanki majhnih sesalcev in ptic), so bolj natančno predstavili tudi Jamnik s sodelavci (2013, sl. 8, najdišče 1/II.).

Jamnik s sodelavci (2013, str. 18, sl. 8) opisujejo tudi najdišče, ki leži na južnem delu kamnoloma in so ga označili kot najdišče 2 (glej sl. 1 in sl. 2, B) in iz katerega omenjajo več ostankov nosoroga *Stephanorhinus* cf. *kirchbergensis* (Jäger). Isto najdišče kot Jamnik s sodelavci (2013) pred njim omenjata in prikazujeta tudi Poharjeva in Kraljeva (2002, sl. 3, 241), ki ga označujeta kot B1-B2. Danes je to najdišče močno zaraščeno (sl. 2, B), a še vedno dostopno in zato tudi ogroženo.

Iz črnokalskega kamnoloma so fosilne ostanke pleistocenske favne opisovali tudi Aguilar s sodelavci (1998) ter Aguilar in Michaux (2011), a ne podajajo natančnih lokacij v kamnolomu. Njihovo najdišče z oznako Črni Kal 3 verjetno ustreza najdišču 1 po Jamniku s sodelavci (2013), ki ga podajamo tudi mi (sl. 2, C-E). Aguilar in Michaux (2011) predstavljata tudi novi vrsti pleistocenskih polhov (*Glis mihevci* Aguilar & Michaux in *Glis perkoi* Aguilar & Michaux) iz črnokalskega kamnoloma.

Novo najdišče pleistocenske favne (Črni Kal, Najdišče 3)

Novo najdišče pleistocenske favne leži na severnem delu črnokalskega kamnoloma (sl. 1B in sl. 3) in je bilo raziskano v februarju 2016. Najdišče je špranjasta jama oz. brezno, ki je bilo v celoti zapolnjeno z različnimi sedimenti (sl. 4). Jama se nahaja približno 14 -15 m od današnjega površja na 330 m nadmorske višine. Zgornji del predstavlja mlajši zarušek zgornjega dela brezna, z večjimi bloki sige in okolne kamnine (alveolinsko-numulitni apnenec).

Fosilonosno plast (sl. 4, B.B.) predstavlja plast kostne breče (debelina okoli 40 cm) s sigastim vezivom rdečkaste do rumeno rjave barve. Med brečo se pojavljajo tudi vložki sivozelene ilovice (glinast material) s hematitnimi konkrecijami (podobnih bobovcem) ter manganovimi dendriti . Ponekod kosti sestavljajo skoraj polovico volumna kostne breče (sl. 5). Nekaj kostnih fragmentov smo dokumentirali tudi na levi strani najdišča, kjer so le ti tako zasigani, da jih je brez poškodb nemogoče izbiti iz breče (sl. 4, B). Spodnji del pleistocenskih sedimentov tvori rumen do rjav glinen sediment debeline približno enega metra, ki pa je brez vidnih fosilnih ostankov.

Glede na model geneze, ki jo podajata Bolliger in Rummel (1994, abb.6) lahko novo črnokalsko Najdišče 3 uvrstimo med tipa B in C, kjer je razlika med spodnjim plastovitim in zgornjim kaotičnim sedimentom dokaj razločna.

Podobna najdišča, kot so črnokalska, lahko zasledimo po vsej Evropi, še posebej na območjih z močnim zakrasevanjem karbonatnih kamnin (predvsem apnencev) različnih geoloških starosti (Dehm & Fahlbusch, 1970; Bonfiglio et al., 1993; Ziegler, 1995; Nagel & Rabeder, 2000; Rathgeber, 2002; Becker et al., 2009; Schöllmann & Schlösser, 2010).

Preliminarne določitve fosilnih ostankov in tafonomija

Na najdišču je bilo zbrano za analizo več blokov kostne breče in posameznih koščkov kosti, ki so izpadli iz sedimenta. Zaradi še vedno trajajoče preparacije fosilnega gradiva tukaj podajamo zgolj preliminarne določitve zbranih fosilnih kosti in zob velikih sesalcev. Vsi fosilni ostanki izhajajo iz plasti kostne breče (sl. 4, C). Med zbranimi gradivom smo že na najdišču lahko določili zob nosoroga, ki pripada rodu *Stephanorhinus* (sl. 5, C). Zob je levi M^3 ter po obliki in dimenzijah lahko pripada vrstama *Stephanorhinus kirchbergensis* (Jäger) (gozdni ali Merckov nosorog) ali *Stephanorhinus hemitoechus* (Falconer) (stepski nosorog), ki sta bili pogosti v srednjem in mlajšemu pleistocenu. Nosorogov zob še nima obrabljene žvekalne površine, zato domnevamo, da še ni bil izrasel iz čeljusti, oziroma je v vsakem primeru pripadal mlademu osebku. Od zoba se je ohranila le krona. Ostalo fosilno gradivo lahko po prvih analizah pripišemo jelenom (družina Cervidae), kjer je zastopana tudi srna (rod *Capreolus*). Od zveri smo našli le dva zoba, ki pa še nista taksonomsko opredeljena. Na osnovi preliminarne taksonomske določitve zbrane favne težko določimo starost najdene fosilne združbe, prisotnost gozdnega nosoroga pa kaže na toplo oziroma interglacialno obdobje. Na interglacialno starost lahko kaže tudi debela plast zdrobljene sige in podornih kamnitih blokov nad plastjo s fosilnimi ostanki. Presenetljivo je dejstvo, da med favno nikjer ni moč zaslediti ostankov jamskih medvedov, ki prevladujejo na najdišču (Bro-

Sl. 3. Položaj novega najdišča pleistocenske favne (Najdišče 3) v severni steni črnokalskega kamnolomu (situacija maja 2016). Koordinate najdišča X 412834,235, Y 46557,704. Fotografija: Matija Križnar.

Fig. 3. Location of new site (Najdišče 3) with vertebrate remains in the northern part of the Črni Kal quarry (situation in May 2016). Coordinates of new site X 412834,235, Y 46557,704. Photo: Matija Križnar.

darjev profil) ob vhodu v kamnolom. Podobno odsotnost jamskega medveda lahko potrdimo tudi na drugih dveh črnokalskih najdiščih (Pavlovec & Pohar, 1997; Pohar & Kralj, 2002; Jamnik et al., 2013), ki podobno kot novo najdišče nista tipični jamski objekt, kjer bi se zadrževali jamski medvedi.

Fosilne kosti so skoncentrirane v eni plasti, kjer sediment lahko opredelimo kot kostno brečo, saj kostni ostanki ponekod predstavljajo več kot polovico sedimenta. Nekatere kosti so bile nekaj časa izpostavljene atmosferskim vplivom, na kar kažejo površinske razpoke, ki so delno zapolnjene s sedimentom oziroma vezivom. Po naših predvidevanjih je plast breče nastajala skozi daljše časovno obdobje, kar sovpada tudi z raziskavami tafonomije recentnih ostankov (Cutler et al., 1999) in tudi fosilnih združb (Behrensmeyer & Miller, 2012). Majhna debelina plasti breče kaže na krajše časovno obdobje sedimentacije. Na debelino plasti sicer lahko vpliva več faktorjev, kot so zaloga sedimentacijskega materiala (prst tipa *terra rossa*), vremenskih pogojev (izpiranje prsti), količina in oddaljenost kostnega gradiva od najdišča ter morfologija terena v času sedimentacije. Na krajšo in enakomerno sedimentacijo kaže tudi odsotnost očitnih sprememb barve sedimenta, oblike ali načina sedimentacije plasti s fosili. Če novo najdišče primerjamo z Brodarjevim profilom, kjer so bili fosilni ostanki najdeni v skoraj 20 plasteh, je sedimentacija gotovo potekala relativno kratek čas. Zasledimo tudi nekoliko drugačne pogoje sedimentacije kot pri črnokalskem najdišču 1 (I. in II.), kjer so bile mnoge kosti , še preden jih je prekril sediment, prevlečene s tanko plastjo karbonatnih prevlek (sige) (Jamnik et al, 2013).

Razdrobljenost in ohranjenost kostnega gradiva kaže na sedimentacijo večjih kostnih odlomkov po predhodni fragmentaciji, ki jih trenutno ne pripisujemo delovanju plenilcev (zveri), čeprav med preliminarno določeno favno najdemo tudi redke ostanke zob zveri. Razdrobljenost kosti lahko pripišemo tudi vremenskim vplivom, ki lahko močno vplivajo na stanje kostnega gradiva pred sedimentacijo oziroma pokopom (Behrensmeyer, 1978). Mnoge od kosti lahko pripišemo fazi 5, kot jih je postavila Behrensmeyerjeva (1978). V tej fazi kosti že fizično razpadajo in večje kosti so težje taksonomsko opredeljive, površina kosti je močno razpokana. Nekatere druge kosti ne kažejo tako močnih znakov razpadanja. Med njimi so ohranjene tudi cele kosti predvsem manjše kosti ekstremitet, kot so prstni členki, ki jih večji del pripisujemo jelenjadi.

Problematika paleontoloških najdišč (pleistocenskih sesalcev) v kamnolomih

Kamnolomi so z naravovarstvenega vidika problematični, ker predstavljajo večji poseg v okolje ter dodatno obremenjujejo okolico s prahom in hrupom. Še toliko bolj so lahko kamnolomi problematični na območju, kjer pogosto delno

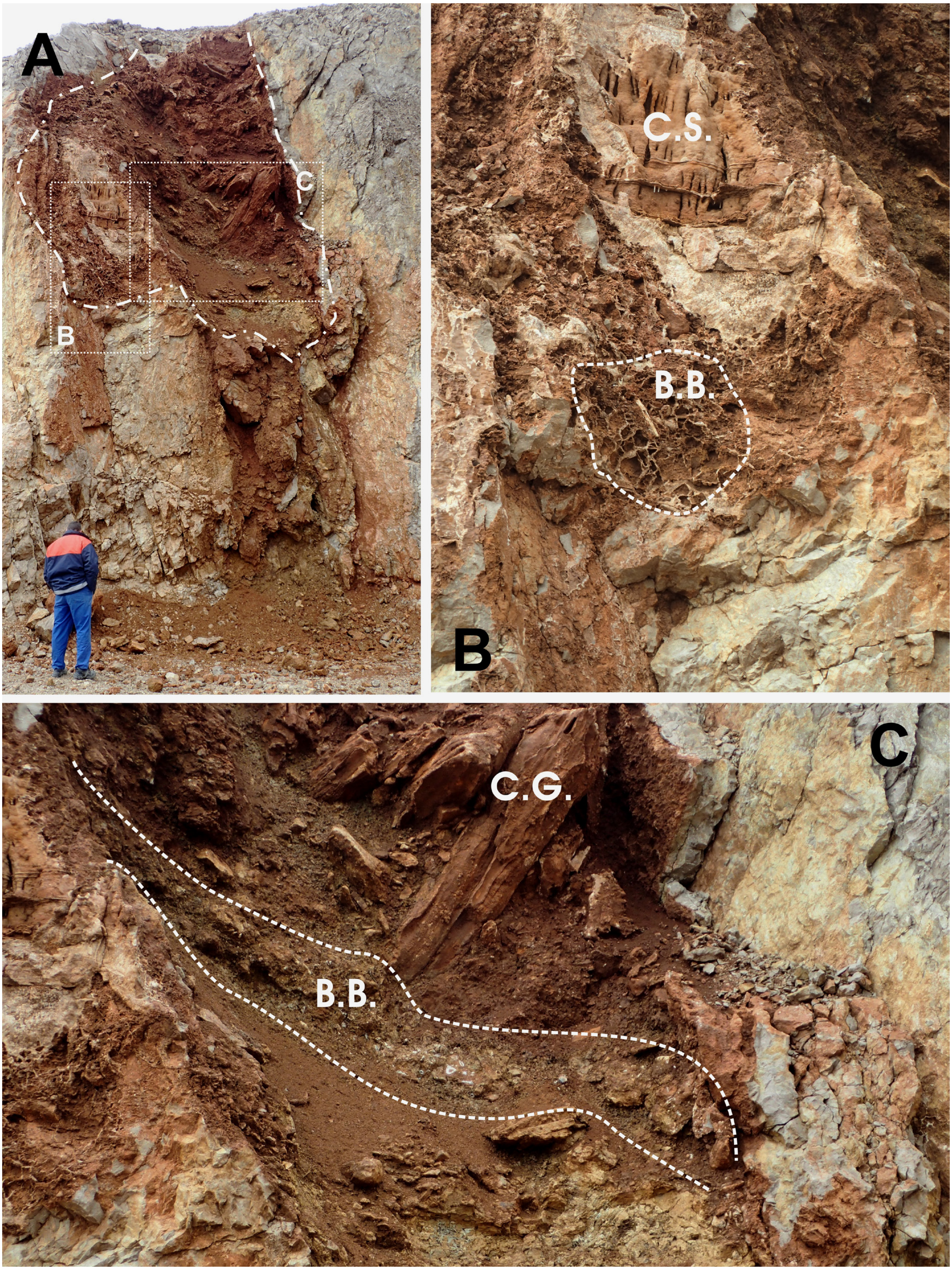

Sl. 4. Pogled na novo najdišče pleistocenske favne. A – s sedimenti zapolnjeno brezno (označena je razprostranjenost sedimentov), B – območje najdišča z ostanki sige (C.S.) in redkimi kostnimi ostanki (B.B.), C – pogled na položaj plasti s kostmi (kostna breča) (B.B.) in velikimi podornimi bloki sige (C.G.), ki zapolnjujejo večji del najdišča. Fotografija: M. Križnar.

Fig. 4. View on the new locality with Pleistocene fauna remains. A – karst fissure cave filled with sediments, B – area with remains of flowstones (C.S.) and rare bone remains (B.B.), C – view on location of the bone breccia (B.B.) and big blocks of broken flowstones (C.G.) on the top of fossil bearing layer. Photo: M. Križnar.

odkrivajo ali celo uničujejo kraške pojave, kot so jame, brezna in vrtače (cona epikrasa in tudi globlje). Predvsem aktivni kamnolomi s svojim delovanjem lahko v zelo kratkem časovnem intervalu odkrijejo najdišče in ga močno poškodujejo ali celo uničijo (celotna odstranitev). Nekoliko manj so problematični predeli kamnolomov, kjer aktivnosti ne potekajo intenzivno ali celo zastanejo v globljih delih kamnolomov. Na razgaljena ležišča fosilov poleg mehanskih poškodb ali odstranitve na daljše obdobje vplivajo tudi:

- vremenski vplivi (izpiranje sedimentov v nižje ležeče dele, sekundarno nahajališče),
- tresljaji ob delovanju kamnoloma (porušitev sedimentov),
- nenadzirano poseganje v najdišče.

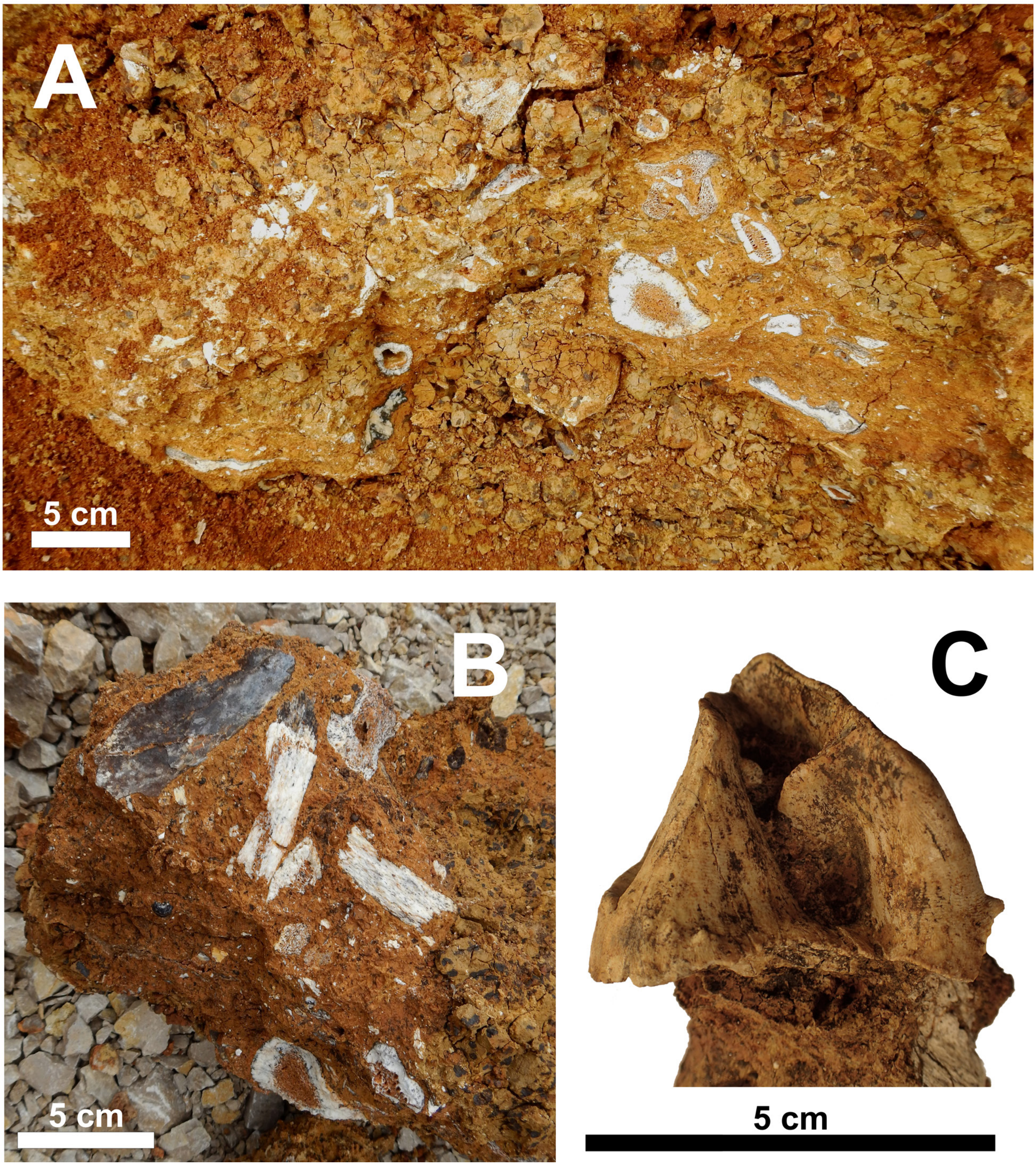

Sl. 5. A – bližnji posnetek plasti kostne breče z večjimi fragmenti kosti pleistocenskih sesalcev, A – odpadli kos kostne breče pod najdiščem, C – zob pleistocenskega nosoroga (*Stephanorhinus* sp. iz plasti kostne breče. Fotografije: D. Preisinger, M. Križnar.

Fig. 5. A – Close photo of bone breccia with large fragments of Pleistocene mammals bones, A – broken and detached block of bone breccia on the quarry road, C – tooth of Pleistocene rhinoceros (*Stephanorhinus* sp.) from bone breccia. Photo: D. Preisinger, M. Križnar.

Hkrati je potrebno poudariti, da kamnolomi ponujajo tudi edinstveno priložnost za odkrivanje novih, običajno nedostopnih paleontoloških (tudi arheoloških) najdišč. Dva izmed teh primerov sta tudi kamnolom pri Črnem Kalu ter nekoliko višje ležeči in večji kamnolom Črnotiče.

Prav črnokalski kamnolom je lep primer, kjer lahko na majhnem območju naštejemo več paleontoloških najdišč s pleistocensko favno (Jamnik et al., 2013), kjer pa se pogosto srečamo s problematiko zaščite teh najdišč, predvsem v aktivnih predelih kamnoloma.

Naše večletne izkušnje so pokazale, da so pri teh najdiščih pomembni:

- redni nadzor, predvsem v aktivnih delih kamnolomov,
- predhodni pregledi, še neaktivnih/zakritih delov kamnoloma z iskanjem morebitnih znakov najdišč (razpoke, manjše vrtače in drugi morfološki znaki),
- dobri odnosi z upravniki/lastniki kamnolomov, kjer lahko s sodelovanjem vsaj delno zaščitimo in dokumentiramo nova najdišča,
- pravilno in redno dokumentiranje stanja (fotografiranje stanja in napredovanj v kamnolomu, izris najdišč) in pravilni strokovni odvzemi paleontološkega, sedimentološkega, arheološkega in drugega gradiva,
- ustrezno objavljanje (z natančno lego najdišč), ozaveščanje o morebitnih novih najdiščih v kamnolomih (predvsem epikraško območje).

Za dosledno dokumentiranje in proučevanje pleistocenskih najdišč v kamnolomih je potrebno tudi poenotiti poimenovanje posameznih najdišč v delih kamnoloma. Problematiko smo že omenili v pregledu dosedanjih črnokalskih najdišč, predvsem z vidika fotografske dokumentacije in topografskih podatkov. Da lahko neprimerno in nedosledno poimenovanje predstavlja problem sta nakazala že Dehm in Fahlbusch (1970) iz pleistocenskih najdišč v nekaterih kamnolomih južne Nemčije.

V Sloveniji preventivnih paleontoloških nadzorov in preventivnih ogledov, kot bi lahko poimenovali nadziranje del in napredovanj v kamnolomih in drugih podobnih posegih (gradnja cest, predorov, vkopov) v naravno kamninsko podlago, ne poznamo v večjem obsegu, kar je morda tudi posledica pomanjkljive (zastarele in nedorečene) zakonodaje. V tujini je to nekako že ustaljena praksa, poznana pod nazivom »mitigation paleontology«, ki jo izvajajo na osnovi nekaterih predhodnih podatkov (teoretični del) in že predhodnih terenskih podatkov (praktični del) (Society of Vertebrate Paleontology, 1995; Murphy et al., 2014).

Podobnih območij z najdišči pleistocenske favne v kamnolomih je v Sloveniji še nekaj in vsi bi bili potrebni podobne obravnave. Sem spada zgoraj omenjeni kamnolom Črnotiči, ki je tudi edini dobro dokumentiran in proučen (Bosak et al., 1999; Mihevc, 2001; Horaček et al., 2007; Jamnik et al., 2013). Aguilar in Michaux (2011) podajata seznam nekaterih podobnih najdišč iz kamnoloma Velika Pirešica blizu Žalca in najdišča pri Sežani. O najdbi zoba azijskega črnega medveda *Ursus thibetanus mediterraneus* Cuvier iz breče v razpoki krednih apnencev v kamnolomu pri Vrhovljah na Krasu poroča Thenius (1958), ki pa ne podaja natančnega najdišča. Mnogi novi kamnolomi v okolici Sežane in na Krasu (Jurkovšek, 2013; Jurkovšek et al., 2013) ponujajo priložnosti za nova odkritja. To območje je danes z obujanjem starih kamnolomov in tradicionalnega izkoriščanja gradbenega (tehničnega) in okrasnega kamna še toliko bolj aktualno. Iz osrednje Slovenije sodi med kamnolome z izjemno pestrostjo kraških pojavov ter tudi najdb pleistocenskih sesalcev (jamski lev *Panthera leo spelea* (Goldfuss) in kosti jelena) tudi kamnolom pri Lesnem Brdu (Rakovec, 1969; Pavlovec, 1965; Křížnar, 2012). Iz kamnoloma oligocenskih konglomeratov na Kamnitniku pri Škofji Loki pa iz podobnih zapolnjenih razpok oziroma brezen Rakovec (1942) opisuje in omenja ostanke gozdnega nosoroga *Rhinoceros mercki* Jäger (=*Stephanorhinus kirchbergensis* (Jäger)). V vseh omenjenih kamnolomih izkoriščajo oziroma so izkoriščali apnenec (in njegove različke).

Zaključek

Novo odkrito najdišče jamske breče s kostmi pleistocenskih sesalcev v kamnolomu Črni Kal je primer dobrega sodelovanja med strokovno službo (Prirodoslovni muzej Slovenije) z zainteresirano javnostjo (zbiralci) in upravo kamnoloma. Na severnem delu črnokalskega kamnoloma smo raziskali delno odkopano paleokraško brezno, ki je nastalo v eocenskih alveolinsko–numulitnih apnencih. Iz plasti kostne breče, ki leži pod debelim nasutjem večjih kosov sige in odlomljenih kosov okoliške kamnine, smo uspeli izluščiti tudi nekaj paleontološkega gradiva, med katerim smo preliminarno ugotovili prisotnost nosoroga rodu *Stephanorhinus* (*Stephanorhinus kirchbergensis* (Jäger) ali *Stephanorhinus hemitoechus* (Falconer)), ostanke jelenov in še nedoločenih zob zveri. Kosti v breči so večinoma zdrobljene in so bile izprane v brezno. Pri raziskavi smo se posvetili tudi ostalim in že znanim najdiščem v kamnolomu Črni Kal ter v luči problematike zaščite podobnih najdb postavili nekatere smernice za boljšo zaščito, pravilno dokumentiranje in ohranjanje podobnih najdišč fosilov v kamnolomih (predvsem aktivnih) širom Slovenije.

New Pleistocene mammal site in Črni Kal quarry (Primorska region, Slovenia) with discussion on problems of protection and preservation of fossil sites in quarries

Summary

The Črni Kal quarry we report on a new Pleistocene mammal locality, which was discovered in northern part of the quarry, situated in alveolinid-nummulitid limestone of Eocene age. The new site is a karst (fissure) sinkhole mostly filled with flowstone rubble and partially with fine grained sediments, mixed with clay. The fossiliferous layer is around 40 cm thick bone breccia close to the bottom of the fissure.

The preliminary results of the analysis of few well preserved vertebrate fossils shows the presence of probable Merck's rhinoceros of the genus *Stephanorhinus* (tooth), bones of deer and few teeth of carnivores. Some discussion was made on the taphonomy of fossil remains, with emphasis on fragmentation of bones and teeth.

Additional we presented all known fossil mammals localities from Črni Kal quarry with some comments of previous research. We also presented and discussed on problems with preserving vertebrate sites in quarries. Most problematic are: weathering of exposed fossilbearing site, destruction (partly or whole site) due to work in a quarry, uncontrolled collecting and excavation on site.The overseeing the Pleistocene vertebrate fossil sites in quarries must include: regularly inspections of quarries (mitigation paleontology), relevant documentation (as photo documentation), exact location in quarry, correct designation/names of fossilbearing localities.

All of the above given suggestions should be apllied to some known Slovenian (active) quarries with simillar paleontological sites (Pleistocene vertebrate sites).

Zahvala

Pri nastajanju, raziskovanju in dokumentiranju novega črnokalskega najdišča je sodelovalo tudi Društvo za raziskovanje jam Kranj, njihovim jamarjem se lepo zahvaljujemo, še posebno Šimnu Žumru. Za pomoč in sodelovanje bi se radi zahvalili tudi vodstvu kamnoloma (gospodoma Marijanu Prešernu in Branku Sosiču) ter delavcem v kamnolomu, ki so v veseljem pomagali pri terenskem delu.

Literatura

Aguilar, J.-P., Crochet, J.-Y., Krivic, K., Marandat, B., Michaux, J., Mihevc, A., Sigé, B. & Šebela, S. 1998: Pleistocene small mammals from some karstic fillings of Slovenia - preliminary results. Acta carsologica, 28/2: 141–150.

Aguilar, J.-P. & Michaux, J. 2011: Pleistocene edible dormice (Rodentia Mammalia) from Slovenia, and their relations to the present day *Glis glis* (Linnaeus 1766). Acta carsologica, 40/2: 369–380.

Bavec, M. & Pohar, V. 2009: Kvartar. In : Pleničar, M., Ogorelec, B. & Novak, M. (eds.): Geologija Slovenije. Geološki zavod Slovenije: 441-464.

Becker, D., Aubry, D. & Detrey, J. 2009: Les dolines du Pléistocène supérieur de la Combe de «Vâ Tche Tchâ» (Ajoie, Suisse): un piège à restes de mammifères et artefacts lithiques. Quaternaire, 20/2: 135-148.

Behrensmeyer, A.K. 1978: Taphonomic and ecologic information from bone weathering. Paleobiology, 4:150–162.

Behrensmeyer, A.K. & Miller, J.H. 2012: Building Links Between Ecology and Paleontology Using Taphonomic Studies of Recent Vertebrate Communities. In: Louys, J. (ed.): Paleontology in Ecology and Conservation. Springer Earth System Sciences: Springer-Verlag Berlin Heidelberg: 69-91, doi: 10.1007/978-3-642-25038-5_5

Bolliger, T. & Rummel, M. 1994: Säugetierfunde aus Karstspalten – Die komplexe Genese am Beispiel eines Steinbruches bei Petersbuch, Südliche Frankenalb (Bayern). Mitteilungen der bayerischen Staatsammlung für Paläontologie und historische Geologie, 34: 239–264.

Bonfiglio, L., Di Stefano, G., Insacco, G. & Marra, A.C. 1993: New Pleistocene fissure--filling deposits from the Hyblean Plateau (South Eastern Sicily). Rivista Italiana di Paleontologia e Stratigrafia, 98: 523-540.

Bosák, P., Mihevc, A., Pruner, P., Melka, K., Venhodová, D. & Langrová, A. 1999: Cave fill in the Črnotiče Quarry, SW Slovenia: palaeomagnetic, mineralogical and geochemical study. Acta Carsologica, 28: 15-39.

Brodar, S. 1958: Črni Kal, nova paleolitska postaja v Slovenskem primorju (Črni Kal, eine neue Paläolithstation im Küstengebiet Sloweniens). Razprave 4. razreda SAZU 4: 271–363.

Brodar, M. & Osole, F. 1979: Nalazišta paleolitskog i mezolitskog doba u Sloveniji. In: Praistorija jugoslavenskih zemalja, 1: Paleolitsko i mezolitsko doba, Akademija nauka i umjetnosti Bosne i Hercegovine: 135–157.

Cutler, A. H., Behrensmeyer, A.K. & Chapman, R. E. 1999. Environmental information in a recent bone assemblage: roles of taphonomic processes and ecological change. Palaeogeography, palaeoclimatology, palaeoecology, 149/1-4: 359-372.

Dehm, R. & Fahlbusch, V. 1970: Zur Bezeichnung fossilführender Spaltenfüllungen. Mitteilungen der Bayerischen Staatssammlung für Paläontologie und historische Geologie, 10: 351–364.

Dietrich, A.K. 1958: *Dicerorhinus kirchbergensis* (Jäger) aus einer Karsthöhle bei Črni Kal (Istrien, Jugoslawien). Razprave 4. razreda SAZU 4: 435-440.

Horáček, I., Mihevc, A., Zupan Hajna, N., Pruner P. & Bosák, P. 2007: Fossil vertebrates and paleomagnetism update of one of the earlier stages of cave evolution in the Classical karst, Slovenia: Pliocene of Črnotiče II site and Račiška pečina Cave. Acta Carsologica, 36/3: 453-468, doi:10.3986/ac.v36i3.179.

Jamnik, P., Križnar, M. & Turk, M. 2013: Novi podatki o paleolitskih in paleontoloških najdiščih v kamnolomih Črni Kal in Črnotiče nad Koprom = New information on the palaeolithic and palaeontological sites in the Črni Kal and Črnotiče quarries above Koper, Slovenia. Arheološki vestnik, 64: 9-25.

Jurkovšek, B. 2013: Geološka karta Krasa = Geological map of Kras (Slovenia). 1:100.00, Geološki zavod Slovenije. Internet: http://www.geo-zs.si/PDF/GeoloskeKarte/Kras_new.pdf (27.9.2016)

Jurkovšek, B., Cvetko Tešović, B. & Kolar-Jurkovšek, T 2013: Geologija Krasa (=Geology of Kras). Geološki zavod Slovenije, Ljubljana: 205 p.

Križnar, M. 2012: Pleistocenski lev pri Lesnem Brdu. Konkrecija, 1: 41-43.

Mihevc, A., 2001: Speleogeneza Divaškega krasa. Zbirka ZRC, 27: 1-180.

Murphy, P.C., Knauss, G.E., Fisk, L.H., Demere, T.A., Reynolds, R.E., Trujillo, K.C. & Strauss, J.J. 2014: A Foundations for Best Practices in Mitigation Paleontology. Dakoterra, 6: 243-285.

Nagel, D. & Rabeder, G., 2000: Mittelpleistozäne Säugetierreste aus einer Spaltenfüllung bei Mannersdorf am Leithagebirge (Niederösterreich). Beiträge zur Paläontologie (Österreichs), 25A:1-9.

Pavlovec, R. 1965: Ostanki ledenodobnih živali v Lesnem Brdu pri Vrhniki. Proteus, 28/6: 155–156.

Pavlovec, R. & Pohar, V., 1997: The Črni Kal Quarry – An example of destroying Geotopes. Geologica Croatica, 50/2: 181–184.

Pavlovec, R. & Pohar, V. 2000: Destroying of geotopes – examples from Slovenia. Memorie Descr. Carta Geologica D'Italia, LIV: 367-369.

Pohar, V. & Kralj, P. 2002: Preservation of Pleistocene natural and cultural heritage in Potočka Zijalka, Križna jama and Črni Kal, Slovenia = Die Erhaltung der Pleistozän Natur- und Kulturerbschaft in Potočka zijalka, Križna jama und Črni Kal, Slowenien. In: 6th Internatiolnal Symposium on Cultural Heritage in Geosciences, Mining and Metallurgy. Idrija, Book of abstracts: 239–242.

Rakovec, I. 1942: Nosorog s Kamnitnika pri Škofji Loki. Razprave – matematično-prirodoslovnega razreda, AZU, 2: 241-262.

Rakovec, I. 1958: Pleistocenski sesalci iz jame pri Črnem Kalu = The Pleistocene Mammalia from the cave Črni Kal in Northern Istria. Razprave 4. razreda SAZU, 4/365–433.

Rakovec, I. 1969: Su nuovi resti di *Panthera* (*Leo*) *spelaea* (Goldf.) rinvenuti in Slovenia (Jugoslovia). Scritti sul Quaternario in onore di Angelo Pasa, museo Civico di storia Naturale: 53–65.

Rathgeber, T. 2002: Fossilführende Karstspalten bei Sonnenbühl-Genkingen = Fossil-bearing karst fissures near Sonnenbühl-Genkingen. Abhandlungen zu Karst- und Höhlenkunde, 34: 83-85.

Schöllmann, L. & Schlösser, M. 2010: Eine fossilführende Karstspalte im Steinbruch Hillenberg bei Warstein. Geologie und Paläontologie in Westfalen, 75: 5-26.

Society of Vertebrate Paleontology (SVP) 1995: Assessment and mitigation of adverse impacts to nonrenewable paleontologic resources: Standarg guidelines. Society of Vertebrate Paleontology News Bulletin, 163:22–27.

Thenius, E. 1958: Über einen Kleinbären aus dem Pleistozän von Slowenien: Nebst bemerkungen zur phylogenese der Plio-Pleistozänen Kleinbären. Razprave 4. razreda SAZU, 4: 631-646.

Ziegler, R. 1995: Pleistozäne Säugetierfaunen von Genkingen bei Reutlingen (Baden-Württemberg) = Pleistocene mammal faunas from Genkingen near Reutlingen (Baden-Württemberg). Stuttgarter Beiträge zur Naturkunde, Serie B (Geologie und Paläontologie), 234: 2-28.

Zupan Hajna, N. 2011: Human intervention in the karst underground through quaries; examples from Slovenia. In: Prelovšek, M. & Zupan Hajna, N. (eds.): Pressures and Protection of the Underground Karst - Cases from Slovenia and Croatia. Inštitut za raziskovanje krasa ZRC SAZU: 93-100.

GEOLOGIJA *60/1*, 99-115, Ljubljana 2017
https://doi.org/10.5474/geologija.2017.008

Early Jurassic foraminiferal assemblages in platform carbonates of Mt. Krim, central Slovenia

Spodnjejurske foraminiferne združbe v plitvomorskih karbonatih na območju Krima, osrednja Slovenija

Luka GALE[1,2] & Matej KELEMEN[3]

[1]University of Ljubljana, Faculty of Natural Sciences and Engineering, Department for Geology, Privoz 11, SI-1000 Ljubljana, Slovenia; e-mail: luka.gale@ntf.uni-lj.si
[2]Geological Survey of Slovenia, Dimičeva ul. 14, SI-1000 Ljubljana, Slovenia; e-mail: luka.gale@geo-zs.si
[3]Ulica Štefana Kovača 9, SI-9000 Murska Sobota, Slovenia

Prejeto / Received 23. 2. 2017; Sprejeto / Accepted 7. 4. 2017; Objavljeno na spletu / Published online 9.6.2017

Key words: External Dinarides, Adriatic Carbonate Platform, biostratigraphy, post-extinction recovery, Triassic-Jurassic boundary, diversity
Ključne besede: Zunanji Dinaridi, Jadranska karbonatna platforma, biostratigrafija, okrevanje po izumrtju, meja trias-jura, diverziteta

Abstract

During the Early Jurassic, the subtropical carbonate platforms of the peri-Tethys Ocean experienced significant changes in their architectures, as well as in their biota compositions. Shallow-water carbonates from the northern part of the ancient Adriatic Carbonate Platform (External Dinarides) were investigated in six sections, which taken together cover the development of the platform from deposition of the uppermost Triassic Main Dolomite to the middle Lower Jurassic, lithiotid limestone. Our aim was to establish a detailed foraminiferal biostratigraphy and to observe the changes in size, abundance and diversity of foraminifera in different types of facies. As a result, the succession was successfully divided into stage or substage levels. Foraminiferal assemblages were shown to experience a gradual change in taxonomic composition (including an increase in the proportion of complex agglutinated forms), a general increase in abundance of specimens, and greater diversity in each facies type, except in bindstone and mudstone. Notable is the difference between Hettangian assemblages, which display fairly uniform compositions in all facies types and the predominance of opportunists, and the post-Hettangian assemblages, which become progressively more species-rich and where the differences in facies are perhaps more pronounced. Changes in the size of the species *Meandrovoluta asiagoensis* Fugagnoli & Rettori, and of the largest specimen in the assemblages, however, are less clear, but are arguably present. Faunal changes roughly correspond to the gradual change from the flat-top platform of the upper Triassic – Hettangian, where biota would be repeatedly subjected to stressed peritidal conditions, to a platform differentiated into lagoon, sand bars and ephemeral emergent areas, offering numerous habitats and perhaps more stable living conditions for organisms.

Izvleček

Karbonatne platforme območja Tetide so v času starejše jure doživljale znatne spremembe v morfologiji in sestavi biote. Plitvomorske karbonate Jadranske karbonatne platforme (Zunanji Dinaridi) smo raziskali v šestih profilih na širšem območju Krima. Profili skupaj zajemajo interval od vrhnjega dela, glavnega dolomita do litiotidnega apnenca. Naš cilj je bil identifikacija foraminifernih biocon. Poleg same taksonomske sestave smo beležili še raznolikost foraminifernih združb, pogostnost (ali gostoto) foraminifer ter spremembo v velikosti vrste *Meandrovoluta asiagoensis* Fugagnoli & Rettori ter v velikosti največjih primerkov v združbah. Po pričakovanjih rezultati kažejo postopne spremembe v taksonomski sestavi foraminifernih združb, vključno z naraščanjem deleža kompleksnih aglutiniranih vrst ter splošen porast gostote primerkov in raznolikosti v vseh faciesih razen v bindstone in mudstone faciesih. Zanimivo je, da hettangijske združbe izkazujejo precejšnjo podobnost v sestavi in prevlado oportunističnih vrst, medtem ko so razlike med združbami glede na facies v mlajših plasteh bolj izrazite. Sprememba v velikosti vrste *M. asiagoensis* je znotraj posamičnega faciesa težko dokazljiva, celokupno gledano pa največji osebki te vrste dosegajo večjo velikost v mlajših plasteh. Podobno velja za velikost največjih osebkov v združbi. Favnistične spremembe približno sovpadajo s postopno spremembo v morfologiji platforme, ki se postopno diferencira v laguno, delno omejeno s peščenimi sipinami.

Introduction

The end-Triassic biocalcification crisis is generally thought to have had a significant influence on carbonate platforms (Galli et al., 2005; Greene et al., 2012). The acidification of oceanic water greatly influenced carbonate-secreting organisms like corals and calcareous sponges, and many of the marine groups experienced elevated extinction rates (Hautmann, 2004; Kiessling et al., 2007, 2009). Among the strongly affected organisms were also foraminifera, microscopically small, mostly marine, unicellular eukaryotes, which by the end of the Triassic formed diverse shallow-water communities composed of Involutinoidea, Duostominidae, Lagenida, Miliolida and Textulariida (Galli et al., 2005; Mancinelli et al., 2005; Gale, 2012; Gale et al., 2012). The change to Early Jurassic assemblages, almost completely dominated by agglutinated forms, is a striking example of community replacement.

The Adriatic (Dinaric sensu Buser, 1989) Carbonate Platform, the remnants of which are presently incorporated into the structurally deformed margin of the Adriatic tectonic microplate (Placer, 1999; Tari, 2002; Csontos & Vörös, 2004), was a platform with a seemingly less dramatic lithological change at the Triassic-Jurassic boundary, as peritidal deposition continues from the Upper Triassic to the lowermost Jurassic (e.g., Miler & Pavšič, 2008; Ogorelec, 2009). Afterwards, the succession records a gradual transition from tidal-flat to restricted lagoon setting, where the present "lithiotid limestone" deposited. This change of the platform topography, however, remains poorly researched, especially due to the lack of biostratigraphically well-defined sections.

This paper has two main aims. First, we show the stratigraphic distribution of foraminifera in six sections from the broader area of Mt. Krim, south of Ljubljana, from the base of the Hettangian Krka Limestone Member to the lower part of the Pliensbachian Lithiotid Limestone Member. Five of the sections were investigated in detail. On the basis of foraminifera, we determine the age of the sections to the stage or substage level. Secondly, we follow changes in terms of taxonomic composition, abundance of foraminifera, diversity, the size of *Meandrovoluta*, and the change in the largest specimen among foraminifera for each of the stages/substages, in order to gain more detailed insight into the origin of the post-extinction community. We do this for each facies type in order to avoid lithologically-induced bias.

Geological Setting and General Stratigraphy

The studied exposures are located in the northern External Dinarides (Fig. 1; Placer, 1999, 2008). The Lower Jurassic succession consists of shallow-marine carbonates deposited on the Adriatic Carbonate Platform (AdCP; Vlahović et al., 2002, 2005), locally also known as the

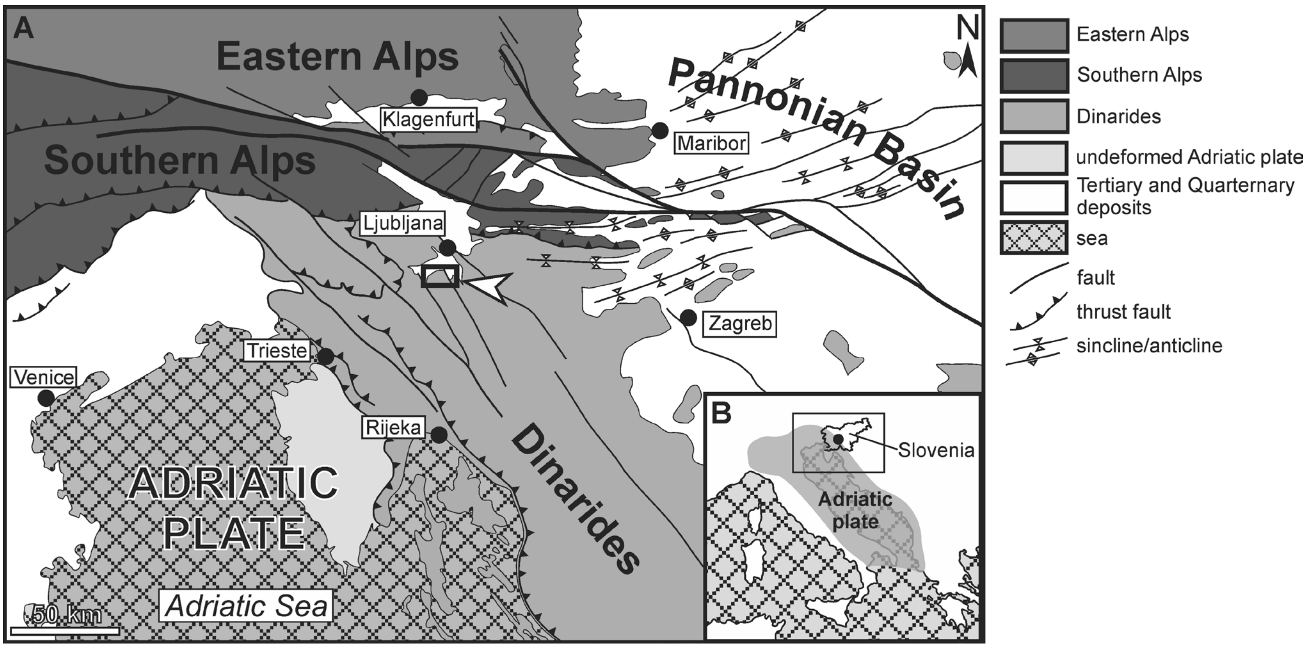

Fig. 1. Regional schematic structural map. The position of the studied area is marked by the white arrowhead. A: Structural map of the north-eastern corner of the present Adriatic tectonic plate. B: Present position of the Adriatic tectonic plate and position of Slovenia. The studied area is marked with a black dot. Modified after Vrabec and Fodor (2006).

Dinaric Carbonate Platform (Buser, 1989; Ogorelec & Rothe, 1993), which was during the Early Jurassic situated at a paleolatitude of approximately 25°N (Stampfli & Mosar, 1999; Stampfli & Kozur, 2006; Bosence et al., 2009; Berra & Angiolini, 2014). The thick sequence of carbonates, which continued to be deposited up until the uppermost Cretaceous (Buser, 1989), was later tilted and broken into several tectonic blocks, and separated by faults that in the studied area run in approximately N-S and WNW-ESE to NW-SE directions, separating tectonic blocks comprising Upper Triassic to Middle Jurassic carbonates (Fig. 2; Buser et al., 1967; Pleničar, 1970; Buser, 1968, 1974).

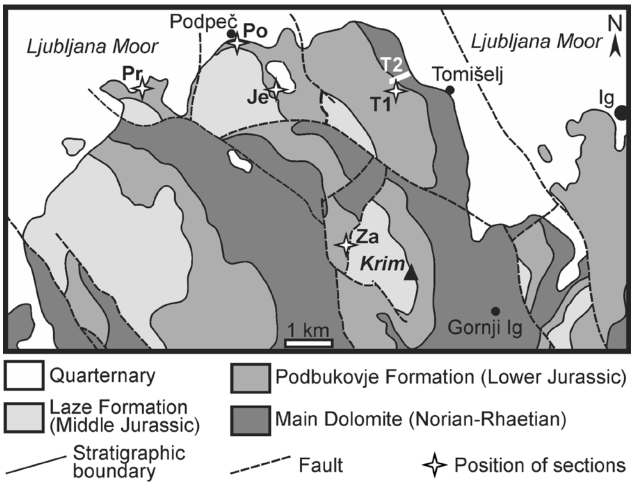

Fig. 2. Simplified geologic map of the studied area and location of studied sections. Modified after Buser et al. (1967) and Buser (1968). Je: Jezero (45°57´30´´ N, 14°26´00´´ E); Po: Podpeč (45°58´22´´ N, 14°25´16´´ E); Pr: Preserje (45°57´56´´ N, 14°23´47´´ E); T1: Tomišelj 1 (45°57´51´´ N, 14°28´06´´ E); T2: Tomišelj 2 (45°58´00´´ N, 14°28´16´´ E); Za: Zalopate (45°56´09´´ N, 14°27´21´´ E).

The lithostratigraphic subdivision of Lower Jurassic carbonates in the External Dinarides was recently revised by Dozet and Strohmenger (2000), Miler and Pavšič (2008), and Dozet (2009) (Fig. 3). The Norian-Rhaetian Main Dolomite is typified by medium- to thick-bedded crystalline dolomite, stromatolitic dolomite, and intraclastic breccia, indicating cyclically interchanging shallow subtidal, intertidal, and supratidal conditions (i.e., Lofer facies in Fischer, 1964) on a flat-topped carbonate platform (Ogorelec & Rothe, 1993). Peritidal sedimentation continued into the earliest Jurassic (Ogorelec, 2009), though the position of the Triassic-Jurassic boundary is merely arbitrary (Miler et al., 2007). The Lower Jurassic Podbukovje Formation (Dozet & Strohmenger, 2000; Predole Beds in Dozet, 2009) consists of five members. The Hettangian-Sinemurian Krka Limestone (i) is composed of crystalline dolomite, laminated (rarely stromatolitic) dolomite, mudstone, wackestone, rarely pellet or ooid grainstone, and intraclastic breccia (Dozet, 1993; Dozet & Strohmenger, 2000; Dozet, 2009; Ogorelec, 2009). Miler and Pavšič (2008) also note thick bodies of mud-supported breccia, which could be indicative of Early Jurassic tectonic activity. The following Upper Sinemurian-Pliensbachian *Orbitopsella* Limestone (ii), Lithiotid Limestone (iii) and Ooidal Limestone (iv) members mark the establishment of lagoons restricted by oolitic bars (Miler & Pavšič, 2008; Dozet, 2009; Gale, 2014). The Podbukovje Formation ends with the Toarcian Spotty Limestone Member (v) with nodular mudstone-wackestone and black ooid packstone (Dozet & Strohmenger, 2000; Dozet, 2009; Kresnik, 2016).

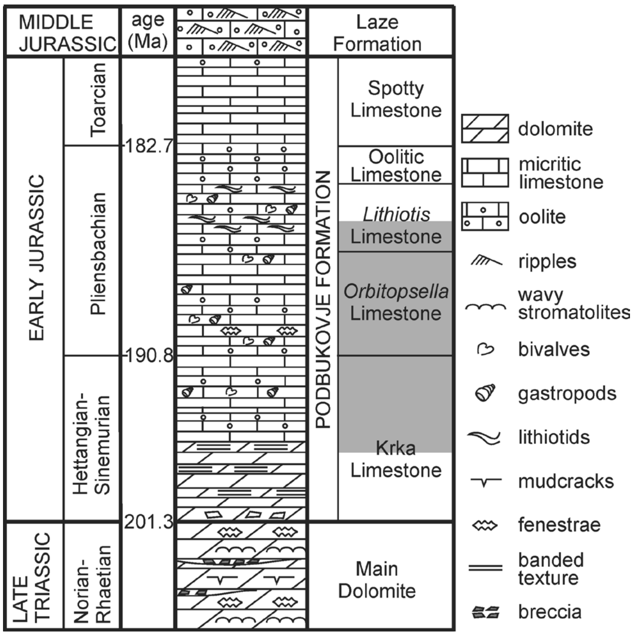

Fig. 3. Schematic lithostratigraphic column of the studied area. Shading indicates the interval covered by the detailed sections (the schematic Tomišelj 2 sections ranges further down to the Main Dolomite). Adopted after Miler and Pavšič (2008), Dozet (2009). Vertical scale is reconciled to thicknesses given in Dozet (2009). Ages for are taken after OGG et al. (2012).

Material and methods

The Lower Jurassic succession was investigated in five detailed sedimentological sections (Preserje, Tomišelj 2, Jezero, Zalopate, Podpeč sections), which structurally belong to the External Dinarides. Together the sections span the interval from the Krka Limestone to the Lithiotid Limestone Member sensu Dozet and Strohmenger (2000). The Preserje section was measured previously by Ogorelec (2009) and is reproduced herein. Although the succession of this section was originally placed near or at the Triassic-Jurassic boundary, we suggest a slightly younger age for these rocks on the basis of lithostratigraphic correlation and foraminiferal biozonation. The sixth, Tomišelj 1 section was measured schematically and reaches to the underlying Main Dolomite.

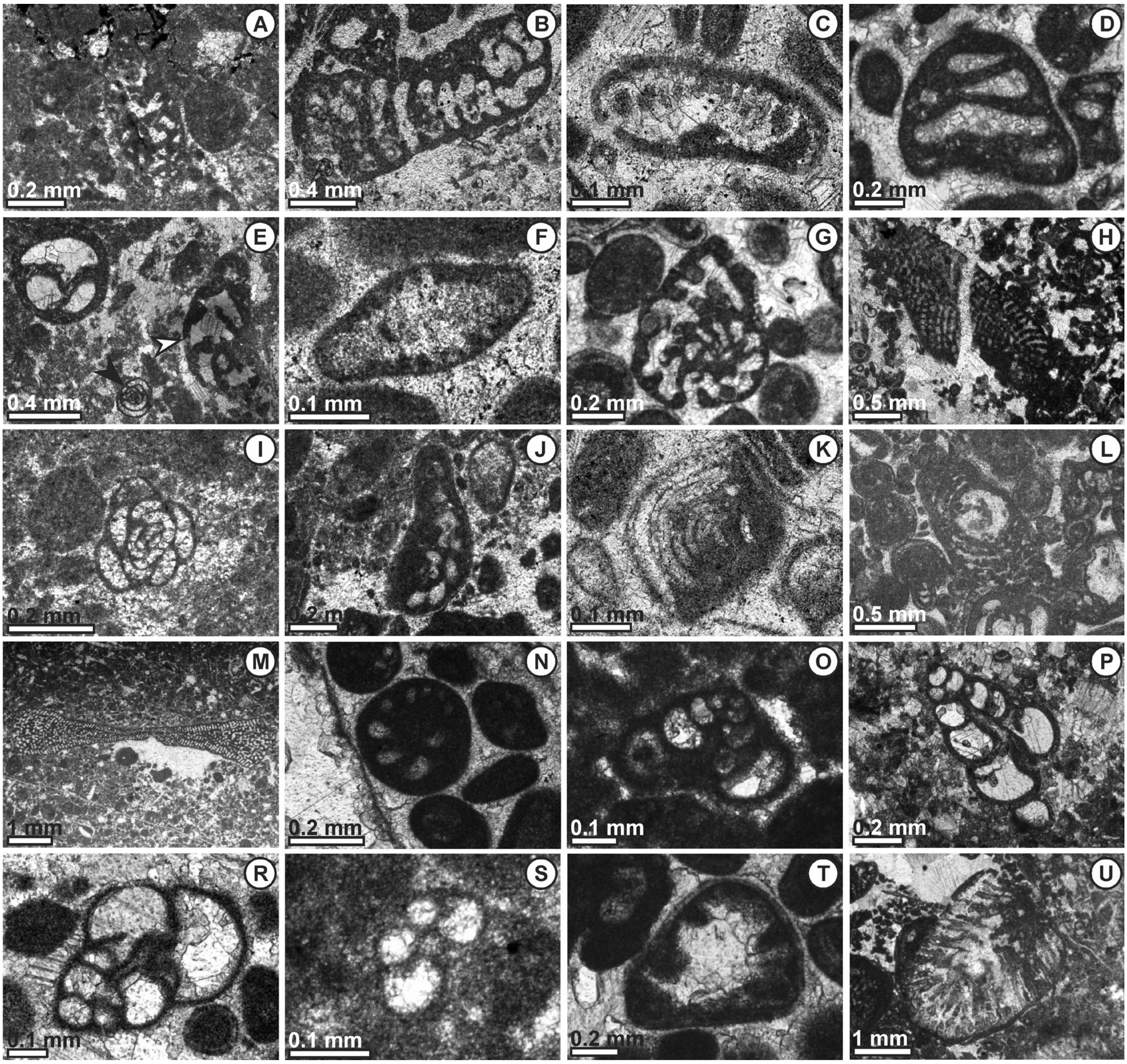

Fig. 4. Early Jurassic foraminifera and algae from the investigated sections.

A*: Amijiella amiji* (Henson). Thin section 535. Section Podpeč. Early Pliensbachian. B: *Bosniella oenensis* Gušić. Thin section 510. Section Podpeč. Early Pliensbachian. C: ?*Coronipora* sp. Thin section 528. Section Podpeč. Early Pliensbachian. D: *Duotaxis metula* Kristan. Thin section 418. Section Zalopate. Late Sinemurian-earliest Pliensbachian. E: *Everticyclammina praevirguliana* Fugagnoli (white arrowhead). Black arrowhead points at *Meandrovoluta asiagoensis*, whereas the section in the upper left corner belongs to *Duotaxis metula*. Thin section 328. Section Zalopate. Late Sinemurian-earliest Pliensbachian. F: *Involutina* sp. Thin section 528. Section Podpeč. Early Pliensbachian. G: *Lituolipora termieri* (Hottinger). Thin section 536. Section Podpeč. Early Pliensbachian. H: *Lituosepta recoarensis* Cati. Thin section 329. Section Zalopate. Late Sinemurian-earliest Pliensbachian. I: *Meandrovoluta asiagoensis* Fugagnoli & Rettori. Thin section 535b. Section Podpeč. Early Pliensbachian. J: *Mesoendothyra*? sp. Thin section 515. Section Podpeč. Early Pliensbachian. K: *Ophthalmidium* sp. Thin section 522. Section Podpeč. Early Pliensbachian. L: *Orbitopsella praecursor* (Gümbel). Thin section 529. Section Podpeč. Early Pliensbachian. M: *Orbitopsella primaeva* Henson. Thin section 535b. Section Podpeč. Early Pliensbachian. N: *Pseudopfenderina butterlini* (Brun). Thin section 510. Section Podpeč. Early Pliensbachian. O: *Siphovalvulina gibraltarensis* BouDagher-Fadel, Rose, Bosence & Lord. Thin section 328. Section Zalopate. Late Sinemurian-earliest Pliensbachian. P: *Siphovalvulina variabilis* Septfontaine. Thin section 412. Section Zalopate. Late Sinemurian-earliest Pliensbachian. R: *Siphovalvulina variabilis* Septfontaine. Thin section 329b. Section Zalopate. Late Sinemurian-earliest Pliensbachian. S: *"Trochammina" almtalensis* Koehn-Zaninetti. Thin section Jezero. Early - Middle Sinemurian. T: *Trocholina* sp. Thin section 325. Section Zalopate. Late Sinemurian-earliest Pliensbachian. U: *Palaeodasycladus mediterraneus* (Pia). Thin section 34. Section Preserje. Early - Middle Sinemurian.

Approximately 200 thin sections 47×28 mm and 75×49 mm in size from 184 beds were investigated for foraminifera (Fig. 4), and assemblages from different facies types were distinguished. Sparse and dense wackestones were distinguished by a borderline value of 30 % of grains. The number of foraminifera in thin sections varies from 0 to 60 per cm^2, with up to 434 specimens counted in a single thin section. Changes in abundance (number of specimens per cm^2), species richness and diversity for each facies type were investigated on the basis of approximately 150 thin sections. When generic or species determination was not possible, open nomenclature was used instead (e.g. Foraminifera indet. sp. A). *Aeolissacus/Earlandia* specimens were not counted due to their indistinct character. Some Nodosariidae were likewise difficult to separate into distinct species. As a result, biodiversity indices do not represent absolute values that could be directly compared to present-day values. The total number of foraminifera in each thin section was divided by the surface area of the investigated area in order to normalize the resulting values. The biodiversity of each sample was estimated on the basis of the Shannon-Wiener diversity index H´ (Hammer & Harper, 2006). In addition to calculating diversity, the maximum specimen size from each biozone was measured (see Payne et al., 2011). We also measured the largest specimen of the most common and widespread species, *Meandrovoluta asiagoensis*, in different facies types.

Description of sections and biostratigraphy

Tomišelj 2

This section serves as a reference section for the easier lithostratigraphic positioning of other sections. Due to the patchy exposure of beds (up the forested slope), no detailed sampling was possible. The section comprises the upper 18 m of the Rhaetian Main Dolomite and almost 300 m of the Lower Jurassic Krka Limestone Member (Fig. 5).

The Main Dolomite consists of medium thick beds of dolomitized bindstone with stromatolites and crystalline dolomite. Birds' eyes, tee-pee structures, desiccation cracks, black pebbles, and irregular bedding surfaces filled with lithified clasts in a clayey matrix are common. Only rare, small agglutinated forms and small Nodosariidae (Lagenida) were found in the uppermost part of the Main Dolomite.

The lower part of the Krka Limestone Member is to a large extent dolomitized. Medium- to very thick-bedded dolomite is coarsely crystalline, or exhibits planar laminae measuring a few millimetres in thickness. Fine-scale wrinkles, typical of stromatolites of the underlying Main Dolomite, are extremely rare. Tee-pee structures, black pebbles, and birds' eyes, however, are still common, as well as occasional irregular and clayey bedding planes. After approximately 70 m, medium- to thick-bedded micritic limestone with mudstone to wackestone texture dominates for 15 m, followed again by crystalline dolomite. Upwards, limestone (mudstone, and rarely wackestone) starts to gradually predominate over dolomite. Laminae, desiccation cracks, and birds' eyes structures are occasionally present. Approximately 100 m from the base of the Krka Limestone Member, the foraminiferal assemblage with *Duotaxis metula*, small Nodosariidae, *Reophax* sp., ?*Siphovalvulina colomi*, *Siphovalvulina variabilis*, ?"*Trochammina*" *almtalensis* and *Textularia* sp. were found. According to Velić (2007), *S. variabilis* first appears in the latest Hettangian.

Approximately 130 m from the base of the Krka Limestone, packstone and grainstone with bioclasts, intraclasts, and peloids are encountered. Leached-out clasts may be abundant. Packstone and grainstone are more common as we move to the uppermost part of the section, although mudstone still predominates. Red and/or irregular clayey bedding-planes and bird's eye vugs are occasionally present. The foraminiferal assemblage is notably more diversified and includes: *Amijiella amiji*, *D. metula*, *Everticyclammina praevirguliana*, Nodosariidae, *Meandrovoluta asiagoensis*, ?*Pseudopfenderina butterlini*, *Reophax* sp., *Siphovalvulina gibraltarensis*, *Siphovalvulina* sp., *Textularia* sp., *Trocholina* sp., and *Valvulina* sp. According to BouDagher-Fadel and Bosence (2007), *E. praevirguliana* first appears in the Middle Sinemurian, but Velić (2007) sets its first appearance already in the Late Hettangian. Furthermore, Velić (2007) sets the first appearance of *S. gibraltarensis* at the beginning of the Sinemurian. This part of the section is thus dated as Early Sinemurian. In the uppermost part of the Tomišelj 2 section, *M. asiagoensis* and ?*Lituosepta recoarensis* were also recorded. *Lituosepta recoarensis* first appears in the Late Sinemurian (BouDagher-Fadel & Bosence, 2007; Velić, 2007).

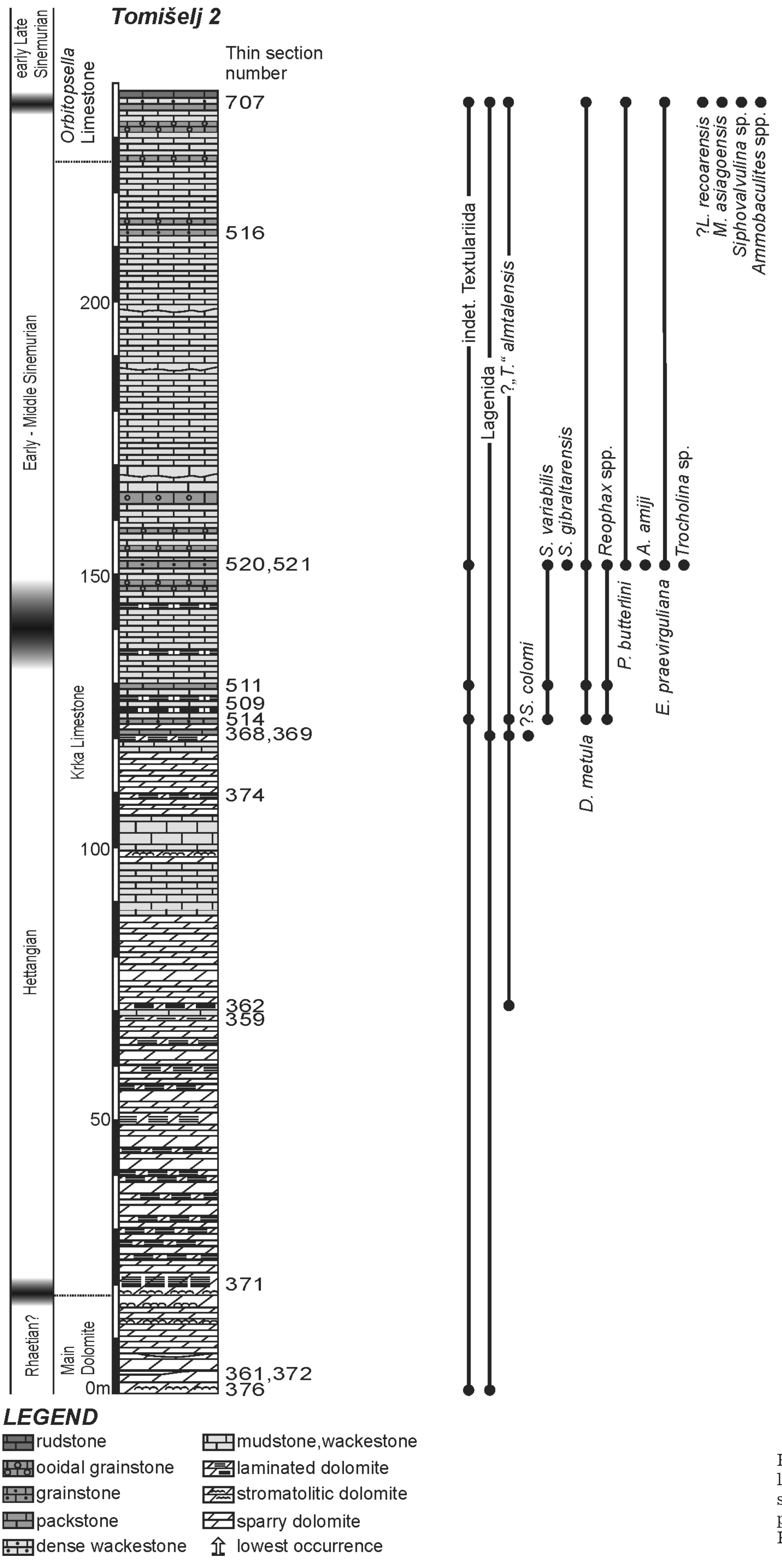

Fig. 5. Schematic stratigraphic log of the Tomišelj 2 section. The section is exposed along the slope from Tomišelj towards Mt. Krim and is partly covered.

Preserje

Medium to thick beds predominate. The lowermost part of the section is strongly dolomitized. Mudstone, bioclast and peloid wackestone predominate throughout the section (Fig. 6). Fragmented thin-shelled bivalves, foraminifera, ostracods, gastropods, echinoderms, green algae (*Palaeodasycladus mediterraneus*), and microproblematica *Thaumatoporella parvovesiculifera* are present among bioclasts. Horizons and beds of laminated dolomite, very rarely stromatolites, and intraclastic breccias are subordinate, as well as oolite with micritized grain-centres. Desiccation cracks and pores are present (Ogorelec, 2009).

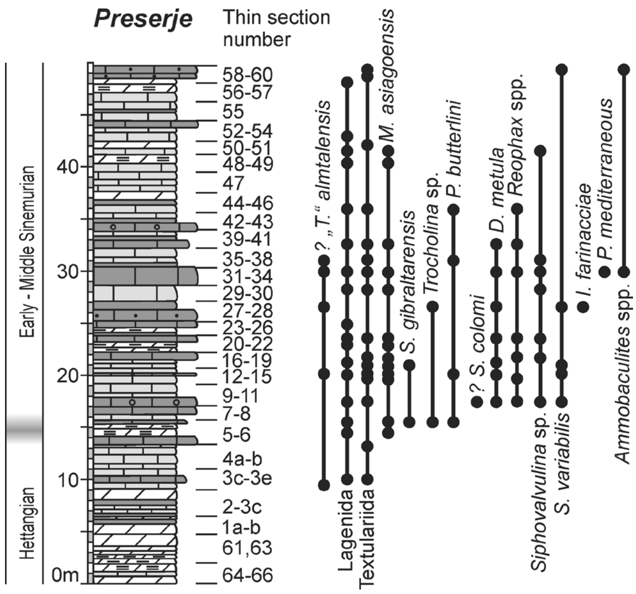

Fig. 6. The Preserje section. Redrawn and simplified after Ogorelec (2009). For the legend see Fig. 5.

The lowermost part of the section contains few foraminifera. Only Nodosariidae, small *Textularia* and ?"*T.*"*almtalensis* were determined. The rest of the section contains *Ammobaculites* sp., *D. metula*, *Involutina* sp., Nodosariidae, *M. asiagoensis*, *P. butterlini*, *Reophax* sp., ?*S. colomi*, *S. gibraltarensis*, *S. variabilis*, *Siphovalvulina* sp., *Textularia* sp., ?"*T.*" *almtalensis*, and *Trocholina* sp. Whereas the previous assemblage could possibly belong to the Hettangian, this assemblage is placed in the Early to Middle Sinemurian according to the stratigraphic chart for the Dinarides in Velić (2007). Additionally, according to BouDagher-Fadel and Bosence (2007), *P. butterlini* first appears in the Early to Middle Sinemurian *Siphovalvulina colomi* zone.

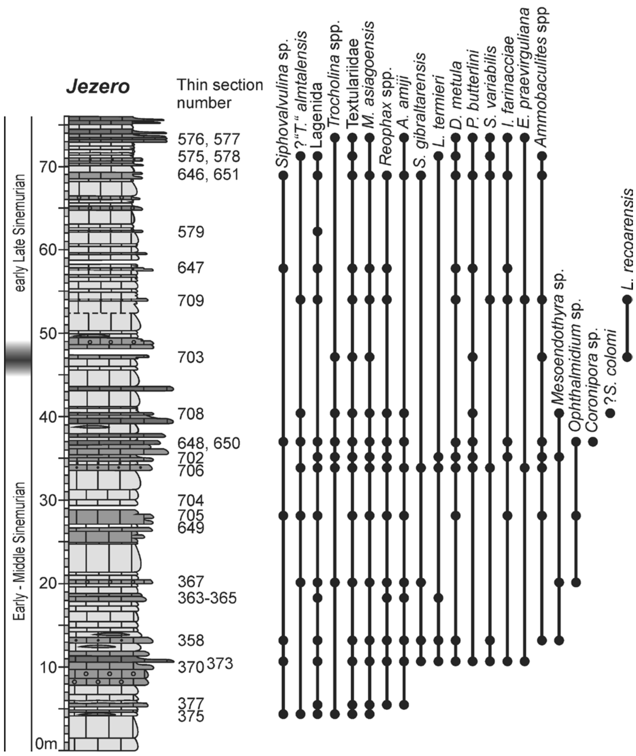

Fig. 7. Jezero section. For the legend see Fig. 5.

Jezero

Beds vary in thickness from thin, rarely even platy, to very thick. Grey and black mudstone and wackestone predominate (Fig. 7). Ooidal limestone is subordinate, sometimes presenting only horizons or lenses. Floatstone with bivalve and gastropod shells is likewise rare, whereas bioclast rudstone is slightly more abundant in the uppermost part of the section. Peloids predominate among clasts. Horizontal lamination in mudstone and gently dipping cross lamination are rare. Small-scale erosion relief, reworked mud chips, shell lags, red clayey bed surfaces, boring and burrowing structures are present.

The foraminiferal assemblage is identical to the one in the Tomišelj 1 section. *Mesoendothyra* sp. first occurs 13 m from the base of the section, and *L. recoarensis* 47 m from its base. Thus, it is possible that the section spans the successive *Mesoendothyra* sp. partial-range zone between the Early and Late Sinemurian, and the *L. recoarensis* partial-range zone of the early Late Sinemurian (Velić, 2007).

Tomišelj 1

Beds are medium- and occasionally very thick (Fig. 8). Mudstone and wackestone with rare intraclasts, peloids, ooids, thin-shelled bi-

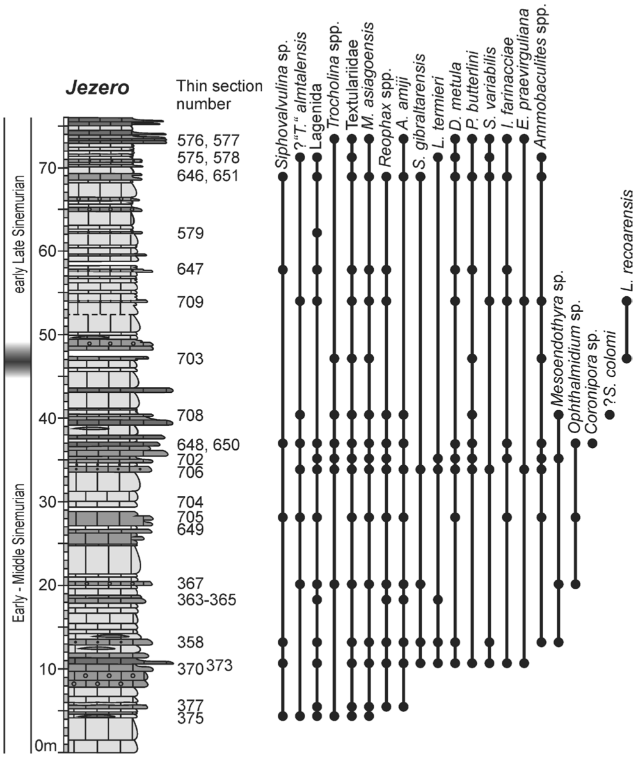

Fig. 8. Tomišelj 1 section. For the legend see Fig. 5.

valves, and small gastropods predominate. Ooid and bioclast-ooid packstone and grainstone are also common. Intraclast rudstone is rare and bivalve floatstone is present only in single horizons. Bioturbation is common in mudstone and wackestone, whereas normal and inverse gradings were rarely noted in ooid grainstone.

The foraminiferal assemblage consists of *A. amiji*, *Ammobaculites* spp., ?*Bosniella oenensis*, *Coronipora* sp., *D. metula*, *E. praevirguliana*, *Involutina* sp., Nodosariidae, ?*Lituolipora termieri*, ?*L. recoarensis*, *M. asiagoensis*, *Mesoendothyra* sp., *Ophthalmidium* sp., *P. butterlini*, *Reophax* spp., ? *S. colomi*, *S. gibraltarensis*, *S. variabilis*, *Siphovalvulina* sp., Textulariidae, ?"*T.*" *almtalensis*, *Trocholina* spp., and *Valvulina* sp..

According to the presence of ?*L. recoarensis* and the absence of *Orbitopsella* sp., this section belongs to the *L. recoarensis* partial-range zone of the early Late Sinemurian. Alternatively, because determination of *Lituosepta* is here questionable, it could belong to the older, *Mesoendothyra* sp. partial-range zone, spanning the transition from the Early to Late Sinemurian (Velić, 2007). According to Bassoullet (1997), this assemblage would be of Late Sinemurian age. Due to the early occurrence of *A. amiji*, the stratigraphic scheme of BouDagher-Fadel and Bosence (2007) seems less appropriate for this assemblage.

Zalopate

The predominant lithology in the Zalopate section is ooid grainstone in mostly medium thick beds (Fig. 9). Bivalve fragments, brachiopods, intraclasts, and oncoids are sometimes accumulated at the base of the oolite, and may be common enough to constitute a bioclast-ooid grainstone. Mudstone, lithiotid rudstone, peloid wackestone with *T. parvovesiculifera*, bivalve floatstone to rudstone with a bioclast-peloid wackestone-packstone matrix, and peloid grainstone are subordinate to grainstone. Normal and inverse grading, red clay partings, scour structures and flow-ripples are occasionally present.

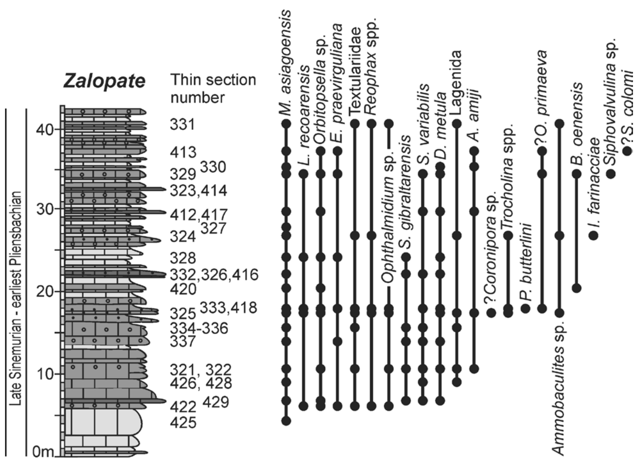

Fig. 9. Zalopate section. For the legend see Fig. 5.

The foraminiferal assemblage comprises *A. amiji*, *Ammobaculites* spp, *B. oenensis*, *Coronipora* sp., *D. metula*, *E. praevirguliana*, *Involutina* sp., Nodosariidae, *L. recoarensis*, *M. asiagoensis*, *Ophthalmidium* sp., *Orbitopsella primaeva*, *Orbitopsella* sp., *P. butterlini*, *Reophax* spp., ?*S. colomi*, *S. gibraltarensis*, *S. variabilis*, *Siphovalvulina* sp., *Textularia* spp., *Trocholina* spp., and *Valvulina* sp. According to the presence of *Orbitopsella* sp. and *O. primaeva*, this section represents the *O. primaeva* partial-range zone of Late Sinemurian to earliest Pliensbachian age (Velić, 2007).

Podpeč

The dominant lithology of the Podpeč section (Fig. 10) is medium to massive bedded grey ooid grainstone and bioclast-ooid grainstone. Also common are peloid wackestone to packstone, and oncoid and bioclast floatstone. Fragments of bivalves are the most frequent bioclasts; terebratulid brachiopods, foraminifera, gastropods and green algae are other common bioclasts. Lithiotid bivalves are mostly accumulated inside red claystone beds, rarely at the bases of limestone beds. Thin to medium thick beds of wackestone and mudstone are subordinate. Irregular bedding planes, red clayey surfaces, parallel lamination and grading are common. Cross-lamination in ooid grainstone was found outside the quarry.

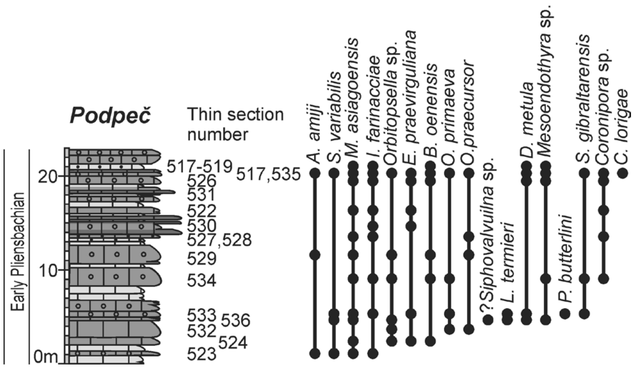

Fig. 10. Podpeč section. For the legend see Fig. 5.

The foraminiferal assemblage consists of *A. amiji*, *Ammobaculites* spp., *B. oenensis*, *Coronipora* sp., *D. metula*, *E. praevirguliana*, *Involutina* sp., Lagenida, *L. termieri*, *M. asiagoensis*, *Mesoendothyra* sp., *Ophthalmidium* sp., *Orbitopsella praecursor*, *O. primaeva*, *Orbitopsella* sp., *P. butterlini*, *Reophax* spp., ?*S. colomi*, *S. gibraltarensis*, *S. variabilis*, *Siphovalvulina* sp., Textularidae, *Trocholina* spp., and *Valvulina* sp. This assemblage belongs to the *O. praecursor* taxon-range zone of Early Pliensbachian age (Velić, 2007).

Trends in foraminiferal assemblages

Stratigraphic distribution of foraminifera is shown in Figures 5-10. Table 1 summarizes the composition of assemblages of successive time intervals and is divided according to facies. The highest abundance of specimens per cm^2 of thin section, the highest number of species and the highest calculated diversity are also given. These parameters, together with corresponding proportions of complex agglutinated foraminifera, are graphically shown in Figure 11. Figure 12 shows the change in size of *M. asiagoensis* and of the absolute largest specimen for each time interval.

Discussion

Facies changes

Lithological succession in the measured sections is summarized as follows:

i) Lofer cycles are typical for the Hettangian part of the succession (Dozet, 1993; Ogorelec, 2009). Irregular surfaces, clay infillings, and black pebbles point to occasional subaerial exposure (Haas et al., 2007), which together with birds' eyes, tee-pee structures, and desiccation cracks indicate intertidal sedimentation on a platform with a flat top.

ii) Mudstone, bioclast and peloid wackestone gradually start to become more common during the Late Hettangian, indicating longer-lasting subtidal conditions and/or the gradual recovery of invertebrates after the end-Triassic mass extinction, while stromatolites and subaerial exposures become less frequent. Transgression may be partly related to the global rise in sea level (Haq et al., 1988; Hallam, 2001) and/or the tectonic subsidence of the AdCP northern margin (Bucković et al., 2001).

iii) During the Early - Middle Sinemurian and in the early Late Sinemurian, bioclastic limestone gradually becomes more common. Red clayey bed surfaces indicate short periods of exposure (Martinuš et al., 2012).

iv) Ooid and bioclast-ooid packstone and well-sorted ooid grainstone with mature ooids become common during the early Late Sinemurian, and predominate in the Late Sinemurian and the Early Pliensbachian. Accumulations of bioclasts and scour structures indicate the influence of occasional storms (see Flügel, 2004: 714). Well-preserved and paired shells of lithiotid bivalves suggest the presence of bivalve bioherms in the vicinity (Fraser et al., 2004; Posenato & Avanzini, 2006; Posenato & Masetti, 2012). Short-lasting emersions are still evident as occasional red and clayey bedding planes. This type of platform was no longer dominated by peritidal conditions, but probably resembled internally differentiated lagoon with accumulations and/or buildups of lithiotid bivalves and oolitic sand shoals (Gale, 2015).

Table 1. The largest values for diversity (H), abundance and number of species per thin section and the list of determined foraminifera.

Microfacies	Age	Max H‘	Max abundance per cm^2	*Max No. species	Assemblage (determined taxa only, without species held in open nomenclature)
Bindstone	Rhaetian – Middle Hettangian	1.00	0.42	3	Nodosariidae, Textulariida
	Late Hettangian	0.56	1.06	2	*Meandrovoluta asiagoensis*, Nodosariidae
	Early – middle Sinemurian	0.75	5.87	6	*Meandrovoluta asiagoensis*, Nodosariidae, *Pseudopfenderina butterlini*, Textulariida, “*Trochammina” almtalensis*, *Trocholina* sp.
	early Late Sinemurian	0	0	0	/
Mudstone	Late Hettangian	0	0.29	1	»*Trochammina*« *almtalensis*
	Early - Middle Sinemurian	1.31	2.26	5	*Meandrovoluta asiagoensis*, Nodosariidae, *Pseudopfenderina butterlini*, *Reophax* sp., *Siphovalvulina* sp., Textulariida
	early Late Sinemurian	0.8	0.97	3	*Ammobaculites* sp., Nodosariidae, *Pseudopfenderina butterlini*
	Late Sinemurian – earliest Pliensbachian	/	0	0	/
Sparse wackestone	Late Hettangian	/	0	0	/
	Early - Middle Sinemurian	2.48	10.77	9	*Amijiella amiji*, *Ammobaculites* sp., ?*Coronipora* sp., *Duotaxis metula*, *Involutina* sp., *Meandrovoluta asiagoensis*, Nodosariidae, *Oph-thalmidium* sp., *Pseudopfenderina butterlini*, *Reophax* sp., *Siphovalvulina* sp., Textulariida, “*Trochammina” almtalensis*, ?*Trocholina* sp.
	early Late Sinemurian	1.98	8.55	11	*Amijiella amiji*, *Everticyclammina praevirguliana*, *Meandrovoluta asiagoensis*, Nodosariidae, *Reophax* sp., *Siphovalvulina* sp., Textulariida
Dense wackestone	Late Hettangian	0.72	10.12	4	*Duotaxis metula, Meandrovoluta asiagoensis,* Nodosariidae, Textulariida
	Early - Middle Sinemurian	1.56	36.13	16	*Amijiella amiji*, *Ammobaculites* sp., *Duotaxis metula*, *Lituolipora termieri*, *Meandrovoluta asiagoensis*, Nodosariidae, *Pseudopfenderina butterlini*, *Reophax* sp., *Siphovalvulina gibraltarensis*, *Siphovalvulina variabilis*, Textulariida, “*Trochammina*” *almtalensis*, *Trocholina* sp.
	early Late Sinemurian	2.06	11.58	13	*Ammobaculites* sp., *Duotaxis metula*, *Everticyclammina praevirguliana*, *Meandrovoluta asiagoensis*, Nodosariidae, *Pseudopfenderina butterlini*, *Reophax* sp., *Siphovalvulina* sp., Textulariida, “*Trochammina*” *almtalensis*
	Late Sinemurian – earliest Pliensbachian	1.83	1.69	7	*Siphovalvulina gibraltarensis*
	Early Pliensbachian	1.94	28.67	20	*Ammobaculites* sp., *Involutina farinnaciae*, *Meandrovoluta asiagoensis*, *Mesoendothyra* sp., Nodosariidae, *Ophthalmidium* sp., *Reophax* sp., Textulariida, *Trocholina* sp.

Packstone	Late Hettangian	1.64	2.94	6	*Duotaxis metula*, *Reophax* sp., *Siphovalvulina variabilis*, Textulariida
	Early – Middle Sinemurian	3.18	14.62	24	*Amijiella amiji*, *Ammobaculites* sp., ?*Coronipora* sp., *Duotaxis metula*, *Everticyclammina praevirguliana*, *Involutina* sp., *Lituolipora termieri*, *Meandrovoluta asiagoensis*, *Mesoendothyra* sp., Nodosariidae, *Ophthalmidium* sp., *Pseudopfenderina butterlini*, *Reophax* sp., ?*Siphovalvulina colomi*, *Siphovalvulina gibraltarensis*, *Siphovalvulina* sp., *Siphovalvulina variabilis*, Textulariida, "*Trochammina" almtalensis*, *Trocholina* sp.
	early Late Sinemurian	2.38	24.28	15	*Amijiella amiji*, *Ammobaculites* sp., ?*Coronipora* sp., *Duotaxis metula*, *Everticyclammina praevirguliana*, *Involutina* sp., *Meandrovoluta asiagoensis*, Nodosariidae, *Ophthalmidium* sp., *Pseudopfenderina butterlini*, *Reophax* sp., *Siphovalvulina gibraltarensis*, *Siphovalvulina* sp., *Siphovalvulina variabilis*, Textulariida, "*Trochammina" almtalensis*, *Trocholina* sp.
	Late Sinemurian – earliest Pliensbachian	2.38	29.82	30	*Amijiella amiji*, *Ammobaculites* sp., ?*Coronipora* sp., *Duotaxis metula*, *Everticyclammina praevirguliana*, *Involutina* sp., *Lituosepta recoarensis*, *Meandrovoluta asiagoensis*, *Mesoendothyra* sp., Nodosariidae, *Ophthalmidium* sp., *Orbitopsella primaeva*, *Orbitopsella* sp., *Pseudopfenderina butterlini*, *Reophax* sp., *Siphovalvulina gibraltarensis*, *Siphovalvulina variabilis*, ?*Siphovalvulina colomi*, Textulariida, *Trocholina* sp.,
	Early Pliensbachian	2.21	59.86	18	*Amijiella amiji*, *Bosniella oenensis*, ?*Coronipora* sp., *Duotaxis metula*, *Everticyclammina praevirguliana*, *Involutina* sp., *Meandrovoluta asiagoensis*, *Mesoendothyra* sp., Nodosariidae, *Ophthalmidium* sp., *Orbitopsella praecursor*, *Orbitopsella primaeva*, *Orbitopsella* sp., *Siphovalvulina gibraltarensis*, *Siphovalvulina variabilis*, Textulariida, *Trocholina* sp.
Grainstone	Late Hettangian	1.63	4.83	6	*Duotaxis metula*, Nodosariidae, *Reophax* sp., *Siphovalvulina variabilis*, Textulariida
	Early – Middle Sinemurian	2.31	18.89	16	*Amijiella amiji*, *Ammobaculites* sp., *Duotaxis metula*, *Everticyclammina praevirguliana*, *Involutina* sp., *Lituolipora termieri*, *Meandrovoluta asiagoensis*, *Mesoendothyra* sp., Nodosariidae, *Planiinvoluta* sp., *Pseudopfenderina butterlini*, *Reophax* sp., *Siphovalvulina gibraltarensis*, *Siphovalvulina variabilis*, *Siphovalvulina* sp., Textulariida, "*Trochammina" almtalensis*, *Trocholina* sp.
	early Late Sinemurian	2.62	26.62	17	*Amijiella amiji*, *Ammobaculites* sp., *Bosniella oenensis*, ?*Coronipora* sp., *Duotaxis metula*, *Everticyclammina praevirguliana*, *Involutina* sp., *Lituolipora termieri*, *Lituosepta recoarensis*, *Meandrovoluta asiagoensis*, *Mesoendothyra* sp., Nodosariidae, *Pseudopfenderina butterlini*, *Reophax* sp., ?*Siphovalvulina colomi*, *Siphovalvulina variabilis*, *Siphovalvulina* sp., Textulariida, "*Trochammina" almtalensis*, *Trocholina* sp.
	Late Sinemurian – earliest Pliensbachian	2.64	29.48	25	*Amijiella amiji*, *Ammobaculites* sp., ?*Coronipora* sp., *Duotaxis metula*, *Everticyclammina praevirguliana*, *Involutina* sp., *Lituosepta recoarensis*, *Meandrovoluta asiagoensis*, Nodosariidae, *Ophthalmidium* sp., *Orbitopsella primaeva*, *Orbitopsella* sp., *Pseudopfenderina butterlini*, *Reophax* sp., *Siphovalvulina gibraltarensis*, *Siphovalvulina variabilis*, Textulariida, *Trocholina* sp.
	Early Pliensbachian	2.02	29.94	24	*Amijiella amiji*, *Ammobaculites* sp., ?*Coronipora* sp., *Duotaxis metula*, *Involutina* sp., *Meandrovoluta asiagoensis*, *Mesoendothyra* sp., Nodosariidae, *Ophthalmidium* sp., *Orbitopsella* sp., *Reophax* sp., *Siphovalvulina* sp., Textulariida, *Trocholina* sp.
Ooidal grainstone	Early – Middle Sinemurian	2.38	3.35	12	*Amijiella amiji*, *Ammobaculites* sp., *Duotaxis metula*, *Involutina* sp., *Meandrovoluta asiagoensis*, *Mesoendothyra* sp., Nodosariidae, *Ophthalmidium* sp., *Reophax* sp., *Siphovalvulina gibraltarensis*, *Siphovalvulina* sp., *Siphovalvulina variabilis*, Textulariida, *"Trochammina" almtalensis*, *Trocholina* sp.
	early Late Sinemurian	2.53	11.03	17	*Amijiella amiji*, *Ammobaculites* sp., *Bosniella oenensis, Duotaxis metula*, *Everticyclammina praevirguliana*, *Involutina* sp., *Lituolipora termieri, Lituosepta recoarensis*, *Meandrovoluta asiagoensis*, *Mesoendothyra* sp., Nodosariidae, *Ophthalmidium* sp., *Pseudopfenderina butterlini*, *Reophax* sp., ?*Siphovalvulina colomi*, *Siphovalvulina gibraltarensis*, *Siphovalvulina* sp., *Siphovalvulina variabilis*, Textulariida, *Trocholina* sp.
	Late Sinemurian – earliest Pliensbachian	2.21	18.08	18	*Amijiella amiji*, *Bosniella oenensis,* ?*Coronipora* sp., *Involutina* sp., *Lituosepta recoarensis*, *Meandrovoluta asiagoensis*, Nodosariidae, *Ophthalmidium* sp., *Planiinvoluta* sp., *Pseudopfenderina butterlini*, *Reophax* sp., ?*Siphovalvulina colomi*, *Siphovalvulina gibraltarensis*, *Siphovalvulina* sp., Textulariida, *Trocholina* sp.
	Early Pliensbachian	2.92	43.39	29	*Amijiella amiji*, *Ammobaculites* sp., *Bosniella oenensis,* ?*Coronipora* sp., *Duotaxis metula*, *Everticyclammina praevirguliana*, *Involutina* sp., *Lituolipora termieri, Meandrovoluta asiagoensis*, *Mesoendothyra* sp., Nodosariidae, *Ophthalmidium* sp., *Orbitopsella primaeva*, *Orbitopsella praecursor*, *Orbitopsella* sp., *Pseudopfenderina butterlini*, *Reophax* sp., *Siphovalvulina gibraltarensis*, *Siphovalvulina variabilis*, ?*Siphovalvulina colomi*, Textulariida, *Trocholina* sp.

* species held in open nomenclature included

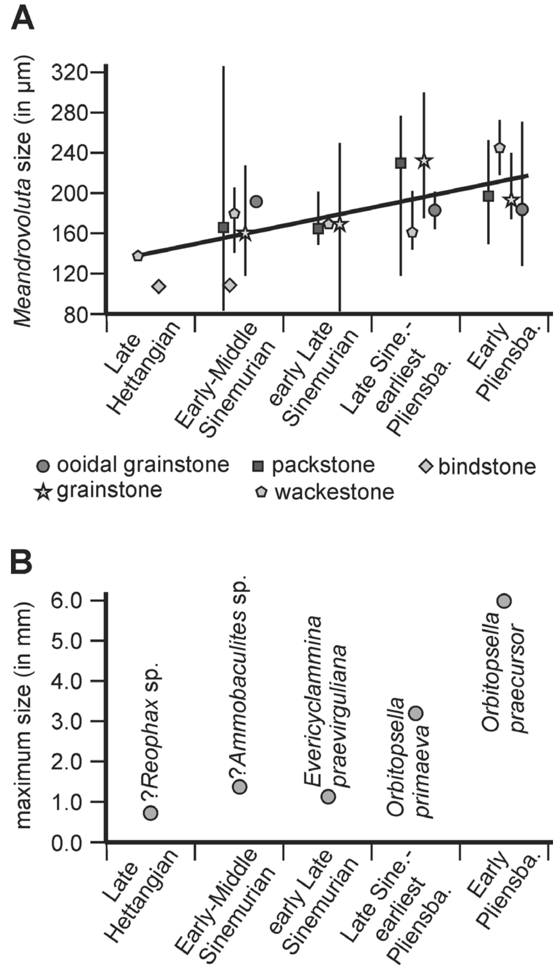

Fig. 12. Trends in sizes of foraminifera. A: A within-genus change of size for *Meandrovoluta* per facies type. Vertical bars indicate variability within distinct facies types, and the symbol the mean size. The oblique solid line represents a general increase in size. B: The among-genus change in size. The largest specimens encountered in different time-slices were measured, regardless of facies type.

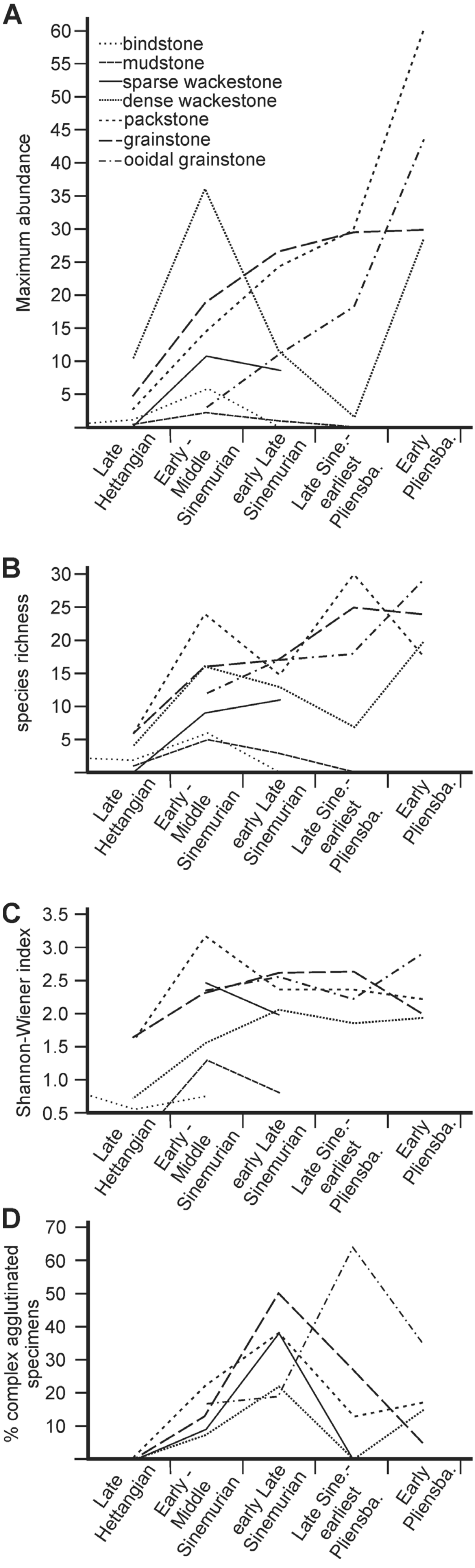

Fig. 11. Changes in foraminiferal assemblages according to different facies. A: Maximum abundance (number of specimens per cm^2 of thin section). B: Maximum number of species (species richness) per facies type. C: Maximum diversity for different facies types. D: Percent of relatively complex agglutinated foraminifera. Specimens with an advanced endoskeleton (e.g., axial infill, pillars) and/or with exoskeletal structures (complex outer wall, possibly for hosting endosymbionts) were counted, and include the genera: *Bosniella, Lituolipora, Pseudopfenderina, Amijiella, Mesoendothyra, Lituosepta, Orbitopsella, Everticyclammina, Cymbriaella*.

Diversification in foraminifera

Foraminiferal assemblages from Hettangian to Pliensbachian undergo significant changes in composition, diversity and abundance, which take place cotemporaneous with a facies change from restricted tidal-flat to predominantly subtidal and normal marine conditions:

i) Until the Late Hettangian, the taxonomic composition is virtually the same in all facies types of the peritidal environment. The assemblage consists of species, that may be considered opportunists (see Fugagnoli, 2004; BouDagher-Fadel, 2008), e.g. *M. asiagoensis*, *Siphovalvulina* spp., and Triassic survivors, e.g. *D. metula*, "*T.*" *almtalensis*.

ii) A strong increase in abundance, species richness, diversity of foraminifera and number of complex agglutinated forms is common to all facies types, except mudstone and bindstone in the Early - Middle Sinemurian. There is a strong possibility of a continued increase in the abundance of foraminifera until the Early Pliensbachian, which is the youngest sampled interval. As such increase occurs in all facies types (except in bindstone and mudstone), we can rule out the possibility of simply sampling a more suitable facies type (i.e., more "grainy" limestone opposed to micritic limestone).

iii) *Bosniella oenensis*, *L. recoarensis*, and *Orbitopsella* spp. are restricted to packstone, grainstone and ooid grainstone since the early Late Sinemurian. These may be more strongly agitated facies types.

iv) Although the size of *M. asiagoensis* varies, there may be a general trend in increase in size; and the size of the largest species in the assemblage also increases.

The recorded succession of faunas parallels the studies of benthic foraminifera elsewhere in the present peri-Mediterranean area (Chiocchini et al., 1994; Zambetakis-Lekkas et al., 1996; BouDagher-Fadel et al., 2001; Eren et al., 2002; Kabal & Tasli, 2003; Barattolo & Romano, 2005; Mancinelli et al., 2005; Pomoni-Papaioannou & Kostopoulou, 2008; Bosence et al., 2009; Tunaboylu et al., 2014). The contrasting Hettangian - Early Sinemurian and Late Sinemurian - Pliensbachian communities are mostly interpreted as survival and recovery communities of the post-extinction period (Barattolo & Romano, 2005; Mancinelli et al., 2005; BouDagher-Fadel & Bosence, 2007; BouDagher-Fadel, 2008; Tunaboylu et al., 2014), and could be interpreted as part of the global community maturation process (Hottinger, 1996, 2014). However, Fugagnoli (2004; see also Septfontaine, 1986) related a low-diversity assemblage dominated by *Glomospira/Planiinvoluta* spp. (i.e., *Meandrovoluta* sp.), together with *Duotaxis*, simple textulariids and valvulinids, to eutrophic conditions (bioturbated mudstone-wackestone alternating with black shale), while the diversity and proportion of complex lituolids increase as conditions changed towards meso- and oligotrophic. The change in nutrient supply and oxygen availability from Hettangian to Pliensbachian is not as strongly supported in the present study, as there is no transition from organic-rich facies (although algal mats contained plenty of organic matter, while well-washed sands in the younger part of the succession were well oxygenated). Rather, environmental stability itself might be more important in establishing more complex associations of foraminifera. Such stability might have been related to stabilization of the physical environment (e.g., ocean chemistry, sea temperature) after the end-Triassic extinction, or to the increasing interactions among organisms, but it might also have come with the transition from highly fluctuating peritidal conditions where there are drastic changes in light intensity, salinity and temperature, to predominantly subtidal and thus more physically stable conditions (see Hallock, 1988). Furthermore, although a steady increase in the size of foraminifera has been recorded after the Permian-Triassic boundary extinction and used as an argument for a true (i.e., not facies-change related) recovery of foraminifera (Payne et al., 2011; Rego et al., 2012), it is not known whether such an increase in size is possible also during the time of rising sea level (Wilmsen & Neuweiler, 2008). In other words, the increased complexity of foraminiferal assemblages in transgression-affected succession should not be attributed solely to post-extinction biotic recovery and diversification, but may instead reflect a rather local re-establishment of suitable habitat.

Conclusions

The precise age of Lower Jurassic carbonates from the Mt. Krim area (External Dinarides) was determined on the basis of foraminifera. Such biostratigraphic framework is obligatory for potential future studies of the northern Adriatic Carbonate Platform. During the Late Hettangian, sedimentation took place on a relatively flat platform with quickly interchanging subtidal and intertidal conditions, as can be concluded from the exchange of micritic limestone/dolomite with laminated (stromatolitic) limestone/dolomite and emersion surfaces. Foraminiferal assemblage, consisting of small opportunists, is identical in all microfacies types, even in rare packstone and grainstone. The low diversity of the assemblage may be attributed to the early stages of recovery after the end-Triassic extinction, or to unstable environmental conditions. Towards the Early – Middle Sinemurian, foraminiferal assemblages of various facies types show an increase in abundance, species richness, and diversity. Larger agglutinated species appear for the first time. This change in the assemblage corresponds to a shift towards predominantly subtidal and more stable conditions. The younger strata show a continuing increase in abundance until the Early Pliensbachian, but the trend is not so clear as regards species richness and diversity. The facies association suggests the contemporaneous development of an internally differentiated lagoon, which hinders distinguishing between the true speciation and the mere colonisation of suitable habitats.

Acknowledgements

This study was financially supported by the Slovenian Research Agency (pr. no. P1-0011). Thin sections were prepared by Mladen Štumergar (Geological Survey of Slovenia). We thank students Maša Jamnik and Primož Oprčkal for their help with the field work. We also thank the reviewers for their constructive remarks.

References

Barattolo, F. & Romano, R. 2005: Shallow carbonate platform bioevents during the Upper Triassic-Lower Jurassic: an evolutive interpretation. Boll. Soc. Geol. It., 124: 123-142.

Bassoullet, J.-P. 1997: Large foraminifera. In: Cariou, E. & Hantzpergue, P. (eds.): Jurassic biostratigraphy of the western Europe and Mediterranean: microfossil distribution and zonations. Bull. Centre Rech. Explor. Product. Elf, 17: 293-304.

Berra, F. & Angiolini, L. 2014: The evolution of the Tethys region throughout the Phanerozoic: a brief tectonic reconstruction. In: Marlow, L., Kendall, C. & Yose, L. (eds.): Petroleum systems of the Tethyan region. AAGP Mem., 106: 1-27.

Bosence, D., Procter, E., Aurell, M., Bel Kahla, A., BouDagher-Fadel, M., Casaglia, F., Cirilli, S., Mehdie, M., Nieto, L., Rey, J., Scherreiks, R., Soussi, M. & Waltham, D. 2009: A dominant tectonic signal in high-frequency, peritidal carbonate cycles? A regional analysis of Liassic platforms from western Tethys. J. Sed. Res., 79: 389-415.

BouDagher-Fadel, M.K. 2008: Evolution and geological significance of larger benthic foraminifera. In: Wignall, P.B. (ed.): Developments in Palaeontology and Stratigraphy: 540 p.

BouDagher-Fadel, M. & Bosence, D.W.J. 2007: Early Jurassic benthic foraminiferal diversification and biozones in shallow-marine carbonates of western Tethys. Senck. Leth., 87: 1-39.

BouDagher-Fadel, M.K., Rose, E.P.F., Bosence, D.W.J. & Lord, A.R. 2001: Lower Jurassic foraminifera and calcified microflora from Gibraltar, western Mediterranean. Palaeontology, 44: 601-621.

Bucković, D., Jelaska, V. & Cvetko Tesović, B. 2001: Facies variability in Lower Liassic carbonate successions of the Western Dinarides (Croatia). Facies, 44: 151-162.

Buser, S. 1968: Basic Geological Map SFRY 1:100.000, Sheet Ribnica, L 33-78. Federal Geological Survey, Beograd.

Buser, S. 1974: Explanatory book for Sheet Ribnica, L 33-78, Basic Geological Map SFRY 1:100.000. Federal Geological Survey, Beograd: 60 p.

Buser, S. 1989: Development of the Dinaric and the Julian carbonate platforms and of the intermediate Slovenian Basin (NW Yugoslavia). Boll. Soc. Geol. It., 40: 313-320.

Buser, S., Grad, K. & Pleničar, M. 1967: Basic Geological Map SFRY 1:100.000, Sheet Postojna, L 33-77. Federal Geological Survey, Beograd.

Chiocchini, M., Farinacci, A., Mancinella, A., Molinari, V. & Potetti, M. 1994: Foraminiferal, dasycladacean and calpionellid biostratigraphy of the Mesozoic carbonates of the Central Apennines (Italy). In: Biostratigraphy of the Central Italy. Studi Geol. Camerti, Roma, spec. vol.: 9-130.

Csontos, L. & Vörös, A. 2004: Mesozoic plate tectonic reconstruction of the Carpathian region. Palaeogeogr., palaeoclimatol., palaeoecol., 210: 1-56.

Dozet, S. 1993: Lofer cyclothems from the Lower Liassic Krka limestone. Riv. Ital. Paleont. Strat., 99: 81-100.

Dozet, S. 2009: Lower Jurassic carbonate succession between Predole and Mlačevo, Central Slovenia. RMZ-materials and geoenvironment, 56: 164-193.

Dozet, S. & Strohmenger, C. 2000: Podbukovje Formation, central Slovenia. Geologija, 43/2: 197-212, doi:10.5474/geologija.2000.014.

Eren, M., Tasli, K. & Tol, N. 2002: Sedimentology of Liassic carbonates (Pirencik Tepe measured section) in the Aydincik (Içel) area, southern Turkey. J. Asian Earth Sci., 20: 791-801.

Fischer, A.G. 1964: The Lofer cyclothems of the Alpine Triassic. In: Merriam, D.F. (ed.): Symposium on cyclic sedimentation. Kansas Geol. Surv. Bull., 169: 107-146.

Flügel, E. 2004: Microfacies of carbonate rocks: Analysis, interpretation and application. Springer-Verlag, Berlin Heidelberg, New York: 984 p.

Fraser, N.M., Bottjer, D.J. & Fischer, A.G. 2004: Dissecting "lithiotis" bivalves: Implications for the Early Jurassic reef eclipse. Palaios, 19: 51-67.

Fugagnoli, A. 2004: Trophic regimes of benthic foraminiferal assemblages in Lower Jurassic shallow water carbonates from northeastern Italy (Calcari Grigi, Trento Platform, Venetia Prealps). Palaeogeogr., palaeoclimatol., palaeoecol., 205: 111-130.

Gale, L. 2012: Rhaetian foraminiferal assemblage from the Dachstein Limestone of Mt. Begunjščica (Košuta Unit, eastern Southern Alps). Geologija, 55/1: 17-44, doi:10.5474/geologija.2012.002.

Gale, L. 2014: Lower Jurassic foraminiferal biostratigraphy of Podpeč Limestone (External Dinarides, Slovenia). Geologija, 57/2: 119-146, doi:10.5474/geologija.2014.011.

Gale, L. 2015: Microfacies characteristics of the Lower Jurassic lithiotid limestone from northern Adriatic Carbonate Platform (central Slovenia). Geologija, 58/2: 121-138, doi:10.5474/geologija.2015.010.

Gale, L., Kolar-Jurkovšek, T., Šmuc, A. & Rožič, B. 2012: Integrated Rhaetian foraminiferal and conodont biostratigraphy from the Slovenian Basin, eastern Southern Alps. Swiss J. Geosci., 105/3: 435-462, doi:10.1007/s00015-012-0117-1.

Galli, M.T., Jadoul, F., Bernasconi, S.M. & Weissert, H. 2005: Anomalies in global carbon cycling and extinction at the Triassic/Jurassic boundary: evidence from a marine C-isotope record. Palaeogeogr., palaeoclimatol., palaeoecol., 216: 203-214, doi:10.1016/j.palaeo.2004.11.009.

Greene, S.E., Martindale, R.C., Ritterbush, K.A., Bottjer, D.J., Corsetti, F.A. & Berelson, W.M. 2012: Recognising ocean acidification in deep time: An evaluation of the evidence for acidification across the Triassic-Jurassic boundary. Earth-Sci. Rev., 113/1-2: 72-93, doi:10.1016/j.earscirev.2012.03.009.

Haas, J., Lobitzer, H. & Monostori, M. 2007: Characteristics of the Lofer cyclicity in the type locality of the Dachstein Limestone (Dachstein Plateau, Austria). Facies, 53/1: 113-126, doi: 10.1007/s10347-006-0087-8.

Hallam, A. 2001: A review of the broad pattern of Jurassic sea-level changes and their possible causes in the light of current knowledge. Palaeogeogr., palaeoclimatol., palaeoecol., 167: 23-37, doi:/10.1016/S0031-0182(00)00229-7.

Hallock, P. 1988: Diversification in algal symbiont-bearing foraminifera: a response to oligotrophy? Rev. Paléobiol., spec. vol. 2 (Benthos, 86): 789-797.

Hammer, Ø. & Harper, D.A.T. 2006: Paleontological data analysis. Blackwell Publishing: 351 p.

Haq, B.U., Hardenbol, J. & Vail, P.R. 1988: Mesozoic and Cenozoic chronostratigraphy and cycles of sea-level change. In: Wilgus, C.K., Hastings, B.S., Posamentier, H., Wagoner, J.V., Ross, C.A. & Kendall, C.G.St.C. (eds.): Sea-Level Changes- An Integrated Approach. SEPM Spec. Publ., 42: 71-108.

Hautmann, M., Benton, M.J. & Tomašových, A. 2008: Catastrophic ocean acidification at the Triassic-Jurassic boundary. N. Jb. Geol. Paläont. Abh., 249: 119-127, doi:https://doi.org/10.1127/0077-7749/2008/0249-0119

Hottinger, L. 1996: The fossil record of the foraminifera, a succession of global community maturation (GCM) cycles, or: How to survive global disruptive events in Earth history. In: Drobne, K., Goričan, Š. & Kotnik, B. (eds.): The role of impact processes in the geological and biological evolution of planet Earth. Scientific Research Centre SAZU, Ljubljana: 35.

Hottinger, L. 2014: Paleogene larger rotaliid foraminifera from the western and central Neotethys doi:10.1007/978-3-319-02853-8. Springer: 196 p.

Kabal, Y. & Tasli, K. 2003: Biostratigraphy of the Lower Jurassic carbonate from the Aydincik area (Central Taurides, S. Turkey) and morphological analysis of *Lituolipora termieri* (Hottinger, 1967). J. Foram. Res., 33: 338-351.

Kiessling, W., Aberhan, M., Brenneis, B. & Wagner, P.J. 2007: Extinction trajectories of benthic organisms across the Triassic-Jurassic boundary. Palaeogeogr., palaeoclimatol., palaeoecol., 244: 201-222, doi:http://dx.doi.org/10.1016/j.palaeo.2006.06.029

Kiessling, W., Roniewicz, E., Villier, L., Léonide, P. & Struck, U. 2009: An Early Hettangian coral reef in southern France: Implications for the end-Triassic reef crisis. Palaios, 24: 657–671, doi:http://dx.doi.org/10.2110/palo.2009.p09-030r

Kresnik, T. 2016: Sedimentological and micropaleontological analysis of Toarcian limestones in External Dinarides, Slovenia. MSc Thesis. Faculty of Natural Sciences and Engineering, Department of Geology, Ljubljana: 47 p. (in Slovenian with English abstract).

Mancinelli, A., Chiocchini, M., Chiocchini, R.A. & Romano, A. 2005: Biostratigraphy of Upper Triassic-Lower Jurassic carbonate platform sediments of the central-southern Apennines (Italy). Riv. Ital. Paleont. Strat., 111: 271-283, doi:http://dx.doi.org/10.13130/2039-4942/6314.

Martinuš, M., Bucković, D. & Kukoć, D. 2012: Discontinuity surfaces recorded in shallow-marine platform carbonates: an example from the Early Jurassic of the Velebit Mt. (Croatia). Facies, 58: 649-669, doi:10.1007/s10347-011-0288-7.

Miler, M. & Pavšič, J. 2008: Triassic and Jurassic beds in Krim Mountain area (Slovenija). Geologija, 51/1: 87-99, doi:10.5474/geologija.2008.010.

Miler, M., Pavšič, J. & Dolenec, M. 2007: Determination of T/J boundary by $\delta^{13}C$ and $\delta^{18}O$ stable isotope analysis (Krim Mountain, Slovenia). Mater. Geoenvir., 54: 189-202.

Ogg, J.G., Hinnov, L.A. & Huang, C. 2012: Chapter 26 – Jurassic. In: Gradstein, F.M., Ogg, J.G., Schmitz, M.D. & Ogg, G.M. (eds.): The geologic time scale. Elsevier BV: 731-791.

Ogorelec, B. 2009: Spodnje jurske plasti v Preserju pri Borovnici. Geologija, 52/2: 193-204, doi:10.5474/geologija.2009.019.

Ogorelec, B. & Rothe, P. 1993: Mikrofazies, Diagenese und Geochemie des Dachsteinkalkes und Hauptdolomits in Süd-West-Slowenien. Geologija, 35: 81-181, doi:10.5474/geologija.1992.005.

Payne, J.L., Summers, B., Rego, B.L., Altiner, D., Wei, J., Yu, M. & Lehrmann, D.J. 2011: Early and Middle Triassic trends in diversity, evenness, and size of foraminifers on a carbonate platform in south China: implications for tempo and mode of biotic recovery from the end-Permian mass extinction. Paleobiology, 37: 409-425.

Placer, L. 1999: Contribution to the macrotectonic subdivision of the border region between Southern Alps and External Dinarides. Geologija, 41: 223-255, doi:10.5474/geologija.1998.013.

Placer, L. 2008: Principles of the tectonic subdivision of Slovenia. Geologija, 51/2: 205-217, doi:10.5474/geologija.2008.021.

Pleničar, M. 1970: Explanatory book for Sheet Postojna, L 33-77, Basic Geological Map SFRY 1 : 100.000. Federal Geological Survey, Beograd: 62 p.

Pomoni-Papaioannou, F. & Kostopoulou, V. 2008: Microfacies and cycle stacking in Liassic peritidal carbonate platform strata, Gavrovo-Tripolitza platform, Peloponnesus, Greece. Facies, 54/3: 417-431 doi:10.1007/s10347-008-0142-8.

Posenato, R. & Avanzini, M. 2006: "Lithiotis" beds of the Rotzo Formation (Calcari Grigi Group, Lower Jurassic) from Albaredo (Rovereto, Trento). Studi Trent. Sci. Natur.- Acta Geol., 81: 23-28.

Posenato, R. & Masetti, D. 2012: Environmental control and dynamics of Lower Jurassic bivalve build-ups in the Trento Platform (Southern Alps, Italy). Palaeogeogr., paleoclimatol., palaeoecol., 361-362: 1-13, doi:http://dx.doi.org/10.1016/j.palaeo.2012.07.001.

Rego, B.L., Wang, S.C., Altiner, D. & Payne, J.L. 2012: Within- and among-genus components of size evolution during mass extinction, recovery, and background intervals: a case study of Late Permian through Late Triassic foraminifera. Paleobiology, 38/4: 627-643, doi:https://doi.org/10.1666/11040.1.

Septfontaine, M. 1986: Milieux de dépôt et foraminifères (Lituolidés) de la plate-forme carbonatée du Lias moyen du Maroc. Rev. Micropal., 28: 265-289.

Stampfli, G.M. & Kozur, H.W. 2006: Europe from the Variscan to Alpine cycles. In: Gee, D.G. & Stephenson, R.A. (eds.): European lithosphere dynamics. Geol. Soc. Mem., 32: 57-82.

Stampfli, G.M. & Mosar, J. 1999: The making and becoming of Apulia. Mem. Sci. Geol., 51: 141-154.

Tari, V. 2002: Evolution of the northern and western Dinarides: a tectonostratigraphic approach. EGU Stephan Mueller Spec. Publ. Ser. (European Geosci. Union), 1: 223-236.

Tunaboylu, B.C., Altiner, D., Isintek, I. & Demirci, D. 2014: Foraminiferal biostratigraphy and sequence stratigraphy of peritidal carbonates at the Triassic-Jurassic boundary (Karaburun Peninsula, Western Turkey). J. Asian Earth Sci., 90: 61-76, http://dx.doi.org/10.1016/j.jseaes.2014.04.015.

Velić, I. 2007: Stratigraphy and palaeobiogeography of Mesozoic benthic Foraminifera of the Karst Dinarides (SE Europe). Geol. Croat., 60: 1-113.

Vlahović, I., Tišljar, J., Velić, I. & Matičec, D. 2002: The Karst Dinarides are composed of relics of a single Mesozoic platform: Facts and consequences. Geol. Croat., 55: 171-183.

Vlahović, I., Tišljar, J., Velić, I. & Matičec, D. 2005: Evolution of the Adriatic Carbonate Platform: Palaeogeography, main events and depositional dynamics. Palaeogeogr., palaeoclimatol., palaeoecol., 220: 333-360, doi:http://dx.doi.org/10.1016/j.palaeo.2005.01.011.

Vrabec, M. & Fodor, L. 2006: Late Cenozoic tectonics of Slovenia: structural styles at the Northeastern corner of the Adriatic microplate. In: Pinter, N., Grenerczy, G., Weber, J., Stein, S. & Medek, D. (eds.): The Adria microplate: GPS geodesy, tectonics and hazards. NATO Sci. Ser., IV, Earth Environ. Sci., 61: 151-168, doi:10.1007/1-4020-4235-3_10.

Wilmsen, M. & Neuweiler, F. 2008: Biosedimentology of the Early Jurassic post-extinction carbonate depositional system, central High Atlas rift basin, Morocco. Sedimentology, 55/4: 773-807, doi:10.1111/j.1365-3091.2007.00921.x.

Zambetakis-Lekkas, A., Pomoni-Papaioannou, F. & Alexopoulos, A. 1996: Biostratigraphy and sedimentology of Liassic carbonate sediments of Tripolitza platform in central Crete. Rev. Paléob., 15: 393-399.

GEOLOGIJA *60/1*, 117-128, Ljubljana 2017
https://doi.org/10.5474/geologija.2017.009

Mineral Deposits of Public Importance (MDoPI) in Slovenia

Nahajališča mineralnih surovin javnega pomena v Sloveniji

Duška ROKAVEC & Kim MEZGA

Geological Survey of Slovenia, Dimičeva ulica 14, SI-1000 Ljubljana, Slovenia;
e-mails: duska.rokavec@geo-zs.si; kim.mezga@geo-zs.si;

Prejeto / Received 15. 3. 2017; Sprejeto / Accepted 25. 5. 2017; Objavljeno na spletu / Published online 9.6.2017

Key words: mineral deposits of public importance (MDoPI), safeguarding mineral deposits, spatial planning, MINATURA2020

Ključne besede: mineralne surovine javnega pomena, varovanje nahajališč mineralnih surovin, prostorsko načrtovanje, MINATURA2020

Abstract

The second pillar of the "Raw materials initiative – meeting our critical needs for growth and jobs in Europe" praises the intention of safeguarding mineral deposits from sterilisation. In the near future, each Member State may protect access to mineral deposits of public importance (MDoPI) in accordance with its national legislation framework. Every Member State should identify its own mineral deposits of public importance to be incorporated into spatial plans. A list of suggested MDoPIs has been created for Slovenia in terms of safeguarding the access to deposits and sustainable mineral supply in the future. The survey of potential MDoPIs is described, and a map of suggested mineral areas is created. 30 areas/deposits have been selected and designated on the national level. On the local/regional level, up to 50 extraction sites were suggested as aggregates supply centres (quarries of crushed stones and gravel pits). Less than 0.5 % of the national territory might be dedicated to future mineral safeguarding. This paper presents the proposed list of potential safeguarded areas of MDoPIs in Slovenia and the MDoPIs map. The list is not closed or finally accomplished, but it is a dynamic system. It will be adopted referring to new geological research results as well as social needs. Nineteen countries are participating in the MINATURA2020 project (Horizon2020 program), and seven of them were selected as case studies (United Kingdom, Italy, Sweden, Portugal, Hungary, Poland, and Slovenia) regarding the differences in the territorial size, types of mineral endowment, and national mineral policies. The project provides an opportunity to engage with the issue and begin the safeguarding process on the national level.

Izvleček

Namera Evropske unije v srednjeročnem obdobju je zavarovati svoja nahajališča mineralnih surovin v skladu z drugim stebrom »Pobude za surovine – zagotavljanje preskrbe z nujno potrebnimi surovinami za rast in delovna mesta v Evropi«. Vsaka država članica bo v prihodnje v skladu s svojo državno zakonodajo zavarovala dostop do nahajališč mineralnih surovin javnega pomena (ang. mineral deposits of public importance - MDoPI). Zato je naloga nacionalnih geoloških zavodov, da strokovno določijo nahajališča mineralnih surovin, ki naj bodo v prihodnje ustrezno opredeljena v prostorskih načrtih in varovana pred poselitvijo. V ta namen smo pripravili nabor slovenskih nahajališč, ki bi jih bilo v prihodnje smotrno varovati za zagotavljanje trajnostne oskrbe z mineralnimi surovinami. V raziskavi smo predlagana nahajališča opredelili, opisali in utemeljili. Na državni ravni smo izbrali 30 nahajališč nekovinskih mineralnih surovin javnega pomena in na regionalni ravni približno 50 centrov preskrbe s kamenimi agregati (tehnični kamen, prod in pesek). Skupna površina ozemlja, ki naj bi se v prihodnosti zavarovala, je glede na predlagan nabor nahajališč, manjša od 0,5 % državnega ozemlja. V prispevku je predstavljen predlog nabora nahajališč s karto predlaganih nahajališč mineralnih surovin javnega pomena. Predlog nahajališč ni dokončen, temveč je dinamičen in se bo, glede na nove rezultate geoloških raziskav in potrebe družbe, skozi čas dopolnjeval. V projektu MINATURA2020 (program Obzorje 2020) sodeluje 19 držav. Sedem držav je bilo izbranih kot testna območja (Velika Britanija, Italija, Švedska, Portugalska, Madžarska, Poljska in Slovenija) glede na različne velikosti državnega ozemlja, raznovrstnost mineralnih surovin ter nacionalno zakonodajo. Projekt ponuja priložnost, da se soočimo s problematiko, in pričnemo s procesom varovanja nahajališč mineralnih surovin na državni ravni.

Introduction

In recent decades, the importance of minerals has increased: prices have risen, as has mineral consumption, due to the increased needs/demands of new growing economies in China, Brazil, etc. (Shields & Šolar, 2004; Šolar, 2015). Insufficient production within the EU and increases of imported raw materials from other parts of the world are reflected in supply shortages. Different land uses, e.g. nature preservation, infrastructure building, water protection, etc., are sharing preferential treatment, while mineral deposits (MD) are often neglected in land-use planning. In general, the consumption of minerals is increasing, and available areas for potential mineral extraction are running short; therefore, continuous reduction of available land for exploration and mineral extraction became a risk.

In November 2008, the European Commission (EC) launched the "Raw materials initiative – meeting our critical needs for growth and jobs in Europe" (RMI) which established an integrated strategy to respond to the different challenges related to access to non-energy and non-agricultural raw materials. The RMI is based on three pillars: (1) *Ensuring the fair and sustainable supply of raw materials from international markets, promoting international cooperation with developed and developing countries*; (2) *Fostering sustainable supply of raw materials from European sources*; and (3) *Reducing consumption of primary raw materials by increasing resource efficiency and promoting recycling* (European Commission, 2008). By identifying mineral deposits of public importance and securing their access, we are also supporting the first pillar.

The Raw materials initiative (European Commission, 2008) and the European Innovation Partnership's (EIP) Strategic Implementation Plan (SIP) (Internet 1; Internet 2) highlight access to mineral deposits as a common EU challenge that also targets Member States. Therefore, national Geo-Surveys endeavours to designate mineral deposits of public importance (MDoPI) reflect the above-mentioned initiatives' aims. Geo-Surveys experts' work and activities contribute to better communication between the mineral sector and the land use planning sector. Current land use planning fails to address mineral potential areas and temporary land use for mineral extraction is neglected as well (e.g. surface extraction of clays) (European Commission, 2000). Constructive dialogue amongst different land users and planners should be straightened.

Recent EU statistics show that every newborn infant will need a lifetime supply of 300 kg of lead, 280 kg of zinc, 560 kg of copper, 1,350 kg of aluminium, 12,200 kg of iron, 9,950 kg of clays, 1,500 kg of salt and 448,000 kg of stone, sand, gravel, and cement (Internet 3). Therefore, the exploitation of minerals in Europe is an indispensable activity and must ensure that the present and future needs of the European society can be met. This requires sufficient access to mineral deposits (University of leoben, 2004). Prospective mineral deposits (taking into account abandoned mines and historical mining sites) should be considered with respect to and in balance with other land uses, such as agriculture, forestry, natural preservation, building, and infrastructure. Furthermore, the access to mineral deposits also needs to meet public demands.

The importance of the minerals supply for the benefit of society and the necessity to develop planning policies that respect the highest environmental and social criteria of sustainability should be recognised. Some deposits of metals, industrial minerals and construction materials (energy minerals are mostly treated properly all over Europe) should be considered of "public importance". This is where information demonstrates that sustainable exploitation could provide economic, social, or other benefits to the EU or the Member States or a specific region/municipality (MINATURA2020 Project Consortium, 2014).

Parallel with geological definitions, a harmonised European regulatory framework for sustainable access and mineral supply should be developed. It will include the "sustainability principle" for exploration and mineral extraction (Shields & Šolar, 2004; Šolar, 2015). The concept of mineral safeguarding should be incorporated.

Geo-Surveys' task is to identify, explore and properly designate MDoPIs on the national and local level that should be safeguarded by incorporation into spatial plans. Therefore, the establishment and maintenance of INSPIRE compliant geo-referenced Mineral Information System is a vital task of every national Geo-Survey.

Slovenia belongs to the group of the countries which apply a safeguarding regulative concept while mineral deposits are included into land use plans only through a permit process. This means that only areas with mining rights are safeguarded. There is no open door for “potential deposits” that still have not been granted mining rights. According to the Slovenian Mining Act (Official gazette RS, 2014), only energy raw materials can be of strategic importance. Currently, Slovenia is preparing a new National Mining Strategy, which is an excellent opportunity to improve the current mineral status in terms of safeguarding minerals and their deposits on the national level.

Materials and methods

Despite its relatively small national territory, Slovenia has numerous mineral deposits. More than 200 extraction sites (almost all of them are open pits and quarries) with mining rights (under concessions) are currently active, with 26 different mineral resources (construction materials, industrial minerals, and energy resources). Slovenia also has around 200 sites of metallic mineral deposits, and occurrences and a few dozen are closed or abandoned mines operations. Today, all metal mines are closed after a long mining period, but there are still ore reserves which could be exploited in the future. Nowadays, extraction of mineral resources in Slovenia is focused on construction, for the industry of building materials, and a few industrial minerals. Annual production of construction materials and industrial minerals is around 15 million tons (aggregates, dimension stone, clays, quartz sand, etc.) not taking into account energy minerals (lignite and hydrocarbon production). Estimation of reserves and resources within mining areas is around 840 million tons. Non-metal mineral resources are used in the construction, ceramic, brick, metallurgy and metalworking industries, for the environment and water purification, glass manufacturing, farming, food industry, etc. (Senegačnik et al., 2016; Senegačnik & Štih, 2016). Mining activities in Slovenia are under the jurisdiction of the Ministry of Infrastructure, precisely under its mining sector.

Natura 2000 (Official gazette RS, 2004b) covers more than 37 % of national territory, not including 12.6 % of protected areas (1 national park, 3 regional parks, 45 landscape parks, 1 strict nature reserve and 54 nature reserves, and 1,163 natural monuments) in Slovenia (Internet 4-7). In Slovenian practice, few natural resources are properly safeguarded (e.g. water, forests and agricultural land), while mineral resources, although non-renewable, are rather neglected. Therefore, an adequate regulatory or guidance framework similar to Natura 2000 should be established in order to equally protect mineral resources as, for example, Natura 2000 sites across the EU.

Slovenians’ shallow geological structures are relatively well-known. Based on extended knowledge on lithological composition and on mineral deposits, the Geological Survey of Slovenia (GeoZS) has established a Mineral Information System on the national level. The Geo-Surveys across the EU also identify their MDoPIs. In Slovenia, industrial minerals and construction minerals/aggregates have been put on the list at this stage. The geological knowledge of deep structures is not sufficient due to lack of deep exploration. There is a possibility of raw material potential in deeper structures. Even some abandoned and closed metal mines could be important in the future.

For the designation of MDoPIs, two different levels were taken into account: the national and local/regional levels. On the national level, a few industrial mineral deposits are selected and on the local/regional level some aggregates supply centres are suggested.

Slovenia is endowed with aggregates (crushed stone, sand and gravel) regarding its geological settings; however, there are many overlapping land use interests and protected areas (Natura 2000, water protection areas, etc.). Therefore, it is very important to define and place locations for aggregate extraction. Due to bulk production, negative environmental impacts also occur. These locations are most delicate to manage, and they are barely incorporated into spatial plans. Therefore, locations should be selected according to their environmental and nature protection requirements, also taking into account other land uses.

Detailed methodology description

Slovenia currently extracts/produces non-metals and energy resources. Since energy resources might be of strategic importance and therefore properly treated, our survey was focused on non-energy minerals (industrial minerals and aggregates). Slovenian MDoPIs were selected due to their uniqueness, rareness, and importance for existing industry or traditional housing use as construction material. Detailed methodology is presented for three cases for MDoPIs selection:

Case a) Dimension stone - limestone in Slovenian Karstic region (Table 1, No. 14-16):

Cretaceous limestone (Fig. 1a) as an autochthonous building material has played a crucial role in the Adriatic area. Massive and platy limestone, are both recognizable elements of the cultural landscape along the Adriatic karstic coast (Vesel, 1980; Jurkovšek et al., 2013; Novak, 2015). Blocks of limestone have been used for housing and as an ornamental stone, platy limestone also as roof tiling, for the construction of dry walls, shepherd cottages, and similar structures. Besides being an element of cultural heritage, it is also important for natural heritage, with often rich and diverse fossil fauna e.g. well-preserved vertebrate fossils. For centuries excavated in regional quarries, few of them are also located in backyards or in small delves near villages. The white limestone blocks with specific polished surfaces were also used in the neighbour trans-border area (e.g. in Italy) as a globally known building (dimension) stone.

Case b) Ilirska Bistrica clay deposit in Southwest region (Table 1, No. 1):

The largest clay deposit in Slovenia is developed on Eocene flysch of Reka synclinal (Fig. 1b). The thickest layer of Plio-Pleistocene clay in Slovenia, situated in 3 km long synclinal, was explored by drilling. This, over 60 m thick, layer consists rather of homogenous clay that had been used as brick and ball clay (Jerše et al., 1986; Jerše, 1990; Rokavec, 2014). The mineral composition is muscovite-illite-montmorillonite, with particle size 25-53 % of clay particles under 2 µm. In the 20^{th} century, the region was producing brick; nowadays, no industry uses clay, and the huge resources and reserves remain intact, although Slovenia imports this type of clay.

Case c) Chert in Mirna Valley in Central – South Slovenia (Table 1, No. 22):

Chert outcrops occur in the Mirna Valley (locations Jersovec, Ogorelke, and Gabrovka) as well as in several smaller deposits (Fig. 1c). The Mirna chert deposit is unique in the country (Šolar, 1994; Skaberne, 2003). Primary chert occurs in Triassic limestones and dolomites, and secondary chert, which is product of weathering processes, occurs in breccias with a clay matrix. The entire production of chert is being exported. This mineral commodity of good quality is used for production of refractories materials.

The source of data and information for this survey were the following references:

- the Mining registry book (MZI, 2015, 2017),
- periodical bulletin "Mineralne surovine" (Senegačnik et al., 2016),
- "Bulletin Mineral resources in Slovenia" (Senegačnik & Štih, 2016),
- papers and monographies (Dimkovski & Rokavec, 2001; Bavec et al., 2009; Jurkovšek et al., 2013; Rokavec, 2014; Miletić & Rokavec, 2015; Rman & Novak, 2016; Rokavec & Miletić, 2016; Rokavec & Mezga, 2017),
- expert reports (Jerše et al., 1986; Šolar, 1994; Skaberne, 2003; Pleničar et al., 2009; Novak, 2015), and other.

Results and discussion

A list of proposed MDoPIs has been created for Slovenia (Table 1 and 2) along with a MDoPI map (Figs. 2-4) for safeguarding the access to deposits and mineral sustainable supply in the future. On the national level non-metal deposits were designated due to their uniqueness, rareness and importance for existing industry or tra-

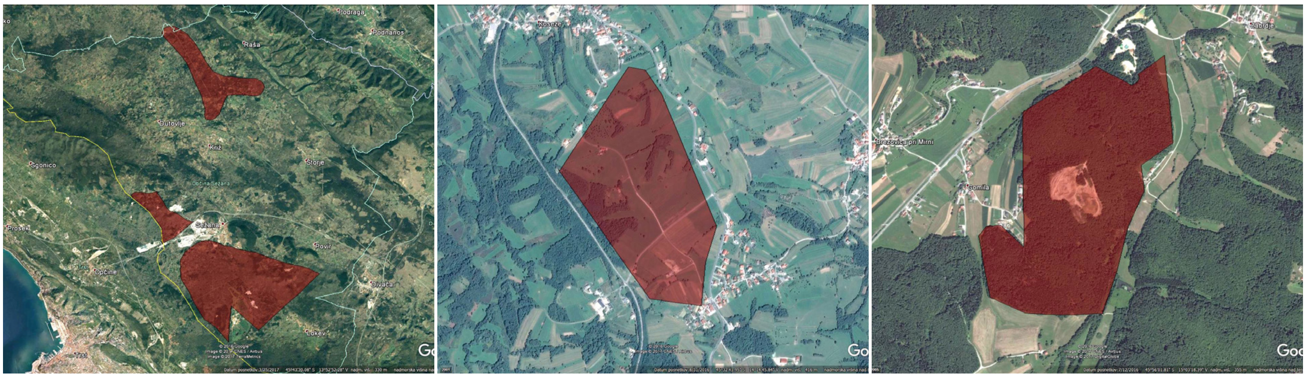

Fig. 1. Examples of three suggested MDoPIs: (a) dimension stone – limestone deposit in Karst, (b) clay deposit in Ilirska Bistrica and (c) chert in Mirna Valley, presented on the Google Earth (2017).

ditional housing use as construction material. On the local/regional level aggregates supply centres are suggested, optimally 1–5 locations per every statistical region. Those locations will serve as regional centres for aggregates supply. National spatial planning strategy (Official gazette RS, 2004a) and National mineral resource management programme (GeoZS, 2009) recommend a few bigger regional supply centres instead of numerous small ones.

Table 1. List of potential areas of mineral deposits.

#	Suggested areas of MD (province)	MDoPI	Age	Estimated surface of MDoPI (km2)	Type of minerals (mineral commodity)	Arguments for MDoPI selection	Existing protected areas*
1	Ilirska Bistrica	Koseze	Pl	0.53	clays (brick and ball clay)	base for existing and future brick and roof tile industry	N2000, EIA
2	Vipavska dolina / Valley	Okroglica	Ps	1.23			N2000, EIA
3		Renče	Ps	0.06			
4		Dolgi hrib	Ps	0.11			
5		Tomaški hrib	Ps	0.07			
6	Savinjska dolina / Valley	Ljubečna	Pl-Q	6.95			N2000, EIA
7		Hom		1.01			/
8	Pomurje area	Boreci	Ps	0.43			N2000, EIA, VNF, WPA (mun.)
9	Podravje area	Hardeška šuma	Ps	1.55			/
10	Jezersko	Jezersko	Pl-Q	0.005	dimension stone- travertine	unique	N2000, EIA, VNF (travertine)
11	Pohorje	Cezlak	Tc	0.24	dimension stone- tonalite and cizlakite	unique	N2000, EIA, VNF
12	Southern Pohorje	Vitanje surrounding	Tc	6.73	ornamental stone - schist gneiss	unique, for traditional buildings	N2000, WPA (mun.), EIA, VNF
13	Hotavlje	Hotavlje	T	0.20	dimension stone- limestone	unique	/
14	Kras	Lipica	K	19.50	dimension stone- limestone	used in natural heritage buildings in karstic area	N2000, EIA, VNF
		Debela Griža					
15		Doline	K	2.99			N2000, EIA
16		Tomaj	K	6.96			N2000, EIA, VNF, WPA (mun.)
		Kazlje					
		Kopriva					
17	Primorska region	Milje	Ec	0.14	dimension stone - flysch sandstone	typical for region	/
18	Globoko and Bizeljsko Region	Globoko and Bizeljsko Hills	Pl	19.10	quartz sand, clay	rare	N2000, EIA, VNF
19	North-Eastern Slovenia	Puconci surrounding	Pl, Ps	1.83	quartz sand	rare	N2000, EIA, VNF, LP
20	Dolenjska Region	Raka-Ravno	Pl	0.98			N2000, EIA, VNF
21	Moravče synclinal	Moravče	Mc	10.3			N2000, EIA, VNF, WPA (mun.)
22	Mirna Valley	Jersovec and other	T3	0.75	chert	unique	VNF
23	Northern Soča Valley	Srpenica	Ps	0.15	chalk	unique	N2000, EIA, VNF
24	Stahovica	Stahovica	T3	0.84	calcite	rare	N2000, EIA, VNF (calcite), WPA (mun.)
25	Zaloška Gorica	Zaloška Gorica	Ol	0.94	bentonite, tuff	unique	/
26	Solkan	Solkan	K	0.36	limestone for cement industry	supports existing lime and cement industry	/
27	Kresnice	Kresnice	T	1.65	limestone for lime industry	supports existing lime and cement industry	WPA (mun.)
28	Anhovo	Anhovo deposits	Pc	2.72	raw material for cement industry	supports existing lime and cement industry	VNF
29	Sečovlje	Sečovlje saltworks	rec.	6.39	sea salt	traditional salt-works, natural heritage	N2000, EIA, VNF (halite), LP
30	Strunjan	Strunjan saltworks	rec.	0.19			N2000, EIA, VNF (halite), LP

*MD – mineral deposit; *N2000 = Natura 2000, EIA = Ecologically important area, VNF = Valuable natural features, LP = Landscape park, WPA = Water protection area, nat. = national level, mun. = municipal level; rec. – recent.*

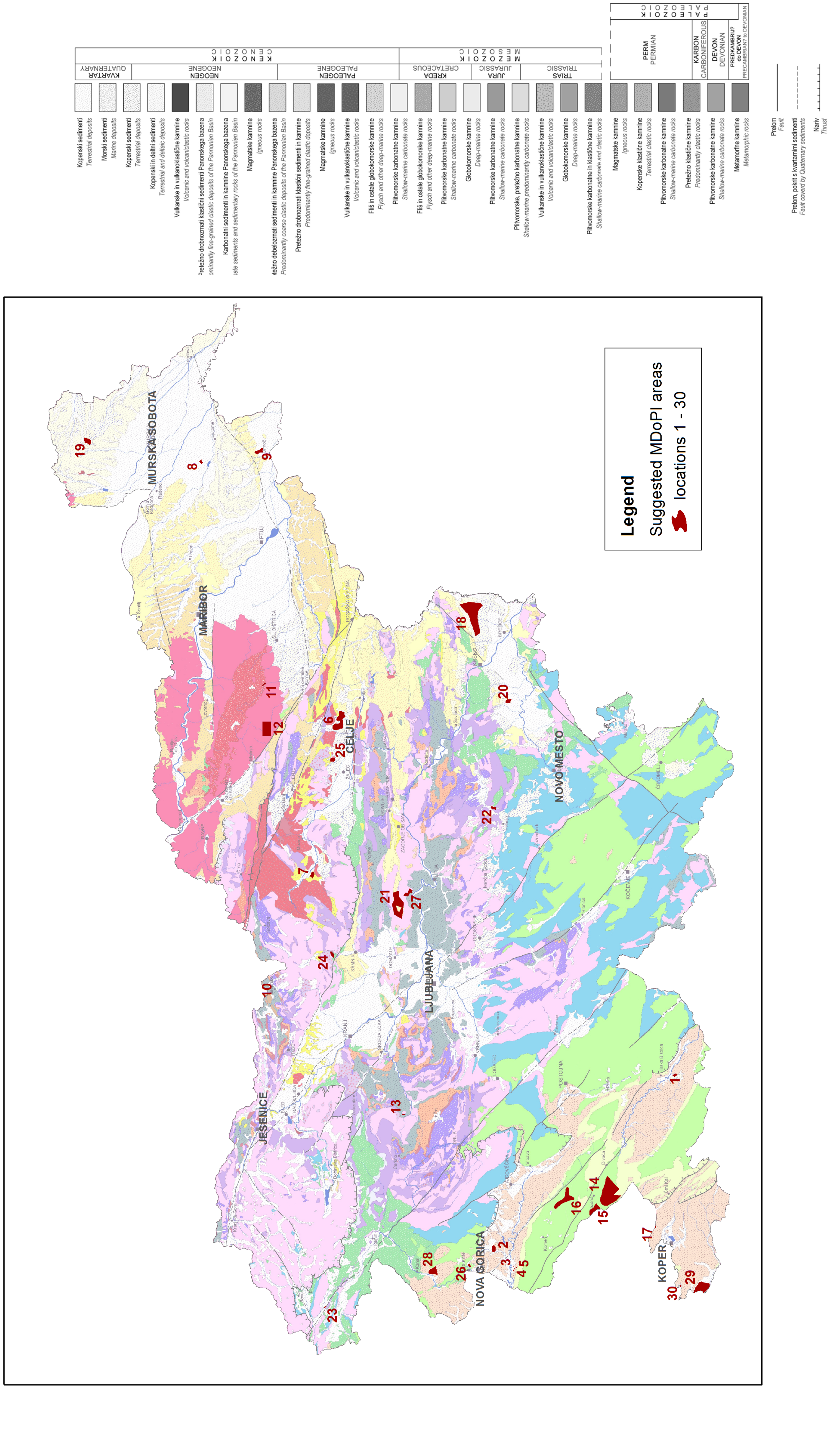

Fig. 2. Suggested MDoPI areas in Slovenia presented on the Geological Map of Slovenia 1:1.000.000 (Bavec et al., 2013).

(a) National level (non-metals /industrial minerals)

On the national level 30 areas of non-metal deposits were designated, mainly clays, dimension stone, quartz sand, chert, chalk, calcite, bentonite, limestone for industrial purpose and others (Table 1, Fig. 2). Due to geological settings, these deposits should be treated as safeguarding priority in land use plans.

The total surface of suggested MDoPI areas in Slovenia is ca. 95 km², which is approximately 0.47 % of state territory, not including aggregates, which also need to be safeguarded. The suggested MDoPIs are mostly located outside urbanised areas, often close to the extraction areas where detailed research has been conducted in response to industry demands.

The designation of MDoPIs has been a specific issue in our work due to various geological compositions, different mineral deposits characteristics and their extension. Two different principles were used for MDoPI designation:

a. The entire geological formation was recognised as a unified MDoPI area (e.g. Karst region) as a carbonaceous (limestone) platform which has an applicable value as an autochthonous building material. The entire designated area is not meant to be safeguarded, but only the access to particular deposits should be secured.
b. Small mineral sites (occurring locally) were recognised due to their limited reserves (e.g. Mirna chert deposits).

(b) Local/regional level (aggregates)

On the local/regional level, one to five locations – aggregate supply centres per statistical region were considered. Up to 50 extraction localities for local/regional aggregates supplies are suggested (Fig. 4, Table 2).

MDoPIs on the national level are displayed as polygons (marked in red, Fig. 4) and aggregates supply centres on the regional level are displayed as points (marked in yellow, Fig. 4) in the ArcGIS (Esri, 2014). The shape file was transferred to an interactive map on Google Earth application (Google Earth, 2017) for an overview of the locations and areas of potential MDoPIs.

The proposed list of MDoPIs and the borders of suggested mineral deposits are not final; the list is a dynamic system that should be adopted referring to new geological research results, as well as knowledge and social demands in the future. The proposed MDoPIs are overlapping mostly forest, agricultural or built-up areas (regarding their land use). In a few cases, they also extend into protected areas (e.g. Natura 2000, ecologically important areas, valuable natural features, landscape parks, etc.). Re-

Table 2. Suggested regional supply centres with aggregates.

No.	Region	Production in the region (tons/year)*	Number of appropriate location	Mineral resource (aggregates)
1.	Central-Slovenian region	2 236 722	5	crushed stone – limestone crushed stone – dolomite sand and gravel
2.	Coastal-Karstic region	1 612 710	3	crushed stone – limestone
3.	Drava region	1 868 529	4	sand and gravel
4.	Gorenjska region	794 148	3	sand and gravel crushed stone – dolomite and silicates (quartz keratophyre)
5.	Goriška region	157 974	1	crushed stone – limestone
6.	Koroška region	206 072	2	crushed stone – dolomite sand and gravel
7.	Notranjsko-karstic region	254 539	2	crushed stone – dolomite crushed stone – limestone
8.	Pomurje region	1 129 366	4	sand and gravel crushed stone – silicates
9.	Savinja region	1 386 377	3	crushed stone – limestone crushed stone – dolomite
10.	Southeastern Slovenia (including Bela Krajina, Kočevska and Dolenjska region)	527 675	4	crushed stone – dolomite
11.	Spodnjeposavska region	785 482	4	crushed stone – dolomite sand and gravel
12.	Zasavje region	92 388	1	crushed stone – dolomite

* (Senegačnik et al., 2016)

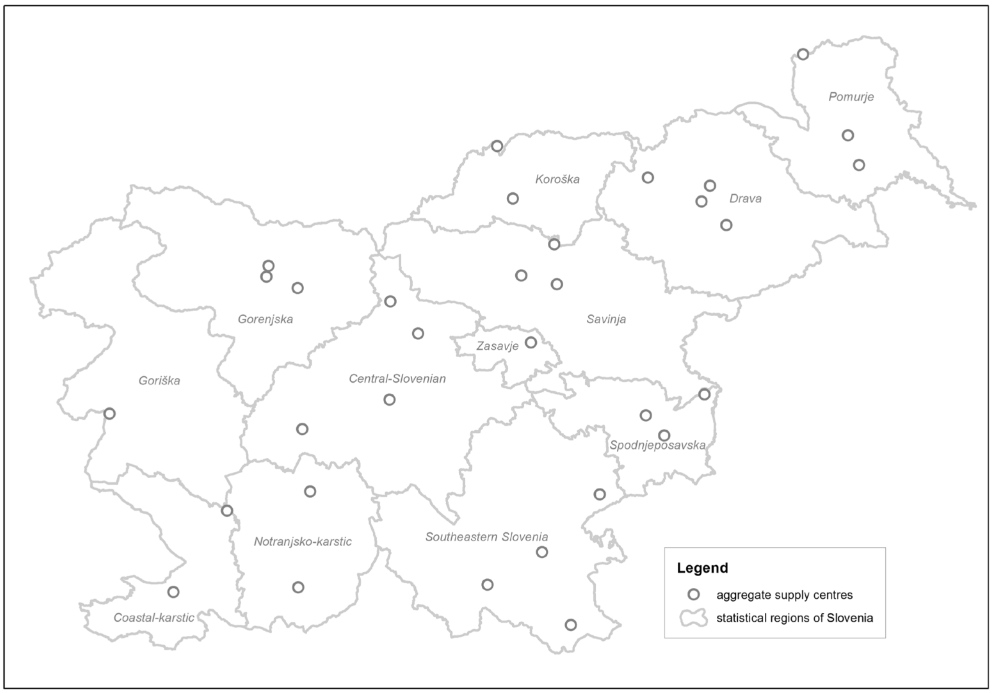

Fig. 3. Future network of aggregate supply centres on the regional level.

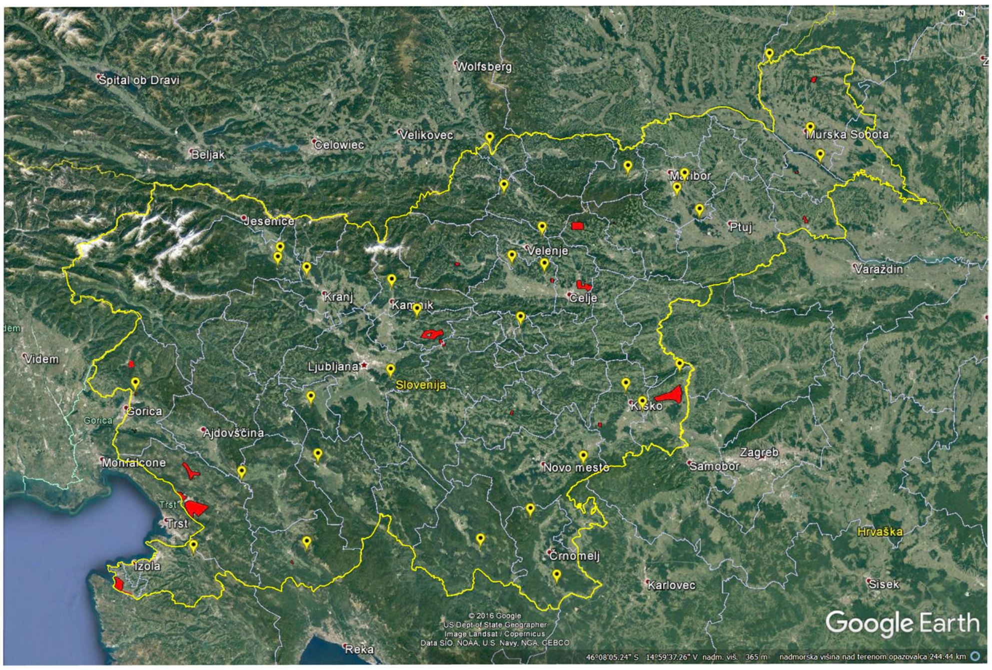

Fig. 4. Suggested MDoPIs in Slovenia displayed in Google Earth (2017; marked in red on the national level and marked in yellow on the local/regional level).

gardless of existing land use, the mineral deposits (at least those that are rare and unique) should be designated in spatial plans and, therefore, safeguarded for future generations. Geological settings/mineral deposits cannot be moved to another location, while most human activities can (e.g. industrial structures, agriculture, and housing). Therefore, Natura 2000 (Habitats Directive 92/43/EEC) does not exclude or even prohibit mineral exploration and extraction but sets certain limits (European Commission, 2010).

Good practices from other EU countries

Twenty-four partners from 19 countries participate in the project MINATURA2000 – "*Developing a concept for a European minerals deposit framework*" (MINATURA2020 Project Consortium, 2014; Internet 8). Some of them were selected as case-study countries, i.e. United Kingdom, Italy, Sweden, Slovenia, Portugal, Hungary, and Poland. These countries differ in territorial size, mineral endowment, and national mineral policies and have been surveyed as well in terms of designating their MDoPI (European Commission, 2000). Due to their territorial size only selected areas (e.g. provinces) have been examined in detailed. Metals, industrial minerals, and aggregate deposits have been suggested for future safeguarding regimes on different levels: national, regional, and local, depending on the national mineral policy and ownership of minerals (Table 3) (Rokavec et al., 2016a).

Italy
- Emilia Romagna Region: 11 deposits of aggregates (alluvial sands and gravels, coastal sands, sandstones and conglomerates, limestones, siliceous rocks).

Portugal
- Tungsten province (national level): 38 deposits of metal ores (W, Sn, Pb, Au, Mo, Ag).
- Rio Maior (local level): Mineral deposit of special Quartz kaolinite-rich sands (Special sands).

Hungary
- Borsot-Aubauj-Zemplen, Hajdu-Bihar, Heves, Szabolcs-Szatmar-Berek): 402 deposits of non-metals (sand, gravel, crushed stone, clay and perlite).

Sweden
- Norrbotten Country: 24 deposits of metal ores (Pb, Ag, Cu, Au, Fe) and non-metals (graphite, dolomite and limestone for industrial purpose, kaolin, magnesite, wollastonite, quartz).

United Kingdom
- South West England & South Wales: 40 deposits on shore (sand and gravel, crushed stone, dimension stones, ball cay, pottery clay, china clay, brick clay, slates, metals), 10 deposits offshore in Celtic and Irish seas (sand and gravel, undersea salt and potash, metals in seabed nodules, crust and extinct smokers).

Poland
- Dolnośląskie Province: 142 deposits with indicated and measured resources (copper-silver ore, nickel ore, barite and fluorite, bentonite, clays (brick, ceramic and fire clays), dimension stone, crushed stone, feldspar, gypsum and anhydrite, kaolin, magnesite, quartzite, aggregates (sand and gravel), sand for lime, sand for glass production.

Raising awareness of the importance of minerals

In order to strengthen the awareness of decision makers of the importance of minerals, EU countries are organising regional and national stakeholder consultations in 2016 and 2017. The aim is to promote the idea of safeguarding mineral deposits, to encourage transparent land use practices and, overall, to exchange experiences and views of different sectors dealing with mineral resources. In Slovenia, the first national stakeholder workshop was organised in February 2016 (Rokavec et al., 2016b) and the second one in January 2017 (Rokavec et al., 2017), both located in Ljubljana.

Table 3. List of potential safeguarded areas (MDoPI) – summary data by countries (SI-Slovenia, I-Italy, PT-Portugal, H-Hungary, S-Sweden, UK-United Kingdom and PL-Poland).

Country	Province	∑No. MDoPI (potential areas)	Level	Type of mineral endowment		
				metals	non-metals	aggregates
SI	Entire state territory	30	national		x	
		max 50	local/regional			x
I	Emilia Romagna Region	11	regional			x
PT	Tungsten province	38	national	x		
	Rio Maior	1	local		x	
H	Borsot-Aubauj-Zemplen, Hajdu-Bihar, Heves, Szabolcs-Szatmar-Berek	402	regional		x	x
S	Norrbotten country	24	national	x	x	
UK	South West England & South Wales (on shore)	40	regional	x	x	x
	South West England & South Wales (off-shore in Celtic and Irish seas)	10	regional	x		x
PL	Dolnośląskie Province	142		x	x	x

Conclusions

Mineral supply is an important condition for economic, social and technological development. Due to Europe's huge mineral consumption, it is highly dependent on the import of some mineral resources. Since the mineral supply is becoming a challenge, European industry has expressed the needs through the "Raw materials initiative". In order to ensure sustainable mineral supplies within the EU, it is of great importance to properly safeguard mineral deposits and foster sustainable mineral supply from European sources.

For the sustainable development of European society, the safeguarding of European mineral deposits is one of the key issues. The access to mineral deposits should be secured in order to encourage, firstly, their exploration and afterward, if viable, also their exploitation. It is important that current mineral extraction does not endanger the supply of future generations. The mineral deposits of public importance should be properly evaluated, taking into account the geological settings and economic viability of exploitation and permitted in accordance with land use and environmental requirements. Urbanisation, nature conservation, and other land use interests often impede the access to potential mineral deposits. Coordinated placement of mining areas with other land uses is challenging in order to avoid conflicts and meet social needs.

Slovenia is preparing the basis for a concept for defining and subsequently protecting mineral deposits of public importance (MDoPI). Different land uses, e.g. nature preservation, infrastructure building, water protection, etc., have preferential treatment, while mineral deposits are often neglected in spatial planning procedures. For this purpose, a list and a map of proposed MDoPIs were established for Slovenia. MDoPIs need to be identified, explored, and properly designated on the national and local levels to facilitate their incorporation into spatial plans. On the national level 30 deposits of non-metals have been designated (e.g. dimension stone, clay, chert, raw materials for cement and lime industry, bentonite, tuff, calcite, and quartz sand) in Slovenia. On the local/regional level, up to 50 extraction sites, optimally one to five locations per every statistical region were suggested as aggregate supply centres (crushed stone, sand and gravel). Less than 0.5 % of national territory is estimated to be under safeguarding regime in the future. The list is not final but dynamic and will be changed according to new geological research results and knowledge of deep geological structures, the market, land uses and other societal conditions. Furthermore, other EU countries, i.e. the United Kingdom, Italy, Sweden, Portugal, Hungary and Poland, are preparing their lists and methodologies for designation of their MDoPIs that should be safeguarded.

Although energy raw materials are of strategic importance (according to Slovenian Mining Act), there is a need to safeguard non-energy mineral resources as well. Slovenia is in a phase of adopting a new National Mining Strategy, which provides an opportunity to improve the current mineral status in terms of safeguarding mineral deposits on the national level.

Acknowledgements

This paper was prepared in the frame of MINATURA2020 project within the WP4 activity "Creating a list of potential protected areas at the case study level". This three-year project (February 2015–January 2018) is funded by the EU Horizon2020 research and innovation programme under grant agreement nº 642139. The project is a part of the thematic area: "H2020-SC5-2014: Growing a Low Carbon, Resource Efficient Economy with a Sustainable Supply of Raw Materials", under the call for proposals "SC5-13a-2014 - Mineral deposits of public importance". The authors would like to thank reviewers for their careful reading of the paper and their valuable comments and suggestions to improve the paper.

References

Bavec, M., Novak, M., Poljak, M. 2013: Geological Map of Slovenia in scale 1: 1.000.000. Geološki zavod Slovenije, Ljubljana.

Dimkovski, T. & Rokavec, D. 2001: Nahajališča nekovinskih mineralnih surovin v Sloveniji: površinski kopi (1. del) (in Slovene). Geološki zavod Slovenije, Ljubljana: 123 p.

Esri, 2014: ArcGIS Desktop: Release 10. Redlands, CA: Environmental Systems Research Institute.

European Commission, 2000: Promoting sustainable development in EU non-energy extractive industry. Communication from the Commission to the Council and the European Parliament, COM(2000) 265 final (3 May 2000), Brussels.

European Commission, 2008: The raw materials initiative – Meeting our critical needs for growth and jobs in Europe. Communication from the Commission to the Council and the European Parliament. COM(2008) 699 final (4 November 2008), Brussels.

European Commission, 2010: Non-energy mineral extraction and Natura 2000 (guidance document). Internet: http://ec.europa.eu/environment/nature/natura2000/management/docs/neei_n2000_guidance.pdf

GeoZS (Geološki zavod slovenije), 2009: National Mineral Resource Management Programme = Državni program gospodarjenja z mineralnimi surovinami (in Slovene). Geološki zavod Slovenije, Ljubljana: 59 p. Internet: http://www.energetika-portal.si/fileadmin/dokumenti/publikacije/dp_min_sur/dp_spl_nacrt.pdf (05. 01. 2017)

Google Earth, 2017: Google Earth application. Internet: https://www.google.com/earth/ (12. 06. 2016).

Habitats Directive 92/43/EEC: Council Directive 92/43/EEC of 21 May 1992 on the conservation of natural habitats and of wild fauna and flora.

Jerše, Z., Grad, K., Štern, J. & Mišič, M. 1986: Raziskave glin na območju Ilirske Bistrice (in Slovene). Geološki zavod Slovenije, Ljubljana: 21 p.

Jerše, Z. 1990: Pregled lastnosti gline pri Ilirski Bistrici (in Slovene). Geološki zavod Slovenije, Ljubljana: 5 p.

Jurkovšek, B., Cvetko Tešović, B. & Kolar-Jurkovšek, T. 2013: Geologija Krasa = Geology of Kras. Geological Survey of Slovenia, Ljubljana: 205 p.

MINATURA2020 Project Consortium, 2014: MINATURA2020 – Description of work: 188 p.

Miletič S. & Rokavec, D. 2015: Mineralne surovine javnega pomena - MINATURA2020. In: Rožič, B. (ed.): 22. posvetovanje slovenskih geologov, Geološki zbornik, 23: 118-122.

MZI (Ministrstvo za infrastrukturo), 2015: Mining registry book (cadastre and register) (in Slovene). Geološki zavod Slovenije, Ljubljana.

MZI (Ministrstvo za infrastrukturo), 2017: Mining registry book (web application) (in Slovene). Internet: https://ms.geo-zs.si/ (03. 03. 2017).

Novak, M. (ed.) 2015: Limestone as the common denominator of natural and cultural heritage along the karstified part of the Adriatic coast – RoofOfRock. Final thematic Report RoofOfRock. Internet: http://www.roofofrock.eu/publication/ (15.07.2016).

Official Gazette of the Republic of Slovenia, 2004a: Decree on Spatial order of Slovenia = Uredba o prostorskem redu Slovenije (ZPNačrt), Nos. 122/04, 33/07.

Official Gazette of the Republic of Slovenia, 2004b: Decree on special protection areas (Natura 2000 areas) = Uredba o posebnih varstvenih območjih (območjih Natura 2000), Nos. 49/04, 110/04, 59/07, 43/08, 8/12, 33/13, 35/13, 39/13 – Constitutional Court Decision 3/14 and 21/16).

Official Gazette of the Republic of Slovenia, 2014: Mining Act = Zakon o rudarstvu (ZRud-1), No. 14/14.

Pleničar, M., Ogorelec, B. & Novak, M. (eds.), 2009: Geologija Slovenije = The geology of Slovenia. Geološki zavod Slovenije, Ljubljana: 612 p.

Rman, N. & Novak, M. (eds.), 2016: Seventy geological wonders of Slovenia. Geological Survey of Slovenia, Ljubljana: 204 p.

Rokavec, D. 2014: Gline v Sloveniji (in Slovene). Geološki zavod Slovenije, Ljubljana: 95 p.

Rokavec, D. & Miletić, S. 2016: Projekt MINATURA2020 – o nahajališčih mineralnih surovin javnega pomena (in Slovene). Mineralne surovine v letu 2015, 12/1: 162-165.

Rokavec, D., Mezga, K. & Miletić, S. 2016a: List of potential protected areas that suit the selected safeguarding criteria in selected case study countries (Version 1.1, Report). Geological Survey of Slovenia, Ljubljana: 66 p.

Rokavec, D., Miletić, S., Kozinc, Z., Dolinar, U. & Pogačnik Ž. 2016b: Nacionalna delavnica projekta MINATURA 2020: Mineralne surovine javnega pomena v Sloveniji (in Slovene). Mineral, 9/44: 28-30.

Rokavec, D., Mezga, K., Kozinc, Z. & Pogačnik, Ž. 2017: 2. nacionalna delavnica projekta MINATURA 2020: Mineralne surovine javnega pomena v Sloveniji (in Slovene). Mineral, 10/50: 30-32.

Rokavec, D. & Mezga, K. 2017: Ustrezno varovanje dostopa do nahajališč mineralnih surovin v Sloveniji (in Slovene). In: Rožič, B. (ed.): 23. posvetovanje slovenskih geologov, Geološki zbornik, 24: 149-153.

Shields, D. J. & Šolar, S.V. 2004: Sustainable Mineral Resource Management and Indicators: case study Slovenia. Geological Survey of Slovenia, Ljubljana: 84 p.

Senegačnik, A., Štih, J. & Burger, A. 2016: Pregled podatkov proizvodnje ter zalog in virov nekovinskih mineralnih surovin (in Slovene). Mineralne surovine v letu 2015, 12/1:16-46.

Senegačnik, A. & Štih, J. 2016: Overview of data on production, reserves and resources of non-metals. Bulletin Mineral resources in Slovenia 2015, 5-10.

Skaberne, D. 2003: Poročilo o geološkem popisu jeder vrtin v površinskem kopu Jersovec II pri Mirni (in Slovene). Geološki zavod Slovenije, Ljubljana: 20 p.

Šolar, S.V. 1994: Elaborat o kategorizaciji, klasifikaciji in izračunu rezerv rožEnca v ležišču Jersovec II pri Mirni na Dolenjskem, stanje 31.12.1992. Dopolnilo k elaboratu - Jersovec III pri Mirni, stanje 31.12.1992 leta (in Slovene). Geološki zavod Slovenije, Ljubljana: 22 p.

Šolar, S.V. 2015: Evropske smeri gospodarjenja in oskrbe z mineralnimi surovinami ter njihova implementacija. Mineralne surovine v letu 2014 (in Slovene), 11/1: 114-118.

University of Leoben, 2004: Minerals Planning Policies and Supply Practices in Europe (Commissioned by the European Commission Enterprise Directorate General under Contract no. ETD/FIF 2003 0781), Austria: 355 p.

Vesel, J. 1980: Geološke raziskave naravnega okrasnega kamna v Sloveniji: poročilo o geoloških raziskavah nahajališč Mali Medvedjak, Lipica in Kopriva ter prospekcije Krasa (in Slovene). Geološki zavod Slovenije, Ljubljana: 79 p.

Internet sources:

Internet 1: https://ec.europa.eu/growth/sectors/raw-materials/policy-strategy_en (12. 1. 2017)

Internet 2: https://ec.europa.eu/growth/tools-databases/eip-raw-materials/en/content/strategic-implementation-plan-sip-0 (17. 01. 2017)

Internet 3: http://www.euromines.org/what-we-do/sustainable-development-issues (12. 12. 2016)

Internet 4: http://www.natura2000.si/fileadmin/user_upload/Primerjava_N2K_2004_2016_20160725_MOP.pdf (12. 7. 2016)

Internet 5: http://www.arso.gov.si/narava/zavarovana%20obmo%C4%8Dja/SeznamParkov.htm (12. 7. 2016)

Internet 6: http://www.arso.gov.si/narava/zavarovana%20obmo%C4%8Dja/ (12. 7. 2016)

Internet 7: http://www.eea.europa.eu/soer-2015/countries/slovenia (12. 7. 2016)

Internet 8: http://minatura2020.eu/ (13. 3. 2017)

GEOLOGIJA 60/1, 129-143, Ljubljana 2017
https://doi.org/10.5474/geologija.2017.010

Investigations of the air – ground temperature coupling at location of the Malence borehole near Kostanjevica, SE Slovenia

Raziskave povezanosti temperatur zraka in plitvega podzemlja na lokaciji vrtine Malence pri Kostanjevici, JV Slovenija

Ana STRGAR[1], Dušan RAJVER[2] & Andrej GOSAR[3,4]

[1]Suhadolčanova ulica 6, SI-1000 Ljubljana, Slovenia; e-mail: ana.strgar@gmail.com
[2]Geological Survey of Slovenia, Dimičeva ulica 14, SI-1000 Ljubljana, Slovenia; e-mail: dusan.rajver@geo-zs.si
[3]ARSO, Seismology and Geology Office, Vojkova 1b, SI-1000 Ljubljana, Slovenia; e-mail: andrej.gosar@gov.si
[4]Faculty of Natural Sciences and Engineering, University of Ljubljana, Aškerčeva 12, SI-1000 Ljubljana, Slovenia

Prejeto / Received 9. 1. 2017; Sprejeto / Accepted 26. 5. 2017; Objavljeno na spletu / Published online 9.6.2017

Key words: air-ground temperature coupling, soil temperature, borehole temperature, thermal conductivity, climate, southeast Slovenia
Ključne besede: povezanost zračnih in talnih temperatur, temperatura tal, temperatura v vrtini, toplotna prevodnost, podnebje, jugovzhodna Slovenija

Abstract

In this paper we present the results of monitoring of temperatures in the air, soil and a borehole V-8/86 at Malence near Kostanjevica in the southeast Slovenia. The results include the temperatures measured in the period from year 2011 to 2015. Highlights of the paper are mainly on the influence of heavy rainfall on temperatures in the upper parts of the shallow subsurface, on understanding how the heat transfers between air and soil and in determination of the warming rate in the shallow subsurface with the assumption that conduction is the prevalent mechanism of heat transfer within the rock. The analysis has shown that heavy rainfall has a greater impact at depth of 1 m in the borehole than at 1 m in the soil, since the sensor at 1 m in the borehole is actually still in the air (inside the borehole) so the rainwater and consequently the air temperature change can reach it faster than the rainwater can infiltrate through soil to depth of 1 m. During infiltration the rainwater's temperature interact with the soil temperature and the change between the rainwater and soil temperatures is no longer evident at 1 m depth in the soil. Based on the measured temperatures from years 2014 and 2015 the rate of warming at the depth of 40 m is 0.011 °C/yr. While analysing the temperature-depth profile of daily means of temperature on the 15th day of each month, we concluded that the influence of seasons can be tracked down to depth of 20 m. At the depth of 20 m temperatures vary within 0.04 °C (2015). The assumption that the conduction is the prevalent mechanism of heat transfer is reasonable, because the theoretical values do not differ much from the measured ones (within 5 %).

Izvleček

V članku so prikazani rezultati merjenja temperatur v zraku, tleh in vrtini V-8/86 v Malencah pri Kostanjevici v jugovzhodni Sloveniji. Podatki obsegajo obdobje od leta 2011 do 2015. Osredotočili smo se predvsem na odzive temperatur v plitvem podpovršju na obilnejše padavine, na prehajanje toplote čez mejo zrak-tla in na določanje stopnje segrevanja v vrtini s predpostavljenim konduktivnim načinom prehajanja toplote znotraj kamnine. Analiza je pokazala, da obilnejše padavine bolj vplivajo na temperaturo v globini 1 m v vrtini kot v globini 1 m v tleh, saj je senzor na 1 m v vrtini dejansko še v zraku in ga deževnica in posledično sprememba zračne temperature doseže hitreje, kot pa se deževnica infiltrira do globine 1 m v tleh. Med pronicanjem se temperatura deževnice približa temperaturi tal in razlike med temperaturama na globini 1 m v tleh ne zaznamo več. Na podlagi podatkov iz leta 2014 in 2015 je trend naraščanja temperature na globini 40 m 0,011 °C/leto. Pri analizi odvisnosti povprečne dnevne temperature za vsak 15. dan v mesecu od globine, smo prišli do sklepa, da letno spreminjanje temperature zraka vpliva do globine 20 m, kjer so razlike med posameznimi meseci samo še znotraj 0,04 °C (2015). Predpostavka konduktivnega načina prehajanja toplote kot prevladujočega za izračun teoretičnega poteka temperatur v odvisnosti od časa in globine je smiselna, saj teoretične vrednosti ne odstopajo bistveno od izmerjenih (znotraj 5 %).

Introduction

Studies of the air-ground temperature coupling get more and more attention as an auxiliary insitu method in research of the long-term temperature variations and therefore climate changes in the present and in the past (Čermák, 1971; Lachenbruch & Marshall, 1986; Šafanda et al., 1997; Smerdon et al., 2004; Bodri & Čermák, 2007). The climate interpretation of the ground surface temperature (GST) history, which is obtained from present-day temperature-depth profiles, measured in deep boreholes, is based on an assumed long-term tracking of the mean annual surface air temperature and the ground surface temperature (i.e. Majorowicz et al., 2004). The reconstructed GST histories are temporal changes of the ground temperature at the upper boundary of the heat conduction domain, which begins somewhere in the soil-rock basement transition zone. Environmental conditions are suspected to be the most important factors influencing the air-soil temperature difference. In 1993 an international project under the NATO scientific programme support and initiative of the Czech Geophysical Institute (GFÚ) was lunched with an aim to explore the assumption on a long-term tracking of the mean annual surface air temperature and the ground surface temperature. Furthermore, this project was initiated also in order to determine the poorly investigated impact of environmental conditions such as soil moisture, type of vegetation cover and the amount and type of precipitation, on heat transfer in the soil and shallow subsurface. Understanding these impacts is essential for understanding how the heat transfers through different layers of shallow subsurface. This knowledge is needed for reconstruction of the past climate based on the temperatures measured along deep boreholes (Beck & Judge, 1969; Čermák, 1971; Shen & Beck, 1991; Kane et al., 2001).

Therefore, a study, based on the air-ground temperature coupling, began in year 1993 to determine how temperatures in the shallow subsurface follow the long-term variations of the air temperatures in different recent climates and how significant is their influence on heat transfer in the shallow subsurface. The main aim of the monitoring is to explore the assumption on a long-term tracking of the mean annual surface air temperature and the ground surface temperature, which is vital for the climatic interpretation of the GST history obtained from present-day temperature-depth profiles measured in deep boreholes. The project comprises permanent temperature measurements in the boreholes in Czech Republic (since 1994), Slovenia (since 2003) and Portugal (since 2005).

One of the most important parameters of heat transfer in the shallow subsurface is thermal diffusivity, which determines how much heat transfers conductively through the material (Gosar & Ravnik, 2007). Thermal diffusivity can be measured directly on the rock sample in a laboratory using e.g. a flash method (Dědeček et al., 2013). Researchers at the aforementioned project *Air-ground temperature coupling in three different climates* decided to use an auxiliary in-situ method for studying the air-ground temperature coupling. With the long-term logging of temperatures at different heights in the air and depths in the soil and borehole every 30 minutes a large database has been generated, covering interval since Nov. 12th 2003 until Dec. 31st 2015 and beyond until today. The 30-minutes interval has been chosen by Czech geophysicists (with longer experience in this matter) as the most appropriate, as it is not too rare (e.g. with regard to precipitation events) neither too dense. This database can be used for determining the effects of environmental conditions and the nature of propagation of surface temperatures into shallow subsurface. By exploring the temperature-time series in three boreholes located in different climates the results can be correlated. Boreholes are located in three experimental sites as follows: a GFÚ-1 borehole of 150 m depth (Šafanda, 1994) in Prague (Czech Republic) at the premises of Czech Geophysical Institute with monitoring down to 38 m depth, a V-8/86 borehole at Malence near Kostanjevica (Slovenia) of 100 m depth and a TGQC-1 borehole of 180 m depth in Caravelinha near Évora (Portugal) (Smerdon et al., 2004, 2006). While the borehole in Prague is in the southeast suburb Spořilov of a metropolitan city, the other two are found in rural areas, at Malence on the edge of meadow, and at Caravelinha in the sparse oak forest near Évora. Both observatories in Slovenia and Portugal monitor temperatures down to 40 m depth (Šafanda et al., 2007).

Herein we present the results of measurements from the Malence Borehole Temperature Observatory (MBTO) near Kostanjevica in the period from 2011 to 2015.

Air-ground temperature coupling

The method of inverting the measured temperatures in deep boreholes in order to reconstruct the GST history was represented by Beck and Judge (1969), who reconstructed the climate in the decade previous to the year of their study. They were soon followed by Čermák (1971), who used the temperature measurements from a borehole in Canada and, although he reconstructed the climate in the past millennium, he also stated that the method needed improvements. The method does not predict the nonconductive heat transfer (Shen & Beck, 1991; Majorowicz et al., 2004). The nonconductive heat transfer, such as infiltration of rain water and freezing or defrosting of the soil, were examined among others by Kane at al. (2001).

First studies of the past climate change in Czech Republic were conducted by Šafanda & Kubík (1992). Analysis of measurements from two boreholes (one in SW and one in NE part of the Czech Republic) has shown an increase of the average surface temperature from -6 °C to 7 °C around 12,000 years ago, a warming by 0.9 °C some 475 years ago, a cooling by 0.5 °C some 36 years ago, followed by an increase of temperature by 1.3 °C nine years ago (as regard to the time of writing the cited paper).

Survey of temperatures obtained from seven boreholes in Slovenia suggests the surface warming by 0.6 to 0.7 °C in the decade 1988-1998 (Rajver et al., 1998). The study has also shown a glacial minimum (3 °C) some 14 to 13 thousand years ago, which was followed by the post-glacial maximum (10.5 °C) around 2 to 3 thousand years ago.

The signature of the last ice age (75 to 10 thousand years ago) in the present subsurface temperatures was studied in boreholes from Slovenia and the Czech Republic by Šafanda & Rajver (2001) who have used temperature-depth (T-z) profiles from 1.5 to 2.4 km deep boreholes. They confirmed a glacial minimum extending 19 to 10 thousand years ago and a postglacial warming of 6 to 15 °C.

The first measurement results from 2003 to 2005 at MBTO were published by Rajver et al. (2006). Data from a period of 2003 to 2009 and a conductive and conductive-convective heat transfer mechanisms were studied by Dědeček et al. (2013).

Heat from surface transfers into the shallow subsurface mainly by conduction. Surface temperature is regulated largely by heat flow from the Sun. Therefore, differences in surface temperature are mostly due to daily and annual cycles. These differences can be tracked down to the depth of about 50 m. Any deeper variations of temperatures, which substantially depart from the conductive heat flow, are the result of a drastic changes in climate (e.g. ice age) (Kappelmeyer & Haenel, 1974).

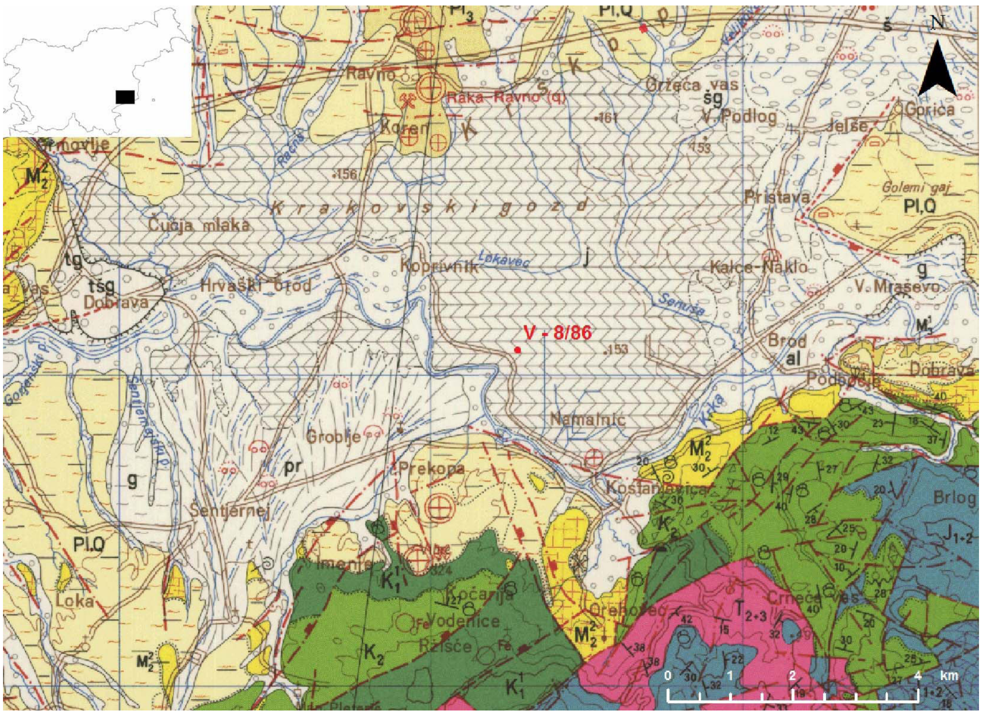

Fig. 1. Location of the V-8/86 borehole at Malence, SE Slovenia. Geology is after OGK Novo mesto (Pleničar & Premru, 1977).

Methodology of temperature measurements in the borehole V-8/86 at Malence

The borehole V-8/86 is located at Malence near Kostanjevica (45°52.1' N, 15°24.5' E, z=152 m a.s.l.) (Fig.1) in the Krško basin in southeast Slovenia. The basin is filled with Tertiary sediments of the Pannonian basin and Quaternary deposits from the Sava river (Pleničar & Premru, 1977) and is part of the Sava folds (Placer, 1998). The borehole was finished in October 1986 and is 100 m deep (Fig. 2a). It was drilled through Quaternary clay, sand and gravel in the first 16 m, below which lies Miocene marl, which gradually becomes more clayey with depth (Rajver et al., 2006; Šafanda et al., 2007; Dědeček et al., 2013). In Figure 2a the last temperature log from August 30th, 2011 is also presented. The borehole is cased with zinc-coated tube of 41.5 mm (1.6 inch) of inner diameter. Temperature was logged four times along the whole borehole depth, from October 1986 to August 2011 (Fig. 2b), using two different temperature sensors. The first two loggings in 1986 and 1987 were done using the Pt-100 sensor, connected to LAGO-T meter (Ravnik & Lakovič, 1984) with a precision of 0.01 °C and accuracy of +/- 0.1 °C, while for the other two loggings the Antares thermistor was used with a resolution of 1 mK and accuracy better than 0.1 K. The thermistor's drift is of the order of first hundredths K over the time the GFÚ team uses the probe (more than 10 years), but the probe is calibrated practically every year, so the effect of possible drift is eliminated (Šafanda, pers. com.). The Pt-100 sensor has been only occasionally calibrated, nevertheless the results are comparable with those of Antares thermistor.

There have been only two rock samples collected, from depths of 0.7 m (sandy clay) and 99 m (clayey marl). On both a thermal conductivity has been measured using different but comparable methods, TCS and transient hot wire, respectively, and results were 1.7 W/(m·K) for the one from 0.7 m and 1.45 W/(m·K) from 99 m (Rajver et al., 2006; Šafanda et al., 2007). Estimation of thermal diffusivity is based on typical density and specific heat values and can differ between 0.6 and $0.8 \cdot 10^{-6}$ m²/s. Due to high specific heat of pore water, it could be as low as $0.4 \cdot 10^{6}$ m²/s (for 30 % total porosity) (Šafanda et al., 2007). Dědeček et al. (2013) extracted thermal diffusivity from subsurface temperature data at Malence. They got $0.2 - 0.3 \cdot 10^{-6}$ m²/s in the top 5 to 10 cm of soil and $0.5 - 0.7 \cdot 10^{-6}$ m²/s within 0.1 to 10 m of the bedrock. Simple calculation using reasonable parameter values shows that with 15 % of water content in the sample and the mineral density

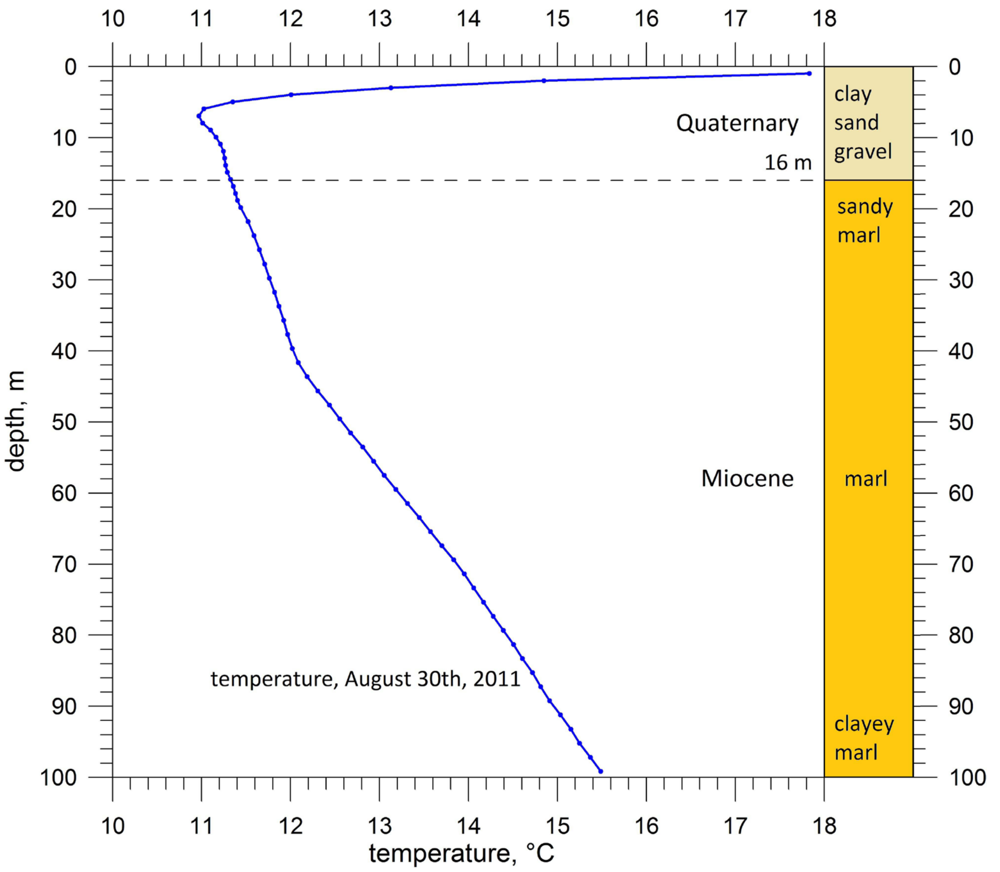

Fig. 2a. Geological column of the V-8/86 borehole with the last T-z profile of August 30th 2011. Lithological data are summarized by Rajver et al. (2006).

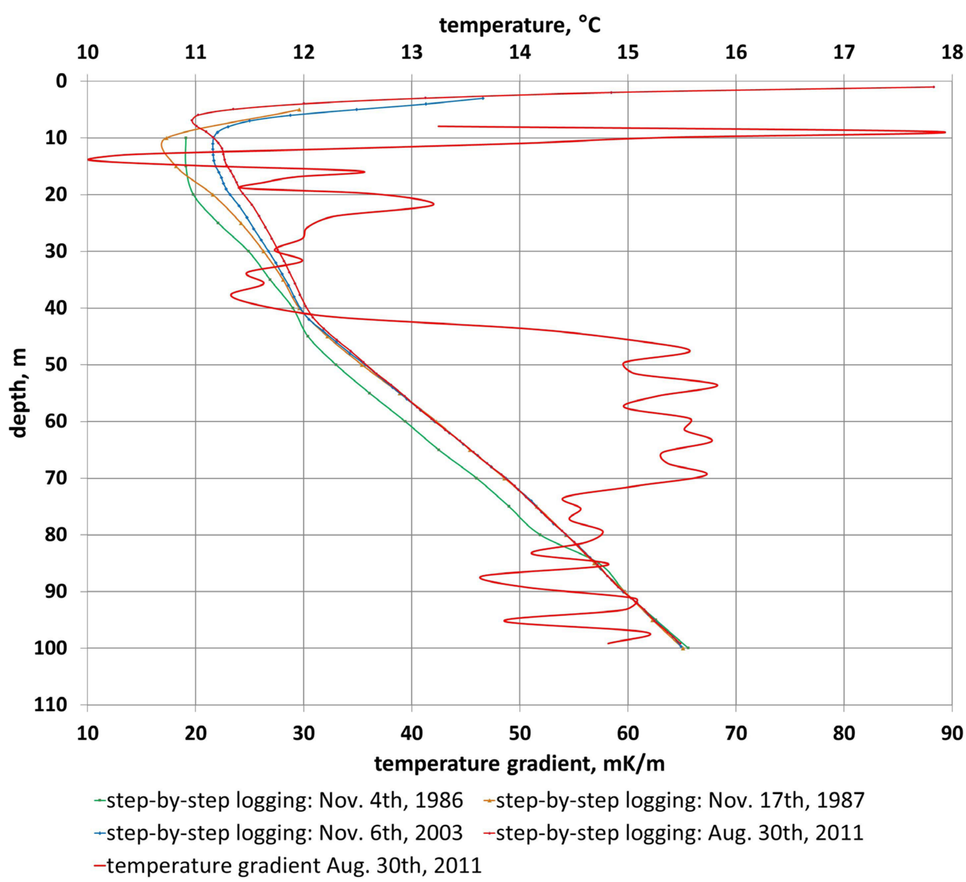

Fig. 2b. The measured temperature (T-z) profiles in the V-8/86 borehole in a period from 1986 to 2011.

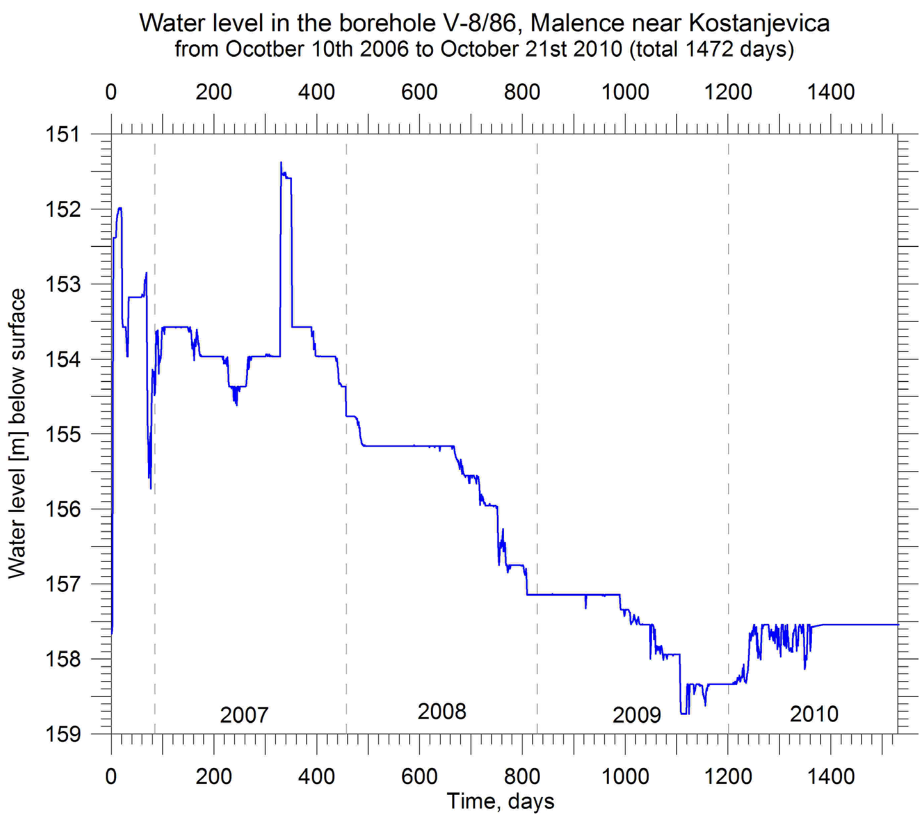

Fig. 3. Water level in the borehole V-8/86, monitored in a period of 4 years (2006 to 2010).

of 2,670 kg/m^3, the effective specific heat (ρ·c) is 2.51·10^6 J/(m^3·K), and thermal diffusivity $\kappa = \lambda / (\rho \cdot c)$ is 0.68·10^{-6} m^2/s. The borehole has been chosen as the most suitable among available and investigated boreholes in Slovenia because of its location with an easy access, a good knowledge on lithology and relatively stable level of groundwater. The water level in the borehole was monitored only in a period from Oct. 10th 2006 to Oct. 21st 2010 (Fig. 3), using the piezometer sensor that has been connected to one of the channels instead of a temperature sensor at 1 m in the borehole. This monitoring showed only slightly water level variations between 151 and 159 cm below ground surface. Since the fluctuation is quite small and does not show any periodic characteristics, we can assume it does not respond to differences in the level of nearby Krka River. Unfortunately, this period does not match with the period of temperature analyses. The borehole is located on the edge of the meadow, which on the north side continues into the forest, so the vegetation around the borehole is more or less constant and in micro location cleaned out when necessary. We have no data on depth of saturated zone in the shallow subsurface. It is believed this zone is at least 1.5 m deep because the soil to this depth consists mostly of clay and sandy clay, and deeper to 16 m also of gravel in mixture with clay and sand. The borehole is located on a private land and data logger with battery is being kept in a locked metal box so the risk of vandalism is quite low.

In order to explore the assumptions of (i) a long-term tracking between the mean annual surface air temperature and the ground surface temperature and (ii) a conductive propagation of soil temperature changes into bedrock, the MBTO station has been established (Fig. 4). It consists of a data logger, battery and sensors for monitoring air temperatures at different heights above the ground level (2 m and 5 cm), soil temperatures at different depths below the surface (2, 5, 10, 20, 50,

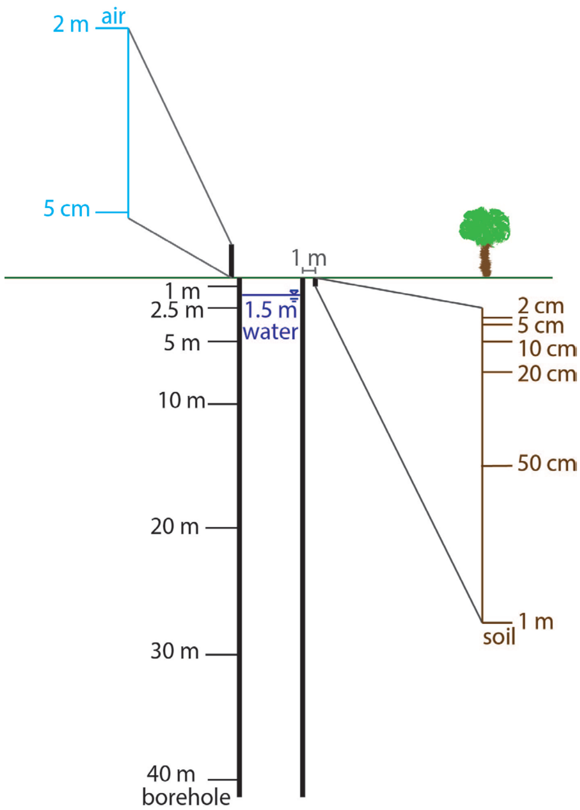

Fig. 5. Layout of the temperature sensors in the air, in the soil and in the borehole V-8/86.

100 cm) and bedrock temperatures in the borehole (1, 2.5, 5, 10, 20, 30, 40 m) (Fig. 5). The platinum sensors (Pt 1000, class A, resolution of the system is 3 mK) were installed in November 2003 for permanent measurements (Rajver et al., 2006; Dědeček et al., 2013). The accuracy < +/- 0.15 °C is

Fig. 4. Malence Borehole Temperature Observatory (in Sept. 2011). Sensors in the soil are buried within depicted trapeze.

given by producer for the users that do not calibrate the sensors. All MBTO sensors are calibrated. The absolute error of the measured temperature can be estimated at 0.01 K (Šafanda, pers. com.). Temperatures are recorded in 30-minute intervals with a data logger system (16 channels, 24 bits A/D converter, 16 bits resolution, producer Fiedler Magr s.r.o., Czech Republic). Data used in this study cover the period from September 2nd 2011 to January 1st 2016. The MBTO station faced several difficulties in monitoring due to hardware malfunctions. For example, in the period of Oct. 21st to Dec 14th, 2010, some abnormally high positive and negative peak oscillations appeared in the measured temperatures at 1 to 40 m depths, resulting also in high peaks of daily averages. We did not notice this immediately and until Aug. 30th, 2011, we couldn't transfer the measured data to computer, which was later discovered as a memory malfunction of the data logger. Consequently, the GFÚ team decided to install a new data logger unit on Aug. 30th, 2011. They also changed two sensors (the borehole's at 10 m and the air sensor at 2 m). The sensors' and data logger's functioning is occasionally but constantly controlled by the GFÚ team, and the sensors are calibrated before their installation. Contrary to thermistors, the platinum sensors are stable in time. Therefore, we are convinced there are no sensor drifts. Later on, the data were lost or are missing in the following periods: Sept. 17th to 23rd, 2011, when voltage regulator was disconnected, Oct. 15th to 17th, 2012, when all the sensors were changed with the new ones, and Sept. 13th to Oct. 22nd, 2014, when five sensors (at 2.5, 5, 10, 20 and 30 m) in the borehole were changed and the time unit was properly set. A short disruption of the borehole data occurred when on Nov. 14th, 2013, all the borehole sensors were replaced with a new set of sensors.

Results of temperature monitoring and discussion

An example of 30-minute data interval is presented for February, 2012 (Fig. 6), which shows an influence of snow on temperatures in the upper part of soil. In the beginning of the month, the temperatures at depths of 2 and 5 cm in the soil stayed roughly at 0 °C since snow acted like an insulator. Review of data from the meteorological (precipitation) station in Kostanjevica – Brod (3 km away) confirmed that there was a snow cover present from 4th – 23rd of February (Internet 1). Another example (Fig. 7) of the influence of the snow cover insulation is shown for a period January 14th – March 2nd, 2013 (Internet 1), and can be tracked down to depth of 100 cm in the soil.

An example of the influence of rain is shown in Figure 8 with 30-minute data for July 2012, where the temperatures in the air at 2 m and 5 cm

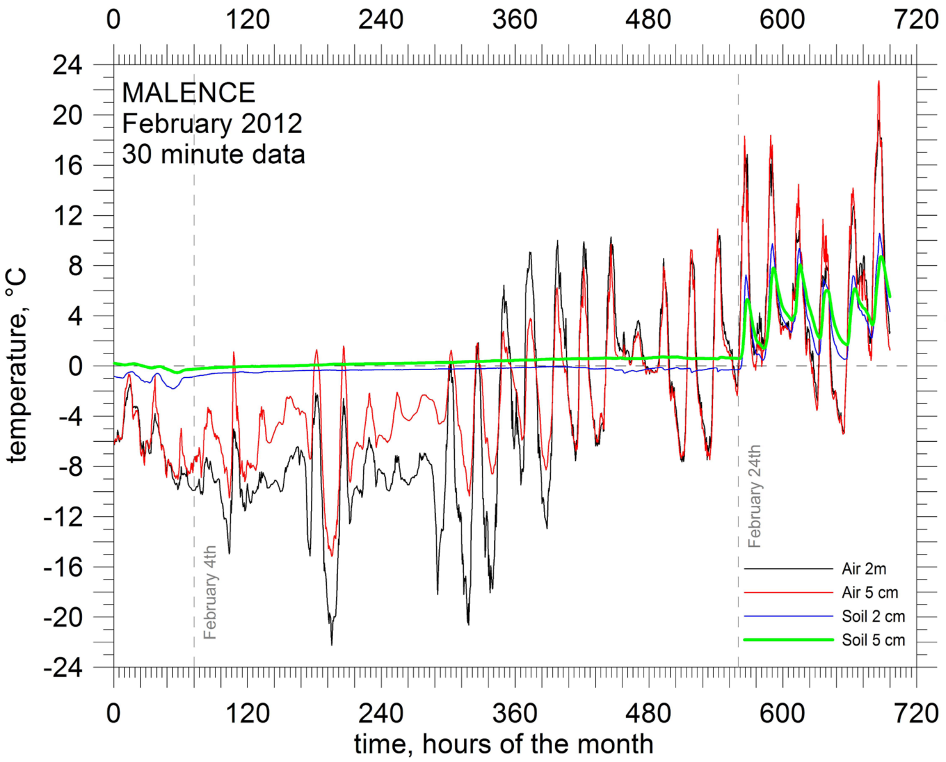

Fig. 6. 30-minute data in February 2012 at 2 and 5 cm in the air and in the soil depths of 2 and 5 cm showing influence of snow cover (February 4th to 24th).

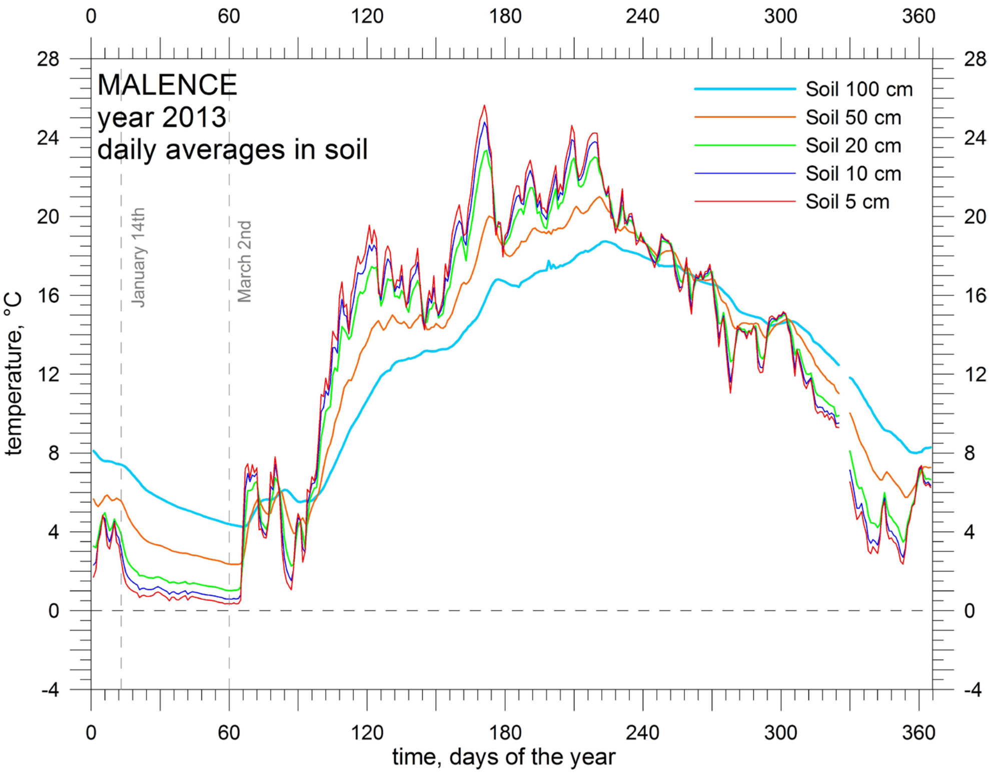

Fig. 7. The average daily temperatures in 2013 at depths from 5 cm to 1 m in the soil showing the influence of snow cover (January 14th to March 2nd) on temperatures to a depth of 1 m.

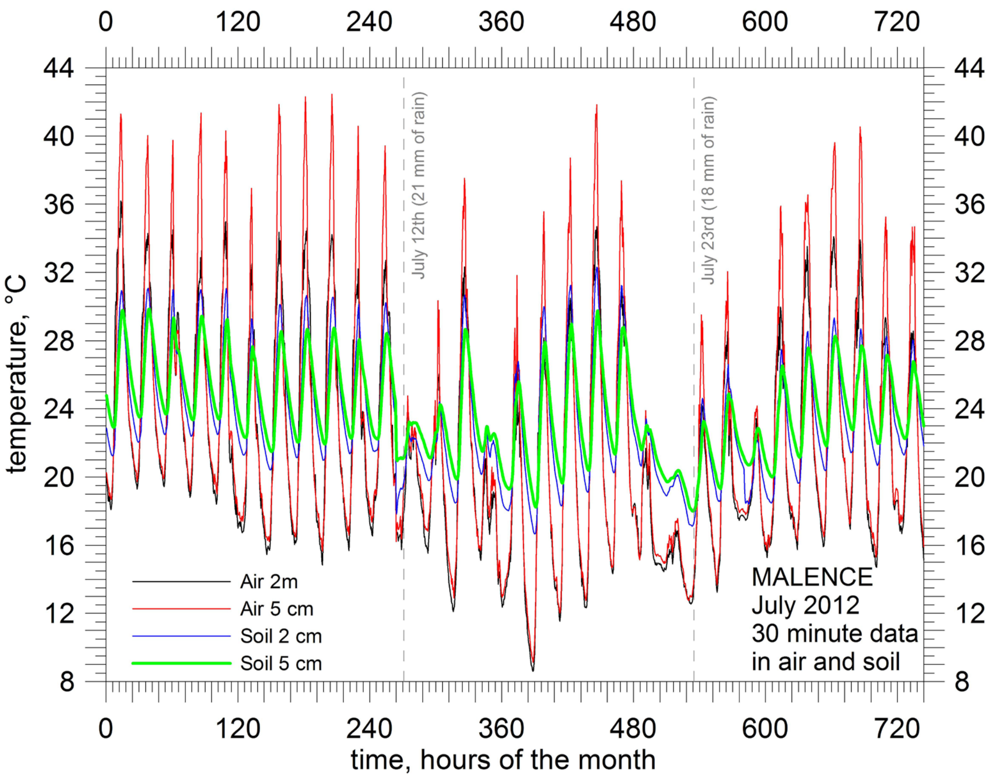

Fig. 8. 30-minute data in July 2012 at 2 m and 5 cm in the air and the soil depths of 2 and 5 cm. Impact of rainfall is evident in two events.

decreased just before the precipitation occurred (Internet 1). Consequently, the temperatures in the soil at 2 cm and 5 cm also decreased. This reaction was due to considerably lower air temperatures of the weather front with the similar precipitation temperatures. Figure 8 also shows typical greater daynight variability at 2 m and 5 cm in the air, which is gradually smoothed in the soil.

How infiltration of the rain water influences the temperature in the soil and in the borehole at depth of 1 m is shown in Figure 9. Due to some non-conductive heat transfer the temperature in the soil at depths of 5 to 20 cm slightly fell after heavy rains in the night from 13th to 14th August, 2014, recorded at Kostanjevica - Brod (Internet 1), which is the result of infiltration of relatively cooler rain water. This influ-

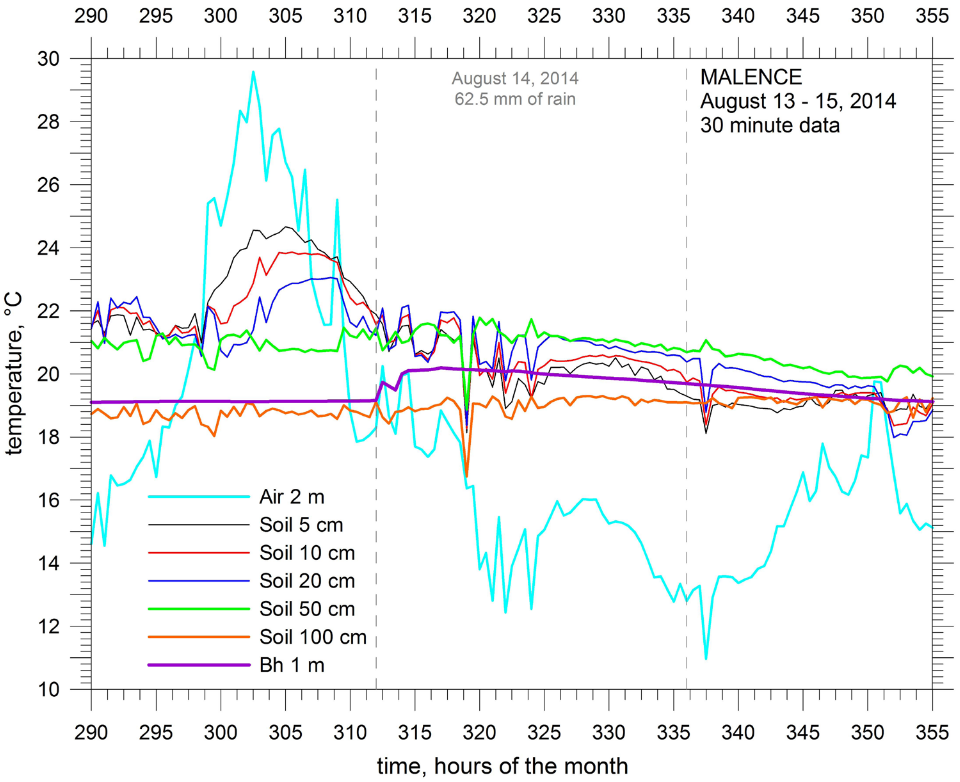

Fig. 9. Measured temperatures in the period between August 13th and 15th 2014 at a height of 2 m in the air and depths ranging from 5 cm to 1 m in the soil and in the borehole at a depth of 1 m showing the temperature response to heavier rainfall.

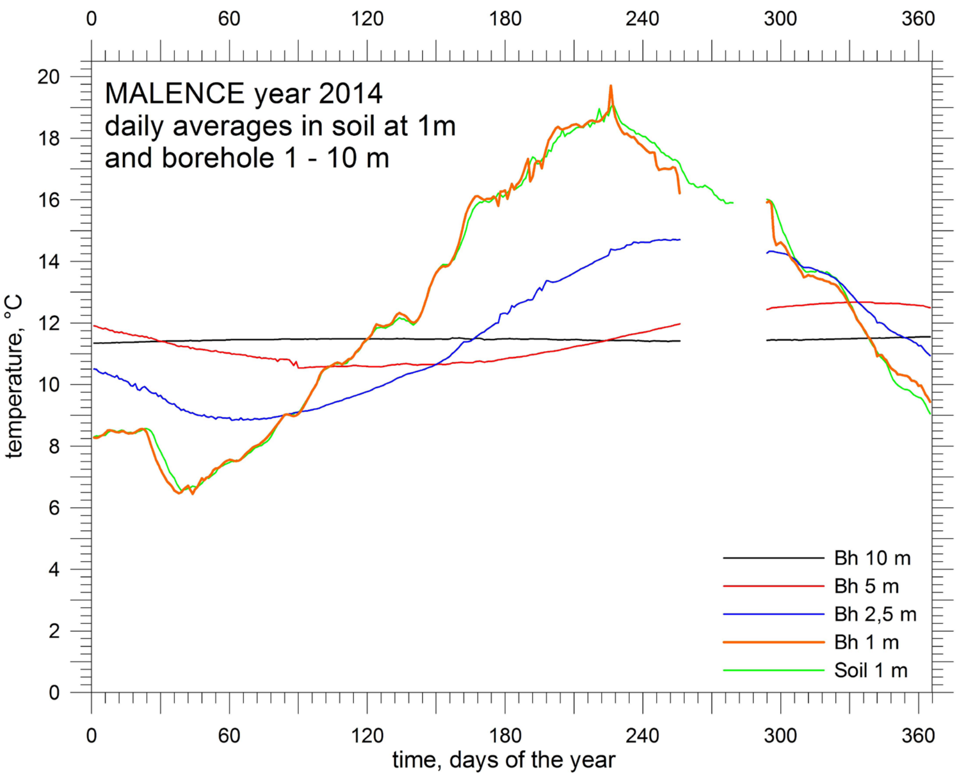

Fig. 10. The average daily temperatures in 2014 at depths of 1 m to 10 m in the borehole showing amplitude decreasing with depth and the delay of the temperature minima and maxima with depth. The sensor at 1 m depth in borehole records the temperature in the air, others record in the water.

ence is not evident any more at depths of 50 and 100 cm in the soil, but there is a sudden warming of 1 °C in ca. 2 hours at depth of 1 m in the borehole. This happened due to slightly warmer rain water temperature (and the air temperature surrounding the rainfall itself) than the air in the top part of the borehole column, but still slightly cooler than the soil down to depth of 50 cm.

Daily temperature averages at depths from 1 to 10 m in the borehole and at 1 m in the soil (Fig. 10) demonstrate the amplitude decrease with depth. Temperatures at 1 m in the soil and 1 m in the borehole nicely fit together and vary within 13 °C, and since the sensor in the borehole at 1 m is in the air, it records the variations just slightly earlier than the sensor at 1 m depth in the soil. Temperatures at a depth of 10 m vary only with-

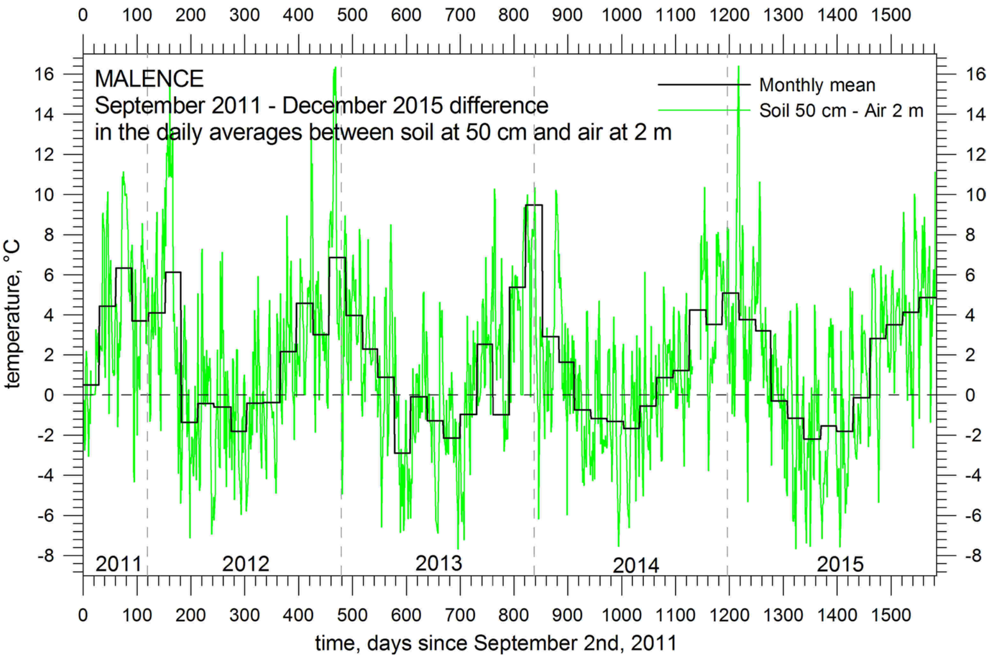

Fig. 11. The average daily and monthly differences between the soil at 50 cm and the air at 2 m from 2011 to 2015.

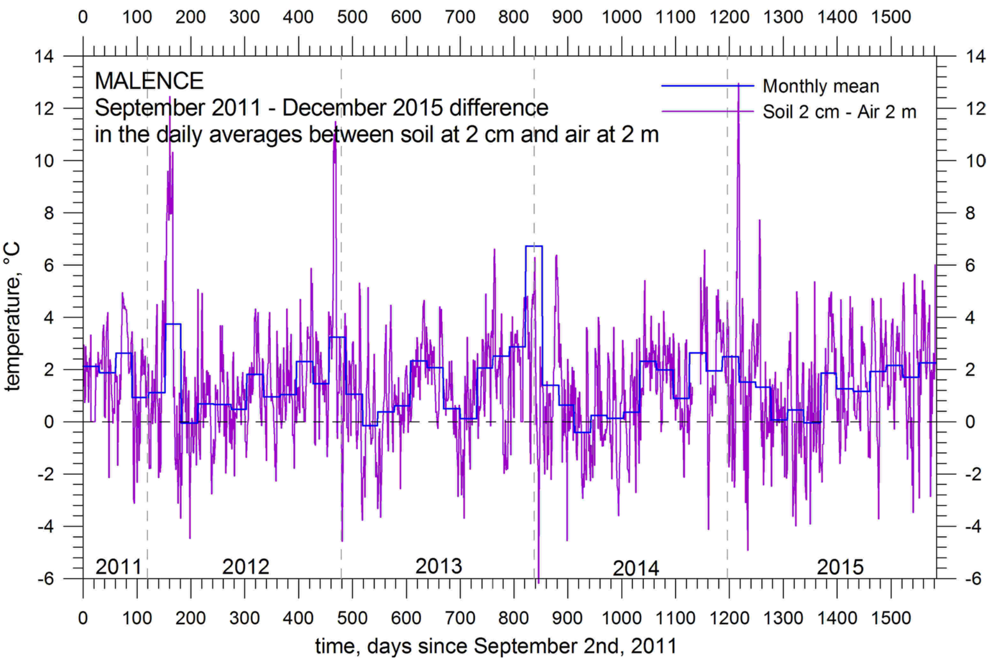

Fig. 12. The average daily and monthly differences between the soil at 2 cm and the air at 2 m from 2011 to 2015.

in 0.5 °C. The gap at the end of the year is due to unfortunate malfunctioning of the sensors in the borehole.

Appropriate differences must be examined to understand the correlation and tracking between the air and soil temperatures. Figures 11 and 12 are examples of daily and monthly differences between the air and the soil in the period from September 2011 to the end of year 2015. Both graphs are useful to show the heat transfer through the air-soil boundary. There is a larger difference in the winter time between the temperatures of soil at 50 cm depth and air at 2 m than between the temperatures of soil at 2 cm depth and air at 2 m height, just because the annual climate changes are more pronounced at shallower soil levels. During the summer time it is usually the opposite. Differences between 50 cm in the soil and 2 m in the air are smaller in the summer time, while there are much smaller variations between the seasons in differences between the soil at 2 cm and the air at 2 m. Temperature differences between 2 cm in the soil and 2 m in the air are mostly positive, which means that the soil in shallow depths is most often warmer than the air at 2 m. At 50 cm depth this is not so much evident, but the temperature differences between the soil at 50 cm and the air at 2 m exhibit that the soil is warmer in the winter time, consequently the differences are greater.

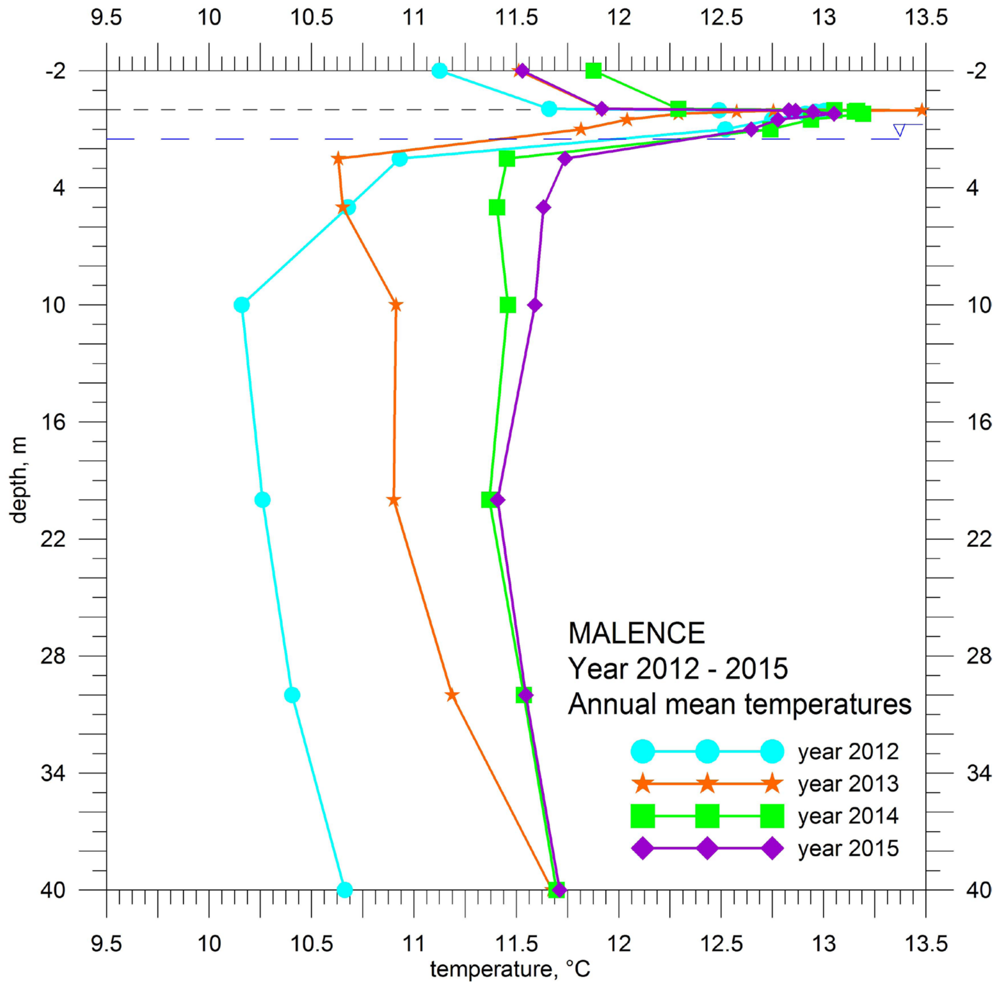

Fig. 13. The mean annual temperatures for the years 2012 to 2015 from a height of 2 m in the air to a depth of 40 m in the borehole. The average water level in the borehole is indicated.

By comparing the mean annual temperatures at all depths down to 40 m (Fig. 13) one can see that temperatures at 2 m in the air are lower than those at 5 cm in the air by about 0.7 to 1.0 °C. This is contrary to the results of the study for years 2004 and 2005 (Rajver et al., 2006). It could be due to general climate warming, which influences strongly the shallow soil levels (2 to 10 cm depth) and consequently the air temperature at 5 cm is presumably under the influence of additional shallow soil heating, therefore in such a way beating the air temperature at 2 m. In this context it is not yet clear if some cleaning of the forest (in summer 2011) just north of the borehole has any influence on air temperatures at 2 m. In the years 2004 and 2005 the mean annual temperatures at shallow soil levels (2 to 5 cm) reached ca 11.7 °C (Rajver et al., 2006), and in later years (2006 to 2009) they increased to 12 to 13.1 °C, while in the 2012 to 2015 period they reached 13 to 13.5 °C, again obviously due to global warming. The temperature is the highest at depth of 20 cm in the soil and gradually decreases with depth to 10 m in 2012, to 2.5 m in 2013 and to 20 m in 2014 and 2015. We have no direct comparison of this effect with other data in other parts of Slovenia. The observation period is too short to make some firm conclusions, as in the period 2004 to 2009 these minima were changing between 2.5 m and 20 m. It is the consequence of the surface temperature variations that propagate into the soil and bedrock and are drawn as mean annual air temperatures. Since the platinum sensors are stable in time, we are not certain about any malfunctioning except the data logger itself, which is also not likely. Below these depths temperature slowly increases due to geothermal gradient. An increase in mean annual temperatures over the years is a result of increase in surface temperature in the past decades as a result of global warming. For the years 2014 and 2015 the mean annual temperature at 20 m was 11.4 °C and at depth of 40 m it was 11.7 °C. We don't have any comparable systematic temperature measurements so far, showing the global warming from Slovenian boreholes. However, from the repeated temperature downhole loggings in several boreholes in Slovenia (Rajver et al., 2006), the global warming is evident in the upper 20 to 30 m. Much more data on the evidence of global warming from borehole temperature loggings are found in many other countries

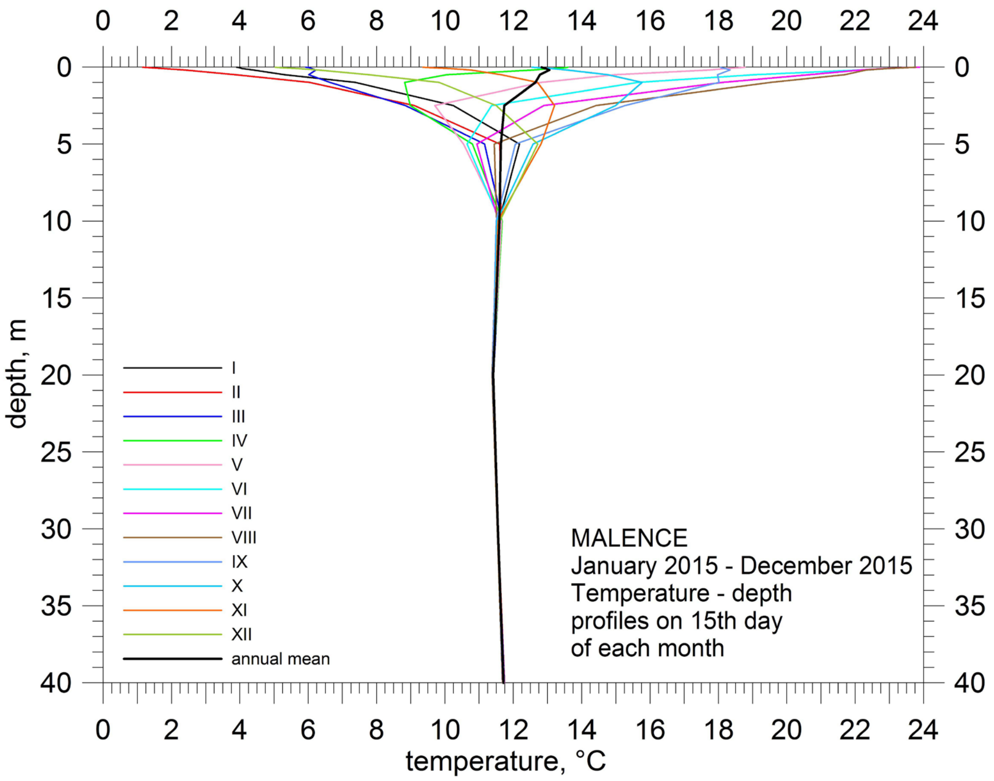

Fig. 14. The average daily temperatures on the 15th day of the month for 2015 in the depths of 0 to 40 m.

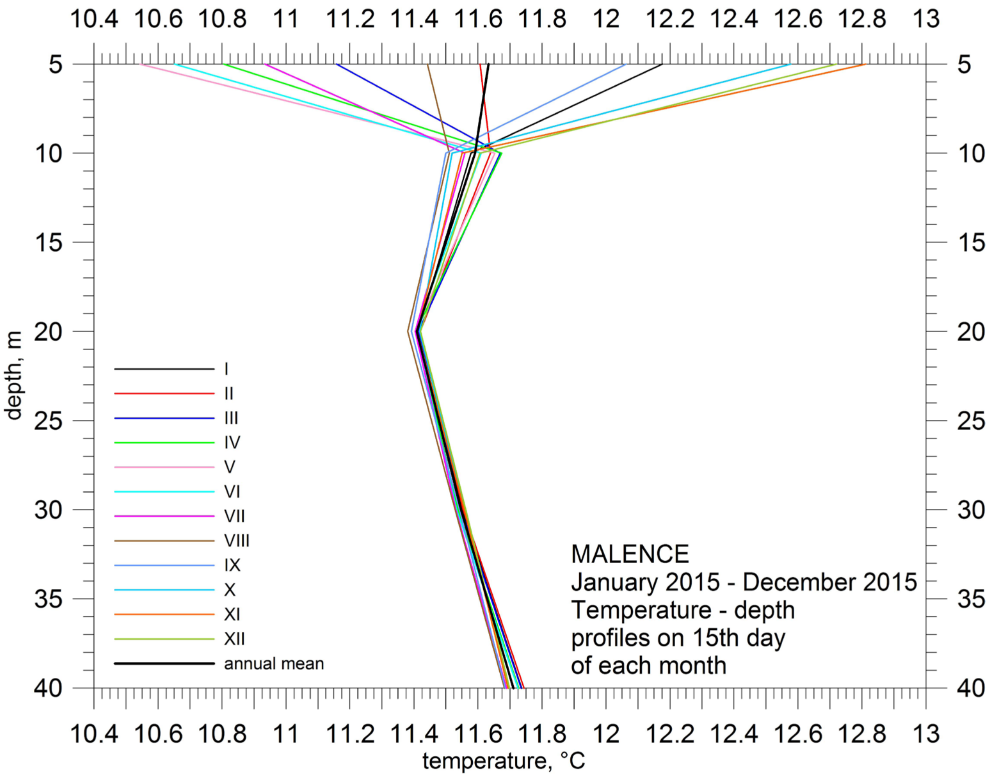

Fig. 15. The average daily temperatures on the 15th day of the month for 2015 in the depths of 5 to 40 m.

(i.e. Bodri & Čermak, 2007). The last three temperature loggings in the V-8/86 borehole clearly revealed the influence of global warming in the shallow underground, more exactly by 0.12 °C in less than eight years and by 0.28 °C in almost 24 years (Fig. 2b).

Temperatures on the 15th day of each month in 2015 are shown in Figures 14 and 15. Temperatures down to depth of 5 m vary significantly throughout the year, but the differences diminish with depth. This is a typical example of the influence of periodic air temperature variations on the subsurface temperatures down to depths of 20 m.

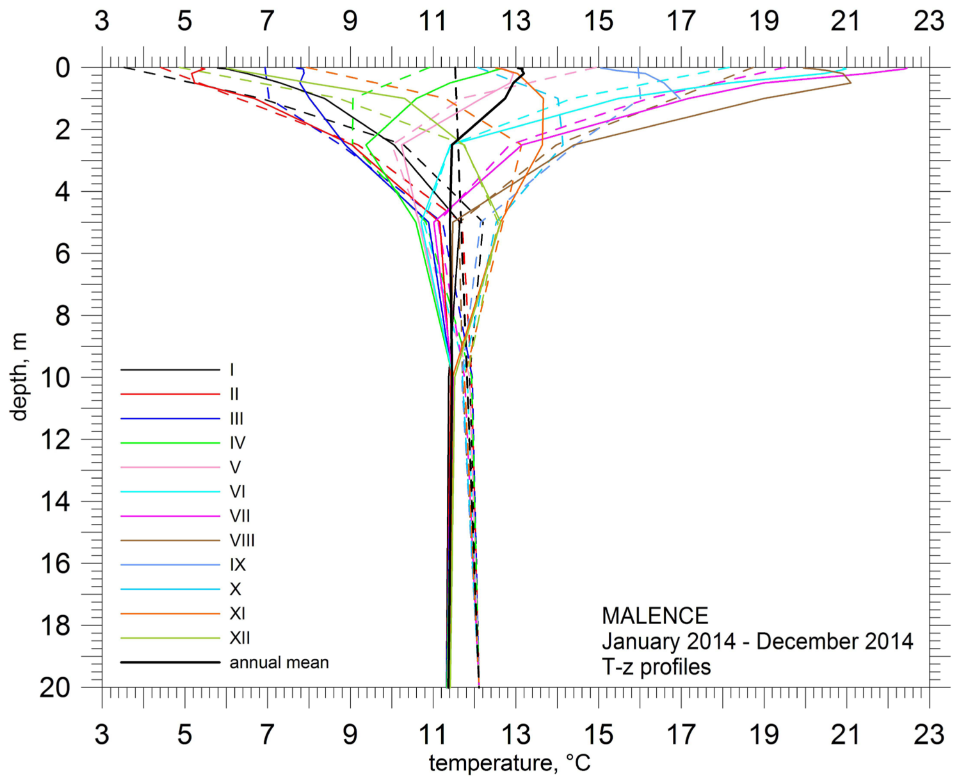

Fig. 16. Comparison of the calculated (dashed curves) and measured (solid curves) average daily temperatures on the 15th of the month for the year 2014 in the depths of 0 to 20 m.

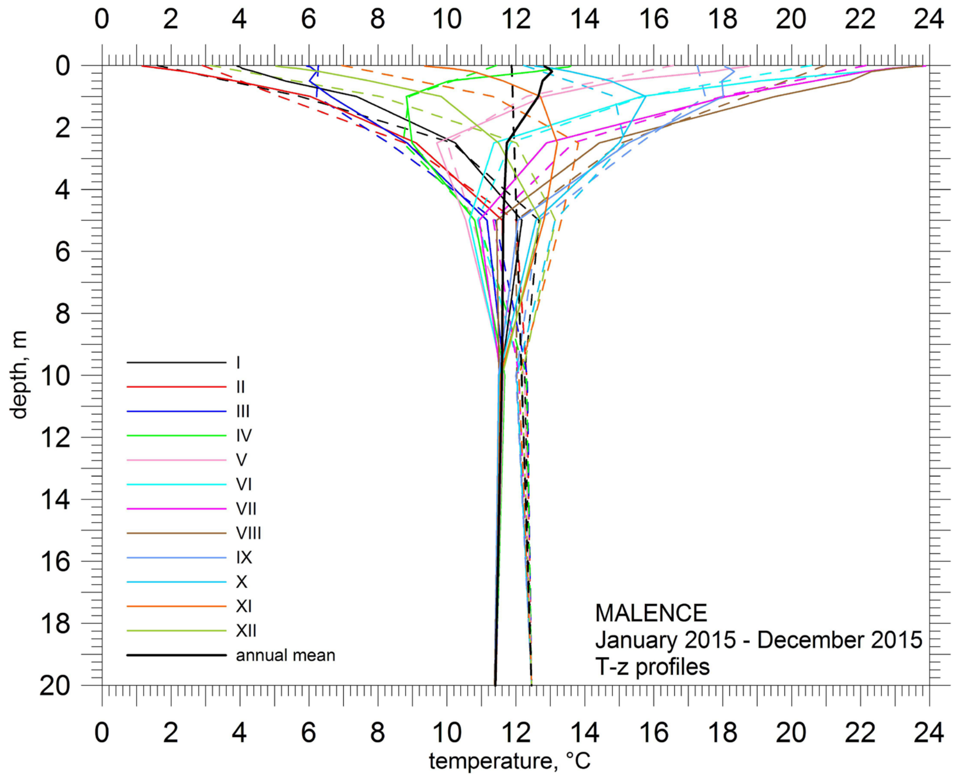

Fig. 17. Comparison of the calculated (dashed curves) and measured (solid curves) average daily temperatures on the 15th of the month for the year 2015 in the depths of 0 to 20 m.

At depth of 20 m the difference between minimum and maximum temperature is 0.04 °C (see Fig. 15 for detail). This is already out of the absolute error of the measured temperature (0.01 K). The influence of variation of surface conditions decreases with depth and loses its effect in most cases somewhere between 10 and 20 m. However, the repeated temperature downhole loggings (everywhere at least 13 years apart) in several boreholes in Slovenia (Rajver et al., 2006) show the influence of surface warming down to depths between 22 and 70 m, which is visible in the comparison of the boreholes' single T-z loggings.

To see the extent of the effect of non-conductive heat transfer we compared synthetic T-z profile, calculated with a diffusion equation (Gosar & Ravnik, 2007), with measured data for the years 2014 and 2015 (Strgar, 2016) (Figs. 16 and 17). Deviations in the upper part indicate that there is some heat transferred non-conductively but is relatively small and can be neglected. On average, the difference between the calculated and measured temperatures at depth of 5 m was -0.20 °C (-1.8 %) in 2014 and -0.39 °C (-3.3 %) in 2015. The difference between the calculated and measured temperatures deeper than 10 m is due to geothermal gradient used in calculations, which was determined by measurements of temperature down to the bottom of the borehole at 100 m in August 2011 (Fig. 2b). The difference is within 5 %, but it could be corrected with trying different input values (e.g. more accurate geothermal gradient). At 40 m the average difference between measured and calculated temperature is -8.5 % (2014) and -11.3 % (2015). Since the difference occurs mostly because of the utilized geothermal gradient, such difference is still small enough and we can confirm that effect of nonconductive heat transfer is low enough and that diffusion equation can be used for further calculations.

Conclusions

The analysis of temperature measurements at the MBTO near Kostanjevica has shown a slight presence of non-conductive heat transfer predominantly in the upper parts of the shallow subsurface. A good example is the influence of the infiltration of precipitation in the soil after heavy rainfalls. The temperature in the soil to depths of 20 cm changes, so it matches the temperature of rain water. While deeper than 20 cm temperatures in the soil stay unaffected, temperature in the borehole at 1 m raises rapidly. The effect of the snow cover, which acts like insulator, can be tracked down to depth of 1 m.

Comparison of the measured T-z profiles with synthetic profile also indicates possibility of the heat transfer mechanisms other than prevailing conductivity regime. However, differences are small enough so the diffusion equation can be used for further calculations.

There has been a slight increase of mean annual temperatures over the years due to global warming of the present climate change. This increase is more noticeable in the upper parts of the shallow subsurface due to the slow propagation of surface temperature variations into the subsurface. The changes in temperature throughout the year affect the temperature down to depths of about 20 m. It is still not possible to acquire a very reliable long-term tendency on this locality at least at 40 m depth also due to difficulties with the sensors and data logger. The long-term warming amounts to 0.011 °C/yr at 40 m depth taking into account a short period of 2014 to 2015 only. Despite it being a quite short period for deep analysis, it coincides with the absolute error of the measured temperature. The trend is comparable to some of the previous periods. For example: the period from July 2004 to January 2008 shows very similar trend at 40 m depth of 0.013 °C/yr. This is a clear evidence of the recent surface warming provided that the conductive heat transfer is the prevalent mechanism.

Acknowledgements

This study is partly realized with the support of the research program P1-0011 financed by Slovenian Research Agency. The constant support of the Czech Geophysical Institute from Prague of the Czech Academy of Sciences through the NATO Science Programme (EST.CLG 980152) for continuation of this research is greatly acknowledged. The authors are grateful to both reviewers for their constructive remarks which significantly improved the paper.

References

Beck, A.E. & Judge, A.S. 1969: Analysis of Heat Flow Data: A Detailed Observations in a Single Borehole. Geophys. J. R. Astron. Soc., 18/2: 145-158.

Bodri, L. & Čermák, V. 2007: Borehole Climatology. A new method on how to reconstruct climate. Elsevier, Amsterdam, 335 p.

Čermák, V. 1971: Underground temperature and inferred climatic temperature of the past millennium. Paleogeogr., Paleoclimatol., Paleoecol., 10/1: 1-19.

Dědeček, P., Rajver, D., Čermák, V., Š., Šafanda, J. & Krešl, M. 2013: Six years of ground-air temperature tracking at Malence (Slovenia): thermal diffusivity from subsurface temperature data. J. Geophys. Eng., 10/2: 1-9, doi:10.1088/1742-2132/10/2/025012.

Dědeček, P., Šafanda, J. & Rajver, D. 2011: Detection and quantification of local anthropogenic and regional climatic transient signals in temperature logs from Czechia and Slovenia. Clim. Change, 113/2: 787-801, doi:10.1007/s10584-011-0373-5.

Gosar, A. & Ravnik, D. 2007: Uporabna geofizika - univerzitetni učbenik za študente geologije, geotehnologije in rudarstva. Naravoslovnotehniška fakulteta, Oddelek za geotehnologijo in rudarstvo, Ljubljana: 218 p.

Kane, D.L., Hinkel, K.M., Goering, D.J., Hinzman, L.D. & Outcalt, S.I. 2001: Non-conductive heat transfer associated with frozen soils. Glob. Planet. Change, 29/3-4: 275-292.

Kappelmeyer, O. & Haenel, R. 1974: Geothermics with Special Reference to Application. Gebrüder Borntraeger, Berlin: 241 p.

Kubík, J. 1990: Subsurface temperature field of the Bohemian Massif. Studia Geoph. Geod., 34/2: 110-128.

Lachenbruch, H. & Marshall, B.V. 1986: Changing climate. Geothermal Evidence from Permafrost in the Alaskan Arctic. Science, 234/4777: 689-696.

Majorowicz, J., Šafanda, J. & Skinner, W. 2004: A Past Surface Temperature Changes as Derived from Continental Temperature Logs—Canadian and Some Global Examples of Application of a New Tool in Climate Change Studies. Advances in Geophysics, 47: 113–174.

Placer, L. 1998: Structural meaning of the Sava folds. Geologija, 41: 191-221, doi:10.5474/geologija.1998.012

Pleničar, M. & Premru, U. 1977: Osnovna geološka karta SFRJ. L 33-79, Novo mesto. 1:100.000. Beograd: Zvezni geološki zavod.

Rajver, D., Šafanda, J. & Dědeček, P. 2006: Monitoring of air-ground temperature coupling and examples of shallow subsurface warming in Slovenia. Geologija, 49/2: 279-293. doi:10.5474/geologija.2006.021

Rajver, D., Šafanda, J. & Shen, P.Y. 1998: The climate record inverted from borehole temperatures in Slovenia. Tectonophysics, 291/1-4: 263-276, doi:10.1016/S0040-1951(98)00045-6.

Ravnik, D. & Lakovič, G. 1984: Temperaturne meritve v plitvih vrtinah. Osnove meritev in opis električnega termometra LAGO-T. Technical report (in Slovene), GeoZS (previously GZL, Dept. for geophysics), Ljubljana: 15 p.

Shen, P.Y. & Beck, A.E. 1991: Least Squares Inversion of Borehole Temperature Measurements in Functional Space. J. Geophys. Res., 96/B12: 19965-19979, doi:10.1029/91JB01883.

Smerdon, J.E., Pollack, H.N., Čermák, V., Enz, J.W., Krešl, M., Šafanda, J. & Wehmiller, J.F. 2004: Air-ground temperature coupling and subsurface propagation of annual temperature signals. J. Geophys. Res., 109/D21107, doi:10.1029/2004JD005056.

Smerdon, J.E., Pollack, H.N., Čermák, V., Enz, J.W., Krešl, M., Šafanda, J. & Wehmiller, J.F. 2006: Daily, seasonal and annual relationships between air and subsurface temperatures. J. Geophys. Res., 111/D07101, doi:10.1029/2004JD005578.

Strgar, A. 2016: Raziskave povezanosti temperature zraka in plitvega podpovršja na lokaciji vrtine V8 v Malencah pri Kostanjevici. Diplomsko delo (in Slovene). University of Ljubljana, Faculty of natural sciences and engineering, Ljubljana: 45 p.

Šafanda, J. 1994: Effects of topography and climatic changes on the temperature in borehole GFÚ-1. Tectonophysics, 239: 187-197.

Šafanda, J. & Kubík, J. 1992: Evidence of ground surface temperature changes from two boreholes in the Bohemian Massif. Glob. Planet. Change, 6/2: 199-208, doi:10.1016/0921-8181(92)90036-A.

Šafanda, J., Čermák, V. & Bodri, L. 1997: Climate history inferred from borehole temperatures, data from the Czech Republic. Surveys in Geophysics, 18/2: 197-212, doi:10.1023/A:1006535926039.

Šafanda, J. & Rajver, D. 2001: Signature of the last ice age in the present subsurface temperatures in the Czech Republic and Slovenia. Glob. Planet. Change, 29/3-4: 241-257, doi:10.1016/S0921-8181(01)00093-5.

Šafanda, J., Rajver, D., Correia, A. & Dědeček, P. 2007: Repeated temperature logs from Czech, Slovenian and Portuguese borehole climate observatories. Clim. Past, 3/3: 453-462, doi:10.5194/cp-3-453-2007.

Internet source:

Internet 1: http://meteo.arso.gov.si/met/sl/archive/ (07.06.2016)

GEOLOGIJA *60/1*, 145-155, Ljubljana 2017
https://doi.org/10.5474/geologija.2017.011

Heterogeneously composed Lozice fossil landslide in Rebrnice area, Vipava Valley

Heterogeni fosilni plaz Lozice na območju Rebrnic v Vipavski dolini

Andrej NOVAK,[1] Timotej VERBOVŠEK[2] & Tomislav POPIT[2]

[1] Prule 19, SI–1000 Ljubljana; e-mail: andrej.i.novak@gmail.com
[2] Naravoslovnotehniška fakulteta, Oddelek za geologijo, Privoz 11, 1000 Ljubljana;
e-mail: timotej.verbovsek@ntf.uni-lj.si; tomi.popit@ntf.uni-lj.si

Prejeto / Received 8.11.2016; Sprejeto / Accepted 29. 5. 2017; Objavljeno na spletu / Published online 9.6.2017

Key words: fossil landslide, sedimentary facies, 3-D model, lidar, Lozice, Rebrnice, Vipava Valley
Ključne besede: fosilni plaz, sedimentni faciesi, 3-D model, lidar, Lozice, Rebrnice

Abstract

The Rebrnice area in the Upper Vipava Valley, SW Slovenia, is covered by Quaternary slope deposits that are very complex in their genesis and composition. Some of the sediments are deposited in the form of heterogeneously composed fossil landslides. One of these landslides in the Rebrnice area is the Lozice fossil landslide located above the village of Lozice. Analysis of this landslide includes geological mapping of the fossil landslide, classification of different sedimentary facies, 3-D modelling of the landslide, and transverse and longitudinal cross-sections. The geological mapping of the fossil landslide is based on field work mapping and analysis of shaded digital terrain models (DTMs) with a resolution of 1 × 1 m obtained by airborne laser scanning. Lithological data from boreholes and excavation trenches have been classified into eight specific sediment facies that had been defined in previous studies. The 3-D model of the landslide was made using the ArcScene application in the program ESRI ArcGIS. For each sediment facies, a surface was made in the form of a Triangulated Irregular Network (TIN), which gave us a wireframe object. TIN nets were merged in Multipatch objects and exported to 3-D Analyst, where a 3-D model was created. In addition, a shaded DTM image was added for a better placement of the 3-D model in space. Previous findings indicate that deposition of fossil landslides in the Rebrnice area was influenced by palaeotopography. Based on borehole data, transverse and longitudinal cross-sections of the fossil landslide were made and indicate concave depressions under the Lozice fossil landslide. Analysis of the Lozice fossil landslide indicates its complex structure of intertwined heterogeneous sedimentary facies.

Izvleček

Območje Rebrnic v Vipavski dolini v jugozahodni Sloveniji prekrivajo kvartarni sedimenti, katerih izvor in sestava sta zelo kompleksna. Nekateri sedimenti so združeni v večkompozitne fosilne plazove, med katerimi je fosilni plaz Lozice, ki se nahaja nad vasjo Lozice v Vipavski dolini. Analiza fosilnega plaz Lozice vključuje geološko karto, klasifikacijo sedimentnih faciesov, izdelavo 3-D modela fosilnega plazu ter vzdolžnega in prečnega profila plazu na podlagi podatkov vrtin. Geološko karto smo izdelali na podlagi terenskega dela ter senčenega digitalnega modela višin, ločljivosti 1 × 1 m, pridobljenega iz lidarskih posnetkov. Litološke opise sedimentov iz vrtin in sondažnih jaškov smo kategorizirali v osem sedimentnih faciesov. 3-D model fosilnega plazu smo izdelali z aplikacijo ArcScene v programskem okolju ESRI ArcGIS Analyst. Za vsak sedimentni facies smo naredili ploskev v obliki nepravilne trikotniške mreže (TIN), s katero smo dobili žičnati model površja. 3-D model smo v prostor umestili tudi z uporabo senčenih digitalnih modelov višin. Dosedanje raziskave kažejo, da so fosilni plazovi na območju Rebrnic vezani na paleotopografsko podlago. Na podlagi podatkov vrtin smo izdelali vzdolžni in prečni profil plazu, ki kažeta na konkavne zajede na območju fosilnega plazu Lozice. Celotna analiza fosilnega plazu Lozice predstavlja kompleksno zgradbo med seboj prepletajočih se sedimentnih faciesov.

Introduction

Due to the geological and morphological characteristics of the landscape, landslides and mass flows are in general very common in Slovenia, causing damage to infrastructure as well as danger to people (Komac, 2009). In the past decades, landslides and mass movements have been very common natural hazards in the Vipava Valley (Kočevar & Ribičič, 2002; Logar et al., 2005; Kočevar, 2011; Petkovšek et al., 2011). In addition to recent mass movements, geomorphological indicators of the extensive fossil landslides can be found (Kočevar, 2011). Studies of fossil landslides help us to understand why the recent landslides occurred. Examples of fossil landslides in Vipava Valley are the Selo landslide, which is also the biggest known landslide in Slovenia (Popit, 2003; Popit & Košir, 2010; Košir et al., 2015) and the Gradiška Gmajna and Podrta gora fossil landslides. All three processes can be attributed to an earthquake-related event that transformed the fractured carbonates into rock avalanches (Verbovšek et al., 2017). Research and analysis of fossil landslides is very important, since they can provide us with a more accurate understanding of why and how recent landslides have occurred and relate them to base rock geology, tectonics, and local/regional climate events in the research area.

In this paper we present sedimentary characteristics of the heterogeneously composed Lozice fossil landslide. The landslide is located above the village of Lozice in the Rebrnice area in the Upper Vipava Valley. Previous research on this area and research done during the construction of the Razdrto–Vipava motorway (Skok, 2001, 2002; Popit & Košir, 2010) showed that half of the Rebrnice area is covered by scree deposits in the morphological shape of a fan (Jež, 2005). These fans were created by sedimentary gravity mass movements (Popit & Košir, 2010). Large quantities of slope deposits are concentrated in the forms of sedimentary bodies, formed as multi-component fossil landslides (Popit & Košir, 2010; Popit et al., 2013; Popit, 2016). On the basis of the lithological, stratigraphic and architectural characteristics of the slope deposit, in total sixteen facies were separated in the broader Rebrnice area, indicating the final articles of diverse sedimentary processes within complex and often interlaced and interdependent transport mechanisms in this area (Popit, 2016). Previous studies (Habič, 1968; Jež, 2005; Popit et al., 2011; Popit et al., 2014; Popit, 2016) also suggest that the deposition of Quaternary slope deposits of fossil landslides is bound by depressions and paleo-ravines in Eocene flysch.

Before and during the construction of the Razdrto–Vipava motorway, a large number of boreholes and excavation trenches were drilled and excavated in the vicinity of the motorway route. During the construction of this motorway, a portion of the Lozice fossil landslide started to creep due to construction (Jež, 2007). To prevent further movement, an intensive geotechnical research was performed. During that time, data were gathered in geotechnical reports (Skok, 2001, 2002), which show that the Lozice fossil landslide is heterogeneously composed of different sediments. In the analysis of the slope deposit of Lozice fossil landslide, these sediments were categorized into eight sedimentary facies (Popit, 2016), which follow in a stratigraphic order.

With a combination of existing information - lithological data from boreholes, studies regarding detailed sedimentological facies definitons (Popit, 2016) and available shaded digital terrain models (DTMs) obtained by airborne laser scanning, we have integrated this data with several new approaches, never published before. First, mapping of the Lozice fossil landslide was performed to outline the landslide and define its basic engineering-geological properties. From all available data, an informative 3-D model of Lozice fossil landslide has been made, based also on a detailed engineering-geological map of the fossil landslide, produced in ESRI ArcGIS. Such 3-D model, based on detailed facies recognition of the very heterogeneously composed Lozice landslide has not yet been done before for any landslide in the broader region, so we consider this an entirely new approach and result. Lidar airborne laser scanning, performed in the period of 2014–2015 (provided by the Surveying and Mapping Authority of the Republic of Slovenia), was also used to determine the extension of the fossil landslide. Lidar technology has already been successfully used in previous studies (Popit et al., 2011; Popit et al., 2014) to determine geomorphological characteristics on Rebrnice area. In addition, on the basis of borehole data, transverse and longitudinal cross-sections of the Lozice fossil landslide have been made to present the paleo-topography underneath the landslide.

Geological setting

The geological structure of the southwest part of Slovenia is composed of thrusts, nappes, and thrust sheets formed due to thrusting in the early Tertiary and neotectonic faults (Placer, 1981, 2008). The Upper Vipava Valley belongs to three different nappes (from structurally lowest to highest): the Komen, the Snežnik and the Hrušica nappes. The Rebrnice area is defined by a thrust front of Mesozoic carbonates of the Hrušica nappe, which is overthrusted on Tertiary flysch of the Snežnik nappe (Fig. 1). The upper part of the slope of the Vipava Valley is marked by steep carbonate cliffs, while the lower parts of the slope are more gently sloping and are composed of flysch bed rock covered by sedimentary bodies and Quaternary slope deposits (Fig. 1) with very complex genesis and composition (Popit & Košir, 2010; Popit et al., 2014; Popit, 2016). These sedimentary bodies are composed of several beds of mud- and matrix- to clast-supported gravel of carbonate and sandstone clasts and/or blocks (Popit, 2016).

The main objectives of the paper were first the combination of engineering-geological map with already existing data from boreholes and lidar-derived DTM. Engineering-geological mapping was used to determine the extension of the fossil landslide, with field mapping of the facies visible on the surface of the fossil landslide. Second objective was to integrate the data into a 3-D model, based on detailed facies recognition of the fossil landslide. Shaded DTM based on airborne laser scanning with a resolution of 1 × 1 m was very helpful at this stage. It provided the bare earth topography without the vegetation or other artificial constructions (buildings). We analysed information from 42 boreholes and eight excavation shafts made during the construction of Razdrto–Vipava motorway. Boreholes are distributed in a small area alongside and topographically above the motorway. Based on lithological data from boreholes and excavation trenches, sediments were categorized according to the specific sedimentary facies that were defined in previous studies (Popit & Košir,

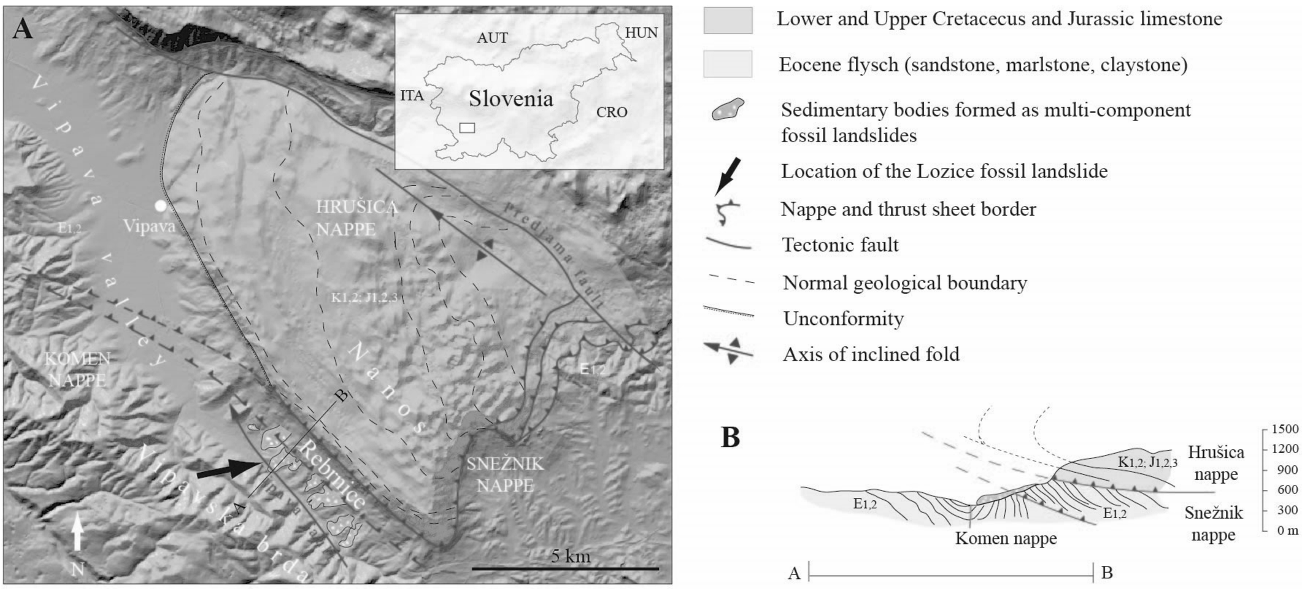

Fig. 1. Location of the studied area with (A) simplified geological map and (B) cross-section of the Vipavska Brda, the Upper Vipava Valley, and the Nanos plateau. Compiled from Placer (1981, 2008) and Popit et al. (2014). The location of the Lozice fossil landslide is marked with a pointer in Fig 1A. *The reader should refer to the online version of the article for the colour figure.*

Methods

Analysis of the Lozice fossil landslide included engineering-geological mapping of the landslide, classification of sediments based on data from geotechnical reports (Skok, 2001, 2002), and classification of facies from previous studies (Popit & Košir, 2010; Popit, 2016), resulting in an informative 3-D model of a part of the fossil landslide and cross-sections through the fossil landslide.

2010; Popit et al., 2013; Popit, 2016). Sedimentary facies were later organized as GIS information layers, including the borehole name, depth, and geographic coordinates, and categorized facies. For each sedimentary facies logged in the borehole or excavation shaft, the data on its thickness and its upper and lower layers are given in metres above sea level and from the depth of the upper and lower sediment layers from the borehole mouth.

The 3-D model of the landslide was made with the ArcScene application in ESRI ArcGIS software. For each facies layer, the upper and lower surfaces were made in the form of Triangulated Irregular Network (TIN) surface, which produced a wireframe object. TINs were made with 3-D Analyst Toolbox and were merged in 3-D Multipatch objects in ArcGIS. These were later exported to 3-D Analyst (Internet 1).

Data from boreholes and excavation shafts were also used to create transverse and longitudinal profiles through the landslide body. In these profiles, each facies is presented in a stratigraphic column with its corresponding thickness. Based on both profiles, a representation of the paleo-topography in the Eocene flysch under the fossil landslide was made, as well as correlations of some facies between the boreholes, in order to gain a better insight in a complex landslide body structure.

Results and discussion

Classification of sedimentary facies and field mapping

Five facies compose the body of the heterogeneously composed fossil landslide, while two form the bedrock underneath the landslide and one represents younger sediments deposited on the surface of the landslide. The facies (Popit & Košir, 2010; Popit et al., 2013; Popit, 2016) (generally ordered by top-most units) are as follows:

- (OGc) Facies of scree deposit of younger limestone gravel sediments, partially covering the surface of the fossil landslide and derives from carbonate cliffs via rock falls and toppling. In the topographically lower parts of its depositional area, the gravel is strongly agglutinated to the carbonate breccia. The facies is not part of the body of the fossil landslide.
- (C(M)Sc) Clast- (conditionally matrix-) supported carbonate gravel with a subordinate amount of carbonate cobbles and big blocks of a few cubic metres. Layers of this facies are from one to a few metres thick with sharp, mainly erosional and normal contacts. The facies is part of the body of the fossil landslide.
- (MCSfc) Matrix- to clast-supported sandstone, marlstone, and mudstone gravel ("flysch" gravel), with subordinate carbonate gravel. Clasts are occasionally normally graded in layers with erosional contacts deposited in the forms of lenses onto older sediments. The facies is part of the body of the fossil landslide.
- (MSf-B) Rare matrix-supported sandstone, marlstone, and mudstone gravel ("flysch" gravel), with clays and silts. Sediment is part of the body of the fossil landslide.
- (MCScf) Matrix to clast-supported carbonate gravel with subordinate sandstone, marlstone, and mudstone gravel ("flysch" gravel) with chaotic textures. The facies is part of the body of the fossil landslide.
- (MScf) Matrix- to clast-supported carbonate gravel, subordinate sandstone, marlstone, and mudstone gravel ("flysch" gravel) with clays and silts. The facies forms layers and lenses a few metres thick with sharp contacts. The facies is part of the body of the fossil landslide.
- (Wf) This facies of weathered Eocene flysch (sandstone, marlstone and mudstone) is part of the bedrock underneath the fossil landslide.
- (f) This facies of Eocene flysch is part of the bedrock underneath the fossil landslide.

Facies OGc, C(M)Sc, MCSfs, and f are visible on the surface and, on the basis of their outcrops, the geological map of the fossil landslide with its boundary was made (Figure 2). On the surface of the fossil landslide, the boundary between facies C(M)Sc and facies OGc is gradual between the heights of 400 and 450 m above sea level. Since the transition from facies C(M)Sc to facies OGc is gradual, the upward extension and the crown of the fossil landslide have been determined mainly by shaded DTMs obtained by airborne laser scanning and also by the last outcrops of the facies C(M)Sc on both flanks of the fossil landslide. With the exception of scree deposits, the surface of the Lozice landslide is covered by facies C(M)Sc and covers an area of 48 ha. It is divided into two fossil landslides, Lozice 1 and Lozice 2 (Fig. 2). Lozice 1 is smaller and covers 6 ha, while the Lozice 2 landslide is bigger and covers an area of 42 ha (Fig. 2). They are divided by a small narrow stream, which cuts and erodes probably all facies down to the bedrock of Eocene flysch (f).

Classification of facies and borehole data of the Lozice fossil landslide

Facies occur at different depths with lateral variableness in all 42 boreholes and eight excavation shafts (Table 1). The most common facies is C(M)Sc, which it is found in 32 boreholes and excavation shafts and overlays all the other facies. This is supported by field work data. Facies Wf is logged in 35 boreholes and excavation shafts and Eocene flysch (f) in 37. Another two

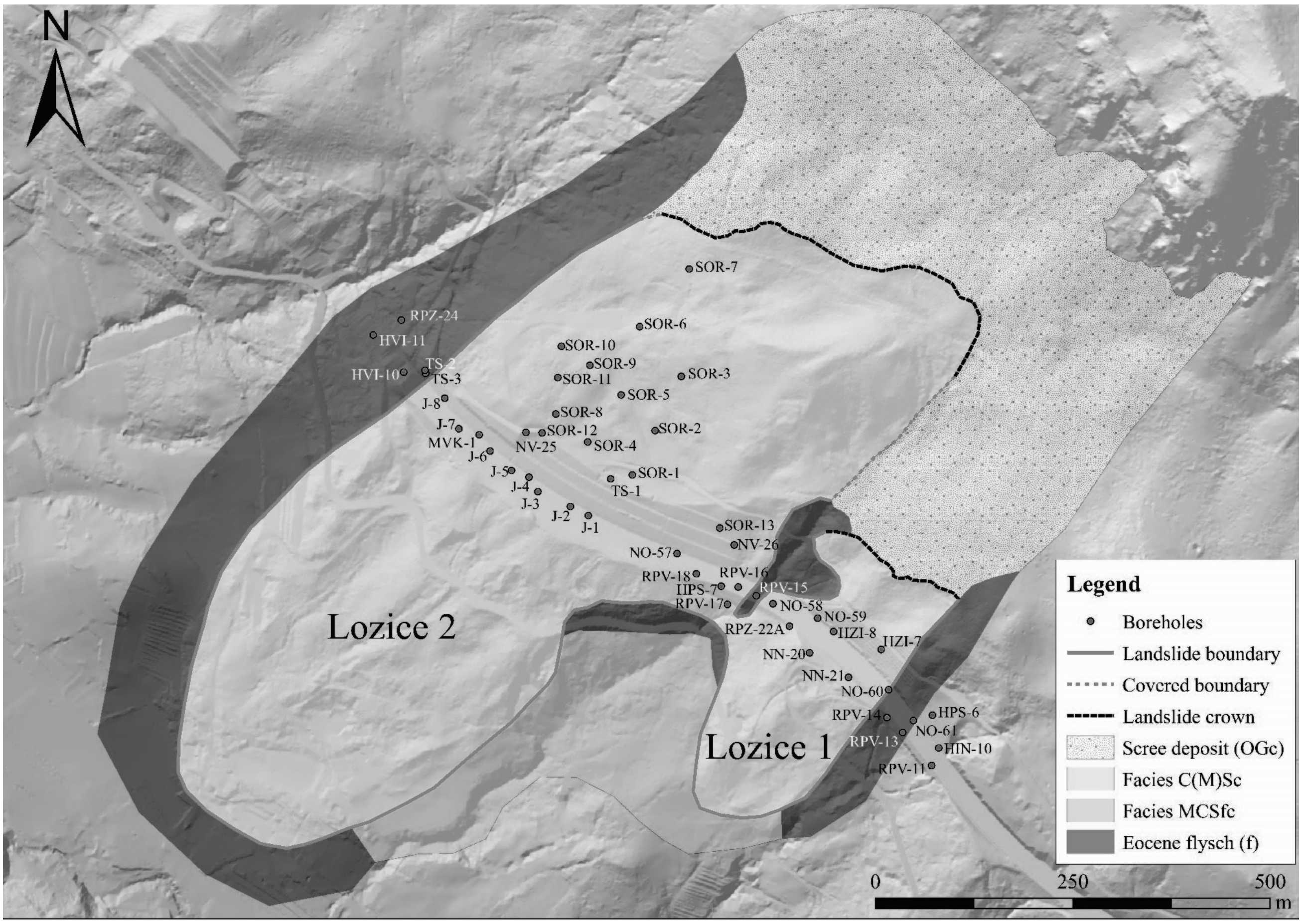

Fig. 2. Engineering-geological map of the heterogeneously composed Lozice fossil landslide, divided into two fossil landslides (after Novak, 2013; Popit, 2016). Boreholes and excavation shafts used as the data source in this research are located alongside the motorway. *The reader should refer to the online version of the article for the colour figure.*

common facies are MCSfc and MSf-B. Facies MCSfc is logged in 23 boreholes and excavation shafts and facies MSf-B in 17 boreholes and excavation shafts. Another two facies, MCScf and MScf, are logged in only a few boreholes or excavation shafts and are scattered all over the body of the Lozice fossil landslide. Later on, in the 3-D model, we represented only the five most common facies [C(M)Sc, MCSfc, MSf-B, Wf, and f] that are found in the body of Lozice fossil landslide. Since the other two types of facies, MCScf and MScf, are less common, we assume that they form lenses in the body of the landslide. Some facies are logged twice in two boreholes (SOR-10 and HZI-7). We assume that the reason for this is the intercalated lenses inside the body of the Lozice fossil landslide. The thickness of the Lozice fossil landslide varies and was estimated from borehole data at their locations. The deepest locations of bedrock based on the depth of facies Wf and f are at 37.7 in borehole SOR-12, 34.9 m in SOR-11, and 34.0 m in SOR-10. Other greater depths are at 21.5 m in SOR-9, 19.9 m in TS-1, 19.3 in SOR-13, 16.8 m in SOR-5, and 16.1 in SOR-4. These boreholes are located in the central and thickest part of the Lozice 2 fossil landslide. In other areas, the landslide is much shallower: it does not exceed 15 m in thickness and has an average thickness of 10.7 m; however the thickness of Lozice 2 fossil landslide is much greater than that of Lozice 1 fossil landslide. Based on borehole data, the average thickness of the Lozice 1 fossil landslide is 6.2 m, while the average thickness of the Lozice 2 fossil landslide is 13.3 m.

The water table was measured in boreholes SOR-1, 2, 3, 4, 6, 7, 8, 9, 10, and 13 between April and May 2002 (except for SOR-13, which was measured in July 2002). Depths to the water table varied a lot in this period, ranging between 8.9 and 20.2 m. There was no spatial correlation among the boreholes. As there was no continuous monitoring of the water tables, we cannot comment on the influence of ground water on the landslide movements. However, the calculated height of the water column above the well bottoms ranged from 1.4 to 30 m (12 m on aver-

Table 1. Distribution of facies in boreholes and excavation shafts of the Lozice fossil landslide. Data for total borehole or excavation shaft depth and facies thickness are given in metres.

SOR-1	**SOR-2**	**SOR-3**	**SOR-4**	**SOR-5**
C(M)Sc (10.3 m)	C(M)Sc (3.8 m)	C(M)Sc (0.8 m)	C(M)Sc (10.2 m)	C(M)Sc (5.6 m)
MScf (0.8 m)	MCSfc (7.7 m)	MCSfc (9.9 m)	MCScf (3.4 m)	MSf-B (11.0 m)
MCSfc (2.0 m)	Wf (0.4 m)	MSf-B (2.6 m)	MCSfc (2,3 m)	Wf (1.0 m)
Wf (5.0 m)	f (9.9 m)	Wf (2.0 m)	Wf (2.7 m)	f (4.2 m)
f (3.2m)	Total depth: 21.8 m	f (8.5 m)	f (5.2 m)	Total depth: 21.8 m
Total depth: 21.3 m		Total depth: 23.8 m	Total depth: 23.8 m	
SOR-6	**SOR-7**	**SOR-8**	**SOR-9**	**SOR-10**
C(M)Sc (5.5 m)	C(M)Sc (1.2 m)	C(M)Sc (11.7 m)	C(M)Sc (10.4 m)	C(M)Sc (9.8 m)
MCSfc (3.3 m)	MCSfc (8.2 m)	MScf (1.2 m)	MSf-B (6.2 m)	MCScf (6.4 m)
Wf (1.8 m)	f (11.4 m)	MCSfc (8.2 m)	MCSfc (4.7 m)	MCSfc (0.8 m)
f (10.9 m)	Total depth: 20.8 m	MSf-B (18,9 m)	Wf (2.8 m)	MSf-B (5.9 m)
Total depth: 21.5 m		Wf (1.0 m)	Total depth: 24.1 m	MCSfc (3.3 m)
		f (3.0 m)		MSf-B (6.1 m)
		Total depth: 44.0 m		MCSfc (1.5 m)
				Wf, (6.0 m)
				Total depth: 39.8 m
SOR-11	**SOR-12**	**SOR-13**	**TS-1**	**TS-2**
C(M)Sc (11.8 m)	C(M)Sc (11.1 m)	C(M)Sc (1.6 m)	C(M)Sc (13.8 m)	f (12 m)
MSf-B (19.1 m)	MSf-B (4.9 m)	MCSfc (16.4 m)	MCScf (0.4 m)	Total depth: (12.0 m)
MCSfc (3.8 m)	MCSfc (21.7 m)	Wf (2.7 m)	MCSfc (5.7 m)	
f (0.2 m)	f (1.3 m)	Total depth: 20.7 m	Wf, (1.1 m)	
Total depth: 34.9 m	Total depth: 39.0 m		Total depth: 21.0	
TS-3	HPS-6	HPS-7	HIN-10	HVI-11
f (12 m)	MCSfc (7.7 m)	C(M)Sc (2.5 m)	MCSfc (10.2 m)	MCSfc (0.9 m)
Total depth: (12.0 m)	f (9.0 m)	MCSfc (2.3 m)	Wf (1.5 m)	Wf (3.5 m)
	Total depth: 16.7 m	Wf (2.0 m)	f (7.0 m)	f (10.4 m)
		f (14,0 m)	Total depth: 18.7 m	Total depth: 14.8 m
		Total depth: 20.8 m		
RPV-11	**RPV-13**	**RPV-14**	**RPV-15**	**RPV-16**
f (16.8 m)	MCSfc (6.4 m)	f (9.8 m)	MCScf (1.4 m)	MCSfc (6.6 m)
Total depth: 16.8 m	Wf (0.5 m)	Total depth: 9.8 m	MCSfc (4.6 m)	f (8.2 m)
	f (6.8 m)		f (5.8 m)	Total depth: 14.8 m
	Total depth: 13.7 m		Total depth: 11.8	
RPV-17	**RPV-18**	**NO-57**	**NO-58**	**NO-59**
MCScf (4.7 m)	C(M)Sc (1.5 m)	C(M)Sc (0.7 m)	MSf-B (0.8 m)	MCScf (1.2 m)
Wf (2.0 m)	MSf-B (2.2 m)	Wf (3.2 m)	Wf (5.0 m)	Wf (2.1 m)
f (6.0 m)	Wf (3.2 m)	f (15.9 m)	f (6.0 m)	f (4.5 m)
Total depth: 12.7 m	f (4.8 m)	Total depth: 19.8 m	Total depth: 11.8 m	Total depth: 7.8 m
	Total depth: 11.7 m			
NO-60	**NO-61**	**HZI-7**	**HZI-8**	**MVK-1**
C(M)Sc (0.6 m)	MSf-B (1.1 m)	C(M)Sc (3.3 m)	C(M)Sc (10.0 m)	C(M)Sc (11.2 m)
Wf (5.2 m)	MCSfc (2.2 m)	MCScf (3.0 m)	MSf-B (0.8 m)	MSf-B (0.7 m)
f (6.9 m)	Wf (0.5 m)	MCSfc (2.8 m)	Wf (6.0 m)	Wf (1,2 m)
Total depth: 12.7 m	f (3.0 m)	MCScf (1.0 m)	f (9.0 m)	f (10.3 m)
	Total depth: 6.8 m	Wf (2.5 m)	Total depth: 25.8 m	Total depth: 23.4 m
		f (8.5 m)		
		Total depth: 21.1 m		
HVI-10	**NN-20**	**NN-21**	**RPZ-22A**	**RPZ-24**
MCSfc (0.6 m)	C(M)Sc (6.0 m)	C(M)Sc (3.6 m)	MScf (3.7 m)	f (5.3 m)
Wf (4.1 m)	Wf (7.6 m)	MScf (1.8 m)	Wf (2.7 m)	Total depth: 5.3 m
f (10.1 m)	f (1.0 m)	Wf (4.7 m)	f (5.3 m)	
Total depth: 14.8 m	Total depth: 14.6 m	f (0.4 m)	Total depth: 11.7 m	
		Total depth: 10.5 m		
NV-25	**NV-26**	**J-1**	**J-2**	**J-3**
C(M)Sc (10.0 m)	C(M)Sc (8.1 m)	C(M)Sc (1.7 m)	C(M)Sc (1.6 m)	C(M)Sc (0.6 m)
Total depth: 10.0 m	Wf (1.9 m)	MSf-B (1.0 m)	MSf-B (1.6 m)	MSf-B (0.8 m)
	f (1.7 m)	Wf (0.4 m)	f (0.2 m)	MCScf (3.0 m)
	Total depth: 11.7 m	Total depth: 3.1 m	Total depth: 3.4 m	Total depth: 4.4 m
J-4	**J-5**	**J-6**	**J-7**	**J-8**
MCScf (1.7 m)	C(M)Sc (0.2 m)	C(M)Sc (3.0 m)	C(M)Sc (1.8 m)	C(M)Sc (4.2 m)
Wf (0.7 m)	MSf-B (1.4 m)	Total depth: 3.0 m	MSf-B (1.0 m)	Total depth: 4.2 m
Total depth: 2.4 m	Wf (0.4 m)		Wf (0.2 m)	
	Total depth: 2.0 m		Total depth: 3.0 m	

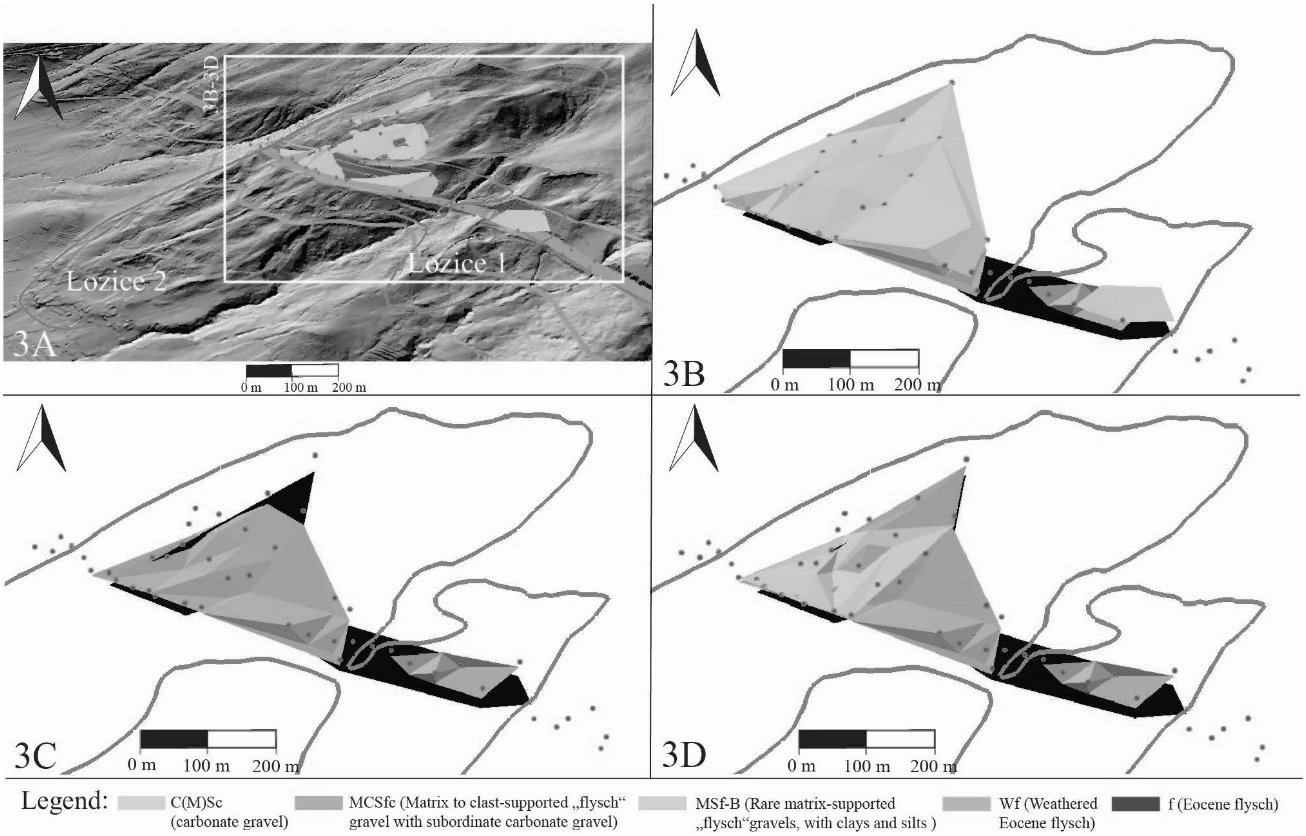

Fig. 3. 3-D model of the Lozice fossil landslide. Fig. 3A shows the fossil landslide on shaded digital terrain models (DTMs) with a resolution of 1 × 1 m obtained by airborne laser scanning with boreholes and facies C(M)Sc, which is visible on the surface of the landslide. Figs. 3B to 3D show the enlarged area of the fossil landslide where the 3-D model is located. Facies C(M)Sc (Fig. 3B, yellow) overlies all the other facies. In Fig. 3C, the Eocene flysch (dark brown) is covered by weathered flysch (light brown) and both facies represent bedrock. Facies MCSfc (violet) and facies MSf-B (light blue) in Fig. 3D lie above bedrock and are intertwined with each other. *The reader should refer to the online version of the article for the colour figure.*

age) in the relatively normal water table season. The height of water above the upper flysch surface was 0.4 to 6 m in the boreholes SOR-1, 2, 3, 4 and 6, 20.8 m in SOR-8, and 2.3 m below the upper flysch surface in SOR-7. Boreholes SOR-9, 10, and 13 did not encounter the flysch facies. Based on these data, we consider the presence of the water to be quite important, as more than 10 m, on average, of saturated sediments and flysch above the borehole bottom and a few metres of saturated deposits above the less permeable flysch contributes to weathering of these sediments and consequently lower their geomechanical properties. Further monitoring of water levels should be performed to investigate the yearly water table fluctuations.

The Razdrto–Vipava motorway is also being built across Lozice fossil landslide. Clast- (conditionally matrix-) supported carbonate gravel deposit of facies C(M)Sc is deposited on facies MSf-B and flysch rocks. The sediment of facies C(M)Sc is unstable and is gradually sliding downslope because of slope inclination, underground water, and clayey zones of MSf-B facies. The recent movements of reactivated parts of the Lozice fossil landslide were measured by means of inclinometer wells and by data from some recent movement in the Rebrnice area. Sliding has already caused regional road deformations, cracks on some new motorway sections, and damage to objects in the village of Lozice. The movements in the geomechanical-inclinometer wells measure between a few millimetres and a maximum of 15 mm monthly. A scarp up to 3 m wide formed high up on the slope. The landslide was stopped by the anchor pile wall (Jež, 2007).

Three-dimensional model of Lozice fossil landslide

Although the map in Figure 2 shows mostly one prevailing facies, the structure of the landslide is much more complex, as inferred from the boreholes. Therefore, a simple 3-D model (Fig. 3) represents the position of the most common facies in the space inside the body of Lozice fossil landslide. Boreholes are not distributed evenly over the surface of the fossil landslide but are

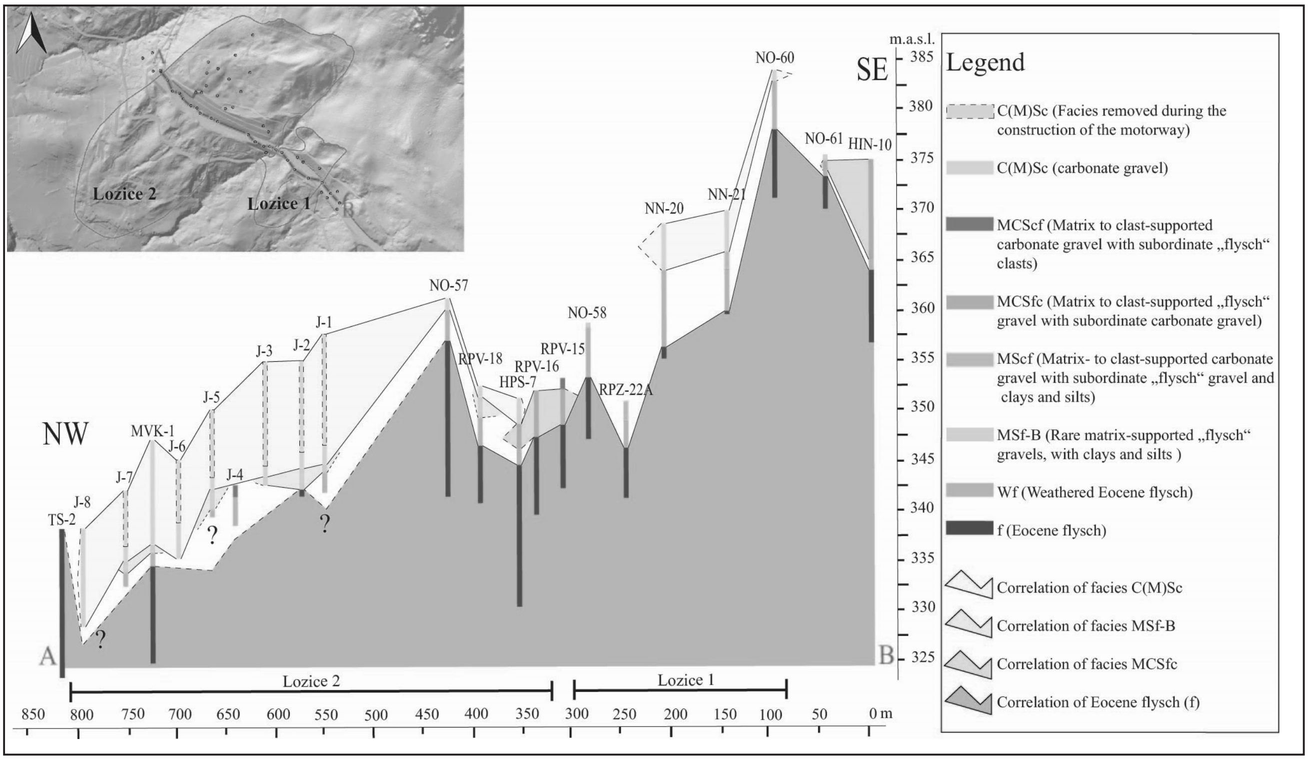

Fig. 4. Transverse cross-section through the Lozice fossil landslide with logged facies and correlations with facies C(M)Sc, MSf-B, MCSfc, and Eocene flysch. *The reader should refer to the online version of the article for the colour figure.*

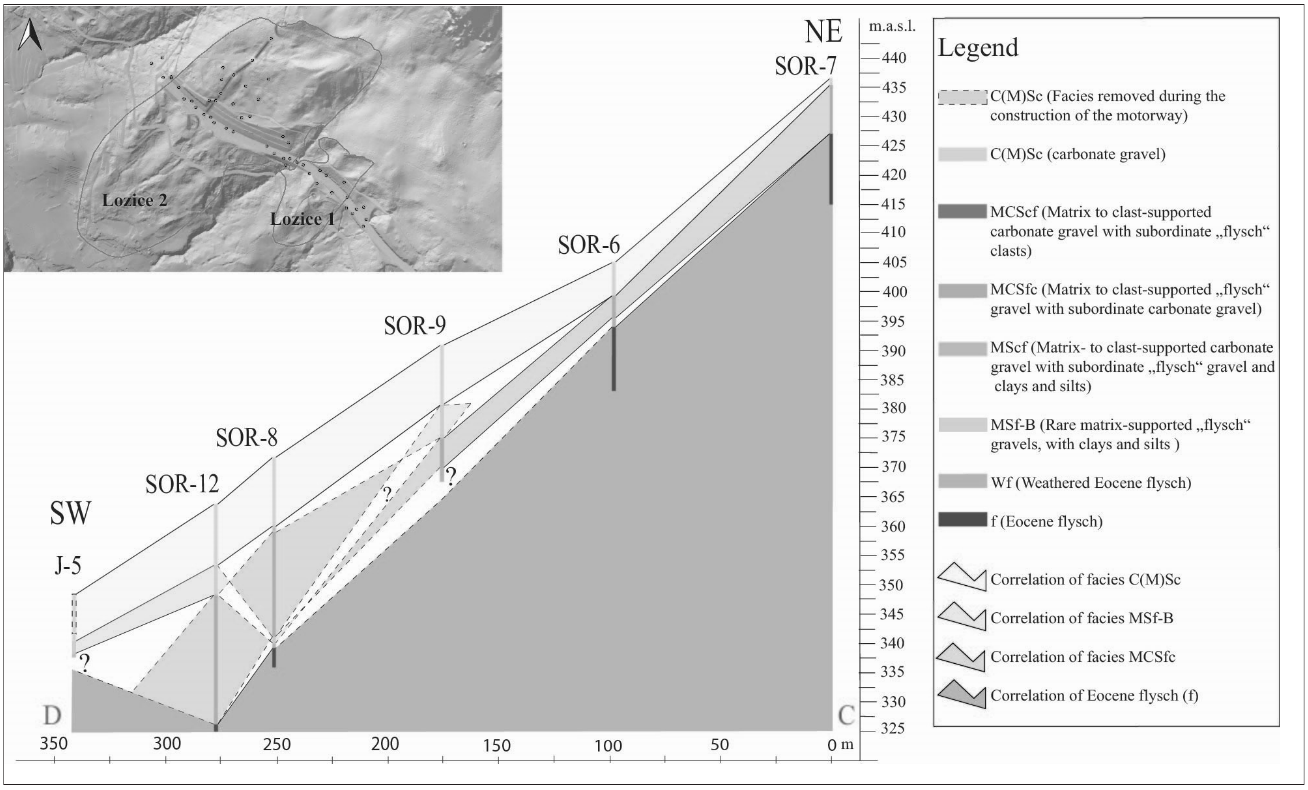

Fig. 5. Longitudinal cross-section through the Lozice 2 fossil landslide with logged facies and correlations with facies C(M)Sc, MSf-B, MCSfc, and Eocene flysch. *The reader should refer to the online version of the article for the colour figure.*

concentrated in a small area alongside and topographically above the motorway. This area covers only 8 ha, which is about one-fifth of the landslide area. That is why the 3-D model, presented in this paper, has an informative nature but still offers a more detailed insight into a smaller part of the landslide. Obviously the facies are distributed vertically in a stratigraphic order. Facies C(M)Sc is stratigraphically the highest and overlays all other facies (Fig. 3A and 3B). It also extends over the complete surface of the landslide, which has also been proven by field mapping. The bedrock is represented by Eocene flysch (f) and weathered Eocene flysch (Wf) facies (Fig. 3C). Flysch (f) and weathered flysch (Wf) facies are overlaid by the MCSfc and MSf-B facies (Fig. 3D) in the Lozice 2 fossil landslide. Facies C(M)Sc, MCSfc, and MSf-B represent the body of the fossil landslide that has been deposited over the flysch facies (f) and weathered flysch (Wf). The facies of MCSfc and MSf-B are clearly intercalated (Fig. 3D), while the facies C(M)Sc overlies all other facies (Fig. 3B). Unfortunately, the data of the Lozice 1 fossil landslide were insufficient to create a 3-D representation of any facies layers other than the bedrock (facies f and Wf) and overlying facies C(M)Sc.

Transverse and longitudinal cross-sections over the Lozice fossil landslide

A transverse cross-section (Fig. 4) based on borehole data shows a complex composition of the fossil landslide. In the area of the fossil landslide Lozice 1, facies C(M)Sc is laying above the facies Wf and f with a few lenses of facies MCSfc and MScf. In the area of Lozice 2, facies C(M)Sc is present on top of all the boreholes. Its thickness varies from 1 m (boreholes RPV-18 and NO-57) up to 10 m (boreholes MVK-1 and J8). In the excavation trenches (from J-1 to J-8) we have estimated the thickness of facies C(M)Sc based on elevation in the topographic map. A portion of facies C(M)Sc was dug and removed during construction of the motorway, but in most of the excavation trenches, it was still present. The thickness of the facies in the cross-section was extended up to the topographic elevation before the construction of the motorway. Other facies are not present in all of the boreholes. Facies MSf-B is most common, with a maximum thickness of 2.5 m, while facies MCScf is present only in the form of thin lenses (not more than 1 m thick). Facies C(M)Sc is not present in boreholes between fossil landslides Lozice 1 and Lozice 2 due to stream erosion. Facies Wf and f lie under the fossil landslide. They are present in almost all boreholes, but only in half of the excavation trenches. At those locations, the depth of the fossil landslide is unknown. Since the cross-section is based on the location of boreholes, it is not perpendicular to the fossil landslide. A perpendicular cross-section would give us a better cross-section of paleo-topography. The paleo-topography is indicated in the Wf and f facies in the transverse cross-section. Concave depressions are best seen in the case of the Lozice 2 fossil landslide, which confirms the findings of previous studies by Habič (1968), Jež (2005), Popit et al. (2011), Popit et al. (2014) and Popit (2016) that the deposition of fossil landslides in the Rebrnice area was bounded by depressions and paleo-ravines in the Eocene flysch bedrock.

A longitudinal cross-section was made for the Lozice 2 fossil landslide and it passes through five boreholes and one excavation trench (Fig. 5). Facies C(M)Sc is again situated on top, and underneath it are other sediments. The thickness of facies C(M)Sc is over 10 m. In the profile, the overlapping and underlapping of facies MCSfc and facies MSf-B are again visible, as in the 3-D model.

Conclusion

In the paper we have integrated previously available data from boreholes (basic lithological descriptions), sedimentological facies definitions and shaded lidar-derived DTM, with new approaches, never published before: mapping of the landslide, resulting in a detailed map, and more importantly, integration of all data in a 3-D model of the landslide. Such a model, based on facies description of the heterogeneously composed Lozice landslide has not yet been done before. Although the model could not be done for the complete area of the landslide due to presence of boreholes only along the narrow band of the highway, our results show that it can be useful in 3-D visualization and further possible volume quantification of very detailed sedimentological descriptions. Such approach also enables to focus on the individual sedimentological unit, often irregularly-shaped and difficult to visualize in 3-D cross-sections. In the future, the model could be improved by drilling additional boreholes in the complete area of the landslide, and most importantly, in such a case it would be possible to calculate the volumes of each sedimentary facies. Field mapping does not reveal what is below the surface, and separate facies cannot be distinguished on such precise level with ground penetrating radar profiling (or other geophysical research). The only possible method of obtaining the data is therefore by drilling several more boreholes and/or excavation trenches. With both of these, lenses and intertwined facies are clearly distinguished.

A detailed engineering-geological map supported with hillshaded DTM shows, that the Lozice fossil landslide covers an area of 48 ha. It can be broadly divided into the smaller eastern fossil landslide (Lozice 1, 6 ha) and the larger western fossil landslide (Lozice 2, 42 ha), separated by a small stream that has already eroded most of the sediments that belong to the body of the fossil landslide. Both parts are composed of several different facies, making them highly heterogeneous. Based on borehole data we determined, in detail, eight different sedimentary facies, which clearly indicate multiple interlaced and interdependent depositional events and various gravity mass-movement processes ranging from slides to flows. The bedrock is composed of facies of Eocene flysch (f) and weathered Eocene flysch (Wf), which form the base on which the landslide sediments are deposited. The base is clearly visible in cross-sections as paleo-topography, thus confirming previous research findings that the fossil landslides in Rebrnice are deposited and bounded by paleo-topography. Among other facies, the three most common, deposited in stratigraphic order, are facies MCSfc, MSf-B, and C(M)Sc. Facies MCSfc is composed of matrix- to clast-supported sandstone, marlstone, and mudstone gravel with subordinate carbonate gravel. Facies MSf-B is formed of rare matrix-supported sandstone, marlstone, and mudstone gravel with clays and silts, while facies C(M)Sc is composed of clast- (conditionally matrix-) supported carbonate gravel with a subordinate amount of carbonate cobbles and of few cubic metres big blocks. Facies C(M)Sc covers the surface of the fossil landslide, while facies MCSfc and facies MSf-B lie below facies C(M)Sc and occasionally intercalate with each other. Facies MCScf and MScf are less common and we assume that they form lenses in the body of the fossil landslide. Similar lenses were also recognized in other fossil landslides in the Rebrnice area (Popit & Košir, 2010; Popit et al, 2013). Sediments of Lozice fossil landslide are now partially covered (especially in the upper part of the landslide) by the youngest scree deposit (OGc). Due to its highly heterogeneous composition, the genesis and movement of the landslide in the geological past is very complex. It's complex structure, presence of the water table, clayey zones and recent reactivated part of the fossil landslide suggest that future movement is possible.

Acknowledgements

Borehole investigation in the Rebrnice area were performed by the GEOT d.o.o. The field work in the Rebrnice area was also performed by the Ivan Rakovec Institute of Palaeontology ZRC SAZU in the framework of the Project of Geological Monitoring on the Motorway Section Razdrto-Vipava, founded by DARS Motorway Company in the Republic of Slovenia.

References

Habič, P. 1968: Kraški svet med Idrijco in Vipavo: prispevek k poznavanju razvoja kraškega reliefa = The Karstic region between the Idrijca and Vipava rivers: a contribution to the study of development of the Karst relief. Dela SAZU, Ljubljana: 243.

Jež, J. 2005: Ocena možnosti nastopanja regionalnih plazov na območju Rebrnic nad Vipavsko dolino. Diplomsko delo. Univerza v Ljubljani, Naravoslovnotehniška fakulteta, Oddelek za geologijo, Ljubljana: 74 p.

Jež, J. 2007: Vzroki in mehanizem zemeljskega plazenja na Rebrnicah v Vipavski dolini. Geologija, 50/1: 55–63, doi:10.5474/geologija.2007.005.

Kočevar, M. 2011: Problem stabilnosti terena ob narivnem robu mezozoiskih karbonatnih kamnin na eocenske fliše v jugozahodni Sloveniji. In: Petkovšek, A. & Klopčič, J. (eds.): 12. Šukljetovi dnevi, Ajdovščina 30. september 2011. Slovensko geotehniško društvo, Zbornik: 39–50.

Kočevar, M. & Ribičič, M. 2002: Geološke, hidrogeološke in geomehanske raziskave plazu Slano blato. Geologija, 45/2: 427–432, doi:10.5474/geologija.2002.043.

Komac, M. 2009: Geološko pogojene nevarnosti. In: Pleničar, M., Ogorelec, B. & Novak, M., (eds.): Geologija Slovenije. Geološki zavod Slovenije, Ljubljana: 589-596.

Košir, A., Popit, T. & Verbovšek, T. 2015: The Selo landslide: A long runout rock avalanche? In: Rožič, B. (ed.): Razprave, poročila = Treatises, reports / 22. posvetovanje slovenskih geologov = 22nd Meeting of Slovenian Geologists. Geološki zbornik, 23: 92-95.

Logar, J., Fifer Bizjak, K., Kočevar, M., Mikoš, M., Ribičič, M. & Majes, B. 2005: History and present state of the Slano Blato landslide. Natural Hazards and Earth System Sciences, 5: 447–457, doi:10.5194/nhess-5-447-2005.

Novak, A. 2013: Fosilni plaz Lozice na območju Rebrnic v Vipavski dolini. Diplomsko delo. Univerza v Ljubljani, Naravoslovnotehniška fakulteta, Oddelek za geologijo, Ljubljana: 42 p.

Petkovšek, A., Fazarinc, R., Kočevar, M., Maček, M., Mejes, B. & Mikoš, M. 2011: The Stogovce landslide in SW Slovenia triggered during the September 2010 extreme rainfall event. Landslides, 8/4: 499–506, doi:10.1007/s10346-011-0270-z.

Placer, L. 1981: Geološka zgradba jugozahodne Slovenije. Geologija, 24/1: 27–60.

Placer, L. 2008: Vipavski prelom = Vipava fault (Slovenia). Geologija, 51/1, 101–105, doi:10.5474/geologija.2008.011.

Popit, T. 2003: Pleistocenski sedimenti blatno-drobirskih tokov pri Selu v Vipavski dolini. Diplomsko delo. Univerza v Ljubljani, Naravoslovnotehniška fakulteta, Oddelek za geologijo, Ljubljana: 80 p.

Popit, T. 2016: Mehanizmi transporta in sedimentacijski procesi kvartarnih pobočnih sedimentov na območju Rebernic. Doktorska disertacija. Univerza v Ljubljani, Fakulteta za gradbeništvo in geodezijo, Ljubljana: 345 p.

Popit, T. & Košir, A. 2010: Kvartarni paleoplazovi na Rebrnicah. In: Košir, A., Horvat, A., Zupan Hajna, N. & Otoničar, B. (eds.): 3. Slovenski geološki kongres, Bovec, 16.–18. September 2010. Povzetki in ekskurzije, ZRC SAZU, Ljubljana: 39–40.

Popit, T., Kokalj, Ž. & Verbovšek, T. 2011: Uporaba lidarja pri proučevanju geomorfoloških oblik na območju Rebrnic in Vipavskih Brd. In: Rožič, B. (ed.). 20. posvetovanje slovenskih geologov, Geološki zbornik, 21: 104–108.

Popit, T., Košir, A. & Šmuc, A. 2013: Sedimentological characteristics of Quarternary deposits of the Rebrnice slope area (SW Slovenia). In: Knjiga sažetka: 3. Znanstveni skup Geologija kvartara u Hrvatskoj s međunarodnim sudjelovanjem, povodom 130 godina rođenja akademika Marijana Salopeka i u spomen znanstvenici Maji Paunović na 10. obljetnicu smrti, Zagreb, 21.–23. 3. 2013. Zagreb, HAZU: 45.

Popit, T., Rožič, B., Šmuc A., Kokalj, Ž., Verbovšek, T. & Košir, A. 2014: A lidar, GIS and basic spatial statistic application for the study of ravine and palaeo-ravine evolution in the upper Vipava valley, SW Slovenia. Geomorphology, 204: 638–645. doi:10.1016/j.geomorph.2013.09.010.

Skok, J. 2001: Geološko-geotehnični elaborat o zgradbi tal in pogojih gradnje HC Razdrto – meja Italija, pododsek 0374 Razdrto-Vipava, km 1,300 – 6,300. Ljubljana, GEOT d.o.o.: 47 p.

Skok, J. 2002: Geološko-geotehnično poročilo o raziskavah ter predlogih sanacij plazu na stranskem odvzemu Rebrnice, v okviru izgradnje HC Razdrto – Vipava, km 4,940 – 5,330. Ljubljana, GEOT d.o.o.: 24 p.

Verbovšek, T., Košir, A., Teran, M., Zajc, M. & Popit, T. 2017: Volume determination of the Selo landslide complex (SW Slovenia): integrating field mapping, Ground Penetrating Radar and GIS approaches. Landslides, doi:10.1007/s10346-017-0815-x.

Internet source:

Internet 1: ArcGIS Help 10.1 3-D Analyst http://resources.arcgis.com/en/help/main/10.1/index.html#/3-D_Analyst_toolbox_licensing/00q90000000v000000/ (20 April 2014)

Nove knjige - New books

Mišo ANDJELOV, Zlatko MIKULIČ, Björn TETZLAFF, Jože UHAN & Frank WENDLAND, 2016:
Groundwater Recharge in Slovenia - Results of a bilateral German-Slovenian Research Project.
Schriften des Forschungszentrums Jülich, Reihe Energie & Umwelt, Jülich: 138 p.
http://juser.fz-juelich.de/record/824161/files/Energie_Umwelt_339.pdf

V letu 2016 je Forschungszentrum Jülich GmbH v okviru svoje zbirke "Spisi raziskovalnega centra Jülich", v zvezku št. 339 niza "Energija in okolje" izdal knjigo "Groundwater Recharge in Slovenia - Results of a bilateral German-Slovenian Research Project", katere avtorji so Mišo Andjelov, Zlatko Mikulič in Jože Uhan z Agencije Republike Slovenije za okolje (ARSO) ter Björn Tetzlaff in Frank Wendland z Raziskovalnega centra Jülich. Knjiga je monografija, ki predstavlja rezultate meddržavnega nemško-slovenskega raziskovalnega projekta, ki sta ga v letih 2009 do 2016 izvajala ARSO in Inštitut za agrosfero pri Raziskovalnem centru Jülich. Kot sledi iz predgovora, ki sta ga sopodpisala direktor Inštituta za agrosfero Raziskovalnega centra Jülich prof. dr. Harry Vereecken in generalni direktor ARSO Joško Knez, so na TAIEX (Technical Assistance and Information Exchange) seminarju o modeliranju podzemnih voda, ki sta ga v Ljubljani skupno organizirala Generalni direktorat za širitev Evropske komisije in ARSO, ocenili, da bi bilo model GROWA možno uporabiti za določanje obnavljanja podzemne vode v Sloveniji. Tej oceni sta sledili zasnova in izvedba bilateralnega raziskovalnega projekta. Projekt z delovnim naslovom 'GROWA-Slovenia' je omogočil prenos hidrološkega vodnobilančnega modela GROWA v Slovenijo in njegovo uspešno nadgradnjo v model 'GROWA-SI', adaptiran na slovenske razmere.

Knjiga obsega naslednja poglavja: 1) Uvod, ki podaja ozadja in cilje projekta, območje raziskav – t.j., ozemlje Republike Slovenije – in osnovne hidrološke definicije; 2) Opis modela GROWA, ki podaja razvoj in stanje modeliranja na nacionalnem nivoju – nemškem in slovenskem, izhodišča za izračun realne evapotranspiracije in celotnega odtoka, izhodišča za določanje količinskega obnavljanja podzemne vode in povzetek modelnih značilnosti in vhodnih plasti modela GROWA; 3) Priprava in regionalizacija podatkov, ki ločeno obravnava klimatske podatke, podatke o zemljiškem pokrovu, pedološke podatke, hidrogeološke podatke, topografske podatke in podatke o pretoku površinskih vod; 4) Rezultati modela, kjer so prikazane določitve realne evapotranspi-

In the Volume 339 of the »Scientific papers of Research Centre Jülich - series Energy & Environment« was in the year 2016 published book »Groundwater Recharge in Slovenia – Results of a bilateral German-Slovenian Research Project«, authored by Mišo Andjelov, Zlatko Mikulič and Jože Uhan from the Slovenian Environment Agency (ARSO), as well as Björn Tetzlaff and Frank Wendland from the Research Centre Jülich (FZJ) in Germany. In the monograph are presented results of the bilateral German-Slovenian research project carried out from 2009 to 2016 by ARSO and Agrosphere Institute IBG-3 of FZJ. As it is pointed out in the foreword co-signed by the director of IBG-3 of FZJ Prof. Dr. Harry Vereecken and the general director of ARSO Joško Knez, the potential of GROWA model for modelling groundwater recharge in Slovenia was identified at the TAIEX (Technical Assistance and Information Exchange) groundwater modelling seminar, jointly organized in Ljubljana by the Directorate-General Enlargement of the European Commission and ARSO. As a follow-up to the seminar a bilateral research project was established. The result of the project was a transfer of water balance model GROWA to Slovenia, as well as the upgrade and adaptation of the original model to the GROWA-SI to suit complex Slovenian physio-geography.

The book comprise following nine chapters: *1) Introduction*, describing project background and project goals, basic information on Slovenian territory, as well as basic hydrological definitions; *2) Description of the GROWA model*, with short historical overview of hydrological modelling development in Germany and Slovenia, describing the method to derive real evapotranspiration, total runoff and to separate it into direct and groundwater runoff, and giving in the end review of all input layers; *3) Data preparation and regionalization*, defining input data into model, namely climate data, landcover data, soil data, hydrogeological data, topography data and hydrological data on river discharge; *4) Model results* where are presented results of real evapotranspiration calculation, total runoff calcularacije, celotnega odtoka in prevladujočih komponent celotnega odtoka, t.j., direktnega odtoka in obnavljanja podzemne vode, pri čemer je kot obnavljanje podzemne vode upoštevana za vrednost medtoka (interflow oziroma, v kraških vodonosnikih, groundwater run-off) zmanjšana vrednost podzemnega odtoka; 5) Validacija in verifikacija modela, ki obravnava ločeno celotni odtok ter ločeno obnavljanje podzemne vode in direktni odtok; 6) Posledice ocene obnavljanja podzemne vode za upravljanje z vodami v Sloveniji; 7) Razširjene uporabe modela GROWA-SI v Sloveniji, kjer so prikazani letno poročanje ocene količinskega stanja podzemne vode, načrt upravljanja s povodjem, vodnobilančni podatki za različne EU in svetovne institucije, obnavljanje podzemne vode kot okoljski indikator, obnavljanje podzemne vode pri podatkovno usmerjenem modeliranju ranljivosti podzemne vode za nitratno onesnaženje, in, na rezultatih modela GROWA osnovano modeliranje dušikovega toka v Sloveniji; 8) Sklepi in obeti; in 9) Reference. Razlage v tekstu so ilustrirane z 68 slikami in podatkovno podprte s 14 tabelami, reference pa obsegajo 179 naslovov.

Pri določanju vodne bilance hidroloških bazenov oziroma povodij se realna evapotranspiracija določa kot odtočni deficit med padavinami in celotnim odtokom. Pristop je zelo natančen za velika povodja, pri manjših povodjih in nepopolnih hidroloških bazenih pa natančnost pada zaradi neugotovljivih dotokov in odtokov podzemne vode vanje ali iz njih. Na osnovi meteorološko določene potencialne evapotranspiracije in njene prevedbe v realno evapotranspiracijo s pomočjo v okviru hidrološkega bazena regionaliziranih parametrov naravnih danosti (topografije, tal, kamninske podlage in vegetacije) ter rabe prostora, izračunamo ob upoštevanju padavin odtok iz hidrološkega bazena. Ta mora ustrezati merjenemu odtoku. Hidrogeološki model postane za hidrološke napovedi uporaben šele potem, ko so za umeritveno obdobje razlike med izračunanimi in izmerjenimi vrednostmi odtoka sprejemljivo majhne.

Za določanje podzemnega odtoka so v uporabi analize hidrogramov in odtočni koeficienti oziroma indeksi, ki določajo podzemni odtok kot delež celotnega odtoka. V sušnih obdobjih napaja pri nizkem vodnem stanju vodotoke le podzemna voda. Zato je za oceno njenega nizkovodnega stanja uporaben indeks baznega odtoka BFI. Zaradi nepopolnosti hidroloških bazenov in s tem povezanega neugotovljivega dotoka ali odtoka podzemnih vod z njihovim zmanjševanjem natančnost

tion, and predominating runoff components, i.e. direct runoff and groundwater recharge separation; *5) Model validation and verification*, where are separately analyzed total runoff, direct runoff and groundwater recharge; *6) Water management implications of groundwater recharge assessment in Slovenia*, giving new insights based on GROWA-SI groundwater recharge calculations; *7) Extended applications of GROWA-SI model in Slovenia* referring to groundwater quantitative status assessment annual report, river basin management plan, water balance data for various EU and global institutions, groundwater recharge as environmental indicator, assessment of climate change impact on groundwater recharge, groundwater recharge in data driven modelling of groundwater vulnerability to nitrate pollution and nitrogen flux modelling in Slovenia based on GROWA-SI results; *8) Conclusions and outlook*; *9) Reference*. The descriptions in the text are accompanied by 68 figures, 14 tables and 179 references.

In water balance of hydrological catchments and river basins is real evaporation determined as a deficit between precipitation and total runoff. This approach gives good results for big river basins while in small catchments or river basins with not well defined boundary conditions accuracy is lower due to the unidentified groundwater inflows and outflows. Climatologically determined potential evapotranspiration which is transferred into real evapotranspiration by taking into account regionalized parameters in hydrological basin (topography, soils, bedrock and vegetation cover) as well as land use and precipitation, data enable calculation of runoff from the basin. This runoff should be equal to measured discharge from the river basin. Hydrogeological model is reliable for hydrological forecasts only when for calibration period difference between calculated and measured runoff is acceptable small.

To calculate groundwater runoff is in use hydrograph analysis and defining runoff coefficients or indices that determine groundwater runoff as a fraction of total runoff. In dry period is river flow completely recharged by groundwater. To assess low flow of the river is used baseflow index BFI. Due to the incomplete river basin boundary conditions causing uncertainties in assessment of groundwater inflow and outflow, in small basins the accuracy of water balance is diminished. The results are also affected by groundwater storage in aquifers. Therefore runoff coefficients and indices are susceptible to great variation. Decades določitev pada. Na izračune vpliva še začasno skladiščenje podzemne vode v vodonosnikih. Odtočni koeficienti oziroma indeksi so zato podvrženi veliki variabilnosti. Habič je zato pri nas pred desetletji z odtočnimi koeficienti ocenjeval variabilnost velikosti prispevnih območij kraških izvirov. Zanesljivi so le odtočni koeficienti oziroma indeksi, izvedeni iz dolgoletnih nizov padavin, celotnega odtoka in podzemnega odtoka.

V knjigi obravnavani model GROWA je numerični hidrološki model, ki parametre naravnih danosti in rabe prostora regionalizira na 100 × 100 m velike celice, razvrščene v pravokotno mrežo. Zanje za izbrano obdobje iz potencialne evapotranspiracije izračunava realno evapotranspiracijo in ob upoštevanju padavin in vodne bilance tudi celotni odtok. Celotni odtok iz hidrološkega bazena je vsota celičnih celotnih odtokov. Biti mora enak v vodomerni postaji na iztoku iz obravnavanega hidrološkega bazena izmerjenemu celotnemu odtoku. Vodna bilanca se računa z letnimi povprečji njenih treh v umeritvenem obdobju izmerjenih oziroma določenih bilančnih postavk. Modeliranje je reševanje inverznega problema - vrednost parametrov v celicah je treba popravljati toliko časa, dokler izračunani odtok ni enak izmerjenemu odtoku. Realna evapotranspiracija za hidrološki bazen je s tem pravilno določena, ustrezne pa naj bi bile tudi za posamezne celice določene vrednosti parametrov. Obnavljanje podzemne vode izračunava GROWA iz celične vrednosti celotnega odtoka s pomočjo celične vrednosti indeksa baznega odtoka BFI, regionaliziranega na podlagi naravnih danosti in rabe prostora. Za hidrološki bazen izračunana vrednost obnavljanja podzemne vode je vsota celičnih vrednosti. Tudi tu mora biti za daljše časovno obdobje izračunana vrednost obnavljanja podzemne vode enaka za isto obdobje s pomočjo povprečne vrednosti najmanjših povprečnih dnevnih mesečnih pretokov izračunanemu povprečnemu letnemu pretoku nizkih vod. In podobno kot prej je tako izračunana vrednost obnavljanja podzemne vode točna za hidrološki bazen, predvidoma pa naj bi bile ustrezne tudi njene celične vrednosti. Velika prednost tega modela je, da je zasnovan na GIS osnovi. Zato je možno vse podatkovne plasti zanj pripraviti v GIS okolju, v GIS okolju pa podaja tudi rezultate izračunov. Jasno je, da so tako podani rezultati nadvse primerni za vse javne in institucionalne rabe.

Model GROWA je bil razvit za severnonemška velika povodja s prevladujočo nekonsolidirano kamninsko podlago, ter uspešno razširjen še na celotno površino več severnonemških zveznih

ago Habič used runoff coefficients to assess area of karst spring catchments in Slovenia. Only reliable runoff coefficients are those determined from long time series data of precipitation, total runoff and underground runoff.

Model GROWA described in the book is numerical hydrological model, regionalizing input data into 100 × 100 m cells in orthogonal mesh. For each cell and chosen time period is calculated real evapotranspiration, and subtracting it from precipitation is calculated total runoff. Total runoff from the basin is a sum of all cell runoffs. Calculated runoff should be equal to the discharge at hydrological station that measures outflow from the river basin. Water balance is calculated from annual means for calibration period of three afore listed water balance components and compared to measured values. Modelling process is an inverse problem solving, i.e. parameter values in the cells are corrected until calculated runoff matches measured runoff. Real evapotranspiration is in this way correctly determined and also other parameter values of the cells are so properly assessed. GROWA calculates groundwater recharge from cell total runoff by applying BFI of the cell which is regionalized taking into account physio-geographical characteristics and land use. Groundwater recharge for entire basin is a sum of all cell values. Calculated groundwater recharge should match measured values of long time series, in this case being multiannual mean of monthly low waters. Thus determined groundwater recharge is accurate for whole river basin as well as giving accurate cell values of recharge. The big advantage of the model is its GIS platform. So, all input parameters are prepared in GIS format, therefore results are also in GIS format, thus being very useful for application in water management.

GROWA model was developed for big river basins with prevailing unconsolidated rocks of northern Germany. Later it was successfully applied to entire territories of several federal states in northern Germany. Upgrading of the GROWA model into GROWA-SI to be used in Slovenian hydrogeological environment of fissured and karst aquifers required adaptation of BFI calculation to take into account Slovenian specific rock types. Mean annual low flow of long term reference period is in GROWA-SI determined from the mean of monthly low flows, calculated by regression analysis taking into account only linear section of the cumulative frequency of low monthly flows. In this way is eliminated interflow component of monthly low flows. It has to država. Njegova nadgradnja v za slovenske hidrogeološke razmere primeren model GROWA-SI je zahtevala razpoklinskim in kraškim vodonosnikom primerno spremembo izračuna indeksa baznega odtoka BFI. Povprečni letni pretok nizkih vod za daljše obdobje je v modelu GROWA-SI določen iz povprečne vrednosti najmanjših povprečnih dnevnih mesečnih pretokov, izračunane s pomočjo z diagramom rastočih vrednosti najmanjših povprečnih dnevnih mesečnih pretokov določene regresijske premice. S tem je kompenzirana v teh vodonosnikih povišana vrednost medtoka. Ob tem je treba opozoriti na dejstvo, da 'obnavljanje podzemne vode', ki za hidrološki bazen podaja minimalno letno količinsko stanje podzemne vode ni enako 'podzemnemu odtoku', ki podaja vrednost vse ponikle vode – tudi tiste, ki napaja medtok.

Izvajalci projekta so opravili izredno veliko in zahtevno delo že s pripravo zanj potrebnih podatkovnih osnov. V za model GROWA-SI potrebne podatkovne plasti so morali v zanj ustrezno GIS okolje prevesti podatke vrste institucij (GURS, GeoZS, UL BF CSES in ARSO). Za umerjanje modela so za obdobje 1971-2000 pripravili tudi klimatološke in hidrološke podatke. Nekatere predstavitve in analize se s tem v zvezi pojavljajo prvič: izračun povprečnih letnih, povprečnih poletnih (maj-okt) in povprečnih zimskih (nov-apr) padavin, količnik zimskih in letnih padavin in povprečna letna potencialna evapotranspiracija za obdobje 1971-2000, prikazi podatkov CORINE za Slovenijo v skladu s standardom ATV-DVWK (2002), karta povprečne globine do podzemne vode, karta tal z visečo talno vodo in karta vrednosti parametra IDPR (Development and Persistence of the River Network) za Slovenijo.

Vsebinsko ključni del projekta pa so predstavljali umerjanje, validacija in verifikacija vodnobilančnega modela GROWA-SI. Posebna odlika knjige je, da poleg rezultatov modela podaja tudi rezultate njegove verifikacije in validacije. Rezultat modela GROWA-SI so za celotno območje Slovenije in za izbrano umeritveno obdobje kartografsko prikazane določitve realne evapotranspiracije, celotnega odtoka in njegovih obeh za upravljanje voda pomembnih komponent, to je, direktnega odtoka in obnavljanja podzemne vode. Kot obnavljanje podzemne vode je bila pri tem upoštevana za vrednost medtoka (interflow oziroma v kraških vodonosnikih fast groundwater run-off) zmanjšana vrednost podzemnega odtoka.

Verifikacija in validacija modela za določanje celotnega odtoka oziroma realne evapotranspira-

be stressed that »groundwater recharge«, which represents minimum annual groundwater quantity in the hydrological basin is not equal to »underground outflow« which represents all seepage including also interflow.

Already preparation of model input data was a very demanding and challenging task. To prepare input layers of GROWA-SI it was required to transfer all data of several institutions (Surveying and Mapping Authority of Slovenia, Geological Survey of Slovenia, University of Ljubljana Biotechnical Faculty, Ministry of Agriculture Forestry and Food, Slovenian Environment Agency) into form suitable for GIS platform. For calibration purpose, data base of climatology and hydrogeology data for 1971-2000 reference period was established. Some of the graphics and analyses have been done for the first time in Slovenia: summer season (May to October) mean precipitation, winter season (November to April) mean precipitation, ratio between winter and summer precipitation, mean annual real evapotranspiration for 1971-2000 period, CORINE map of Slovenia according to ATV-DVWK (2002) standard, map of mean depth to groundwater table, map of perched groundwater and adapted map of IDPR values (Index of Development and Persistence of the River Network).

The crucial part of the project was calibration, validation and verification of the water balance GROWA-SI model. Special valuable feature of the book is that besides the results of model calculations are presented results of model validation and verification. Result of GROWA-SI model are the maps of Slovenia for the chosen reference period that show real evapotranspiration, total runoff together with both components of it very important in water management: direct runoff and groundwater recharge. Groundwater recharge was taken as underground runoff deducted by interflow (in karst fast groundwater runoff component).

Validation and verification process of the model results for total runoff and real evapotranspiration was carried out for 95 gauging stations and corresponding contributing hydrological catchments distributed in all climate regions of Slovenia. Comparison of GROWA-SI model total runoff results to results of classical water balance model of Slovenia by ARSO for 1971-2000 period with regionalized parametres according to physio-geographical characteristics and land use, published in 2008, and compared for the same river basins and gauging stations showed correlation coefficient R^2=0.99. That means, regioncije sta bili izvedeni s pomočjo po vseh klimatskih območjih Slovenije porazdeljenih 95 vodomernih postaj in tem postajam pripadajočih kontrolnih hidroloških prispevnih območij. Primerjava rezultatov klasično zasnovanega bilančnega izračuna za obdobje 1971 - 2000 in temu primerno regionaliziranih parametrov naravnih danosti in rabe prostora, ki so ga na ARSO opravili in objavili že leta 2008, z modelom GROWA-SI izračunanih vrednosti celotnega odtoka za ista hidrološka prispevna območja vodomernih postaj, ima koeficient determinacije R^2=0,99. To pomeni, da je za modelne celice modela GROWA-SI izvedena regionalizacija parametrov obravnavanih hidroloških prispevnih območij enakovredna klasični regionalizaciji teh parametrov; verificirana je torej kot izjemno uspešna. Validacija modela je bila opravljena s primerjavo za kontrolna prispevna območja vodomernih postaj z modelom GROWA--SI izračunanih vrednosti celotnega odtoka in na pripadajočih vodomernih postajah izmerjenih vrednosti tega odtoka. S koeficientom determinacije R^2=0,93 je dokazala, da tako določene slike skoraj vseh hidroloških prispevnih območij od popolne korelacije odstopajo za manj kot 25 %. Ob upoštevanju natančnosti določanja padavin in odtoka ter dejstva, da gre za razmeroma majhna hidrološka prispevna območja, je to povsem sprejemljivo. Z naraščanjem na vodomernih postajah merjenega odtoka se deviacija merjenih in računskih rezultatov zelo zmanjša. Nekaj vrednosti, ki to mejo pri razmeroma majhnih vrednostih celotnega odtoka presegajo, pa kaže, da bi bilo v model GROWA-SI med vplive človeka oziroma urbanizacije treba vključiti še vodne zadrževalnike oziroma površinska vodna telesa. Evaporacija s proste vodne površine je namreč bistveno večja od z modelom GROWA-SI za z njimi prekrita območja izračunanih vrednosti realne evapotranspiracije.

Umerjanje modela GROWA-SI za izračun obnavljanja podzemne vode, je bilo izvedeno na 46 umeritvenih hidroloških prispevnih območjih, validacija modela pa na 27 kontrolnih hidroloških prispevnih območjih za ta dva namena izbranih vodomernih postaj. Verifikacija modelnih izračunov je bila v tem primeru uspešno izvedena s primerjavo za 46 umeritvenih hidroloških prispevnih območij z modelom GROWA-SI izračunanih vrednosti obnavljanja podzemne vode in grafoanalitično, s pomočjo regresijske premice, določenih povprečnih vrednosti najmanjših povprečnih dnevnih mesečnih pretokov. V bistvu je bila na tak način preverjena ustreznost za modelne cealization of the parametres in GROWA-SI cells matches classical water balance regionalization and has been outstandingly successful. Comparison of total runoff calculated by GROWA-SI for 95 control catchments to the measured discharges showed correlation coefficient R^2=0.93, with mean deviation being lower than 25 %. Taking into account uncertainty of precipitation and discharge measurements, and taking into account relatively small catchments area the model results are completely acceptable. Increasing values of measured discharge at gauging stations result in smaller deviation of modelled values from the measured. Some results with high deviation at catchments of small total runoff indicate that GROWA-SI should include impact of water reservoirs i.e. surface water bodies. Namely, evaporation from free water surface is much higher than "real evaporation" calculated by GROWA-SI.

Calibration of GROWA-SI for calculation of groundwater recharge was carried out at 46 calibration hydrological catchments, while validation was carried out at 27 hydrological control catchments. Validation was carried out by comparing GROWA-SI results to monthly lows determined by graph-analytical method of regression curve. Actually, in this way are controlled values of base flow index BFI for model cells. In similar way was carried out verification of the model for control hydrological catchments. Both comparisons were performed also for direct runoff i.e. fast runoff component. Since they were determined as difference between total runoff and groundwater recharge this validation does not offer big added value. For both groundwater recharge and direct runoff is deviation from perfect correlation within 25 %. In the first case is correlation coefficient R^2=0.94 and in the second it is R^2=0.91. In both cases deviation of calculated values from the measured does not decrease with increasing runoff. The cause could be in values of BFI for karst catchments or imperfect boundary conditions of control hydrological catchments. Unfortunately, there is not a list of 46 calibration and 27 validation control hydrological catchments that could offer opportunity to analyze in more detail this problem. For sure it will be a lot of opportunity to do it in course of future use of GROWA-SI model.

From presented validation and verification of GROWA-SI model it could be concluded, that calculation of groundwater recharge in control hydrological catchments offers satisfactory relice privzetih vrednosti indeksa baznega odtoka BFI. Na podoben način je bila za 27 kontrolnih hidroloških prispevnih območij izvedena še validacija modela. Za oba računska pristopa je zato za ta območja podana primerjava za obnavljanje podzemne vode in za direktni (t.j., hitri) odtok izračunanih vrednosti. V obeh primerih ležijo skoraj vsi računski rezultati znotraj 25 % odstopanja od popolne korelacije. V prvem primeru je skladnost obeh izračunov potrjena s koeficientom determinacije R^2=0,94, v drugem primeru pa s koeficientom determinacije R^2=0,91. Direktni odtok pa je bil določen kot razlika celotnega odtoka in obnavljanja podzemne vode, zato zadnji koeficient ne ponuja bistveno nove informacije. Ob tem je treba ugotoviti, da deviacija modelnih in računskih rezultatov z naraščanjem pretoka iz hidroloških prispevnih območij tu ne upada. To je lahko posledica za kraška območja privzetih vrednosti indeksa baznega odtoka BFI, ali pa nepopolnosti kontrolnih hidroloških bazenov. Žal v knjigi ni podana tabela s seznamoma 46 umeritvenih in 27 kontrolnih hidroloških prispevnih območij, kar onemogoča tehtnejši razmislek o vzrokih ugotovljene deviacije. Gotovo bo pa za to še dovolj časa pri nadaljnji uporabi modela GROWA-SI.

Na osnovi prikazane verifikacije in validacije modela GROWA-SI lahko ugotovimo, da izračunava model v kontrolnih hidroloških prispevnih območjih za obnavjanje podzemne vode dovolj verodostojne vrednosti. Na tej podlagi je bila lahko njegova uporaba upravičeno razširjena na celotno območje Republike Slovenije.

Sodim, da je pričujoča knjiga kapitalno delo slovenske hidrologije in hidrogeologije. Uporaba in rezultati za GIS okolje razvitega vodnobilančenga modela GROWA-SI jo operativno prestavljajo v 21. stoletje. Določanje količin in stanja podzemnih voda se s tem vrača tja kamor sodi – v okvir določanja vodnih bilanc posameznih hidroloških bazenov oziroma povodij. Vsi, ki smo že na samem začetku pozdravili idejo, da naj se model GROWA nadgradi in adaptira za Slovenijo, smo lahko z doseženimi rezulati več kot zadovoljni. Posebna vrednost modela GROWA-SI je tudi v tem, da omogoča od obstoječe razmejitve podzemnih vodnih teles povsem neodvisno oceno količinskega obnavljanja podzemne vode. Njihova strokovno utemeljena nadaljnja členitev ali preoblikovanje bosta lahko zato takoj podprti z zanje ustrezno oceno obnavljanja podzemne vode. V poglavju o posledicah ocene obnavljanja podzemne vode za upravljanje voda v Sloveniji je na primeru liable values. Based on these results it could be supposed that the model was rightly applied for entire territory of Slovenia.

I do hold that the book is pioneering breakthrough achievement of Slovenian hydrology and hydrogeology. Use and results of water balance GROWA-SI model developed on GIS platform are operational tools for 21st century. Groundwater quantity assessment is so coming back to its proper place – determination of water balance for hydrological basins and catchments. All of us, who have supported idea of upgrading and adapting of GROWA for Slovenia could be more than satisfied with the achieved results. Great value of GROWA-SI is its feature to calculate groundwater recharge independently of current groundwater bodies delineation. Future groundwater delineation could be immediately supported by qualified assessment of groundwater recharge. In the chapter on water management implications of groundwater recharge assessment was shown use of the model for assessing groundwater recharge per current groundwater bodies, specific groundwater recharge and coefficient of variation of groundwater recharge. In the chapter on extended applications of the GROWA-SI model in Slovenia, it was presented the use of the model results to determine available groundwater, as well as indicating groundwater quantity of critical dry years in 1981-2014 period, assessing groundwater abstraction rate in groundwater bodies, for river basin management plan preparation and in modelling of aquifer vulnerability to nitrate pollution. Some time ago Breznik found out that for some of Slovenian major karst springs are critical two dry years in succession with precipitation below 70 % of multiannual mean. GROWA-SI could be very useful tool to study such exceptional events on groundwater recharge and groundwater quantitative status.

Successful use of GROWA-SI already led to the upgrade to GROWA – DENUZ / WEKU for modelling nitrogen flux. So, in the book are already shown preliminary results of mean total leachate rate that will be used in nitrogen flux modelling. The leachate rate is defined as difference between total runoff and surface runoff i.e. it is sum of groundwater recharge and interflow. To my opinion model GROWA-SI should be for nitrogen flux modelling supplemented with data on clay cover depth at Lower Carniola low karst, as well as depth to groundwater table in high karst region and Alpine karst region of Slovenia. In the obstoječih teles podzemne vode prikazana uporabnost modela za določanje stopnje obnavljanja podzemne vode, njenega specifičnega obnavljanja in koeficienta variacije njenega obnavljanja. V poglavju o razširjenih uporabah modela GROWA-SI v Sloveniji pa je med drugim prikazana njegova uporabnost za določanje razpoložljive podzemne vode in na primerih za obdobje 1981-2014 uporabnost za določanje za stanje podzemnih vod kritičnih suhih let, določanje stopnje izkoriščenosti podzemne vode v podzemnih telesih, njegova uporabnost pri izdelavi načrtov upravljanja voda in pri modeliranju ranljivosti vodonosnikov na nitratno onesnaženje. Ob tem je treba opozoriti, da je pred leti Breznik pokazal, da je za minimalne pretoke nekaterih naših največjih kraških izvirov kritično zaporedje dveh sušnih let z manj kot 70% padavin dolgoletnega padavinskega povprečja. Z modelom GROWA-SI bi zato veljalo proučiti tudi vplive takšnih izjemnih dogodkov na obnavljanje in količinsko stanje podzemne vode.

Zaradi njegove uspešnosti se modelu GROWA--SI že obetata nadgradnji z modelom GROWA--DENUZ/WEKU za modeliranje nitratnega toka. S tem v zvezi so že prikazani prvi rezultati izračuna velikostne stopnje izcedne vode. Te predstavljajo razliko med celotnim odtokom in površinskim odtokom; predstavljajo torej vsoto obnavljanja podzemne vode in medtoka. Sodim, da bo s tem v zvezi model GROWA-SI treba dopolniti s podatki o debelini glinasto-meljnatega pokrova dolenjskega nizkega krasa in podatki o globini podzemne vode tudi za območja visokega krasa in visokogorskega krasa. S prvimi zato, ker lahko v nekaj metrov debelem pokrovu potekajo denitrifikacijski procesi, z drugimi pa zato, ker v debeli nezasičeni coni vodonosnikov poteka oksidacija v vodi prisotnih dušikovih spojin. Poseben izziv bo predstavljal tudi prenos modela mGROWA v Slovenijo. Ta naj bi omogočil modeliranje vodnobilančnih komponent na dnevni osnovi. Priznam, da sprejemam zaradi omejitev v uporabnosti indeksa baznega odtoka BFI za kratka obdobja to napoved z zadržkom – razen, če ne gre le za napovedovanje dnevnih odstopanj od dolgoletnih povprečij.

first case due to important denitrification process in several meter soil cover, and in the second case due to the oxidation of nitrogen compounds in deep unsaturated zone. Special challenge will be transfer of mGROWA model to Slovenia. It is supposed to enable modelling of water balance components on daily scale. I have to express my skepticism concerning this forecasting due to the limitations of baseflow index BFI use for short time scale – except if it goes for forecasting of daily deviations from multiannual mean.

prof. dr. Miran Veselič

GEOLOGIJA *60/1*, 163-166, Ljubljana 2017

Poročila

Predstavitev Slovenskega geološkega društva in letno poročilo za leto 2016

Matevž NOVAK

Geološki zavod Slovenije, Dimičeva ul. 14, SI-1000 Ljubljana; e-mail: matevz.novak@geo-zs.si

Slovensko geološko društvo (SGD) si je kot nevladna in neprofitna organizacija prostovoljno združenih strokovnjakov in ljubiteljev geologije zadalo za temeljni cilj napredek znanosti in prakse na področju vseh vej geologije, ki je zapisan tudi v njegovem statutu.

Skozi vsa leta društvo deluje v skladu z določili statuta in s programom dela, ki je sprejet na sejah IO društva v vsakem koledarskem letu. V letu 2016 sta bili dve seji razširjenega Izvršnega odbora društva in sicer 19. januarja in 1. decembra. Večji del zastavljenega programa je bil realiziran.

Strokovna predavanja

Sarah Halvorson (Oddelek za geografijo Univ. v Montani, ZDA), *»Large-Scale Environmental Transformations in Western Montana: From Glacial Lake Missoula to 21st Century Restoration Science«*, 10. marec 2016 ob 17. uri v Ljubljani v dvorani Zemljepisnega muzeja Geografskega inštituta Antona Melika ZRC SAZU, Gosposka 16. Predavanje je bilo izvedeno v soorganizaciji z Geomorfološkim društvom Slovenije.

Michele Morsilli (Univ. v Ferrari), *»Internal waves: their impact on sedimentary systems and benthic communities«,* 22. marec 2016 ob 17. uri v Ljubljani na Oddelku za geologijo NTF, Privoz 11.

Mihael Brenčič (NTF, GeoZS), *»Popotovanje po moskovskih geoloških muzejih«,* 7. aprila 2016 ob 17. uri v Ljubljani na Oddelku za geologijo NTF, Privoz 11. Predavanje je bilo izvedeno v soorganizaciji s Prirodoslovnim društvom Slovenije.

Strokovna posvetovanja, seminarji in okrogle mize

Slovensko geološko društvo je sodelovalo pri organizaciji terenske delavnice »27th *European Dendroecological Fieldweek«*, ki je potekala med 12. in 18. septembrom 2016 v Kranjski gori in dolini Tamar. Delavnico je organiziral Švicarski gozdarski inštitut (WSL) v sodelovanju z Naravoslovnotehniško fakulteto UL in Gozdarskim inštitutom Slovenije.

V okviru tedna Univerze v Ljubljani je bila v četrtek, 8. 12. 2016 v soorganizaciji Oddelka za geologijo NTF in Slovenskega geološkega društva izvedena *Delavnica o popularizaciji geologije*. Namen delavnice je bil pregled dosedanjega dela na področju popularizacije ter delu na področju šolskega in neformalnega izobraževanja, cilji za prihodnost in vizija skupnih idej na tem področju. Delavnica je potekala v prostorih Oddelka za geologijo na Privozu 11 (predavalnica P-114) s pričetkom ob 9. uri. Udeležilo se je 24 poslušalcev. Poročilo o delavnici je bilo objavljeno v reviji Geologija: RMAN, Nina, ŽVAB ROŽIČ, Petra. Delavnica o popularizaciji geologije, 8. 12. 2016, Oddelek za geologijo, NTF (http://www.geologija-revija.si/dokument.aspx?id=1291).

Sodelovanje na domačih dogodkih in druge aktivnosti

SGD je tudi v letu 2016, 10. junija, sodelovalo na dogodku *BioBlitz – 24 ur z reko Muro* v Veržeju v organizaciji Zavoda RS za varstvo narave, Območne enote Maribor. Izvedeni sta bili geološka delavnica o kamninah, mineralih in fosilih ter predstavitev na stojnici skupaj z Geološkim zavodom Slovenije in Oddelkom za geologijo Naravoslovnotehniške fakultete.

20. avgusta 2016 je Društvo Fran Govekar Ig v sodelovanju z Inštitutom za arheologijo ZRC SAZU na Igu organiziralo *Koliščarski dan*. Z geološko delavnico je SGD sodelovalo skupaj z Oddelkom za geologijo NTF in Geološkim zavodom Slovenije (www.vdezelikoliscarjev.si/).

Vaščani vasi Dešen pri Kresnicah so lansko leto zaprosili Zavod RS za varstvo narave, Oddelek za geologijo NTF in SGD za pomoč pri predstavitvi zanimive geologije kamnoloma nad vasjo in za donacijo za postavitev interpretacijske table. SGD je obema prošnjama ustreglo in oktobra 2016 je bila v Dešnu postavljena informativna točka.

GeoTEK

Slovensko geološko društvo je 13. oktobra 2016 organiziralo GeoTEK na Šmarno goro. Ta športno-rekreativni družabni dogodek nameravamo izvajati vsako leto na drugi, geološko zanimivi lokaciji. Pri organizaciji prvega je sodeloval Geološki zavod Slovenije.

Mednarodno delovanje SGD in članstvo v tujih in domačih zvezah

SGD je včlanjeno v tuje zveze: European Federation of Geologists (EFG), International Union for Quaternary Research (INQUA), European Association for the Conservation of the Geological Heritage (ProGeo), European Mineralogical Union (EMU) in International Mineral Association (IMA). Včlanjeni smo tudi v Slovensko inženirsko zvezo (SIZ).

Kot član Evropskega združenja geologov (European Federation of Geologists – EFG) je Slovensko geološko društvo leta 2015 začelo sodelovati v velikih evropskih projektih Obzorje 2020 (Horizon 2020). Skupaj z več drugimi nacionalnimi geološkimi društvi sodelujemo kot neodvisni partner preko pogodbe z EFG kot vodilnim projektnim partnerjem. V letu 2016 je bila naša vloga v projektu INTRAW – Mednarodno sodelovanje na področju oskrbe z mineralnimi surovinami (*International Cooperation on Raw materials*) posredovanje informacij o projektu in širjenje rezultatov projekta v Sloveniji. Večjo vlogo ima SGD v projektu KINDRA – Zbirka znanja za hidrogeološke raziskave (*Knowledge Inventory for Hydrogeology Research*), kjer je poleg obveščanja o rezultatih projekta v Sloveniji zadolženo tudi za zbiranje nacionalnih podatkov o hidrogeoloških raziskavah in njihovo opredelitev po novem enotnem sistemu klasifikacije raziskav.

V začetku leta 2016 smo podpisali pogodbi o sodelovanju še v dveh projektih: UNEXMIN – *An Autonomous Underwater Explorer for Flooded Mines* in CHPM 2030 – *Combined Heat, Power and Metal extraction from ultra-deep ore bodies.*

Član SGD, Marko Komac je bil novembra izvoljen v izvršni svet EFG kot External Relations Officer.

V letu 2016 smo prvič delovali kot polnopravni član Mednarodne zveze za raziskovanje kvartarja (International Union for Quaternaty Research – INQUA). Slovenski odbor INQUA (SINQUA) je posodobil svojo spletno predstavitev in med slovensko zainteresirano javnostjo razširjal informacije INQUA, vključno z razpisi za financiranje raziskovalnih projektov s poudarkom na podpori raziskav mlajšim raziskovalcem.

19. 4. 2016 smo se udeležili sestanka na Dunaju v okviru European Geosciences Union General Assembly 2016 (http://meetingorganizer.copernicus.org/EGU2016/session/22383), ki je bil organiziran s strani pobudnikov predloga INQUA fokusne skupine (IFG) z naslovom *„The Legacy of Mountain Glaciation“*. Namen ustanovitve omenjene IFG je oceniti relativno pomembnost različnih geomorfnih in podnebnih procesov pri razvoju alpskih ledenikov po vsem svetu.

Med 30. 5. in 3. 6. 2016 smo se udeležili *„7th INQUA International Workshop on Active Tectonics, Paleoseismology and Archaeoseismology (PATA)“* v Crestone, Colorado, ZDA, ki je bil glavni dogodek INQUA fokusne skupine „Earthquake Geology and Seismic Hazards“ (IFG EGSHaz). V okviru delavnice smo se udeležili sestanka IFG EGSHAz, na katerem smo se seznanili z aktivnostmi te skupine v prejšnjem obdobju (pod imenom *„Paleoseismology and Active Tectonics“* - IFG PALACTE) in načrtovanimi aktivnostmi v obdobju 2016–2019.

V sodelovanju z NC Hrvaške smo začeli organizirati 5th Scientific meeting Quaternary geology in Slovenia and Croatia, ki bo novembra 2017 na Hrvaškem. Pričakujemo, da bo ta dogodek spodbudil povečanje članstva.

SGD je včlanjeno v Slovensko inženirsko zvezo – SIZ. S tem je izpolnjen pogoj o obveznem članstvu SGD v SIZ za pridobitev naziva Evro inženir (EUR ING). Čakamo člane za pobude.

V letu 2017 so načrtovane in delno že izvedene naslednje dejavnosti društva:

Strokovna predavanja

Bálazs Székely (Univerza Eötvös Loránd v Budimpešti), *»Attempts to integrate David with Goliath: lessons learnt on differential uplift in a flatland«,* 14. marec 2017 ob 17. uri v Ljubljani na Oddelku za geologijo NTF, Privoz 11.

Giovanni Monegato (Inštitut za geoznanosti in zemeljske vire italijanskega Nacionalnega raziskovalnega sveta), *»An updated overview of* *last glacial maximum on the southern side of the Alps: comparisons and climate considerations«,* 23. marec 2017 ob 18. uri v Ljubljani na Geološkem zavodu Slovenije, Dimičeva ul. 14. Predavanje izvedeno v soorganizaciji s Slovenskim nacionalnim odborom INQUA (SINQUA).

Mirijam Vrabec o rezultatih geoloških raziskav v zadnjih letih na območju Pohorja. Predvideni datum je druga polovica junija 2017.

Marc Ostermann z Univerze v Innsbrucku na temo zemeljskih plazov je predvideno v začetku poletja.

Bojan Djurić (Oddelek za arheologijo FF v Ljubljani) na temo geoarheologije in uporabe naravnega kamna v rimski Emoni bo predvidoma v jeseni 2017.

Strokovne ekskurzije

V juniju 2017 bo ogled naravnega kamna na ljubljanskih ulicah vodil Matevž Novak.

Junija 2017 je predvidena strokovna ekskurzija na Pohorje pod vodstvom Mirijam Vrabec. Tema ekskurzije bo predstavitev novih dognanj o sestavi magmatskih in metamorfnih kamnin Pohorja.

Skupna ekskurzija SKIAH in SGD je načrtovana 13. in 14. oktobra 2017. Teme bodo mineralne vode, vulkaniti in geotermalna energija v SV Sloveniji in Z Madžarski. Obiskali bomo mofete v Slovenskih goricah, Vulkanijo na Goričkem, geotermalne vrtine v Moravskih Toplicah, rastlinjake v Renkovcih ali Dobrovniku, termalno jezero Heviz in pokrajinski muzej Balaton. Pri izvedbi bodo sodelovali tudi madžarski kolegi iz MFGI in zdravilišča Heviz.

Strokovna posvetovanja in okrogle mize

Slovensko geološko društvo je soorganiziralo *23. posvetovanje slovenskih geologov* 31. marca 2017 v Ljubljani na Oddelku za geologijo NTF, Privoz 1. Na posvetovanju je Društvo sodelovalo s predstavitvami mednarodnih projektov, v katere je vključeno.

SGD bo soorganizator *4. svetovnega foruma o plazovih* z naslovom »Landslide Research and Risk Reduction for Advancing Culture of Living with Natural Hazards«, ki bo v Ljubljani med 29. majem in 2. junijem (http://www.wlf4.org/hosts/).

SGD bo sodelovalo pri organizaciji 3. *regionalnega simpozija o zemeljskih plazovih v Jadransko Balkansko regiji (ReSyLAB)*, ki bo potekal od 11. do 13.10. 2017 v Ljubljani v soorganizaciji Geološkega zavoda Slovenije, Fakultete za gradbeništvo in geodezijo ter Naravoslovnotehniške fakultete Univerze v Ljubljani.

Med 6. in 12. novembrom 2017 bo potekalo 5. *regionalno znanstveno srečanje za kvartarno geologijo*, posvečeno geološko pogojenim nevarnostim. Organizatorji srečanja so Hrvaški nacionalni odbor INQUA (Hrvaška akademija znanosti in umetnosti, Oddelek za naravoslovje), Inštitut za kvartarno paleontologijo in geologijo, Slovenski nacionalni odbor INQUA, Slovensko geološko društvo, Geološki zavod Slovenije in Hrvaški geološki inštitut. Srečanje bo 9. In 10. 11. v kraju Starigrad Paklenica na Hrvaškem, pred im po srečanju pa bosta 3- in 2-dnevni ekskurziji v Sloveniji in na Hrvaškem.

Delovna akcija čiščenja geološkega profila

V soboto, 25. 3. 2017 je bila izvedena prestavljena delovna akcija čiščenja zarasti na geoloških naravnih vrednotah. V sodelovanju z Zavodom RS za varstvo narave (ZRSVN) in Občino Tržič smo očistili profil v Naravnem spomeniku Dovžanova soteska.

GeoTEK in GeoLOV

Slovensko geološko društvo bo oktobra 2017 organiziralo drugi tradicionalni GeoTEK. Natančen datum in lokacija še nista določena.

Poleg GeoTEKa smo uvedli še eno ekipno družabno akcijo, povezano z geološko vsebino – GeoLOV (»geocaching«). Prvi GeoLOV je bil v soboto, 8. aprila 2017 v okolici Lesnega Brda.

Sporočilo članom Slovenskega geološkega društva

SGD je z Geološkim zavodom Slovenije začel z aktivnostmi za ureditev pravno-formalnega statusa "geološkega zakona". 25. avgusta 2016 se je M. Novak skupaj z direktorjem Geološkega zavoda Slovenije in njegovim pomočnikom udeležil sestanka s predstavniki MiZŠ, MOP in MZI v prostorih MiZŠ. Dogovorjeno je bilo sodelovanje pri reševanju problematike na področju zbiranja, hranjenja in razpoložljivosti geoloških podatkov oz. podatkov o geosferi. V skladu z dogovorom na sestanku smo ministrstvom poslali kratek opis stanja, problematiko ter predlog ureditve.

Popularizacija geologije. Znotraj SGD so se močno intenzivirale aktivnosti, namenjene promociji geološke znanosti. Formirana je bila Skupina za popularizacijo geologije z jasno zastavljenimi cilji in s podrobnim načrtom lastnih akcij ter s koledarjem prireditev, na katerih bomo sodelovali.

Sodelovanje s sorodnimi društvi. Iz poročila je razvidno, da smo močno okrepili ter vzpostavili nove stike s tujimi geološkimi društvi (predvsem Hrvaškim in Srbskim) ter z drugimi društvo s sorodnimi cilji (Geomorfološkim društvom Slovenije – GDS, Prirodoslovnim društvom Slovenije – PDS, Društvom slovenski komite mednarodnega združenja hidrogeologov – SKIAH).

Med 20. in 22. oktobrom je bila na sedežu Univerze v Beogradu proslava in kratka konferenca za počastitev 125-letnice Srbskega geološkega društva. M. Novak se je prireditve udeležil kot vabljeni častni gost.

16. decembra smo na povabilo Hrvaškega geološkega društva sodelovali na njihovi 34. redni skupščini. T. Verbovšek je imel predavanje *„Slovensko geološko društvo – povijest, aktivnosti i ideje za suradnju s Hrvatskim geološkim društvom“*.

Postavitev nove spletne strani. Društvo je sredi postopka temeljite posodobitve društvenega spletnega portala, ki bo omogočal hitrejše obveščanje o društvenih dogodkih, objavo koledarja dogodkov, izmenjavo mnenj registriranih uporabnikov ter naročanje na prejemanje teh obvestil. S tem želi društvo doseči večjo prepoznavnost društva in povečanje števila članov.

Navodila avtorjem

GEOLOGIJA objavlja znanstvene in strokovne članke s področja geologije in sorodnih ved. Revija od leta 2000 izhaja dvakrat letno. Članke recenzirajo domači in tuji strokovnjaki z obravnavanega področja. Ob oddaji člankov avtorji predlagajo **tri recenzente**, vendar pa si uredništvo pridržuje pravico do izbire recenzentov po lastni presoji. Avtorji morajo članek popraviti v skladu z recenzentskimi pripombami ali utemeljiti zakaj se z njimi ne strinjajo.

Avtorstvo: Za izvirnost podatkov, predvsem pa mnenj, idej, sklepov in citirano literaturo so odgovorni avtorji. Z objavo v GEOLOGIJI se tudi obvežejo, da ne bodo drugje objavili prispevka z isto vsebino.

Jezik: Članki naj bodo napisani v angleškem, izjemoma v slovenskem jeziku, vsi pa morajo imeti slovenski in angleški izvleček. Za prevod poskrbijo avtorji prispevkov sami.

Vrste prispevkov:

Izvirni znanstveni članek
Izvirni znanstveni članek je prva objava originalnih raziskovalnih rezultatov v takšni obliki, da se raziskava lahko ponovi, ugotovitve pa preverijo. Praviloma je organiziran po shemi IMRAD (**I**ntroduction, **M**ethods, **R**esults, **A**nd **D**iscussion).

Pregledni znanstveni članek
Pregledni znanstveni članek je pregled najnovejših del o določenem predmetnem področju, del posameznega raziskovalca ali skupine raziskovalcev z namenom povzemati, analizirati, evalvirati ali sintetizirati informacije, ki so že bile publicirane. Prinaša nove sinteze, ki vključujejo tudi rezultate lastnega raziskovanja avtorja.

Strokovni članek
Strokovni članek je predstavitev že znanega, s poudarkom na uporabnosti rezultatov izvirnih raziskav in širjenju znanja.

Diskusija in polemika
Prispevek, v katerem avtor ocenjuje ali dokazuje pravilnost nekega dela, objavljenega v Geologiji, ali z avtorjem strokovno polemizira.

Recenzija, prikaz knjige
Prispevek, v katerem avtor predstavlja vsebino nove knjige.

Oblika prispevka: Besedilo pripravite v urejevalniku Microsoft Word. Prispevki naj praviloma ne bodo daljši od 20 strani formata A4, v kar so všetete tudi slike, tabele in table. Le v izjemnih primerih je možno, ob predhodnem dogovoru z uredništvom, tiskati tudi daljše prispevke.

Članek oddajte uredništvu vključno z vsemi slikami, tabelami in tablami v elektronski obliki po naslednjem sistemu:
- *Naslov članka (do 12 besed)*
- *Avtorji (ime in priimek, naslov, e-mail naslov)*
- *Ključne besede (do 7 besed)*
- *Izvleček (do 300 besed)*
- *Besedilo*
- *Literatura*
- *Podnaslovi k slikam in tabelam*
- *Tabele, Slike, Table*

Citiranje: V literaturi naj avtorji prispevkov praviloma upoštevajo le tiskane vire. Poročila in rokopise naj navajajo le v izjemnih primerih, z navedbo kje so shranjeni. V seznamu literature naj bodo navedena samo v članku omenjena dela. Citirana dela, ki imajo DOI identifikator, morajo imeti ta identifikator izpisan na koncu citata. Za citiranje revije uporabljamo standardno okrajšavo naslova revije. Med besedilom prispevka citirajte samo avtorjev priimek, v oklepaju pa navajajte letnico izida navedenega dela in po potrebi tudi stran. Če navajate delo dveh avtorjev, izpišite med tekstom prispevka oba priimka (npr. Pleničar & Buser, 1967), pri treh ali več avtorjih pa napišite samo prvo ime in dodajte et al. z letnico (npr. Mlakar et al., 1992). Citiranje virov z medmrežja v primeru, kjer avtor ni poznan, zapišemo (Internet 1). V seznamu literaturo navajajte po abecednem redu avtorjev.

Imena fosilov (rod in vrsta) naj bodo napisana poševno, imena višjih taksonomskih enot (družina, razred, itn.) pa normalno. Imena avtorjev taksonov naj bodo prav tako napisana normalno, npr. *Clypeaster pyramidalis* Michelin, *Galeanella tollmanni* (Kristan), Echinoidea.

Primeri citiranja članka:

Mali, N., Urbanc, J. & Leis, A. 2007: Tracing of water movement through the unsaturated zone of a coarse gravel aquifer by means of dye and deuterated water. Environ. geol., 51/8: 1401–1412, doi:10.1007/s00254-006-0437-4.

Pleničar, M. 1993: *Apricardia pachiniana* Sirna from lower part of Liburnian beds at Divača (Triest-Komen Plateau). Geologija, 35: 65–68.

Primer citirane knjige:

Flügel, E. 2004: Mikrofacies of Carbonate Rocks. Springer Verlag, Berlin: 976 p.

Jurkovšek, B., Toman, M., Ogorelec, B., Šribar, L., Drobne, K., Poljak, M. & Šribar, Lj. 1996: Formacijska geološka karta južnega dela Tržaško-komenske planote – Kredne in paleogenske kamnine 1: 50.000 = Geological map of the southern part of the Trieste-Komen plateau – Cretaceous and Paleogene carbonate rocks. Geološki zavod Slovenije, Ljubljana: 143 p., incl. Pls. 23, 1 geol. map.

Primer citiranja poglavja iz knjige:

Turnšek, D. & Drobne, K. 1998: Paleocene corals from the northern Adriatic platform. In: Hottinger, L. & Drobne, K. (eds.): Paleogene Shallow Benthos of the Tethys. Dela SAZU, IV. Razreda, 34/2: 129-154, incl. 10 Pls.

Primer citiranja virov z medmrežja:

Če sta znana avtor in naslov citirane enote zapišemo:

Čarman, M. 2009: Priporočila lastnikom objektov, zgrajenih na nestabilnih območjih. Internet: http://www.geo-zs.si/UserFiles/1/File/Nasveti_lastnikom_objektov_na_nestabilnih_tleh.pdf (17. 1. 2010)

Če avtor ni poznan zapišemo tako:

Internet: http://www.geo-zs.si/ (22. 10. 2009)

Če se navaja več enot z medmrežja, jim dodamo še številko

Internet 1: http://www.geo-zs.si/ (15. 11. 2000)
Internet 2: http://www.geo-zs.si/ (10. 12. 2009)

Slike, tabele in table: Slike (ilustracije in fotografije), tabele in table morajo biti zaporedno oštevilčene in označene kot sl. 1, sl. 2 itn., oddane v formatu TIFF, JPG ali EPS z ločljivostjo 300 dpi. Le izjemoma je možno objaviti tudi barvne slike, vendar samo po predhodnem dogovoru z uredništvom. Obvezno je treba upoštevati zrcalo revije **172 x 235 mm**. Večjih formatov od omenjenega zrcala GEOLOGIJE ne tiskamo na zgib, je pa možno, da večje oziroma daljše slike natisnemo na dveh straneh (skupaj na levi in desni strani) z vmesnim »rezom«. V besedilu prispevka morate omeniti vsako sliko po številčnem vrstnem redu. Dovoljenja za objavo slikovnega gradiva iz drugih revij publikacij in knjig, si pridobijo avtorji sami. Table pripravite v formatu zrcala naše revije.

Če je članek napisan v slovenskem jeziku mora imeti celotno besedilo, ki je na slikah in tabelah tudi v angleškem jeziku. Podnaslovi naj bodo čim krajši.

Korekture: Te opravijo avtorji člankov, ki pa lahko popravijo samo tiskarske napake. Krajši dodatki ali spremembe pri korekturah so možne samo na avtorjeve stroške.

Prispevki so prosto dostopni na spletnem mestu: http://www.geologija-revija.si/

Oddajanje prispevkov:

Avtorje prosimo, da prispevke pošljejo na naslov uredništva:
GEOLOGIJA
Geološki zavod Slovenije
Dimičeva ulica 14, 1000 Ljubljana
bernarda.bole@geo-zs.si ali urednik@geologija-revija.si

Uredništvo Geologije

Instructions for authors

Scope of the journal: GEOLOGIJA publishes scientific papers which contribute to understanding of the geology of Slovenia or to general understanding of all fields of geology. Some shorter contributions on technical or conceptual issues are also welcome. Occasionally, a collection of symposia papers is also published.
All submitted manuscripts are peer-reviewed by at least two specialists. When submitting their paper, authors should recommend at least **three reviewers**. Note that the editorial office retains the sole right to decide whether or not the suggested reviewers are used. Authors should correct their papers according to the instructions given by the reviewers. Should you disagree with any part of the reviews, please explain why. Revised manuscript will be reconsidered for publication.

Author's declaration: Submission of a paper for publication in Geologija implies that the work described has not been published previously, that it is not under consideration for publication elsewhere and that, if accepted, it will not be published elsewhere.

Language: Papers should be written in English or Slovene, and should have both English and Slovene abstracts.

Types of papers:

Original scientific paper
In an original scientific paper, original research results are published for the first time and in such a form that the research can be repeated and the results checked. It should be organised according to the IMRAD scheme (**I**ntroduction, **M**ethods, **R**esults, **A**nd **D**iscussion).

Review scientific paper
In a review scientific paper the newest published works on specific research field or works of a single researcher or a group of researchers are presented in order to summarise, analyse, evaluate or synthesise previously published information. However, it should contain new information and/or new interpretations.

Professional paper
Technical papers give information on research results that have already been published and emphasise their applicability.

Discussion paper
A discussion gives an evaluation of another paper, or parts of it, published in GEOLOGIJA or discusses its ideas.

Book review
This is a contribution that presents a content of a new book in the field of geology.

Style guide:
Submitted manuscripts should not exceed 20 pages of A4 format (12 pt typeface, 1 line-spacing, left justification) including figures, tables and plates. Only exceptionally and in agreement with the editorial board longer contributions can also be accepted.
Manuscripts submitted to the editorial office should include figures, tables and plates in electronic format organized according to the following scheme:
- *Title (maximum 12 words)*
- *Authors (full name and family name, postal address and e-mail address)*
- *Key words (maximum 7 words)*
- *Abstract (maximum 300 words)*
- *Text*
- *References*
- *Figure and Table Captions*
- *Tables, Figures, Plates*

References: References should be cited in the text as follows: (Flügel, 2004) for a single author, (Pleničar & Buser, 1967) for two authors and (Mlakar et al., 1992) for multiple authors. Pages and figures should be cited as follows: (Pleničar, 1993, p. 67) and (Pleničar, 1993, fig. 1). Anonymous internet resources should be cited as (Internet 1). Only published references should be cited. Manuscripts should be cited only in some special cases in which it also has to be stated where they are kept. Cited reference list should include only publications that are mentioned in the paper. Authors should be listed alphabetically. Journal titles should be given in standard abbreviated form. A doi identifier, if there is any, should be placed at the end as shown in the first case.
Taxonomic names should be in italics, while names of the authors of taxonomic names should be in normal, such as *Clypeaster pyramidalis* Michelin, *Galeanella tollmanni* (Kristan), Echinoidea.

Articles should be listed as follows:
Mali, N., Urbanc, J. & Leis, A. 2007: Tracing of water movement through the unsaturated zone of a coarse gravel aquifer by means of dye and deuterated water. Environ. geol., 51/8: 1401–1412, doi:10.1007/s00254-006-0437-4.
Pleničar, M. 1993: *Apricardia pachiniana* Sirna from lower part of Liburnian beds at Divača (Triest-Komen Plateau). Geologija, 35: 65–68.

Books should be listed as follows:
Flügel, E. 2004: Mikrofacies of Carbonate Rocks. Springer Verlag, Berlin: 976 p.
Jurkovšek, B., Toman, M., Ogorelec, B., Šribar, L., Drobne, K., Poljak, M. & Šribar, Lj. 1996: Formacijska geološka karta južnega dela Tržaško-komenske planote – Kredne in paleogenske kamnine 1: 50.000 = Geological map of the southern part of the Trieste-Komen plateau – Cretaceous and Paleogene carbonate rocks. Geološki zavod Slovenije, Ljubljana: 143 p., incl. Pls. 23, 1 geol. map.

Book chapters should be listed as follows:
Turnšek, D. & Drobne, K. 1998: Paleocene corals from the northern Adriatic platform. In: Hottinger, L. & Drobne, K. (eds.): Paleogene Shallow Benthos of the Tethys. Dela SAZU, IV. Razreda, 34/2: 129-154, incl. 10 Pls.

Internet resources should be listed as follows:
Known author and title:
Čarman, M. 2009: Priporočila lastnikom objektov, zgrajenih na nestabilnih območjih. Internet: http://www.geo-zs.si/UserFiles/1/File/Nasveti_lastnikom_objektov_na_nestabilnih_tleh.pdf (17. 1. 2010)
Unknown authors and title:
Internet: http://www.geo-zs.si/ (22.10.2009)

When more than one unit from the internet are cited they should be numbered:
Internet 1: http://www.geo-zs.si/ (15.11. 2000)
Internet 2: http://www.geo-zs.si/ (10.12. 2009)

Figures, tables and plates: Figures (illustrations and photographs), tables and plates should be numbered consequently and marked as Fig. 1, Fig. 2 etc., and saved as TIFF, JPG or EPS files and submitted at 300 dpi. Colour pictures will be published only on the basis of previous agreement with the editorial office. The maximum size of full-page illustrations and tables is **172 x 235 mm**. Larger formats can only be printed as a double-sided illustration (left and right) with a cut in the middle. All figures should be referred to in the text and should normally be numbered in the sequence in which they are cited. The approval for using illustrations previously published in other journals or books should be obtained by each author.
When a paper is written in Slovene it has to have the entire text which accompanies illustrations and tables written both in Slovene and English. Figure and table captions should be kept as short as possible.

Proofs: One set of page proofs (as pdf files) will be sent by e-mail to the corresponding author. Corrections are made by the authors. They should correct only typographical errors. Short additions and changes are possible but should be paid by the authors.

Geologija is an open access journal, all pdfs can be downloaded from the website: http://www.geologija-revija.si/en/

Submission: Authors should submit their papers to the address of the editorial office:

GEOLOGIJA
Geological Survey of Slovenia
Dimičeva ulica 14, 1000 Ljubljana, Slovenia
bernarda.bole@geo-zs.si or urednik@geologija-revija.si

The Editorial Office

GEOLOGIJA
št.: 60/1, 2017
www.geologija-revija.si

ISSN 0016-7789

GeoZS
Geološki zavod Slovenije